MONTANA STATE UNIVERSITY

Mountains & Minds

Department of Earth Sciences

Geology Field Camp Manual

Summer 2014



Instructors:

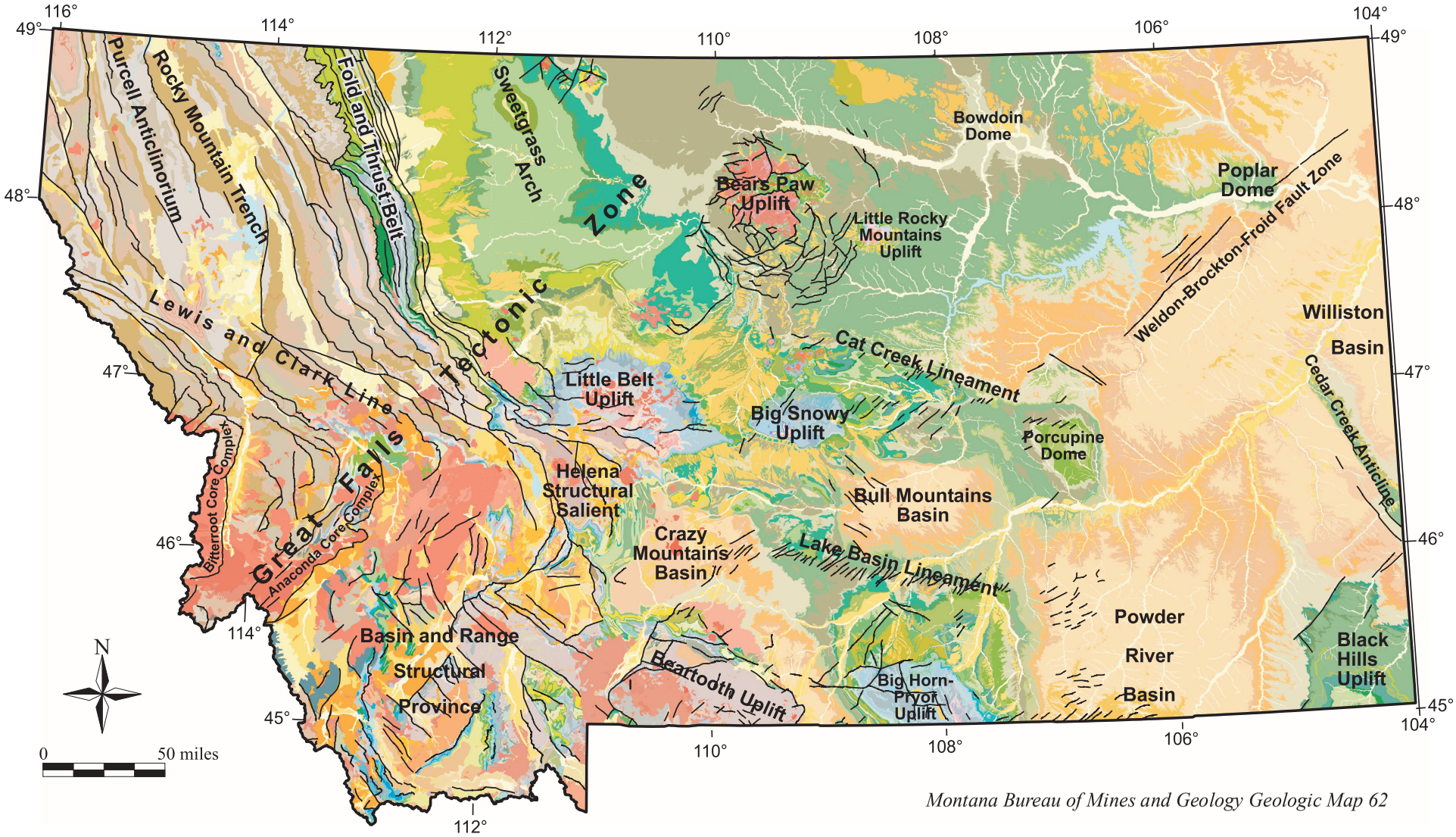
Dr. Jean Dixon

Dr. Todd C. Feeley

Dr. David W. Lageson

Dr. David Mogk

Dr. Colin A. Shaw



Montana Bureau of Mines and Geology Geologic Map 62

TABLE OF CONTENTS

Frontmatter

Geologic Map of Montana Frontspiece/Cover

Field Camp Schedule 4

Equipment, Supplies & First Aid 5

Field Methods

Introduction to Field Mapping of Geologic Structures – D.W. Lageson 7

FieldMove Clino Pro User Guide – Midland Valley 25

Articles, Background Reading & Field Trip Guidebooks

The Method of Multiple Working Hypotheses – T.C. Chamberlain 59

Evolution of the North American Cordillera – W.R. Dickinson 65

Yellowstone National Park and Vicinity Field Trip Guide 121

Reference Material 163

Comparison Charts for Estimating Percentage Composition …

IUGS classification for Igneous Rocks & Guide to Igneous Minerals …

Metamorphic Zones and Facies – AFM Diagrams and Petrogenetic Grids …

Structural Framework and Igneous Province Maps of Montana – MBMG …

Magnetic Declination Chart for Continental U.S. (2010) …

GSA Geologic Time Scale (1999) …

Three Forks Area Stratigraphic Column – W.J. McMannis …

Stratigraphic Column for N. Gallatin & Bridger Ranges, MT – J.W. Montagne Back Cover

Field Camp Schedule Worksheet

	Year	**2014**		***Instructional Days***	**30**
	Start Date	**9-Jun**		***Days off***	**4**
	End Date	**12-Jul**		***Total Days***	**34**
	Date	**Day**	**Exercise**	**Instructor**	**Accomodations**
	***arrive at Gaines Hall parking area by 0700 - depart by 0800**				
1	9-Jun	Mon	Structural Mapping I	Shaw	Camping Dillon
2	10-Jun	Tue	Structural Mapping I	Shaw	Camping Dillon
3	11-Jun	Wed	Structural Mapping I	Shaw	Camping Dillon
4	12-Jun	Thu	Structural Mapping I	Shaw	Camping Dillon
5	13-Jun	Fri	Structural Mapping I	Shaw	Camping Dillon
6	14-Jun	Sat	***Day off***		Camping Dillon
7	15-Jun	Sun	Structural Mapping II	Lageson	Camping Dillon
8	16-Jun	Mon	Structural Mapping II	Lageson	Camping Dillon
9	17-Jun	Tue	Structural Mapping II	Lageson	Camping Dillon
10	18-Jun	Wed	Structural Mapping II	Lageson	Camping Dillon
11	19-Jun	Thu	Structural Mapping II	Lageson	Bozeman
12	20-Jun	Fri	***Day off***		Bozeman
13	21-Jun	Sat	Geomorph	Dixon/Lageson	Jack Creek
14	22-Jun	Sun	Geomorph	Dixon/Lageson	Jack Creek
15	23-Jun	Mon	Geomorph	Dixon/Lageson	Jack Creek
16	24-Jun	Tue	Mm'ic - Bar 7?	Mogk/Shaw	Jack Creek
17	25-Jun	Wed	Mm'ic - Bar 7?	Mogk/Shaw	Jack Creek
18	26-Jun	Thu	Mm'ic - Bar 7?	Mogk/Shaw	Bozeman
19	27-Jun	Fri	***Day off***		Bozeman
20	28-Jun	Sat	Plutonic mapping	Feeley	Camping
21	29-Jun	Sun	Plutonic mapping	Feeley	Camping
22	30-Jun	Mon	Plutonic mapping	Feeley	Camping
23	1-Jul	Tue	Plutonic mapping	Feeley	Camping
24	2-Jul	Wed	Volcanic - YNP/map	Feeley	Camping
25	3-Jul	Thu	Volcanic - YNP/map	Feeley	Camping
26	4-Jul	Fri	Volcanic - YNP/map	Feeley	Bozeman
27	5-Jul	Sat	***Day off***		Bozeman
28	6-Jul	Sun	Research Project	Staff	TBA
29	7-Jul	Mon	Research Project	Staff	TBA
30	8-Jul	Tue	Research Project	Staff	TBA
31	9-Jul	Wed	Research Project	Staff	TBA
32	10-Jul	Thu	Research Project	Staff	Bozeman
33	11-Jul	Fri	Lab-Day	Staff	Bozeman
34	12-Jul	Sat	Present & Clean-up	Staff	Bozeman

FIELD GEOLOGY EQUIPMENT CHECKLIST

Essential Field Gear/Drafting Supplies

_____ Field text (*Compton*, *McClay* etc. as assigned)
_____ 10x hand lens (Hastings Triplet recom.)
_____ Rock hammer (~22 oz.)
_____ **Two**-field notebooks (bookstore)
_____ Technical pens (0.25mm, 0.5mm)
_____ **Two**-mechanical pencils (0.5mm)
_____ Replacement pencil lead (0.5mm)
_____ Stick-style eraser
_____ **Two** Plastic ruler-protractors (bookstore)
_____ Pad of drafting vellum for stereonets (50 sheets)
_____ Sharpee/permanent marker
_____ Set of coloring pencils (at least 12)
_____ Safety pins (for marking maps/photos)
_____ Pocket knife (2-4" blade)
_____ Small first-aid kit
_____ Field belt – non -magnetic (to carry compass/pouch/etc.)
_____ Sturdy field boots (see note above)
_____ **Two** liter canteens or water bottles
_____ Waterproof-breathable parka
_____ Sun hat
_____ Sun glasses
_____ Sun screen (SPF 30 or greater)
_____ Wrist/pocket watch
_____ Field back-pack

Recommended Field Gear

_____ Field pouch (for notebook/pencils)
_____ Wind/rain pants
_____ Large garbage bag for pack
_____ Leather work gloves
_____ Hammer holder for belt
_____ Small binoculars
_____ Camera & film
_____ Photo scale
_____ Calculator with trig functions
_____ Grain-size card
_____ Rock classification charts (in notebook)
_____ Swing magnet
_____ GPS unit

Essential Personal Gear

_____ Duffel bag/backpack
_____ Field clothing
_____ Underclothing & work socks
_____ Cold-weather clothing layers (sweaters etc.)
_____ Warm hat
_____ Warm winter coat
_____ Warm gloves or mittens
_____ Personal toilet kit
_____ Prescription medicine, contact lenses, personal health needs as needed
_____ Sleeping bag
_____ Tent (share w/1-2 friends)
_____ Towel/washcloth

Recommended Personal Gear

_____ Camp/town clothing
_____ Camp shoes or sandals
_____ Reading book, stationary, stamps
_____ Travel alarm clock
_____ D-cell headlamp/flashlight & batteries
_____ Personal cup/plate/bowl/cutlery
_____ Laundry bag & detergent
_____ Camp chair

Equipment Supplied by Department

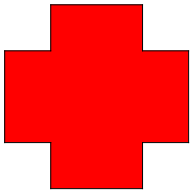
This equipment will be signed out to you and must be returned in good condition.

_____ Brunton and/or Silva compass
_____ iPad/tablet computer (as needed)
_____ Map board
_____ Acid dropper bottles
_____ Air photos/reference maps (as needed)
_____ Field geology reference library
_____ MSU Field Camp Manual
_____ Kitchen Gear: camp stoves, pots/pans, cooking utensils, dishwashing system, coolers etc.

Expendables

_____ 10% HCl
_____ Base map copies
_____ Stereonet/equal area net templates, thumbtacks

GEOL 423 – Field Course
Montana State University



MEDICAL PREPARATION

- ***Students are required to carry their own medical insurance – no exceptions! Be sure to carry insurance cards and/or policy numbers with you.***
- Have you had a tetanus shot within the last few years?
- Do you have medical issues that we need to know about?
- Are you allergic to anything that is potentially life threatening (bee-stings, food, plants, etc.)?

Personal First Aid Kit

Students are required to carry their own personal first aid kit while in the field (in your pack). Be sure to stock it with any items that have been prescribed by a doctor for you, such as inhalers, glucose, or an "epi-pen" for allergic reactions (epinephrine for anaphylactic shock from insect bites, food, plant allergies, etc.). It is recommended that these supplies be carried in a small waterproof stuff-sack.

For trauma care:

- ✧ Several assorted sizes of adhesive strips (band aids), including some large ones
- ✧ One or more rolled ace bandage (elastic wrap)
- ✧ Water-proof medical tape (1- and 2-inch rolls)
- ✧ Several assorted sizes of non-stick sterile dressings
- ✧ Alcohol wipes
- ✧ Triple antibiotic ointment (over-the-counter)
- ✧ Small bottle of sterile saline eye wash
- ✧ Tweezers (good for pulling cactus needles, etc.) & extra safety pins
- ✧ One pair rubber gloves

Miscellaneous supplies:

- ✧ Pocket mask for CPR
- ✧ Pain and/or anti-inflammatory medication (your choice – some people have allergies that dictate what they can take or tolerate, so follow whatever your doctor recommends for you)
- ✧ Small flashlight or head lamp (not left in your tent)
- ✧ Insect repellent (not recommended unless it is extremely buggy)
- ✧ Moleskin or molefoam or other pads and bandages for blisters on your feet
- ✧ Other prescription or non-prescription medications (decongestant for hay fever, antacid, throat lozenges, etc.)?
- ✧ Something for upset stomach and/or diarrhea

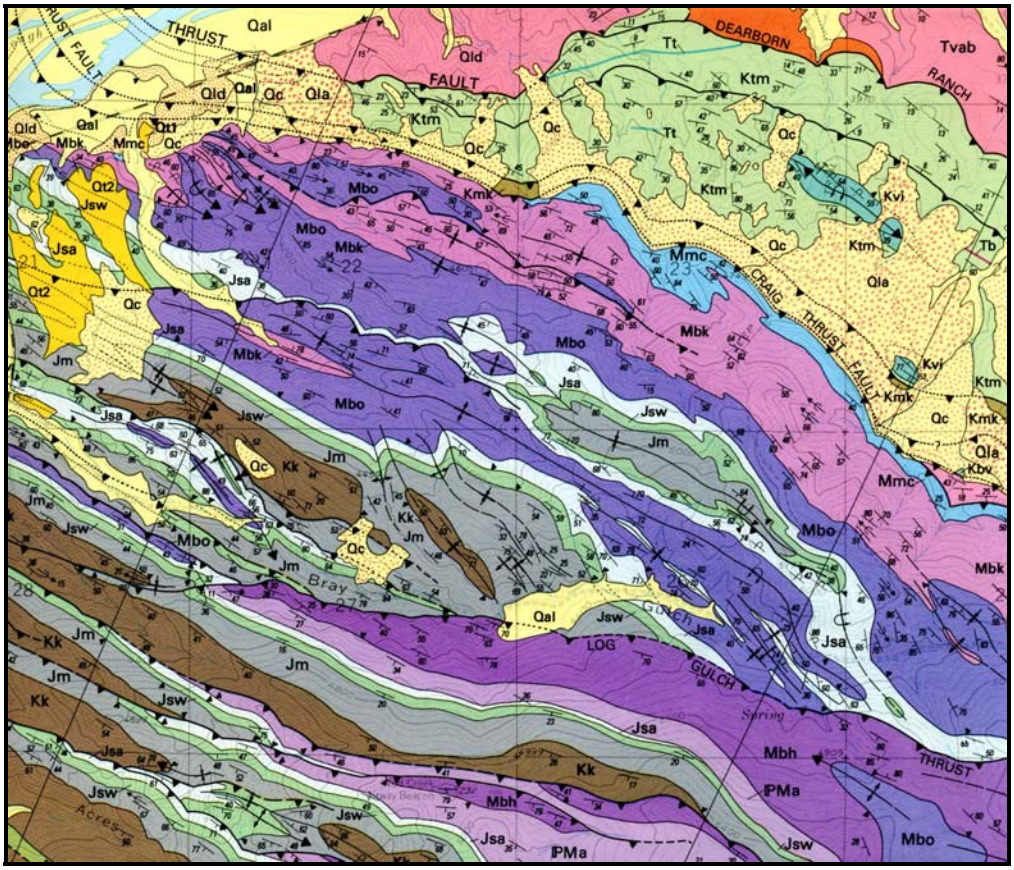
NOTE: If you are a certified First Responder, WFR, or EMT, let your instructors know and bring additional equipment as per your medical rating.

INTRODUCTION TO FIELD MAPPING OF GEOLOGIC STRUCTURES

GEOL 429 – Field Geology

Department of Earth Sciences
Montana State University

Dr. David R. Lageson
Professor of Structural Geology



Source: Schmidt, R.G., 1977, Geologic map of the Craig quadrangle, Lewis and Clark and Cascade Counties, Montana: U.S. Geological Survey GQ-1411, 1:24,000.

CONTENTS

Topic	Page
Introduction	3
Deliverables	4
Constructing a geologic map in the field	4
Procedure	5
Types of contacts	7
Air photos	8
Common symbols used on geologic maps	9
Surficial deposits	10
The issue of scale	10
The importance of thinking	10
Structural measurements	11
Map and cross-section key (explanation)	12
Appearance	13
Written report	14
Field notes	14
Grading criteria	15
Goals to strive for	15
Common criticisms	16
Ethics in field work	17

The author respectfully acknowledges Professor Gray Thompson's unpublished paper entitled "Geologic Mapping" (University of Montana), which was revised and used extensively in the compilation of this handout.

3

INTRODUCTION

Structural analysis proceeds through three linear stages: 1) **description** of the structural geometry of a deformed field area (bedding attitudes, planar fabrics, linear fabrics, folds, faults, joints, etc.); 2) **kinematic** analysis (movements responsible for the development of structures [translation, rotation, distortion, and dilation] and relative timing); and 3) **dynamic** analysis (interpretation of forces and stresses responsible for the deformation). Stage 1, descriptive structural analysis, is the product of careful field mapping.

Although maps are two-dimensional sheets of paper, they portray the geology in three-dimensions. This is because most structures tend to dip or plunge and, therefore, one can infer the direction and degree of dip or plunge through outcrop patterns. Also, we use special geologic symbols to indicate 3-dimensionality on our maps. Therefore, a geologic map is nothing more than the representation of 3-d structures on an arbitrary 2-d horizontal plane. Put another way, a geologic map is a cross-section of dipping and plunging structures projected on a horizontal plane. Clearly, it is necessary to carefully map out this 2-d view before one can visualize the 3-d geometry of deformed rocks. A well-done geologic map can provide a powerful *down-plunge view* of the 3-d structural geometry in a "true" cross-section view that is $\perp$ to plunge.

Field mapping can be physically and mentally challenging. Hundreds of questions arise, dictating that hundreds of decisions must be made during the course of a single day. Where should I go? What unit is this? Why does this bed abruptly end? Thus, field mapping is the ultimate application of the scientific method – a good field mapper is constantly testing predictions about the next outcrop and evaluating multiple hypotheses about the structure. In the midst of this mental workout, it is important to maintain your focus and purpose by remembering the goals of your project or research. Try to maintain a good sense of humor and enjoy the day. After all, didn't most of us decide to go into geology because we like being outdoors and we like thinking about the Earth?

To get started with structural field mapping, here are some tips:

- Eat a good breakfast
- Drink plenty of water throughout the day
- It is humanly impossible to take "too many" strike-and-dips
- In structural geology, accuracy and neatness count heavily!
- Force your mind to think in 3-d; with time and experience, this will come naturally
- Use your time in the field efficiently - always have a plan in the field!

4

DELIVERABLES

Each mapping/structural field project in GEOL 423 requires the following deliverables (i.e., products to be turned in), typically at a designated time/place on the evening of the last day of the project:

- Geologic map – lightly colored and burnished
- Structural cross-section(s) – lightly colored and burnished
- Key or explanation that describes all rock units and explains structural symbols, etc.
- Written report, usually based on a set of questions posed at the onset of the project; some reports may require accompanying stereonets
- Field notebook

In order to accomplish this (on time), it is essential to work during each and every evening during the course of a multi-day project. An evening work plan might be the following:

- Evening 1 – construct your topo-profiles and "boxes" for your cross-section(s) lines; begin work on the key; start to ink your field map; plan your next day (perhaps following a cross-section line)
- Evening 2 – continue to ink your field map; start to make cross-section sketches; continue work on the key; plan your next day
- Evening 3 – continue to ink your field map; finish one of your cross-sections (assuming you have more than one cross-section); make an initial outline of your report; plan your next day
- Evening 4 – continue to ink your field map; finish your second cross-section; spend some more time thinking about your report, particularly how you are going to answer the questions (compile strike-dip data on stereonets); plan your final day to maximize in-filling of your map in critical areas
- Evening 5 – finish inking and coloring your map and key; finalize your report (deadline = mid-evening)

This suggested work schedule would obviously be compressed with mapping projects that span less than five days, so plan accordingly.

CONSTRUCTING A GEOLOGIC MAP IN THE FIELD

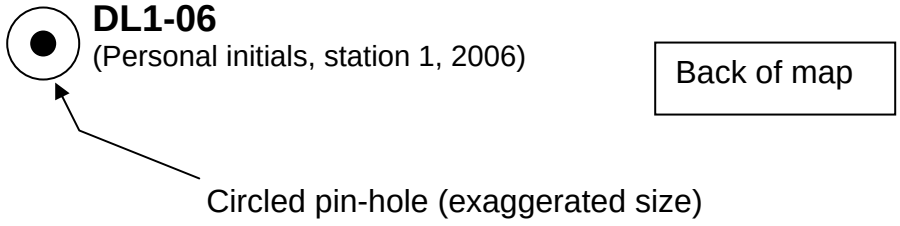
The art and science of geologic mapping involves the accurate depiction of contacts between rock units on a base map of some sort. This is what it's all about – being able to draw a contact on a topo-map or air photo! Obviously, this task is best done in the field where you can visually verify the location of contacts (don't try to "dry lab" a geo-map back in camp). Your ability to construct a reasonable geologic map in the field fundamentally depends on two things. **First**, you must know exactly where you are on a topo-sheet or aerial photo at all times – being lost is simply not an option! **Second**, you must know where you

5

are in the stratigraphic section, which sometimes requires a little scrambling around (this obviously becomes easier with experience in an area). Unless you know where you are and what you're standing on, it is impossible to draw a contact. Therefore, the overriding goal is accurate mapping of contacts and related geologic features (faults, etc.); it is not good enough to depict the "general idea" – we insist on accurately mapped contacts.

Procedure:

1. Keep track of your location on the map or aerial photo continuously as you traverse an area; typically, you will want to plan your traverses perpendicular to strike, thus crossing as many units as possible.
2. Orient the map in the direction that you are traversing: if you are walking east, then you should be looking eastward on the map. Always look ahead to where you want to go next on the topographic map, so when you get there you have already anticipated the topography - *have a plan!*
3. When you encounter a contact between two mappable units, stick a pin through the map at your location, turn the map over, circle the pinhole, and assign a station number to it; then, enter the station number in your field notebook as the heading for entries relating to that map station.
4. A typical station number might be abbreviated in the following manner:



5. Typical notebook entries for a given station might include:
   - Rock descriptions
   - Identification of formations (or other mappable units) at the contact
   - Nature of the contact (disconformity; gradational; fault; igneous; etc.)
   - Strike-and-dip, trend-and-plunge, etc.
   - Estimates of formation thickness
   - Observations on topographic expression of rock units
   - Structural cross-section sketch
   - Stereonet sketch (to help visualize structural data)
   - Sketch of complex outcrop relationships

   (Be sure to distinguish facts/observations from interpretations)

   Good field notes are richly illustrated with clean, clear sketches; one good picture is worth a thousand words!

6. Next, draw the contact on your map as far as you can confidently see it, either on the ground or the air photo (use a thin/sharp pencil with a soft touch, in case you need to erase it). Do not forget the Rule of V's, but

6

don't exaggerate the contact migration in valleys. The contact location on your map should be accurate not generalized or theoretical. Your map IS data.

7. Then move on quickly to the next contact. Remember, try to cover as much ground as possible each day and NEVER plan to return to the same outcrop later – chances are, you never will.

   Also, don't stash your daypack expecting to return to it later. Once you get to a new spot, you may see something that dictates a different route than you planned on. Carry all your gear with you, all the time (this is a basic USGS rule of mapping).

8. To save time and energy, plan your traverse so it crosses the structural grain at a high angle (perpendicular to strike). Work back and forth over an area in a series of traverses, spaced according to the topography and complexity of the geology.

9. Take advantage of hilltops to check your mapping, refine your contacts, refine your traverse route, and predict contacts on the next leg of your traverse. Sometimes in rugged, high mountains, the view from a peak may be your only way to map cliffs, cirque headwalls, and other inaccessible places. In such instances, a good pair of lightweight field binoculars may be your best friend (the so-called "Swiss rock hammer").

10. On your geologic map, depict the hinge lines of folds at the point of maximum curvature and be sure that your strike-and-dip data support the interpretation. **Use medium-weight blue lines for fold hinges**.

11. **Use heavyweight red lines for faults** and apply the appropriate design for different fault types (e.g., barbs in the hanging wall of thrust faults).

7

TYPES OF CONTACTS

There are many different types of contacts between mappable units (refer to geologic map and structure symbols). However, for this field course, three types of contacts will be used to express your level of confidence:

- Solid line = definite contact (you are sure you have located the contact within the line width on your map); sometimes you can show the dip direction and amount with an arrow, as below (intrusive igneous contacts can sometimes dip inwards):



Figure 1. Contact position known well (50 ft on a 1:24,000 map)

- Dashed contact = the contact is reasonably well located, but possibly not within a line width on the map



Figure 2. Contact known with less precision

- Dotted contact = concealed contact (i.e., beneath Quaternary alluvium)

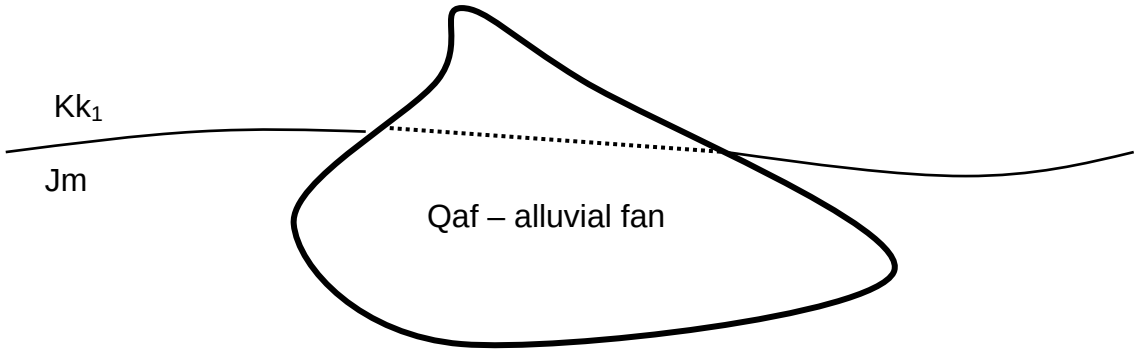


Figure 3. Contact concealed below a surficial unit.

If the rocks are well exposed (as they generally are in field camp), you should be able to draw solid contacts with confidence in most cases. Dotted contacts are certainly permissible where you need to extrapolate a contact beneath Quaternary cover. Dashed contacts should be used rarely in this class because, again, you are mapping some incredibly well exposed areas!

8

Air photos:
When available, air photos can be a great help in locating contacts. Even with black-and-white air photos, contacts can sometimes be clearly seen as tonal boundaries. Just be sure (through ground truthing) that a change in tone corresponds to a mappable contact (formational boundary) and not simply a change in vegetation; if the tone change does correspond to a contact, then you may be able to extrapolate the contact well beyond the area of your traverse and then transfer these data back to your topographic base map. Color air photos work even better for this application! Of course, working with stereo-pairs can assist in visualizing the 3-d relationship of contacts to topography. Be aware that distortion increases on an air photo from the center to its margins, thus affecting the shape of outcrops near the margins of the photo.

When traversing about a field area, pay attention to the plant cover that grows on different rock units. This will assist in your interpretation of air photos.

9

COMMON SYMBOLS USED ON GEOLOGIC MAPS

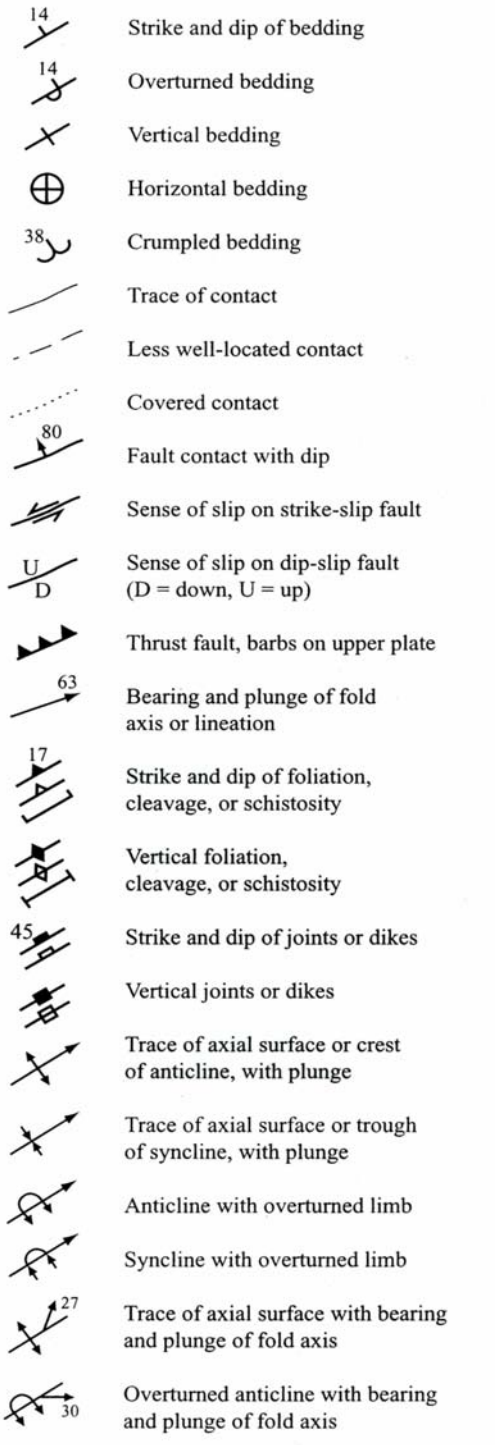


Figure 4. Common symbols on a geologic map (from Rowland et al., 2007, appendix F)

10

SURFICIAL DEPOSITS

Do not get carried away with mapping Quaternary alluvium in every little creek and arroyo; reserve the mapping of Qal for big creeks and rivers with broad, deep floodplains. If bedrock mapping is your goal, then map surficial deposits only where they hopelessly obscure bedrock; alternatively, if your goal is to map surficial deposits, then do not let the bedrock detain you. Do not map surficial deposits as "undifferentiated cover" and do not invent some meaningless designation, such as Quaternary hill wash.

Here is a short-list of some commonly encountered Quaternary deposits that you might need to map:

- Qal – alluvium
- Qaf or Qf – alluvial fan, typically at the base of a range
- Qls – landslide
- Qt – talus (particularly a talus apron at the base of a cliff)
- Qm - moraine

THE ISSUE OF SCALE

The amount of detail you can show on your map depends on its scale – basically on what you have room to draw. You can generally show more detail by resorting to a larger scale, depending of course on the size of the structures in your field area. When selecting a map scale for your field project (something you don't have to worry about in field camp), consider the following:

- What is the goal or purpose of my mapping?
- What scale of structures do I want to "capture" through mapping?
- How much time do I have (is this a reconnaissance project, or can I go slow and map in great detail)?

The typical scale for USGS mapping projects is 1:24,000. At this scale, the USGS rule-of-thumb pace of mapping is one mile^2 per day. For projects involving detailed structural analysis, a better scale may be 1:12,000 and a pace of ~0.5 mile^2 per day.

THE IMPORTANCE OF THINKING

People who wander aimlessly from one outcrop to the next, with no traverse plan, are probably wasting their time. You should always have in mind one or more ***working hypotheses*** that predicts what rocks you will find at the next outcrop or ridge, based on an overall hypothesis about the structure. Geologic field mapping is the ultimate application of continuous hypothesis testing and juggling multiple hypotheses in your mind – the essence of scientific methodology! ***Every outcrop you visit should test one or more hypotheses.***

For this reason, good field mappers are generally very good scientists. The Classic paper *The Method of Multiple Working Hypotheses* by T.C. Chamberlain (1890) explains the benefits of this method in eloquent 19th century scientific prose. The paper is included in this tome for your edification. If you find that you do not have a working hypothesis, it is important to stop and think until you have one. Alternatively, if you find that you are able to consistently predict the next outcrop with ease, don't become too confident and allow your model to dictate the mapping, for Mother Nature has a way of throwing curve balls that can humble even the most experienced field mappers!

STRUCTURAL MEASUREMENTS

Every student in field camp is required to have successfully completed structural geology (GEOL 315 or equivalent from another university). Here are some points to keep in mind:

- Make sure the magnetic declination on your compass is set correctly (based on up-to-date information)
- There are a variety of ways to measure dip and strike with a compass:
    1. Observe an outcrop exposed in three dimensions (most accurate (Compton, 1962, p. 29)):
        - Step back from outcrop 10 feet or so.
        - Move until the bedding surface just disappears.
        - Sight a level line and read the azimuth (Fig. 2A)
        - Maintain position and measure the dip looking along the azimuth line (Fig. 2B).

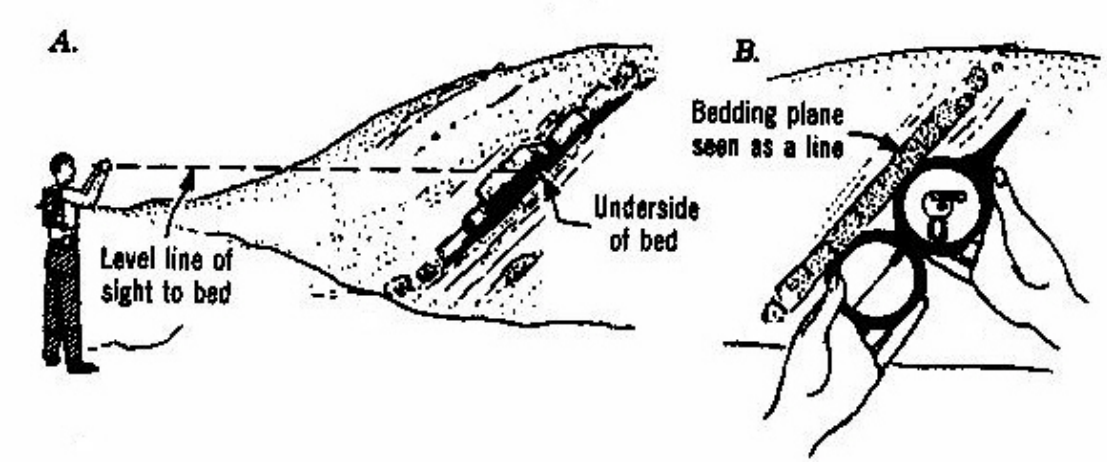


Figure 5. Dip and strike from outcrop 10 feet away (from Compton, 1962, p. 29)

2. On an outcrop (beware of surface irregularities)

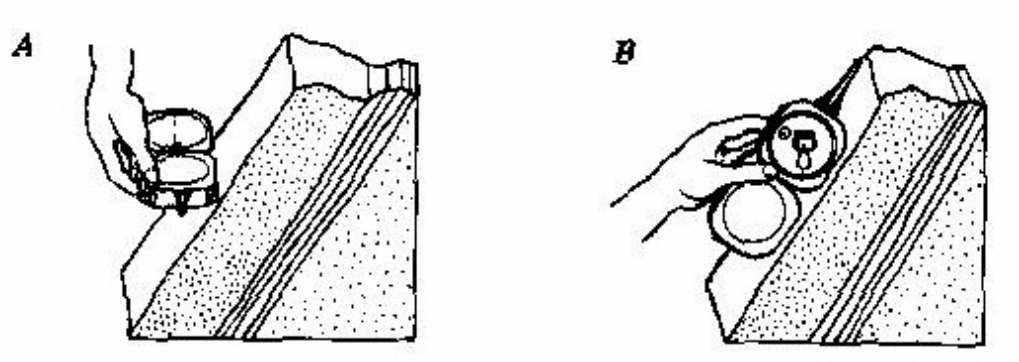


Figure 6. Measurement of dip and strike on outcrop (from Compton, 1962, p. 30).

3. On an outcrop with low dip angle splash water on surface and measure dip parallel to water flow and strike perpendicular to that (Compton, 1962, p. 31)
4. Visually sight a strike-and-dip across an outcrop or across a ravine; these are generally more accurate than measuring directly on an outcrop surface (especially an irregular bedding surface) unless there is a fault in the ravine that offsets the contact.

- For a given outcrop, you and your partner should both take a structural measurement. This provides a quick double-check of your measurement and allows you to take a numerical average, thus accounting for Mother Nature's variability. Your measurements should be within 5^{o} of one another; if not, then find out why.
- With accurate mapping of contacts across topography, you can also determine strike-and-dip through the application of the **three-point method** (three points in space define a plane); this is especially useful for measuring the dip of thrust faults.
- Record a strike-and-dip as: S = 305, 45 SW (always indicate dip direction!)
- Alternatively, record dip and dip direction as: 45, 215
- Record plunge and trend as: 35, 045 (i.e., 35^{o} in the direction 045^{o})
- Never record a bunch of numbers without knowing exactly what they mean; take thorough field notes with lots of structure sketches and stereonet sketches
- Remember, if the trace of a contact (or dike) crosses irregular topography in a straight line, it is vertical or nearly so. If the map trace of a contact follows topographic contours, it must be horizontal. If the map trace of a contact wanders across irregular topography, then it dips!

- One can measure plunge and trend of the hinge line of a fold in one of two ways:
    - Stand on the nose of a fold and take a direct measurement of plunge angle and plunge direction at the point of maximum curvature, or
    - Simply plot strike-and-dip measurements on a stereonet from the limbs of a fold and determine the β-point or π-point (S-pole diagram) – this is the preferred method
- Structure sections should be drawn according to the MSU cross-section formatting rules, with no vertical exaggeration.
- Don't forget Occam's Razor: use the simplest explanation that fits your observed and measured field data.

MAP AND CROSS-SECTION KEY (EXPLANATION)

You will typically be asked to create one key for both the geologic map and cross-section(s). The key should provide the basic information needed to read the map, leaving nothing to guess about. It should be complete, yet concise and very clear. The key should include the following elements:

- The key should be on a separate piece of paper
- Every mapped rock unit should be identified by a colored box that matches the color on the map and cross-section(s), pattern (if used), symbol, and age
- Units should be vertically stacked from youngest at the top to oldest at the bottom
- Show igneous rocks in a separate section of the key (not lumped with sedimentary rocks)
- In some cases, you may be asked to represent stratigraphy as a columnar section instead of colored boxes – but you will receive specific instructions on this
- Each mapped unit should have a brief description adjacent to it, such as color (weathered versus fresh), texture, composition, thickness, outcrop expression, etc. – this information should be gathered by you in the field and recorded in your field notebook
- All structure and contact symbols must have an explanation (faults, folds, strike-and-dip of bedding and foliation, lineations, fold hinges, mine adits and trenches, etc.)
- The key should be specific to the project – it should not include units that do not appear on the map or cross-section

APPEARANCE

Geologic maps, cross-sections, keys, and field notes should please the eye and inform the mind. Always present your work as attractively and professionally as possible.

- Smooth, even, finely drawn ink lines inspire confidence; wavering and uncertain lines inspire doubt. Thick, sloppy lines virtually guarantee a very poor grade on the mapping project.
- Dashed and dotted lines should make smooth, continuous curves, not wayward chicken tracks.
- Lettering should be neat, precise, and easily readable.
- Letter your formation symbols on the map so they read the same way; don't have some upside-down, some sideways, and some right-side-up.
- If you do not have room within the contacts of a unit, place the symbol outside with a thin line connecting it to the unit.
- Be sure the cross section contact location matches the position on the map.

WRITTEN REPORT

We normally require a written report of a page or more on the important geologic aspects of the field area. The written report should be based solely on your own interpretations, not those of your instructors or fellow students. Furthermore, it is unethical to copy and/or slightly modify another student's field report.

- Field reports should address the questions posed in the project handout.
- Reports should not rehash rock descriptions and stratigraphy, unless you are so instructed.
- Reports should not rehash "Laramide history" or some other aspect of regional geology – keep the report focused on the geology of your map area and the leading questions.
- Spelling counts! Use dictionaries (geological and English language)
- The written report should be carefully phrased for the same reason your map and cross-section should be carefully drawn. No one wishes to struggle through a mess of superfluous verbiage and tortured syntax. Nothing makes you look worse than a written report that conveys the impression that you do not comprehend your own map!

FIELD NOTES

Field notes should be neat, clear, well organized, and richly illustrated. They should be written in such a manner that another geologist could easily comprehend what you wrote down. You should be able to pick up your notebook in 20 years and not guess about what your columns of numbers meant (like strike-and-dip). Many agencies (USGS) and companies catalog all field

notebooks as archival records of your work. Your notebooks are part of your legacy, part of your professional reputation. Someone may read your notebook and form an impression of you long after you are gone, or worse, long before you are gone! Therefore, as always in your geologic work, strive for ***high-quality professionalism!***

- Use a bound notebook; two will be required for field camp.
- Use permanent ink or a hard pencil lead that will not smear; it is useful to have two separate pencils, a soft thin pencil for mapping and a harder-lead pencil for notes.
- You should start each day's notes with the date, location, identity of the map and/or air photos you are using, and other pertinent information about the field project (project number, land ownership, township-range-section, GPS coordinates, etc.)
- Basically, organize your notes by station number and GPS coordinates (if you are recording GPS).
- Enter your observations in an orderly manner. Try to be <u>consistent</u> in the order that you write down field data and observations.
- For structural data, it may be useful to place the appropriate structural symbol along the left margin, and then enter the numbers next to it (as a way to keep track of what the numbers represent).
- Consider making a "running" structural section along your line of traverse.
- **Make numerous sketches!** Many students resist sketching in their notebooks on the grounds that they are not artists and therefore cannot draw; if that logic were to prevail, then most could easily resist taking written notes on grounds that they are not published authors. Even a poorly executed sketch depicts ideas with clarity difficult to attain verbally.
- Many noted geologists recommend organizing notes with the left page reserved for writing and the right page for sketching, cross-sections, or columnar sections.
- Keep facts and interpretations physically separate and clearly identifiable.
- If you invent your own abbreviations (as we all tend to do), it is imperative to explain them with a "key" in the back of the notebook. An example might be "RBS" – rocks badly shattered – no one would have the foggiest idea what RBS meant without an explanation.

<u>GRADING CRITERIA</u>

Goals to strive for-

Map: accuracy, neatness, all map units present on the map, proper symbols and use of colors, logical field relationships, sufficient number of stations, and sufficient number of structural measurements.

16

Key: all units and symbols on map and cross-section are also on the key, mapping units in proper sequence (oldest on the bottom), accurate lithologic descriptions, and neatness.

Cross-section(s): consistent with your map, logical structural relationships (admissible), consistent bed thickness, properly formatted, and neatness.

Written report: addresses questions, succinct, correct sentence structure, correct spelling, and overall flow.

Stereonets: neat and clearly labeled, good explanation for each sheet, color or symbol coded if multiple fabrics are plotted on one sheet.

Field notes: organization, orderly presentation of data and interpretations, lots of clear sketches, running cross-sections, columnar sections where applicable, neatness, and overall readability.

PITFALLS

Common criticisms of geologic maps:

1. Inaccurately located contacts
2. Incorrect map symbol
3. Illogical contacts or other map relations (including missing mappable units – mostly commonly Jm)
4. Insufficient number of stations (strike-and-dips); in most field areas, you should easily be able to make at least 20 stations per day
5. Missing or inaccurately located fold hinge line, or the hinge is not drawn through the entire fold at all stratigraphic levels
6. Coloring so dark and streaky that it obscures the map
7. Inked lines too thick and/or not neatly drawn

Common criticisms of keys:

1. Map units or structure symbols missing
2. Poor lithologic descriptions
3. Improper sequence in the stratigraphic column
4. Sloppy lettering

Common criticisms of cross-sections:

1. Inconsistent with the geologic map
2. Inconsistent bed thickness (especially for competent units)
3. Illogical relationships – weak structural interpretation
4. Symbols missing
5. Formatting errors

17

Common criticisms of written reports:

1. Poor writing or spelling
2. Report does not address the salient questions posed at the onset of the project

Common criticisms of field notes:

1. Weak organization and/or lack of neatness
2. Using a pencil that is too soft, resulting in smudges and smears
3. Missing or inadequate sketches of structures and other relevant geologic features
4. Not enough structural data and/or poor organization of measurement data in the notebook
5. Inadequate lithologic descriptions
6. Overall inability to clearly follow what was written down

ETHICS IN FIELD WORK (King, 1977)

You will be required to work with a mapping partner, for the sake of field safety. That does not give you license to copy and plagiarize data. It is fine to discuss where a contact might be, or to compare strike-and-dip measurements to achieve a mean value, or to discuss rock descriptions, or to discuss and debate field relations, but it is not fine to blatantly copy from another student.

- Draw your own contacts on your own map – don't copy someone else's map
- Write your own field notes and do not "dry lab" them from another student in the evening
- Draw your own cross-sections and make your own interpretations
- Treat the land with respect and tread lightly, don't litter, don't carve your initials in rock, and don't break down fences (step through or crawl under when possible)
- *Be honest and set high standards for yourself, in geology field camp and in daily life! Take the ethical high road – it's a better view!*

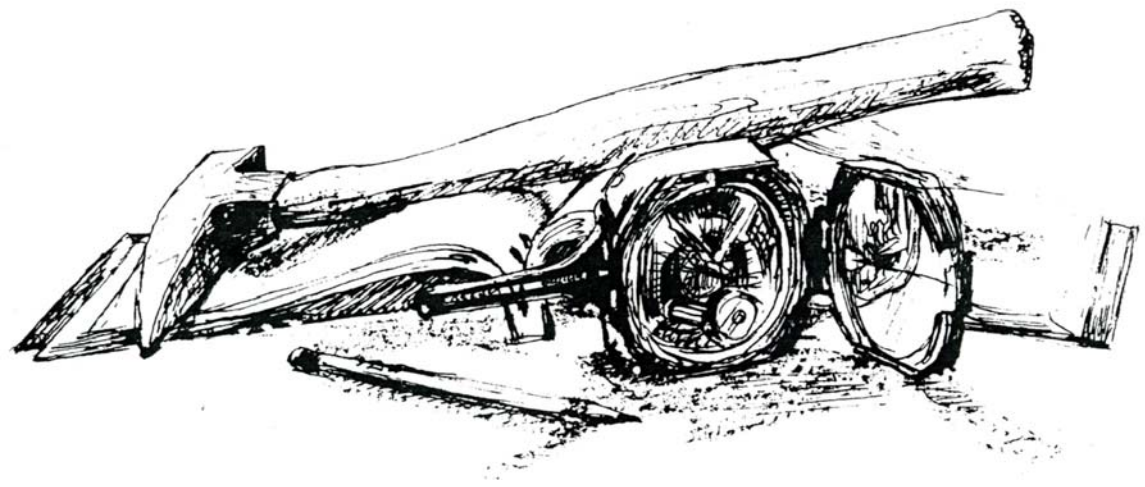
REFERENCES CITED

Compton, R.R., 1962, *Manual of Field Geology*: New York, John Wiley and Sons, 378 p.

King, P.B., 1977, The *Evolution of North America* (revised edition): Princeton University Press, Princeton, N.J., 197 p.

Rowland, S.M., Duebendorfer,E.M., and Schiefelbein, I.M., 2007, *Structural Analysis and Synthesis. A Laboratory Course in Structural Geology* (3rd edition): Oxford, Blackwell Publishing, 300 p.

Chamberlain, T.C., 1890, The method of multiple working hypotheses: *Science*, v. 15, p. 92-97. Reprinted in *Science*, v. 148, p. 754-759 (1965).



midland valley
the structural geology experts



clino Fieldmove

clino pro Fieldmove



iPhone User Guide

Contents

This is a guide to using FieldMove Clino and the **FieldMove Clino Pro** features.

Introduction 2

Disclaimer 3
Important safety note.

Definitions 4
Glossary of terms used in the app and their definitions.

Side Panel 5
Navigation between the app pages.

Compass / Clino 6
Setting a bearing using the compass and recording planar and linear data.

Notes & Images 11
Chronological record of all the data in your project, much like a field notebook.

Map 14
Display the data that has been collected on the phone, import maps and for **FieldMove Clino Pro**, draw on the map.

Stereonet 19
View structural data on an equal area or equal angle stereonet (**FieldMove Clino Pro** only).

Project 20
Details of the active project.

Switch Project 21
Switching between active projects and accessing settings.

Settings 23
Defining GPS, conventions and for **FieldMove Clino Pro** only, line picking accuracy. Contains information of version and acknowledgements.

Export 24
Exporting data, the data format, and how to import data into other software applications.

Digital Compass Calibration 26
Our advice on how to calibrate a digital compass.

FAQs 28
Concise answers to commonly asked questions.

Our Experience 31
Battery life, performance and checks.

System Requirements 33
Minimum platform requirements and other available platforms.

About Midland Valley 34

Introduction



FieldMove Clino is a digital compass-clinometer for data capture on smartphones. The app allows an iPhone or Android phone (see the Android user guide) to be used as a traditional hand-held bearing compass and clinometer for measuring and capturing the orientation of planar and linear features in the field. The field notebook and camera are an integral part of this new technology allowing the capture and storage of georeferenced photographs and text notes. **FieldMove Clino Pro** allows stereonets to be plotted, lines and polygons to be drawn on maps and map symbols to be chosen.

FieldMove Clino supports online Google Maps as well as offline maps as georeferenced MBTile basemaps. Projects can be exported to CSV (.csv comma-separated values), Move™ (.mve) and, with **FieldMove Clino Pro**, Google Earth (.kmz).

This document outlines functionality and recommends workflows to use within FieldMove Clino.

Disclaimer

The use of GPS devices and smartphones as navigation aids

The internal GPS in your device can be used to automatically set location information in the app, which is recorded as latitude and longitude.

Global Positioning System (GPS) devices are commonly used to aid navigation, having grown in popularity over the past decade. Over the last few years, this has extended to smartphones and digital compasses, which are often equipped with GPS functionality.

GPS is a valuable aid to navigation during fieldwork, however it is important to keep safety at the forefront, and we draw your attention to the advice given by a number of mountaineering councils:

"Everyone heading into the hills needs to learn how to read a map, and be able to navigate effectively with a paper map and traditional magnetic compass, especially in poor visibility."

The FieldMove Clino App requires online data transfers for some features (Maps, sharing exported files, etc.). Using such functionality over mobile network services (such as 3G) may incur costs from your provider. If you use the app and services on your mobile phone, you are responsible for any fees that your phone service provider charges for data services, etc. Your phone service provider is not the provider of the FieldMove Clino App.

Midland Valley accepts no liability or loss, resulting from the use or misuse of this product.

Definitions

Terms used in FieldMove Clino

Project
A project is a set of localities, structural data, notes and images related to a specific mapping area. When exporting data it is the whole project that is exported.

Localities
Localities are a way of grouping data and are user definable. For example, localities can be applied to an outcrop or for a new day in the field.

Stratigraphy
User defined list that is used to assign a colour to structural measurements or line objects i.e. to define a rock type or a fault. This information is recorded as an attribute on the object.

Data Type
Defined as planar and linear data. Location can be set automatically using the device GPS.

Comments
These are linked to specific measurements, for example describing in detail the surface where a dip measurement has been taken from.

Notes
Notes are geo-referenced descriptions, such as a sample location or notable change in vegetation. This is akin to the notes taken in a field notebook while mapping. Photos may be added to notes.

Maps
Images can be shown over the online map on the **Map** page. Map overlays can be loaded in as MBTile files.

Side Panel

The **Side Panel** can be opened from any page using the ≡ icon or by swiping from the left edge of the page.

The **Side Panel** allows navigation between the following pages:

Compass / Clino
Take a bearing or record structural planes and lineations with a range of attributes, and create new localities.

Notes & Images
Keeps a chronological record of data captured and allows georeferenced notes and photos to be taken, which can be edited and deleted.

Map
Displays structural data on online and offline maps, and in **FieldMove Clino Pro**, allows line drawing.

Stereonet
Available in **FieldMove Clino Pro**, the stereonet displays data as poles and planes on an equal area or equal angle stereonet plot.

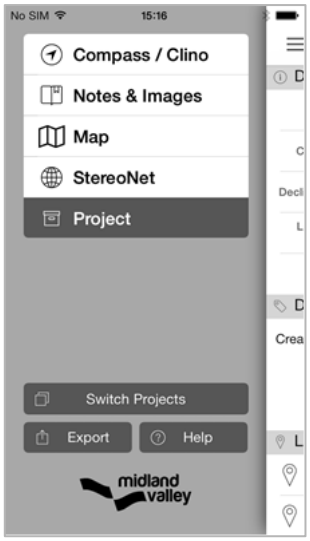
Project
Details of the active project.

Switch Projects
The **Project List** page displays all the projects stored on the phone, allows creation of new projects, and gives access to additional settings and access to import.

Export
Data can be exported as a CSV, Move and, in **FieldMove Clino Pro**, as Google Earth Files.

Help
Access to **Quick Help** or **Extended Help** (this guide).

Side Panel



Compass / Clino

Navigate to the **Compass / Clino** page from the **Side Panel**.

A hand bearing compass or clinometer face will be activated. The active face can be switched between by tapping on the small face.

Note: always give the compass and clinometer a few seconds to stabilize before tapping the clinometer to lock the reading. This will help to ensure the data is consistent.

Compass

To take a bearing with the compass rotate the phone in the desired heading and tap on the compass face. When the phone is rotated a red bar shows the deviation from the set bearing to the current orientation. Tap the compass face again to stop tracking the bearing.

The red arrow on the compass face displays True North and the red outline arrow displays Magnetic North. Declination can be user defined or calculated by the device on the project **Settings** page.

Note: the compass works best when the phone is held level. See our guide on **Digital Compass Calibration**.

Clinometer

The display on the clinometer shows a dip symbol if planes are being recorded or an arrow symbol if lineations are being recorded.

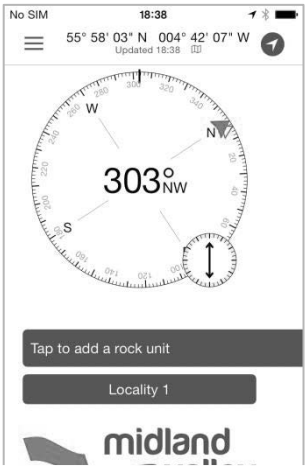
To lock the reading, tap the clinometer face. The icon will change from **red (active)** to **black (locked)**. The reading can be manually overwritten by tapping on the dip and azimuth, or dip and strike numbers for a plane; or plunge and plunge azimuth numbers for a lineation.

To measure the orientation of a **planar feature** the **back** of the phone should be placed flat on the **plane** to be recorded.

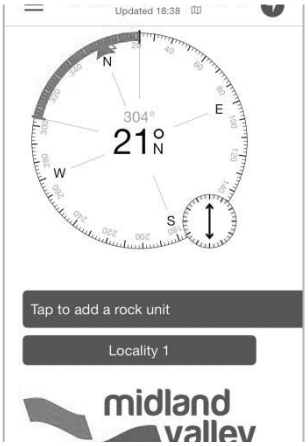
To take a **lineation reading** the long **edge** of the phone should be placed **parallel** to the **lineation,** ideally with the **back** of the phone on the **plane**.

Note: the dip icon orientation corresponds to the phones orientation, not north.

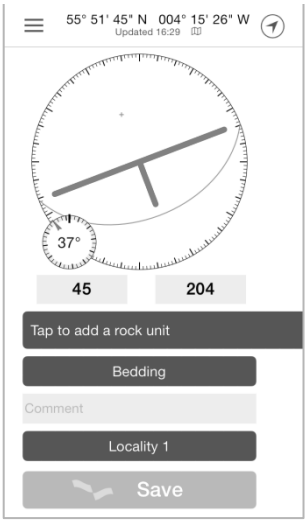
Compass / Clino page



Compass face. Tap to set a bearing.



Compass face. The set bearing is shown by the red bar.



Clinometer face

Compass / Clino

Location

Location is displayed as a latitude and longitude at the top of the page, ①. Below this, the time of the last location update is displayed. The text gives an indication of how the location was set; **Updated** indicates that the location was received from the GPS, whilst **Edited** indicates it was manually set.

Note: UTM co-ordinates are only displayed in the exported data tables.

② **Active** or ⊙ **Idle GPS**

When taking a reading from the **Compass / Clino** or **Map** page an arrow icon is displayed in the top right corner of the iPhone (below the battery icon). There are two modes, **active** and **idle** which can be toggled by tapping on the arrow icon.

Active

The **white arrow with black background** indicates that the phone's GPS is in use, and the current location is being updated. The time stamp in the top bar shows the last time a new position was found.

⊙ **Idle**

The **black arrow with a white background** indicates that the phone's GPS is idle. Any new data point or note will be assigned to the last location update the app received, either from the GPS or set by the user.

Automatic positioning using the GPS and updates

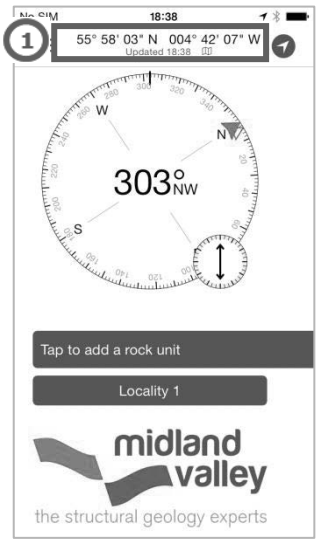
FieldMove Clino uses the iPhone's inbuilt GPS unit for two tasks:

- Finding your location when taking a reading.
- Showing where you are on the map.

In the **Location** page, the last GPS location is shown as a glowing blue dot. The red pin represents a manually set location.

Note: the GPS is constantly trying to update when the circle behind the arrow is black (**active**). This is battery intensive and the **idle** (white background) mode can be used to preserve battery when GPS is not required.

Location



Tap the coordinates ① to open the **Location** page. Long press on the map to set the location manually, the GPS will be set to **idle**



Active GPS ②, last updated GPS position is shown by blue dot and the current location by the red pin

Compass / Clino

Setting location manually

Locations can be set manually without using the GPS functionality, in Degrees / Minutes / Seconds, from the **Compass / Clino** page. On the **Compass / Clino** page tap on the latitude / longitude (lat / long) value in the **Top Bar** this will open the lat / long **Edit Location** page. The current data location is shown by the red pin.

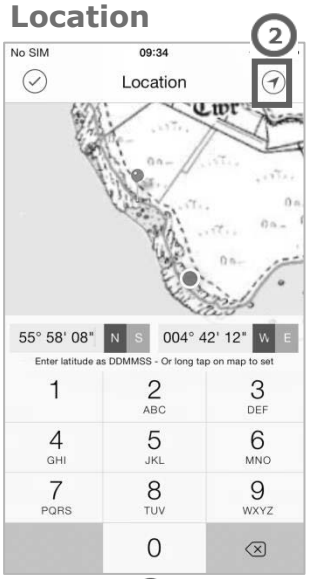
The GPS or current location can be manually overwritten by using a long press on the map to set a new position. This will automatically set the GPS to **idle**. Alternatively, lat / long values can be entered in Degrees / Minutes / Seconds using the number key pad.

If you tap the GPS arrow the GPS will turn on (**active**) and the red arrow jumps to the received location on the map, shown as a blue dot.

Declination convention

Measurements in and exported by the app are given relative to True North. All data is automatically adjusted to True North. True North is calculated using the declination value set in the **Project Details** page.

Location



Idle GPS (2), last updated GPS position is shown by blue dot and the current location by the red pin

Compass / Clino

Stratigraphy
All clinometer readings must be assigned to a unit in the Stratigraphy Column i.e. rock type or object colour, such as a fault or joint. When using the app for the first time, the **Stratigraphy Column** is blank.

① Tap to add rock unit or on the plus icon ⊕ (on pre-existing columns) to open the **Stratigraphy / Rock Types** page. In the **Stratigraphy / Rock Types** page tap the plus icon ⊕ to add new rock units.

② To change the name of a unit, tap on the text to activate the on screen keyboard.

③ To change the colour of a unit tap on the pencil icon ✎ on the right hand side of the page. Select a new colour from the options and tap the tick icon ✓ in the top left corner to apply.

④ Units can be reordered by dragging them to the correct position in the list. To do this, long press on the three vertical dots on the left hand side of the unit. The unit row will expand to indicate it can now be dragged. Move it to the desired location and lift your finger from the screen to drop it.

⑤ Stratigraphy can be imported from pre-existing FieldMove Clino projects or from Move as .csv files. Press the import icon ⍗ to open the **Import** page. Tap the cross icon ⊗ to cancel import.

Note: to change the active unit on the **Compass / Clino** page, tap on the desired unit in the **Stratigraphy Column** on the right hand side of the page.

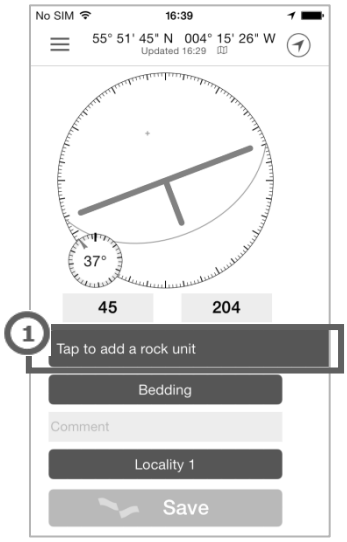
Tap the tick icon ✓ when complete.

Deleting a unit from the stratigraphic column

A rock unit can be deleted from the **Stratigraphy / Rock Type** page by swiping from right to left on the right hand side of the unit. This will display a bin 🗑 icon. Tap to delete.

Locality
To change which locality new data will be created in, tap this button and select the desired locality from the list. Tap the plus icon ⊕ to create a new locality.

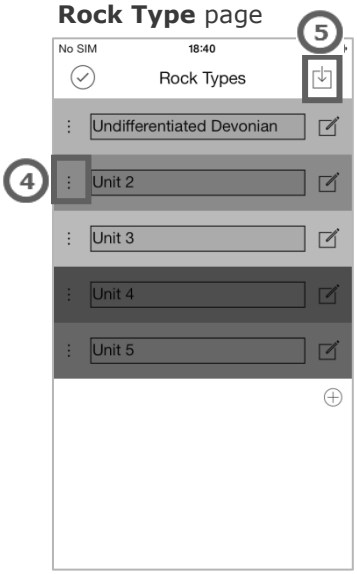
Stratigraphy



Clinometer face



Rock Type page



Units added to Rock Type List

Compass / Clino

Refer to the **Project** section to find out more about the automatic naming of localities, and **Editing Data** for more information on editing locality details.

Data type

① Tap this option to choose between a range of planar and linear data types. Open the **Select Data Type** page by tapping on the current plane or lineation type. Tap any symbol to assign it to the current data or tap above to dismiss.

In **FieldMove Clino Pro** this list can be customized:

Select the **Settings** icon ⚙. This opens the list of currently collectable planar and linear data types.

② Selecting an existing data type allows the icon and name to be edited or the symbol deleted. Any data assigned to a symbol that is deleted will be set to the default symbol of its type. For this reason, the default bedding and lineation symbols cannot be deleted.

③ New icons (icon and name) can be added to the current list by pressing the plus icon ⊕ at the top right hand corner of the **Edit Symbol** page. Press the tick icon ⊘ to apply or the cross icon ⊗ to cancel.

Comments

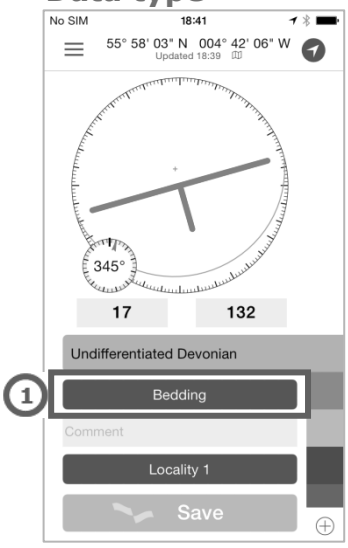
Add a comment which will be saved with the reading.

Save

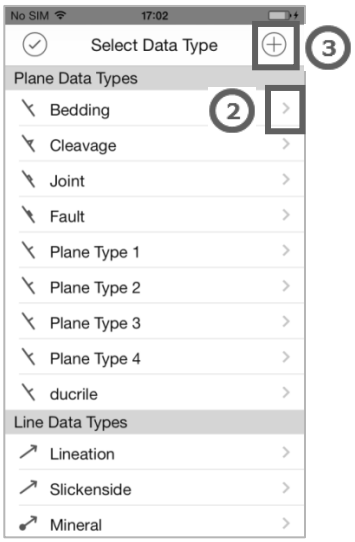
Click **Save** to store the reading which is displayed in the note book and on the map. Make sure the confirmation popup **Saved!** is displayed or the reading will not have been stored.

The **Save** button will be disabled if the clinometer is active or if the stratigraphy table is empty.

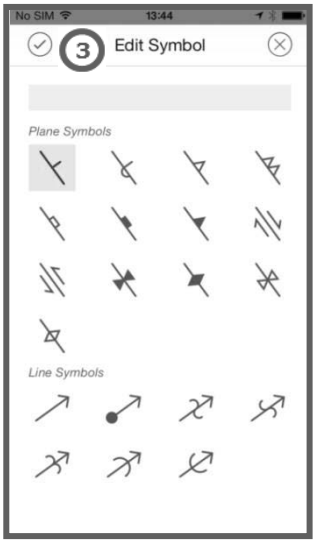
Data type



Clinometer face



Data Type page



Edit Symbol page

Notes & Images

Navigate to the **Notes & Images** page from the **Side Panel**. The **Notes & Images** page provides a chronological record of all the data in your project, much like a field notebook.

Data list
Data is captured from the **Compass / Clino**, **Map** and **Stereonet** pages, and is recorded here under the associated locality in reverse chronological order. Localities are listed in chronological order. However, the active locality will always be at the top of the list.

A summary of each piece of data is shown in this list. Tapping on each item allows the details to be viewed and editing of the fields detailed below. Notes and images can be added to the data list from this page.

Editing structural data

FieldMove Clino does not allow the user to modify existing structural readings; however the rock unit, data type, comment and location can be edited. The rock unit and comments can be edited in the same way as on the **Compass / Clino** page.

When editing the data type, the data cannot be converted from a line type to a plane type or vice versa. Data can only be changed to a different symbol of the same data type. Structural data can be moved by selecting the **Move Data** option. See the **Setting location manually** section for more details on setting locations.

Editing notes and images

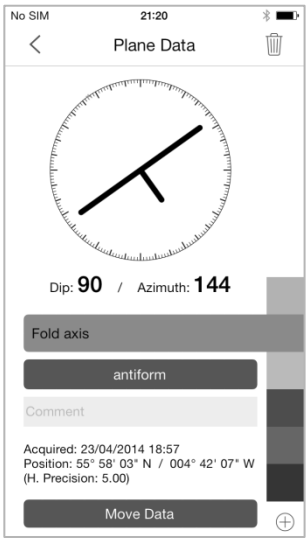
FieldMove Clino allows the user to update the text and location in **notes & images**. The text can be edited by tapping on it. The location can be changed by selecting the **Move Data** option. See the **Setting location manually** section for more details on setting locations. Images can be viewed full screen by tapping the image preview. To return from the full screen view, tap the image once to bring up the tick icon. Tap the tick icon to close the full screen view.

Note: it is not possible to edit an image, or add a new one, after the note has been created.

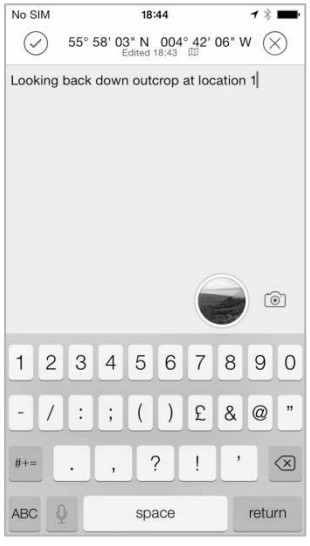
Notes & Images



Notes & Image page



Example of **Edit** page



Note page

Notes & Images

Editing localities

When editing a locality, the user can change the name, description, colour and location. The colour of localities defaults to grey, and has no association to rock units. The colour can by selected by tapping the colour square ① next to the locality name.

The location of a locality can be changed by long pressing at the new location on the map, or by entering the latitude and longitude manually. Refer to the **Setting location manually** section for more information.

Deleting note book entries

In the **Notes & Images** page, orientation data, notes, photographs, line or polygon objects can be deleted by swiping from right to left on the right hand side of the unit. This will display a bin icon. Tap the icon to delete the chosen object. When editing note book entries, tapping the bin icon will also delete the entry.

Filters allow the **Notes & Images** page to be filtered to display **All** data, or just **Notes**, **Datum** or **Lines**. They can be accessed by scrolling to the top of the list (by tapping in the status bar). The active filter will be dark grey. Tap on the filter to apply it to the list.

Screen Options

Side Panel
Refer to **Side Panel** section.

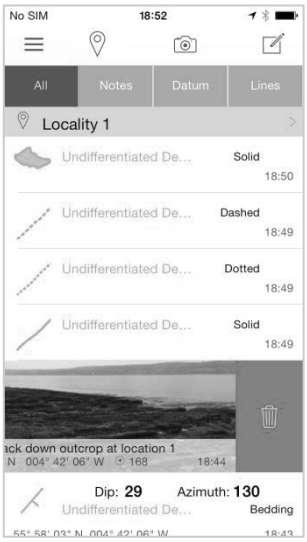
Localities
This displays a list of localities that have been created, and allows the user to create a new one. The currently selected locality is displayed with a tick.

Camera
This option will open up the camera, allowing the user to take a georeferenced photo which automatically records the bearing the camera is facing. Take the photograph by tapping the white circle at the bottom of the display. An option to **Retake** or **Use Photo** will become active. Tap **Use Photo** to keep the image. A page displaying the current location and an option to type a note or description of the photograph will become active. Tap the tick icon when complete. Tap the cross icon to cancel saving the photo.

Edit and Delete



Edit Locality page



Example of **Delete**

Notes & Images

Note

Creating notes allows the user to write longer descriptions which would normally feature in a field notebook. An image can be attached to the note by tapping the camera icon. The image can be selected from the camera roll, or a new photo can be taken. Tap the tick icon when complete. Tap the cross icon to cancel saving the note.

Map

Navigate to the **Map** page from the ≡ **Side Panel**. The **Map** can display the location of all the data that has been collected, as well as **Base Maps** that have been imported into the project.

Navigate around the map by dragging it with a finger. To zoom in, use two fingers pinched together, move them apart to zoom out.

Icons on the map can be selected to display more details, and tapping the ⓘ icon opens the **Edit Data** page.

Screen Options

≡ Side Panel
Refer to **Project Set up and Settings** section.

Locality
Toggle the localities which are displayed on the map from the drop down **Locality Menu**.

Base Maps
Choose which map is used as the base map from the drop down menu. Refer to **Importing Map** section for more information.

Drawing
FieldMove Clino Pro allows lines and polygons to be drawn on the map. Tapping the **Drawing** option activates drawing mode. In drawing mode, lines and polygons can be drawn using a finger. To pan around the map in drawing mode, use 2 fingers pinched together. Drawing mode displays four additional options at the bottom of the map:

Undo
This option allows the user to undo the most recent drawing action. Note that there is no redo option.

Unit colour ① and transparency ②
Tap to select the colour of the line. Each line is associated with a rock unit, so only the colours used in the rock unit list are available. Tap to activate the **Rock Type**.

Long press and slide up to activate transparency. Sliding a finger horizontally over the button will adjust the transparency.

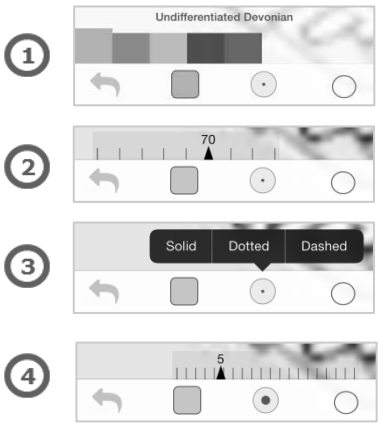
Map



Map page, with satellite overlay displayed. Blue dot shows current GPS position



Drawing options



Map

⊙ to ● **Line style ③ and width ④**
Tap to choose the style of the line. Lines can be solid, dotted or dashed.

Long press and slide up to activate width. Slide a finger horizontally over the button to adjust the line width.

○ or ◉ **Line ⑤ or polygon ⑥ drawing**
Tap to toggle between line (white) and polygon (black) drawing.

Lines can be **extended** or **joined** together. To extend an existing line, tap on it to selected it (it will be highlighted in yellow). Start drawing from the end of the existing line to **extend** it. **Join two lines** by drawing from one end of first line to one end of the second line. Only one of the existing lines needs to be selected.

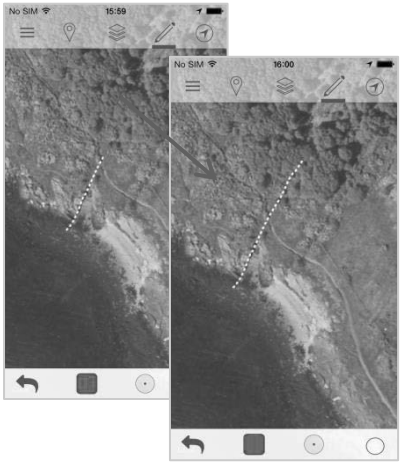
Note: Joining and extending lines is only possible when a line is selected and if they belong to the currently selected **Rock Unit**. **Lines** cannot be closed to create polygons.

Polygons cannot be edited in the current version.

Drawing



Example of line styles



Select line (highlighted in yellow) and continue drawing to extend



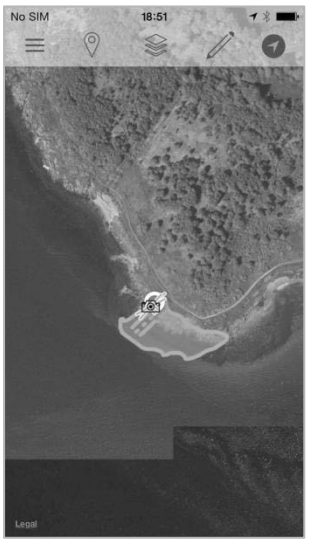
Example of a polygon

Map

Active or **Idle GPS**

When the black arrow is displayed, the map will centre on the current location and will keep your position centred in the map as you move around your mapping area. Tapping again, the map will spin to **show facing direction** . This means the map will be rotated to match your orientation. Tapping the compass again will switch the map back to being oriented with north at the top of the screen.

When the GPS mode is active, any new data point or note will be assigned to the last updated location provided by the sensors.



Map Page with **Active GPS**



Map Page, showing facing direction

Map

Changing Maps

Maps will show either the satellite or the road map of the current area. To change the map display, touch the **Maps** icon and select the map so that it has been ticked. This chosen map will now display in the **Map** page over the iPhone's default map.

You can also import your own overlay map using MBTiles files (see below). The imported maps will show in this list and you can tap a filename to select it. Only one overlay map can be displayed at a time. Overlay maps will be displayed over either the satellite or the road map (which ever was active last).

To view the image in a project, navigate to the **Map** page:

① Tap the **Base Maps** icon.
② Select **Edit Base Maps**.
③ All the maps that are added to the FieldMove Clino **Documents** folder, via iTunes, will be listed here as **New Maps**.
④ Tap on the ⊕ icon to add the selected map to the current **Project Map List**.
⑤ Tap on the icon to add maps to the **New Maps** list from iTunes.

If you tap on the currently active overlay map, the map view will zoom to fit the extents of that overlay.

Loading Maps

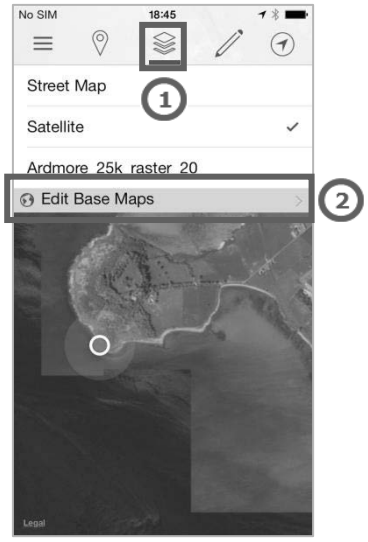
Maps (which may contain geological, topographic and geophysical information) can be imported into FieldMove Clino as MBTiles which are created from georeferenced images (GeoTIFF, JPEG 2000, KMZ etc.).

There are a variety of programs that can perform the conversion of georeferenced images into MBTiles, including:

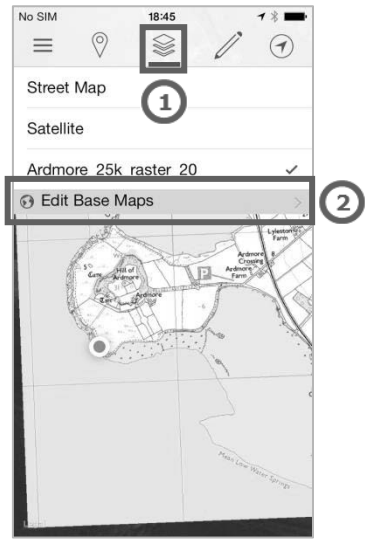
- Move2014 (http://www.mve.com) [Windows/Mac OS X/Linux]
- Global Mapper [Windows]
- Map Tiler (free demo available) [Windows/Mac OS X/Linux]
- Arc2Earth plugin for ArcGIS [Windows]

Note: Make sure the image you use has a high enough resolution for the scale of mapping being performed. In

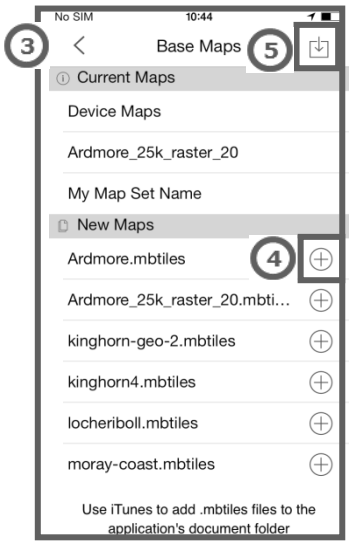
Viewing Map Overlays



Satellite display



MBTile overlay



MBTile loading

low resolution files the higher you zoom in, the more distortion will be seen in the image.

Note: MBTiles files are locked at a minimum and maximum zoom level. Each zoom level increases the magnification by a factor of two, and as a result the size of the MBTiles file approximately increases by a factor of two as well. This means that low zoom level files take up less space on the phone, but not as useful for mapping as higher zoom levels. Be wary of the file size when increasing the zoom level beyond 16, as the file size grows exponentially.

Zoom Level	Metres / pixel
1	78272
2	39136
3	19568
4	9784
5	4892
6	2446
7	1223
8	611
9	306
10	153
11	76
12	38
13	19
14	9.6
15	4.8
16	2.4
17	1.19
18	0.6
19	0.3
20	0.15

Guide to zoom levels

Exporting MBTiles from Move2014

To export an MBTiles file from Move first make sure you have an image present in a georeferenced .move file. Select the image and click the right mouse button. Select the **Export As** option then **Export MBTiles**.

The **Set MBTiles Properties** dialogue box will appear. Select the **Minimum Zoom Level** and **Maximum Zoom Level**. An **Estimated Output** number of tiles and the size of the file will be displayed. An MBTiles file will be exported to the chosen location.

For topographical maps, a scale of 1m/pixel will produce a very large file with a scale that will show paths, streams etc. For satellite images, a scale that fits the resolution of the satellite is suitable. For geological maps, finer resolution than the map itself may be more suitable as this will allow high levels of zoom. It is also worth making all the small zoom levels available (typically a zoom of above 1:2,000,000). This will ensure that the image can be seen in relation to the global map, and will only take up a small amount of the phone's memory. It is worth taking some time to experiment with the scale of the map before going into the field.

Import MBTiles files into FieldMove Clino

Once images are saved in the MBTiles format, they can be added to the FieldMove Clino **Documents** folder via iTunes.

In iTunes, to add the files to the documents folder, select the **Add...** button at the bottom of the right-hand column, and navigate to where the maps are stored. This process will need to be repeated if maps are stored in different locations on your PC.

Stereonet

The **Stereonet** page in **FieldMove Clino Pro** allows the user to view structural data on an equal area or equal angle stereonet. The user can use filters to display a subset of the collected data.

Mean Dip / Azimuth
This option displays the **mean resultant plane** of all the planar data visible on the stereonet. The switch toggles whether the plane and pole are visible on the stereonet. The mean resultant plane is displayed as the thicker black pole and great circle.

① Display settings
There are three display settings to choose from, **Poles**, **Plane**, or **Both**. Tap one to activate it. The active display setting is shown as dark grey.

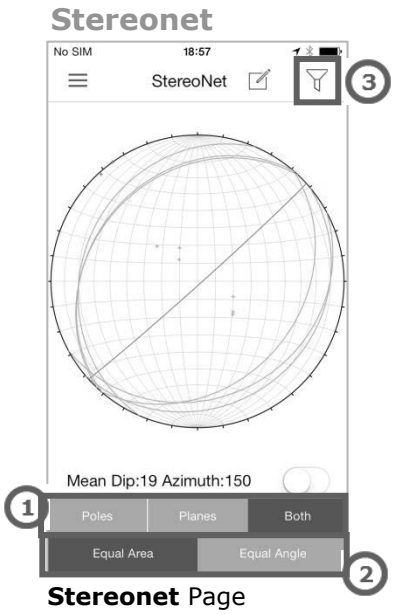
② Stereonet plot
There are two settings to choose from **Equal Area** (Schmidt Net) and **Equal Angle** (Wulff Net).

③ Filter
Choose the data to be displayed. Individual data points can also be toggled on or off. A tick within a black circle ✔ indicates the data is being displayed.

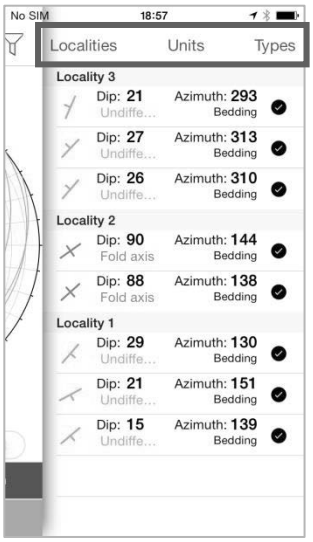
Data can be filtered by locality, unit or type by selecting the relevant data type. **Localities** allow the user to toggle visible localities; **Units** allows the user to filter data by specific rock units; and, **Types** allows the user to filter data by planar or linear data types.

≡ Side Panel
Refer to **Side Panel** section.

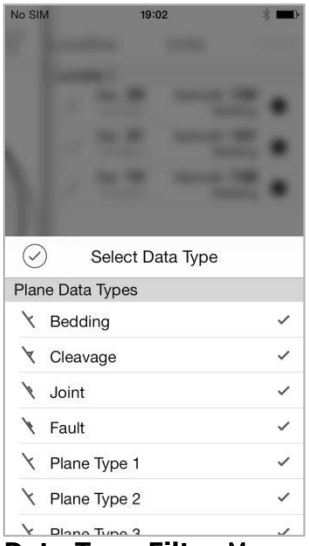
Notes
Save an image of the stereonet to the **Notes & Images** page.



Stereonet Page



Data Display Page



Data Type Filter Menu

Project

Locality Prefix
By default this is **Locality** #. Changing the locality prefix changes the default names given to localities when they are created. The hash (#) indicates the position of the number in the name. If it is excluded the locality number will just be appended to the prefix given.

Folder
Where to find the folder your project is stored in when you connect your device to a computer.

Description
Add a description of the project. By default it will give the creation date and the name of the device it was created on.

Localities
A list of the localities defined in the project, with creation date and time. Localities can be deleted by swiping to the left on the locality.

Deleting a locality

Locations can be deleted from the edit location page accessed from the notebook, as well as swiping from right to left on a locality in the **Project Details** page. Note that the active locality cannot be deleted. Change the active locality from the **Compass / Clino** or **Notes & Images** pages.

Delete Project

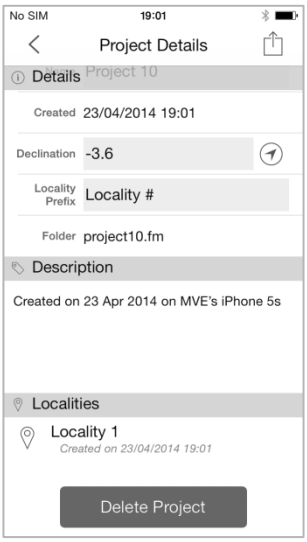
This will permanently remove the project from the device. See **Switch Project** section for more details.

Note: this option is only available when opened from the **Switch Projects** page.

Project Details



Project page opened from the **Side Menu**



Project page opened from the **Switch Projects** page

Switch Project

The **Projects List** page lists all the current projects stored in the phone.

There are four button options at the bottom of this page:

App Setting
Turn the **GPS on and off**, define the units, set the **Angle Convention** and in **FieldMove Clino Pro**, the **Line Picking** accuracy. The **Version** and **Acknowledgments** are also available from this page. See the **Settings** section (below) for more information.

E-mail feedback
We are still developing this app and are always keen improve our products so please let us know what you think and if you have any wishes for future development.

Import
Projects can be re-imported to the iPhone after they have been copied onto a computer. This includes projects created on the Android version of FieldMove Clino.
To import a project from a computer to the iPhone, follow the steps below.

First find the .fm folder saved onto your computer and use Zip to create an archive, as iTunes does not handle moving folders directly to an iPhone. Once zipped, bring the zip file across and extract it on the phone. Plug the iPhone in so it is linked to iTunes. Go to the app page in the iPhone folder and find FieldMove Clino. Now drop the .fm.zip file into the app directory. Once this is finished copying across to the app, eject the iPhone.

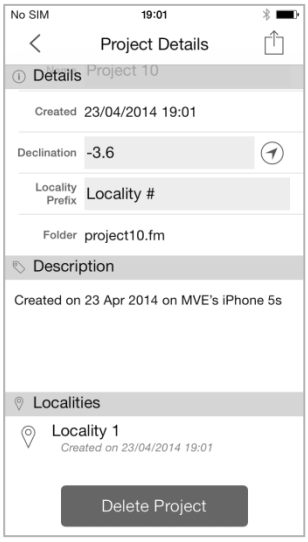
Open up FieldMove Clino on the iPhone and navigate to the switch projects page. Tap the import button at the bottom. A list of .fm.zip files that are present on the phone will be shown. Tap on one of those files to un-archive it. The app will automatically unzip this and, if successful, add the project to the list of projects on the phone.

Please note that while the import will not overwrite an existing project, it does not ensure the project name not already in use. This may lead to several projects having the same name. In the list of .fm.zip file, swipe to delete archives that are no longer needed.

Switch Project



Project List page



Project page opened from the **Switch Projects** page

Switch Project

⊕ **New Project**
Create a new project, this opens the **Project Details** page.

Deleting a Project

To delete a project, navigate to the **Switch Project** page and select the information ⓘ icon for the project you wish to delete.

This will display the project details. Scroll to the bottom and select **Delete Project**. This will remove the project from the device.

Note: you cannot delete an active project. To delete the active project, you will have to switch to another project, and then return to the project details from the **Switch Project** page.

Settings

The **App Settings** ⚙ gives options for:

Location Services
Turns GPS functionality on and off. Turning off saves battery, but be wary that the location won't update when the GPS is turned off.

Unit
Metric or imperial units can be displayed when an elevation reading is available.

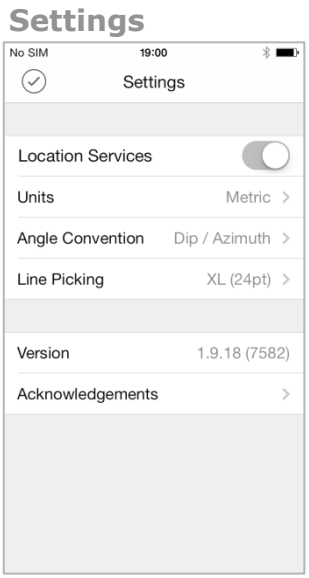
Angle Convention
Choose between **Dip / Azimuth** (default) or **Dip / Strike** for the right hand rule (RHR). Both conventions are used when the project is exported.

Line Picking
In **FieldMove Clino Pro**, define the sensitivity that should be used to select a line in the **Map** page. With a larger setting it will be easier to extend lines but picking will not be as accurate.

Version
The version of the app currently installed on your iPhone. Please provide this information along with your operating system when reporting bugs.

Acknowledgements
This lists copyright notices for the third party software libraries used by FieldMove Clino.

Tap the tick icon ✓ when complete.



Settings page

Export

Projects can be exported by selecting the export option from the **Side Panel** or **Project Details** page. Data can be exported as:

- CSV (.csv);
- Move (.mve);
- Google Earth (.kmz) in **FieldMove Clino Pro**.

Tap the selected file type to export the data. The operation can be cancelled by tapping **Cancel** on the progress pop-up.

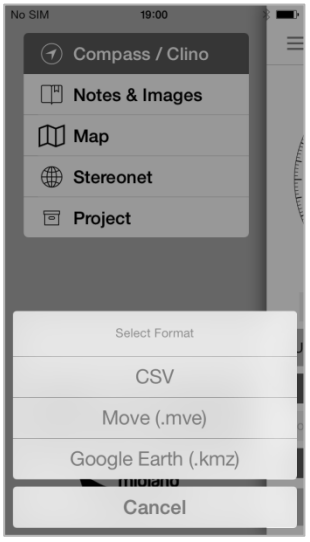
Note: exporting a project with a large number of pictures and data can take some time.

Once the export is complete, an option to **Share** data is available on pop-up box. Data can be shared by:

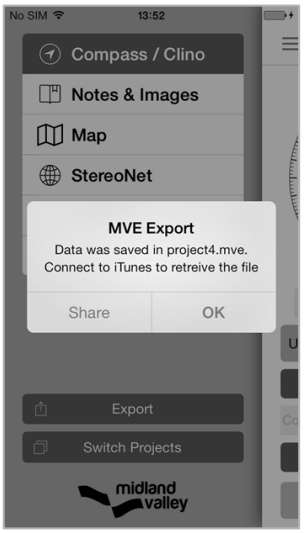
- **AirDrop** – share data wirelessly with another Apple device.
- **Mail** – email the exported project as an attachment. Be aware that large projects may be too big to attach to an e-mail.
- **Dropbox** – This will let you upload the exported file straight to Dropbox. This requires network connectivity. The first time, you will be asked to grant permission so that FieldMove Clino can access your Dropbox. This will be done from the Dropbox app if it's installed, or otherwise via a web interface.
  You can then browse your Dropbox folder and press **Choose** when you are ready to upload the file. Please note .kmz and .mve files can be quite large if you contain images.
- **Open In** – open exported data in another installed app. For example. The **Google Earth** (.kmz) export can be directly opened in the Google Earth app if installed.

Exported CSV files will be stored in their project folder, whilst Google Earth or Move exports will be located in the documents folder. To access this data connect the phone to iTunes on a laptop or desktop PC. Select the device from the iTunes toolbar and choose Apps from the device option panel. The device may need to be synced to see these options. Scroll down to the list of apps and select FieldMove Clino. A list of associated documents will appear on the right-hand column. Select the files to copy from the iPhone and click **Save to**.

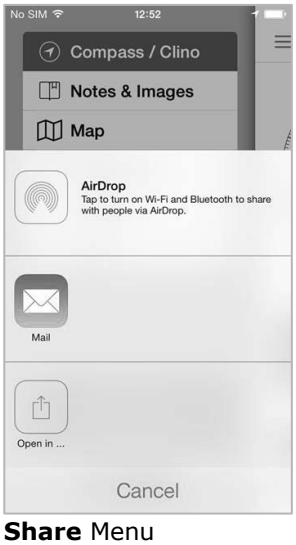
Exporting Data



Export Menu



Share pop-up option



Share Menu

Export

Opening exported projects

CSV files are comma delimited and store georeferenced point data and photo locations. The first line of each file gives the column titles. Each .csv file contains a single data type, and is named as such. For example, all localities are saved *localities.csv* and plane data is stored in *planes.csv*. Whilst localities and their data are stored in separate files, they can be easily cross referenced using the **localityId** which is assigned to each locality and data point. CSV files can be imported directly into many GIS software packages as CSV/ASCII data. Files can be viewed quickly by opening them in simple text editors such as Notepad, or spreadsheet software such as Excel. Note that images are not exported in the CSV export. Instead the geographic location of each photo is found in the image CSV file, along with the name of the image file. All images can be found in the **images** folder, which is stored in the project folder on the iPhone.

Note: CSV files do not contain lines or polygon information.

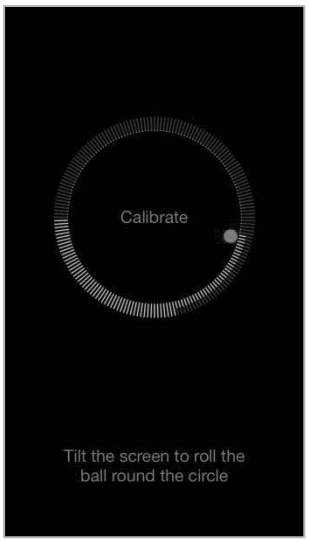
Move files (.mve) can be opened directly in Move. Move is designed for 2D and 3D model building, interpretation and validation in 4D. You can also load .mve files into FieldMove for digital mapping on a tablet PC, or into Midland Valleys free 3D visualization software - MoveViewer.

Note: When importing the data into Move it is advisable to set up the projection in a new document and insert the .mve file into this new document. Doing so avoids UTM calculation issues and misplaced data for larger spanning projects. This process will also flag up any UTM calculation issues on the import summary and is a good check of data location / projection validity.

KMZ files can be opened in Google Earth.

Note: KMZ files do not preserve line style.

Digital Compass Calibration



Most new smartphones contain electronic magnetometer, gyroscope, and accelerometer chips that, either individually or when combined, provide orientation information about the device. These electronic components vary in quality and are subject to a number of limitations. For example, magnetometers can be strongly influenced by the magnetized iron, steel or other permanent magnets in the device (the hard iron effect), as well as being influenced by external magnetic material in the natural and built environment. Gyroscopes often suffer from gyro-drift – an error caused by the accumulation of the unique bias present in each gyroscope. We can counteract these limitations by attempting to calibrate the sensors, or using a combination of their output data to provide an improved result.

However, some smartphones perform more consistently than others. This variation between devices can be caused by:

- differences in phone hardware and firmware
- differences in the built-in noise filtering and sampling frequency
- the different sensor combinations (sensor fusion) or compensation algorithms

There are also differences between the mobile operating systems and how they allow developers to access and manipulate the sensors available on each device.
We are reluctant to recommend specific devices to run FieldMove Clino, however there are significant variations in the quality of the components that are currently being used by the various manufacturers, and we feel strongly that we should make users aware of some of our recent findings.

Calibration for iPhones

The iPhone 4S, 5 and 5C contain good quality components and the compass readings are generally accurate to ±1 degree – better than can be achieved with a traditional hand-held Brunton or Silva compass. Unfortunately the magnetometer/gyroscope/accelerometer combination in the iPhone 5s is of lower quality and the compass is only accurate to ±5 degrees. This is a known issue which has been widely documented online and in the press. Apple have produced a firmware fix for this issue but we have not yet had the opportunity to test the device with the installed update. To calibrate, Apple phones display a black screen with a small red ball that must be rotated within the confines of a graduated circle. The compass clinometer within FieldMove Clino will not become active until this operation has been performed.

Digital Compass Calibration

We have found that some devices do not correctly report inclination. This is obvious when a device is on a flat horizontal surface, yet FieldMove Clino still reports a dip. We believe this is due to components in the device not being seated properly, as we have tested other devices of the same make and model and not observed any problems. To counteract this, we have added an accelerometer calibration option in the app settings. In all cases, calibration resulted in devices correctly reporting inclination.

To get the most out of your smartphone we recommend that you collect data with the device in a variety of orientations and compare this against a traditional hand-held compass clinometer to work out the best orientation to collect data in. Many Android devices work better when held against the rock in landscape mode (long-axis horizontal) rather than in portrait mode (long-axis vertical). When measuring lineations, some Android phones will only record sensible measurements of plunge azimuth in one orientation - when the device is held with the top of the screen pointing down- or up-plunge depending on the manufacturer. This does not seem to apply to the iPhone (all models) with good data being recorded irrespective of the orientation of the phone.

These questions may help you:

- Does the phone have reasonable consistency with itself in all orientations and situations?
- Does the phone have reasonable consistency with a control analogue compass-clinometer in all orientations and situations?
- Are there any orientations (e.g. device long-axis vertical or horizontal) that provide more consistent and accurate results? If so, make sure to collect data only in these orientations.

As with an analogue compass, be aware of sources of interference. This can come from magnets, ferrous metals, electronic devices, another analogue compass or electronic device, watch or phone case (beware of magnetic clasps) to name a few.

..and finally

FieldMove Clino is designed to make data collection quick and easy, facilitating the collection of large, statistically valid data sets. We have found that there are tremendous advantages to using FieldMove Clino on a well-calibrated smartphone. Most users will have experience with traditional analogue devices, where often a single reading at each station is taken with the assumption that each of these readings will have a high level of both precision and accuracy. This assumption is normally wrong. We always recommend taking several readings at each location, which can then be treated statistically to provide both improved accuracy and an understanding of measurement error.

Frequently Asked Questions

How do I load a base map?

Base maps can be loaded into the app as MBTiles files. Use iTunes to import the MBTiles file into FieldMove Clino. Base maps are added to a project from the **Edit Base Maps** option in the **Map** page. The active base map can be selected from the base map list and is indicated with a tick.

Refer to the **Maps** section for more detailed information.

How do I change the project name?

The project name can be changed on the **Project Details** page, which is accessed from the **Project** option in the **Side Panel**, or by tapping the information icon in the **Switch Project** page.

Refer to the **Project** or **Switch Project** sections for more detailed information.

How do I set a bearing?

Navigate to the **Compass / Clino** page. If required activate the compass by tapping on the small compass. Tap the compass face to set the bearing, deviations from this set bearing will be displayed by a red bar. To stop tracking the bearing, tap the compass face again.

Refer to the **Compass / Clino** section for more detailed information.

How do I take a reading using the Compass / Clino?

Planar or linear readings are taken from the **Compass / Clino** page. If required, activate the clinometer by tapping on the small clinometer to the right of the compass face. At least one rock unit is required before taking a reading, so select the **Tap to add a rock unit** option first or select the rock unit you wish to assign to the data you are about to collect. Set the **Data Type** to be collected from the list of planar or linear types. The clinometer page will update to reflect the **Data Type**.

To measure the orientation of a **plane**, the **back of the phone** should be placed on the surface to be measured. To take a **lineation reading**, the **edge of the phone** should be placed along the lineation, preferably with the back of the phone on the surface – but this is not essential.

To lock the reading, tap the clinometer face. The display will change from **red (active)** to **locked (black)**. Check the location reading and associated properties, unit type, locality and add an optional comment before tapping **Save**.

Refer to the **Compass / Clino** section for more detailed information.

How do I create a georeferenced note?

In the **Notes & Image** page select the **Note** icon to take a georeferenced note.

Refer to the **Notes & Images** section for more detailed information.

Frequently Asked Questions

How do I take a georeferenced photo?

In the **Notes & Images** page select the **Camera** icon to take a georeferenced photo. If you want to insert an image as a georeferenced image, use the camera option within the **Note** page.

Refer to the **Notes and Images** section for more detailed information.

How do I view and edit recorded data?

All data can be viewed in the **Notes & Images** page, which can be opened from the **Side Panel**. In **FieldMove Clino Pro** data can be filtered and displayed on a stereonet. Data can also be viewed on the **Map.**

Refer to the **Notes & Images** section for more detailed information.

How do I change a locality name?

Locality names and positions can be changed on the **Edit Locality** page, which is accessed from the **Notes & Images** or **Project** pages. Tap on the locality in the list to open the **Edit Locality** page.

The name of future localities can be set by changing the **Locality** Prefix in the **Project Details** page, accessed from the **Side Panel.**

Refer to the **Notes & Images** or **Project** sections for more detailed information.

How do I delete data?

The **Project** can be deleted from the **Switch Project** page. Active projects cannot be deleted. Switch projects to delete an active project. **Rock Units** can be deleted from the **Rock Types** page. **Localities** can be deleted from the **Notes & Images** page or the **Project Details** page. Notebook entries can be deleted from the **Notes & Images** page.

Swiping from right to left on an item will display the **Delete** icon.

Refer to the **Compass / Clino, Notes & Images** or, **Project** sections for more detailed information.

How do I export the data?

Data can be exported in CSV, Move and Google Earth file formats. The export option is accessed from the **Side Panel** and **Project Details** page.

Refer to the **Export** section for more detailed information.

Frequently Asked Questions

How do I use FieldMove Clino offline?

FieldMove Clino requires online connectivity for the basic maps (satellite or street views) and for accessing Dropbox. If you disable online connectivity, the map view will still work but will only show a basic grid in places where there is no cached data. Please note that activating airplane mode will also turn off the GPS. To disable online services but preserve the GPS, please navigate to the **Settings** page and disable **Cellular Data**.

Refer to the **Settings** section for more detailed information.

Our Experience



Collecting data on folded Devonian sediment at Ardmore Point

The following comments are based on our experience of testing FieldMove Clino with an iPhone 5 running iOS 7.

Hardware

Battery can last for a full field day (~8hours, with the GPS on but when other apps and data streaming are turned off). This is highly dependent on the phone and we recommend experimenting with your phone to get the best out of usage time.

When your iPhone is locked, the GPS will become inactive and will not drain the battery.

There are plenty of tough cases and water proof pockets on the market that project the phone and make it waterproof and robust, such as LifeProof, Idry, Aquapac etc.

Preparation

A common hindrance to successful digital geologic mapping is a lack of advance preparation before leaving for the field. In addition to collation of digital base maps, elevation models, and existing geologic maps, the most important aspect of preparation is practice using the software and hardware tools. As with any compass, orienteering, and basic mapping skill, advance practice ensures that the mapping device is not the focus of the user's attention, leaving the field mapper to focus on 3D spatial analysis of rock units. We find that these issues are relatively easily overcome with advance planning and training, as well as an appreciation for the potential benefits of digital field mapping.

We recommend testing and calibrating the phone against a compass before going to the field. See our guide on **Digital Compass Calibration**.

Our Experience

Things to watch out for when mapping with a smartphone

1. Make sure that you **lock** your iPhone **when it is in your pocket**. This will ensure that you don't end up with 'ghost' readings while you're en route to the next outcrop.

2. Check that the **GPS location has updated** to your current location, **before saving** a reading. Look at the time stamp (underneath the lat / long values) and check that this has the lat / long values for your current location. If you are still unsure if the GPS has placed you correctly, tap the lat / long reading (this will bring up the Map page) where you can check that your current location is correct on the map.

3. Make sure that your iPhone has **enough storage space** for a day's data collection. We recommend that, at the end of each day, you copy your files from your phone to your PC and back these up. You can then delete the project from your phone and start a new project, to free up memory. To put a project back onto your iPhone, simply paste it from its saved location on your PC into the app folder through iTunes.

4. At the start of the day, **check** your phone's **calibration** before taking a reading. Make sure that you are away from buildings, cables, vehicles and jewellery and compare the readings from your iPhone with a traditional compass-clinometer.

5. Take care to check that you have made the **right lithology and structure type** choices before hitting the **Save** button. It is very easy to collect incorrectly classified data, which cannot be used later (e.g. you have recorded a cleavage measurement as bedding or vice-versa).

Note on the geology of Ardmore Point

All the screen shots and photos in this guide are taken from Ardmore Point which is approximately 30km north-west of Glasgow. The strata exposed on the shore are Devonian in age, with excellent antiform and synform structures, faults and fractures with exposures of the Lower and Upper Old Red Sandstone. We frequently run training course at this location and other sites. Please get in touch if you would like to join us to learn more about digital field mapping from the experts.

Closing remarks

We find that digital mapping tools improve the 3D spatial interpretation process by facilitating more analysis and less data management than traditional techniques, especially in the "field office" during the evenings. With a digital mapping workflow, data organisation largely occurs in the field upon data collection, transcription from paper to digital format is unnecessary, and data backup can be as simple as copying digital files to external hard drives. Digital mapping allows more time in the evenings for problem solving, targeting areas of uncertainty, and formulating effective field plans.

The Method of Multiple Working Hypotheses

With this method the dangers of parental affection for a favorite theory can be circumvented.

T. C. Chamberlin

As methods of study constitute the leading theme of our session, I have chosen as a subject in measurable consonance the method of multiple working hypotheses in its application to investigation, instruction, and citizenship.

There are two fundamental classes of study. The one consists in attempting to follow by close imitation the processes of previous thinkers, or to acquire by memorizing the results of their investigations. It is merely secondary, imitative, or acquisitive study. The other class is primary or creative study. In it the effort is to think independently, or at least individually, in the endeavor to discover new truth, or to make new combinations of truth, or at least to develop an individualized aggregation of truth. The endeavor is to think for one's self, whether the thinking lies wholly in the fields of previous thought or not. It is not necessary to this habit of study that the subject-material should be new; but the process of thought and its results must be individual and independent, not the mere following of previous lines of thought ending in predetermined results. The demonstration of a problem in Euclid precisely as laid down is an illustration of the former; the demonstration of the same proposition by a method of one's own or in a manner distinctively individual is an illustration of the latter; both lying entirely within the realm of the known and the old.

Creative study, however, finds its largest application in those subjects in which, while much is known, more remains to be known. Such are the fields which we, as naturalists, cultivate; and we are gathered for the purpose of developing improved methods lying largely in the creative phase of study, though not wholly so.

Intellectual methods have taken three phases in the history of progress thus far. What may be the evolutions of the future it may not be prudent to forecast. Naturally the methods we now urge seem the highest attainable. These three methods may be designated, first, the method of the ruling theory; second, the method of the working hypothesis; and, third, the method of multiple working hypotheses.

In the earlier days of intellectual development the sphere of knowledge was limited, and was more nearly within the compass of a single individual; and those who assumed to be wise men, or aspired to be thought so, felt the need of knowing, or at least seeming to know, all that was known as a justification of their claims. So, also, there grew up an expectancy on the part of the multitude that the wise and the learned would explain whatever new thing presented itself. Thus pride and ambition on the one hand, and expectancy on the other, developed the putative wise man whose knowledge boxed the compass, and whose acumen found an explanation for every new puzzle which presented itself. This disposition has propagated itself, and has come down to our time as an intellectual predilection, though the compassing of the entire horizon of knowledge has long since been an abandoned affectation. As in the earlier days, so still, it is the habit of some to hastily conjure up an explanation for every new phenomenon that presents itself. Interpretation rushes to the forefront as the chief obligation pressing upon the putative wise man. Laudable as the effort at explanation is in itself, it is to be condemned when it runs before a serious inquiry into the phenomenon itself. A dominant disposition to find out what is, should precede and crowd aside the question, commendable at a later stage, "How came this so?" First full facts, then interpretations.

Premature Theories

The habit of precipitate explanation leads rapidly on to the development of tentative theories. The explanation offered for a given phenomenon is naturally, under the impulse of self-consistency, offered for like phenomena as they present themselves, and there is soon developed a general theory explanatory of a large class of phenomena similar to the original one. This general theory may not be supported by any further considerations than those which were involved in the first hasty inspection. For a time it is likely to be held in a tentative way with a measure of candor. With this tentative spirit and measurable candor, the mind satisfies its moral sense, and deceives itself with the thought that it is proceeding cautiously and impartially toward the goal of ultimate truth. It fails to recognize that no amount of provisional holding of a theory, so long as the view is limited and the investigation partial, justifies an ultimate conviction. It is not the slowness with which conclusions are arrived at that should give satisfaction to the moral sense, but the thoroughness, the completeness, the all-sidedness, the impartiality, of the investigation.

It is in this tentative stage that the affections enter with their blinding influence. Love was long since represented as blind, and what is true in the personal realm is measurably true in the intellectual realm. Important as

Thomas C. Chamberlin (1843–1928), a geologist, was president of the University of Wisconsin at the time this lecture was written. Later he was professor and director of the Walker Museum of the University of Chicago. In 1893 he founded the *Journal of Geology*, which he edited until his death. In 1908 he was president of the AAAS. The article is reprinted from *Science* (old series), **15**, 92 (1890).

Reprints of this article are available.

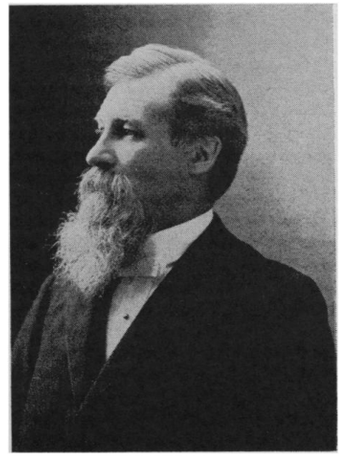
Prices (*cash with order*):	
1	50 cents (*or* 25 cents and stamped, self-addressed envelope)
2 to 9	45 cents each
10 to 24	30 cents each
25 or more	20 cents each

Address orders to AAAS, Chamberlin Reprints, 1515 Massachusetts Ave., NW, Washington, D.C. 20005.

the intellectual affections are as stimuli and as rewards, they are nevertheless dangerous factors, which menace the integrity of the intellectual processes. The moment one has offered an original explanation for a phenomenon which seems satisfactory, that moment affection for his intellectual child springs into existence; and as the explanation grows into a definite theory, his parental affections cluster about his intellectual offspring, and it grows more and more dear to him, so that, while he holds it seemingly tentative, it is still lovingly tentative, and not impartially tentative. So soon as this parental affection takes possession of the mind, there is a rapid passage to the adoption of the theory. There is an unconscious selection and magnifying of the phenomena that fall into harmony with the theory and support it, and an unconscious neglect of those that fail of coincidence. The mind lingers with pleasure upon the facts that fall happily into the embrace of the theory, and feels a natural coldness toward those that seem refractory. Instinctively there is a special searching-out of phenomena that support it, for the mind is led by its desires. There springs up, also, an unconscious pressing of the theory to make it fit the facts, and a pressing of the facts to make them fit the theory. When these biasing tendencies set in, the mind rapidly degenerates into the partiality of paternalism. The search for facts, the observation of phenomena and their interpretation, are all dominated by affection for the favored theory until it appears to its author or its advocate to have been overwhelmingly established. The theory then rapidly rises to the ruling position, and investigation, observation, and interpretation are controlled and directed by it. From an unduly favored child, it readily becomes master, and leads its author whithersoever it will. The subsequent history of that mind in respect to that theme is but the progressive dominance of a ruling idea.

Briefly summed up, the evolution is this: a premature explanation passes into a tentative theory, then into an adopted theory, and then into a ruling theory.

When the last stage has been reached, unless the theory happens, perchance, to be the true one, all hope of the best results is gone. To be sure, truth may be brought forth by an investigator dominated by a false ruling idea. His very errors may indeed stimulate investigation on the part of others. But the condition is an unfortunate one. Dust and chaff are mingled with the grain in what should be a winnowing process.



Thomas Chrowder Chamberlin was noted for his contributions to glaciology and for his part in formulating the Chamberlin-Moulton (planetesimal) hypothesis of the origin of the earth.

Ruling Theories Linger

As previously implied, the method of the ruling theory occupied a chief place during the infancy of investigation. It is an expression of the natural infantile tendencies of the mind, though in this case applied to its higher activities, for in the earlier stages of development the feelings are relatively greater than in later stages.

Unfortunately it did not wholly pass away with the infancy of investigation, but has lingered along in individual instances to the present day, and finds illustration in universally learned men and pseudo-scientists of our time.

The defects of the method are obvious, and its errors great. If I were to name the central psychological fault, I should say that it was the admission of intellectual affection to the place that should be dominated by impartial intellectual rectitude.

So long as intellectual interest dealt chiefly with the intangible, so long it was possible for this habit of thought to survive, and to maintain its dominance, because the phenomena themselves, being largely subjective, were plastic in the hands of the ruling idea; but so soon as investigation turned itself earnestly to an inquiry into natural phenomena, whose manifestations are tangible, whose properties are rigid, whose laws are rigorous, the defects of the method became manifest, and an effort at reformation ensued. The first great endeavor was repressive. The advocates of reform insisted that theorizing should be restrained, and efforts directed to the simple determination of facts. The effort was to make scientific study factitious instead of causal. Because theorizing in narrow lines had led to manifest evils, theorizing was to be condemned. The reformation urged was not the proper control and utilization of theoretical effort, but its suppression. We do not need to go backward more than twenty years to find ourselves in the midst of this attempted reformation. Its weakness lay in its narrowness and its restrictiveness. There is no nobler aspiration of the human intellect than desire to compass the cause of things. The disposition to find explanations and to develop theories is laudable in itself. It is only its ill use that is reprehensible. The vitality of study quickly disappears when the object sought is a mere collocation of dead unmeaning facts.

The inefficiency of this simply repressive reformation becoming apparent, improvement was sought in the method of the working hypothesis. This is affirmed to be *the* scientific method of the day, but to this I take exception. The working hypothesis differs from the ruling theory in that it is used as a means of determining facts, and has for its chief function the suggestion of lines of inquiry; the inquiry being made, not for the sake of the hypothesis, but for the sake of facts. Under the method of the ruling theory, the stimulus was directed to the finding of facts for the support of the theory. Under the working hypothesis, the facts are sought for the purpose of ultimate induction and demonstration, the hypothesis being but a means for the more ready development of facts and of their relations, and the arrangement and preservation of material for the final induction.

It will be observed that the distinc-

tion is not a sharp one, and that a working hypothesis may with the utmost ease degenerate into a ruling theory. Affection may as easily cling about an hypothesis as about a theory, and the demonstration of the one may become a ruling passion as much as of the other.

A Family of Hypotheses

Conscientiously followed, the method of the working hypothesis is a marked improvement upon the method of the ruling theory; but it has its defects—defects which are perhaps best expressed by the ease with which the hypothesis becomes a controlling idea. To guard against this, the method of multiple working hypotheses is urged. It differs from the former method in the multiple character of its genetic conceptions and of its tentative interpretations. It is directed against the radical defect of the two other methods; namely, the partiality of intellectual parentage. The effort is to bring up into view every rational explanation of new phenomena, and to develop every tenable hypothesis respecting their cause and history. The investigator thus becomes the parent of a family of hypotheses: and, by his parental relation to all, he is forbidden to fasten his affections unduly upon any one. In the nature of the case, the danger that springs from affection is counteracted, and therein is a radical difference between this method and the two preceding. The investigator at the outset puts himself in cordial sympathy and in parental relations (of adoption, if not of authorship) with every hypothesis that is at all applicable to the case under investigation. Having thus neutralized the partialities of his emotional nature, he proceeds with a certain natural and enforced erectness of mental attitude to the investigation, knowing well that some of his intellectual children will die before maturity, yet feeling that several of them may survive the results of final investigation, since it is often the outcome of inquiry that several causes are found to be involved instead of a single one. In following a single hypothesis, the mind is presumably led to a single explanatory conception. But an adequate explanation often involves the co-ordination of several agencies, which enter into the combined result in varying proportions. The true explanation is therefore necessarily complex. Such complex explanations of phenomena are specially encouraged by the method of multiple hypotheses, and constitute one of its chief merits. We are so prone to attribute a phenomenon to a single cause, that, when we find an agency present, we are liable to rest satisfied therewith, and fail to recognize that it is but one factor, and perchance a minor factor, in the accomplishment of the total result. Take for illustration the mooted question of the origin of the Great Lake basins. We have this, that, and the other hypothesis urged by different students as the cause of these great excavations; and all of these are urged with force and with fact, urged justly to a certain degree. It is practically demonstrable that these basins were river-valleys antecedent to the glacial incursion, and that they owe their origin in part to the pre-existence of those valleys and to the blocking-up of their outlets. And so this view of their origin is urged with a certain truthfulness. So, again, it is demonstrable that they were occupied by great lobes of ice, which excavated them to a marked degree, and therefore the theory of glacial excavation finds support in fact. I think it is furthermore demonstrable that the earth's crust beneath these basins was flexed downward, and that they owe a part of their origin to crust deformation. But to my judgment neither the one nor the other, nor the third, constitutes an adequate explanation of the phenomena. All these must be taken together, and possibly they must be supplemented by other agencies. The problem, therefore, is the determination not only of the participation, but of the measure and the extent, of each of these agencies in the production of the complex result. This is not likely to be accomplished by one whose working hypothesis is pre-glacial erosion, or glacial erosion, or crust deformation, but by one whose staff of working hypotheses embraces all of these and any other agency which can be rationally conceived to have taken part in the phenomena.

A special merit of the method is, that by its very nature it promotes thoroughness. The value of a working hypothesis lies largely in its suggestiveness of lines of inquiry that might otherwise be overlooked. Facts that are trivial in themselves are brought into significance by their bearings upon the hypothesis, and by their causal indications. As an illustration, it is only necessary to cite the phenomenal influence which the Darwinian hypothesis has exerted upon the investigations of the past two decades. But a single working hypothesis may lead investigation along a given line to the neglect of others equally important; and thus, while inquiry is promoted in certain quarters, the investigation lacks in completeness. But if all rational hypotheses relating to a subject are worked co-equally, thoroughness is the presumptive result, in the very nature of the case.

In the use of the multiple method, the re-action of one hypothesis upon another tends to amplify the recognized scope of each, and their mutual conflicts whet the discriminative edge of each. The analytic process, the development and demonstration of criteria, and the sharpening of discrimination, receive powerful impulse from the co-ordinate working of several hypotheses.

Fertility in processes is also the natural outcome of the method. Each hypothesis suggests its own criteria, its own means of proof, its own methods of developing the truth; and if a group of hypotheses encompass the subject on all sides, the total outcome of means and of methods is full and rich.

The use of the method leads to certain peculiar habits of mind which deserve passing notice, since as a factor of education its disciplinary value is one of importance. When faithfully pursued for a period of years, it develops a habit of thought analogous to the method itself, which may be designated a habit of parallel or complex thought. Instead of a simple succession of thoughts in linear order, the procedure is complex, and the mind appears to become possessed of the power of simultaneous vision from different standpoints. Phenomena appear to become capable of being viewed analytically and synthetically at once. It is not altogether unlike the study of a landscape, from which there comes into the mind myriads of lines of intelligence, which are received and co-ordinated simultaneously, producing a complex impression which is recorded and studied directly in its complexity. My description of this process

T. C. Chamberlin published two papers under the title of "The method of multiple working hypotheses." One of these papers, first published in the *Journal of Geology* in 1897, was quoted by John R. Platt in his recent article "Strong inference" (*Science*, 16 Oct. 1964). Platt wrote: "This charming paper deserves to be reprinted." Several readers, having had difficulty obtaining copies of Chamberlin's paper, expressed agreement with Platt. One wrote that the article had been reprinted in the *Journal of Geology* in 1931 and in the *Scientific Monthly* in November 1944. Another sent us a photocopy. Several months later still another wrote that the Institute for Humane Studies (Stanford, Calif.) had reprinted the article in pamphlet form this year. On consulting the 1897 version, we found a footnote in which Chamberlin had written: "A paper on this subject was read before the Society of Western Naturalists in 1892, and was published in a scientific periodical." Library research revealed that "a scientific periodical" was *Science* itself, for 7 February 1890, and that Chamberlin had actually read the paper before the Society of Western Naturalists on 25 October 1889. The chief difference between the 1890 text and the 1897 text is that, as Chamberlin wrote in 1897: "The article has been freely altered and abbreviated so as to limit it to aspects related to geological study." The 1890 text, which seems to be the first and most general version of "The method of multiple working hypotheses," is reprinted here. Typographical errors have been corrected, and subheadings have been added.

is confessedly inadequate, and the affirmation of it as a fact would doubtless challenge dispute at the hands of psychologists of the old school; but I address myself to naturalists who I think can respond to its verity from their own experience.

Drawbacks of the Method

The method has, however, its disadvantages. No good thing is without its drawbacks; and this very habit of mind, while an invaluable acquisition for purposes of investigation, introduces difficulties in expression. It is obvious, upon consideration, that this method of thought is impossible of verbal expression. We cannot put into words more than a single line of thought at the same time; and even in that the order of expression must be conformed to the idiosyncrasies of the language, and the rate must be relatively slow. When the habit of complex thought is not highly developed, there is usually a leading line to which others are subordinate, and the difficulty of expression does not rise to serious proportions; but when the method of simultaneous vision along different lines is developed so that the thoughts running in different channels are nearly equivalent, there is an obvious embarrassment in selection and a disinclination to make the attempt. Furthermore, the impossibility of expressing the mental operation in words leads to their disuse in the silent process of thought, and hence words and thoughts lose that close association which they are accustomed to maintain with those whose silent as well as spoken thoughts run in linear verbal courses. There is therefore a certain predisposition on the part of the practitioner of this method to taciturnity.

We encounter an analogous difficulty in the use of the method with young students. It is far easier, and I think in general more interesting, for them to argue a theory or accept a simple interpretation than to recognize and evaluate the several factors which the true elucidation may require. To illustrate: it is more to their taste to be taught that the Great Lake basins were scooped out by glaciers than to be urged to conceive of three or more great agencies working successively or simultaneously, and to estimate how much was accomplished by each of these agencies. The complex and the quantitative do not fascinate the young student as they do the veteran investigator.

Multiple Hypotheses and Practical Affairs

It has not been our custom to think of the method of working hypotheses as applicable to instruction or to the practical affairs of life. We have usually regarded it as but a method of science. But I believe its application to practical affairs has a value coordinate with the importance of the affairs themselves. I refer especially to those inquiries and inspections that precede the coming-out of an enterprise rather than to its actual execution. The methods that are superior in scientific investigation should likewise be superior in those investigations that are the necessary antecedents to an intelligent conduct of affairs. But I can dwell only briefly on this phase of the subject.

In education, as in investigation, it has been much the practice to work a theory. The search for instructional methods has often proceeded on the presumption that there is a definite patent process through which all students might be put and come out with results of maximum excellence; and hence pedagogical inquiry in the past has very largely concerned itself with the inquiry, "What is the best method?" rather than with the inquiry, "What are the special values of different methods, and what are their several advantageous applicabilities in the varied work of instruction?" The past doctrine has been largely the doctrine of pedagogical uniformitarianism. But the faculties and functions of the mind are almost, if not quite, as varied as the properties and functions of matter: and it is perhaps not less absurd to assume that any specific method of instructional procedure is more effective than all others, under any and all circumstances, than to assume that one principle of interpretation is equally applicable to all the phenomena of nature. As there is an endless

variety of mental processes and combinations and an indefinite number of orders of procedure, the advantage of different methods under different conditions is almost axiomatic. This being granted, there is presented to the teacher the problem of selection and of adaptation to meet the needs of any specific issue that may present itself. It is important, therefore, that the teacher shall have in mind a full array of possible conditions and states of mind which may be presented, in order that, when any one of these shall become an actual case, he may recognize it, and be ready for the emergency.

Just as the investigator armed with many working hypotheses is more likely to see the true nature and significance of phenomena when they present themselves, so the instructor equipped with a full panoply of hypotheses ready for application more readily recognizes the actuality of the situation, more accurately measures its significance, and more appropriately applies the methods which the case calls for.

The application of the method of multiple hypotheses to the varied affairs of life is almost as protean as the phases of that life itself, but certain general aspects may be taken as typical of the whole. What I have just said respecting the application of the method to instruction may apply, with a simple change of terms, to almost any other endeavor which we are called upon to undertake. We enter upon an enterprise in most cases without full knowledge of all the factors that will enter into it, or all of the possible phases which it may develop. It is therefore of the utmost importance to be prepared to rightly comprehend the nature, bearings, and influence of such unforeseen elements when they shall definitely present themselves as actualities. If our vision is narrowed by a preconceived theory as to what will happen, we are almost certain to misinterpret the facts and to misjudge the issue. If, on the other hand, we have in mind hypothetical forecasts of the various contingencies that may arise, we shall be the more likely to recognize the true facts when they do present themselves. Instead of being biased by the anticipation of a given phase, the mind is rendered open and alert by the anticipation of any one of many phases, and is free not only, but is predisposed, to recognize correctly the one which does appear. The method has a further good effect. The mind, having anticipated the possible phases which may arise, has prepared itself for action under any one that may come up, and it is therefore ready-armed, and is predisposed to act in the line appropriate to the event. It has not set itself rigidly in a fixed purpose, which it is predisposed to follow without regard to contingencies. It has not nailed down the helm and predetermined to run a specific course, whether rocks lie in the path or not; but, with the helm in hand, it is ready to veer the ship according as danger or advantage discovers itself.

It is true, there are often advantages in pursuing a fixed predetermined course without regard to obstacles or adverse conditions. Simple dogged resolution is sometimes the salvation of an enterprise; but, while glorious successes have been thus snatched from the very brink of disaster, overwhelming calamity has in other cases followed upon this course, when a reasonable regard for the unanticipated elements would have led to success. So there is to be set over against the great achievements that follow on dogged adherence great disasters which are equally its result.

Danger of Vacillation

The tendency of the mind, accustomed to work through multiple hypotheses, is to sway to one line of policy or another, according as the balance of evidence shall incline. This is the soul and essence of the method. It is in general the true method. Nevertheless there is a danger that this yielding to evidence may degenerate into unwarranted vacillation. It is not always possible for the mind to balance evidence with exact equipoise, and to determine, in the midst of the execution of an enterprise, what is the measure of probability on the one side or the other: and as difficulties present themselves, there is a danger of being biased by them and of swerving from the course that was really the true one. Certain limitations are therefore to be placed upon the application of the method, for it must be remembered that a poorer line of policy consistently adhered to may bring better results than a vacillation between better policies.

There is another and closely allied danger in the application of the method. In its highest development it presumes a mind supremely sensitive to every grain of evidence. Like a pair of delicately poised scales, every added particle on the one side or the other produces its effect in oscillation. But such a pair of scales may be altogether too sensitive to be of practical value in the rough affairs of life. The balances of the exact chemist are too delicate for the weighing-out of coarse commodities. Despatch may be more important than accuracy. So it is possible for the mind to be too much concerned with the nice balancings of evidence, and to oscillate too much and too long in the endeavor to reach exact results. It may be better, in the gross affairs of life, to be less precise and more prompt. Quick decisions, though they may contain a grain of error, are oftentimes better than precise decisions at the expense of time.

The method has a special beneficent application to our social and civic relations. Into these relations there enter, as great factors, our judgment of others, our discernment of the nature of their acts, and our interpretation of their motives and purposes. The method of multiple hypotheses, in its application here, stands in decided contrast to the method of the ruling theory or of the simple working hypothesis. The primitive habit is to interpret the acts of others on the basis of a theory. Childhood's unconscious theory is that the good are good, and the bad are bad. From the good the child expects nothing but good; from the bad, nothing but bad. To expect a good act from the bad, or a bad act from the good, is radically at variance with childhood's mental methods. Unfortunately in our social and civic affairs too many of our fellow-citizens have never outgrown the ruling theory of their childhood.

Many have advanced a step farther, and employ a method analagous to that of the working hypothesis. A certain presumption is made to attach to the acts of their fellow-beings, and that which they see is seen in the light of that presumption, and that which they construe is construed in the light of that presumption. They do not go to the lengths of childhood's method by assuming positively that the good are wholly good, and the bad wholly bad; but there is a strong presumption in their minds that he concerning whom

they have an ill opinion will act from corresponding motives. It requires positive evidence to overthrow the influence of the working hypothesis.

The method of multiple hypotheses assumes broadly that the acts of a fellow-being may be diverse in their nature, their moves, their purposes, and hence in their whole moral character; that they may be good though the dominant character be bad; that they may be bad though the dominant character be good; that they may be partly good and partly bad, as is the fact in the greater number of the complex activities of a human being. Under the method of multiple hypotheses, it is the first effort of the mind to see truly what the act is, unbeclouded by the presumption that this or that has been done because it accords with our ruling theory or our working hypothesis. Assuming that acts of similar general aspect may readily take any one of several different phases, the mind is freer to see accurately what has actually been done. So, again, in our interpretations of motives and purposes, the method assumes that these may have been any one of many, and the first duty is to ascertain which of possible motives and purposes actually prompted this individual action. Going with this effort there is a predisposition to balance all evidence fairly, and to accept that interpretation to which the weight of evidence inclines, not that which simply fits our working hypothesis or our dominant theory. The outcome, therefore, is better and truer observation and juster and more righteous interpretation.

Imperfections of Knowledge

There is a third result of great importance. The imperfections of our knowledge are more likely to be detected, for there will be less confidence in its completeness in proportion as there is a broad comprehension of the possibilities of varied action, under similar circumstances and with similar appearances. So, also, the imperfections of evidence as to the motives and purposes inspiring the action will become more discernible in proportion to the fulness of our conception of what the evidence should be to distinguish between action from the one or the other of possible motives. The necessary result will be a less disposition to reach conclusions upon imperfect grounds. So, also, there will be a less inclination to misapply evidence; for, several constructions being definitely in mind, the indices of the one motive are less liable to be mistaken for the indices of another.

The total outcome is greater care in ascertaining the facts, and greater discrimination and caution in drawing conclusions. I am confident, therefore, that the general application of this method to the affairs of social and civic life would go far to remove those misunderstandings, misjudgments, and misrepresentations which constitute so pervasive an evil in our social and our political atmospheres, the source of immeasurable suffering to the best and most sensitive souls. The misobservations, the misstatements, the misinterpretations, of life may cause less gross suffering than some other evils; but they, being more universal and more subtle, pain. The remedy lies, indeed, partly in charity, but more largely in correct intellectual habits, in a predominant, ever-present disposition to see things as they are, and to judge them in the full light of an unbiased weighing of evidence applied to all possible constructions, accompanied by a withholding of judgment when the evidence is insufficient to justify conclusions.

I believe that one of the greatest moral reforms that lies immediately before us consists in the general introduction into social and civic life of that habit of mental procedure which is known in investigation as the method of multiple working hypotheses.

Education as a Way of Life

Traditional arrangements for education must be supplemented by a system designed for lifelong learning.

John W. Gardner

Nothing is more obsolete than the notion that education is something that takes place in a solid block of years between, roughly, ages 6 and 22. From now on, the individual is going to have to seek formal instruction at many points throughout his career.

Under such a system, much of the present anxiety over young people who quit school prematurely will disappear. The anxiety stems from the fact that today leaving school signifies the end of education. Under the new system there will be no end to education.

Unfortunately, our institutional arrangements for lifelong education are ridiculously inadequate. Most educational institutions are still designed for young people who have nothing else to do. They are ill suited to men and women who must fit their learning into a busy life.

For years a small number of devoted educators have sought to meet the needs of this latter group, but they have not received much cooperation from the rest of the academic world. That state of affairs appears to be changing.

In the making now are some highly flexible arrangements to make education available to anyone able and willing to learn, under circumstances suited to his needs. To indicate in concrete terms what such a system might look like, I am going to describe certain activities of an imaginary university—let us call it Midland State University. (It is not necessary that all these activities be sponsored by a university—a point which I discuss later.)

The author is president of Carnegie Corporation of New York, 589 Fifth Avenue, New York 10017.

Annu. Rev. Earth Planet. Sci. 2004. 32:13–45
doi: 10.1146/annurev.earth.32.101802.120257
Copyright © 2004 by Annual Reviews. All rights reserved
First published online as a Review in Advance on November 10, 2003

EVOLUTION OF THE NORTH AMERICAN CORDILLERA

William R. Dickinson
Department of Geosciences, University of Arizona, Tucson, Arizona 85721; email: wrdickin@geo.arizona.edu

Annu. Rev. Earth Planet. Sci. 2004.32:13-45. Downloaded from arjournals.annualreviews.org
by Montana State University - Bozeman on 03/20/07. For personal use only.

Key Words continental margin, crustal genesis, geologic history, orogen, tectonics

■ **Abstract** The Cordilleran orogen of western North America is a segment of the Circum-Pacific orogenic belt where subduction of oceanic lithosphere has been underway along a great circle of the globe since breakup of the supercontinent Pangea began in Triassic time. Early stages of Cordilleran evolution involved Neoproterozoic rifting of the supercontinent Rodinia to trigger miogeoclinal sedimentation along a passive continental margin until Late Devonian time, and overthrusting of oceanic allochthons across the miogeoclinal belt from Late Devonian to Early Triassic time. Subsequent evolution of the Cordilleran arc-trench system was punctuated by tectonic accretion of intraoceanic island arcs that further expanded the Cordilleran continental margin during mid-Mesozoic time, and later produced a Cretaceous batholith belt along the Cordilleran trend. Cenozoic interaction with intra-Pacific seafloor spreading systems fostered transform faulting along the Cordilleran continental margin and promoted incipient rupture of continental crust within the adjacent continental block.

INTRODUCTION

Geologic analysis of the Cordilleran orogen, forming the western mountain system of North America, raises the following questions: 1. When was the Cordilleran system born, and from what antecedents; 2. which rock masses are integral to the Cordilleran continental margin, and how were they formed; 3. which rock masses were incorporated into the Cordilleran realm by tectonic accretion, and what were their origins; and 4. what geologic processes are promoting distension and disruption of the Cordilleran system today?

Figure 1 is a chronostratigraphic diagram of Cordilleran rock assemblages showing their relationships to major phases of Cordilleran evolution. The Cordilleran edge of the Precambrian basement, which forms the Laurentian craton, was first delineated by rifting to form a passive continental margin, along which a thick Neoproterozoic to Devonian miogeoclinal prism of sedimentary strata was deposited. From Late Devonian to Early Triassic time, oceanic allochthons were successively thrust across the miogeoclinal strata as internally deformed tectonic

Annu. Rev. Earth Planet. Sci. 2004.32:13-45. Downloaded from arjournals.annualreviews.org
by Montana State University - Bozeman on 03/20/07. For personal use only.

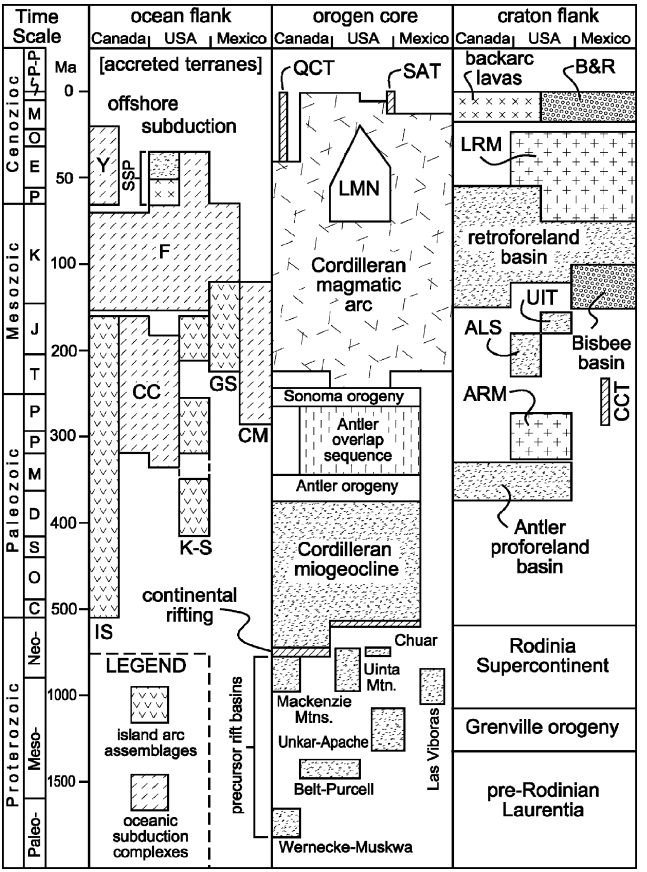


Figure 1 Schematic chronostratigraphic diagram of major Cordilleran rock assemblages (note changes in timescale at 100 Ma and 500 Ma). Canada includes the adjacent panhandle of southeastern Alaska, and Mexico includes the USA-Mexico border region south of the Colorado Plateau. Accreted island-arc assemblages: GS, Guerrero superterrane; IS, Insular superterrane; K-S, accreted arcs of Klamath Mountains and Sierra Nevada foothills. Subduction complexes: CC, Cache Creek; CM, central Mexico; F, Franciscan; Y, Yakutat. Transform faults (*diagonally ruled bars*): CCT, California-Coahuila; QCT, Queen Charlotte; SAT, San Andreas. Other features: ALS, Auld Lang Syne backarc basin; ARM, Ancestral Rocky Mountains province; B&R, Basin and Range taphrogen; LRM, Laramide Rocky Mountains province (LMN, Laramide magmatic null); SSP, accreted Siletzia and overlying forearc basin; UIT, Utah-Idaho trough.

Annu. Rev. Earth Planet. Sci. 2004.32:13-45. Downloaded from arjournals.annualreviews.org
by Montana State University - Bozeman on 03/20/07. For personal use only.

assemblages accreted to the continent. An arc-trench system initiated along the modified continental margin in Triassic time was the tectonic regime that produced Mesozoic-Cenozoic subduction complexes and batholiths most characteristic of the Cordilleran orogen. During the subduction of oceanic lithosphere beneath the Cordilleran margin, Jurassic-Cretaceous accretion of intraoceanic island arcs contributed to the outward growth of the continental block. Beginning in mid-Cenozoic time, impingement of intra-Pacific seafloor spreading systems on the subduction zone at the continental margin gave birth to transform fault systems lying near the edge of the continental block and to associated inland deformation that distended continental crust previously overthickened by Cordilleran orogenesis.

On paleotectonic maps showing the distributions of Cordilleran rock assemblages adapted in part from Dickinson (2000, 2001, 2002) and Dickinson & Lawton (2001a,b; 2003), rock masses are plotted on present geography, with state and province boundaries for orientation, without palinspastic restoration to correct for distortion of rock masses by deformation. Offsets of rock masses across major Cenozoic strike-slip faults are shown, however, and curvatures of tectonic trends by oroclinal bending are indicated by annotations where appropriate.

To aid analysis of accretionary tectonics, the North American Cordillera has been subdivided into nearly 100 formally named tectonostratigraphic terranes (Coney et al. 1980) separated by faulted boundaries of varying tectonic significance and structural style (Silberling et al. 1992). For graphic display at feasible scale, various terranes are combined into generic groupings.

CORDILLERAN OROGEN

The Cordilleran mountain chain of western North America is an integral segment of the Circum-Pacific orogenic belt, which extends along a great circle path for 25,000+ km from the Antarctic Peninsula to beyond Taiwan (Figure 2). The length of the Cordilleran orogen from the Gulf of Alaska to the mouth of the Gulf of California is ~5000 km, or ~20% of the total length of the orogenic belt.

Characteristic geologic features of the Circum-Pacific orogenic belt derive from persistent subduction of oceanic lithosphere at trenches along the flanks of continental margins and offshore island arcs linked spatially to form a nearly continuous chain along the Pacific rim (Figure 2). The rock assemblages of subduction zones where oceanic plates are progressively consumed and of the parallel magmatic arcs built by related igneous activity are the prime signatures of Circum-Pacific orogenesis in the rock record. The oldest rock assemblages of the Cordilleran continental margin that reflect this style of tectonism mark initiation of the Cordilleran orogenic system in mid-Early Triassic time. Older rock assemblages exposed within the mountain chain record preceding tectonic regimes of different character.

Global Orogenic Patterns

In the Philippine-Indonesian region, the Circum-Pacific orogenic belt intersects the Alpine-Himalayan orogenic belt, which is aligned along a different great circle

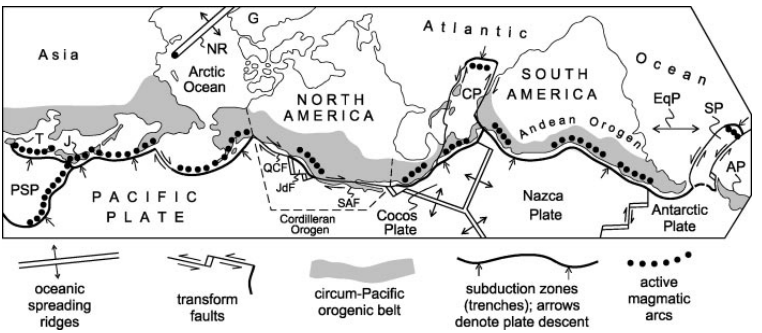


Figure 2 Position of the Cordilleran orogen of western North America along the Circum-Pacific orogenic belt (after Dickinson et al. 1986). Mercator projection with pole at 25° N Lat, 15° E Long (EqP is equatorial plane of projection). AP, Antarctic Peninsula; C, Cascades volcanic chain; CP, Caribbean plate; G, Greenland; J, Japan; JdF, Juan de Fuca plate; NR, Nansen Ridge (northern extremity of Atlantic spreading system); PSP, Philippine Sea plate; QCf, Queen Charlotte fault; SAf, San Andreas fault; SP, Scotia plate; T, Taiwan.

Annu. Rev. Earth Planet. Sci. 2004.32:13-45. Downloaded from arjournals.annualreviews.org
by Montana State University - Bozeman on 03/20/07. For personal use only.

of the globe (Figure 3). Both orogenic belts relate to the breakup of the Permian-Triassic supercontinent of Pangea beginning early in Mesozoic time, but in different ways, as the Atlantic and Indian oceans opened to disrupt Pangea by seafloor spreading. Alpine-Himalayan evolution has involved the successive juxtaposition of disparate continental blocks (e.g., Africa, India, Australia against Eurasia) at suture belts marking the former positions of trenches where intervening ocean basins were closed by plate consumption (Figure 3), but no crustal blocks of comparable size have lodged against the Pacific margin of the Americas.

The ancestral Circum-Pacific orogenic system along the margin of Pangea was born along a great circle path (Le Pichon 1983), rimming an ocean (Panthalassa) that was effectively a paleo-Pacific realm with a Tethyan gulf that projected into the angle between Laurasian and Gondwanan segments of Pangea (Figure 4). The great circle configuration was maintained as expansion of the Atlantic and Indian Oceans led to a modern Pacific only 60% the size of the paleo-Pacific (Le Pichon et al. 1985) by insertion of Australia and its surrounding seas into the Pacific arena to step the Pacific rim eastward for ∼5500 km along the Indonesian archipelago (Figure 3). During Circum-Pacific evolution, intra-Pacific seafloor spreading renewed oceanic lithosphere so rapidly that no vestiges of pre-Jurassic paleo-Pacific seafloor remain (Dickinson 1977).

Supercontinent History

The composite supercontinent of Pangea (Figure 4) formed during late Paleozoic time when Gondwana lodged against Laurasia along the Appalachian-Hercynian

Annu. Rev. Earth Planet. Sci. 2004.32:13-45. Downloaded from arjournals.annualreviews.org
by Montana State University - Bozeman on 03/20/07. For personal use only.

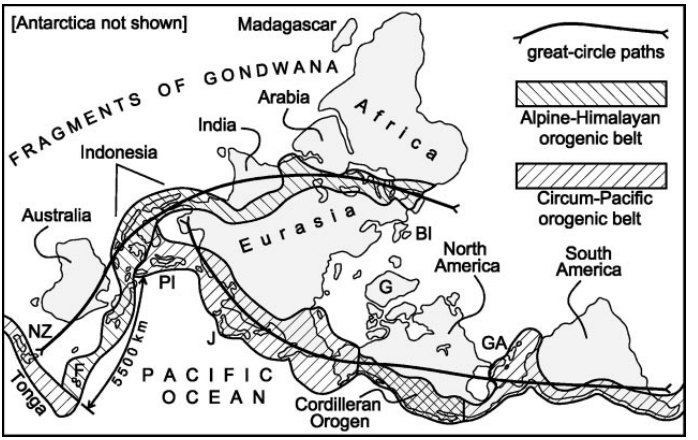


Figure 3 Distribution of continents in relation to the Alpine-Himalayan and Circum-Pacific orogenic belts (Cordilleran orogen: *cross-hatched*) in "circular" projection (after Challand & Rageau 1985). BI, British Isles; F, Fiji; G, Greenland; GA, Greater Antilles; J, Japan; NZ, New Zealand; PI, Philippine Islands.

orogen, a Paleozoic precursor of the modern Alpine-Himalayan system in that both achieved assembly of supercontinents (Pangea and Eurasia) through juxtaposition of previously separate continental blocks. Gondwana was a paleocontinent assembled in Neoproterozoic time (800–550 Ma) by juxtaposition of continental fragments across multiple internal suture belts (Meert & Van der Voo 1997). Laurasia included the ancient continental nuclei of Laurentia (North America) and Baltica (Europe), which had been conjoined in early Paleozoic time and linked in mid-Paleozoic time with Siberia. The Paleozoic precursor of the modern Circum-Pacific system was the Gondwanide orogenic belt, which lay along the Panthalassan (paleo-Pacific) margin of Gondwana, from South America past Antarctica to Australia (Figure 4), where consumption of oceanic lithosphere proceeded without interruption during the progressive assembly of Pangea (Ramos & Aleman 2000, Foster & Gray 2000).

The assembly of Pangea and its subsequent breakup during the assembly of Eurasia over the course of Phanerozoic time finds a Precambrian parallel in the geologic history of an earlier supercontinent, Rodinia, from which continental fragments were at first widely dispersed and then rearranged to form Gondwana and eventually Pangea. Rodinia was aggregated during Grenville orogenesis in Mesoproterozoic time (1325–1050 Ma), and the Cordilleran continental margin first took shape from Neoproterozoic breakup of Rodinia. As yet, however, there is no final consensus on the arrangement of continental cratons within the Rodinian

Annu. Rev. Earth Planet. Sci. 2004.32:13-45. Downloaded from arjournals.annualreviews.org
by Montana State University - Bozeman on 03/20/07. For personal use only.

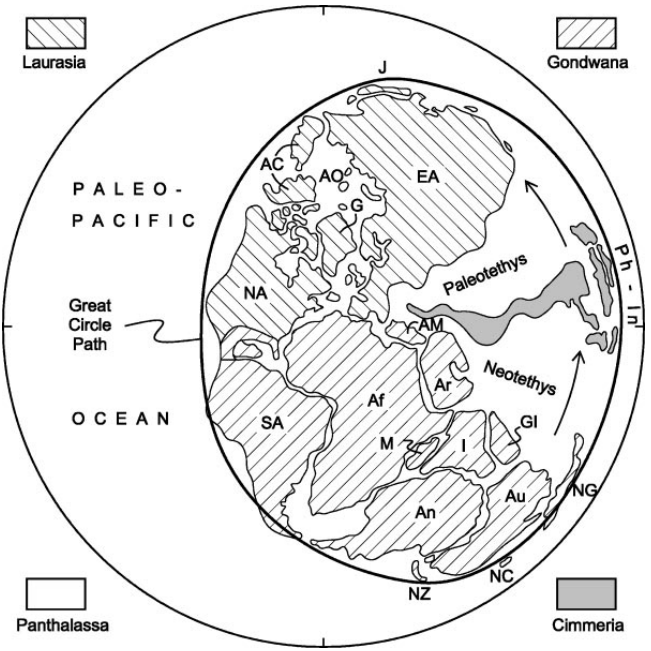


Figure 4 Permian-Triassic configuration of Pangea (Gondwana after Lawver & Scotese 1987) surrounded by Panthalassa (global sea including paleo-Pacific ocean and Tethys gulf) in Lambert equal-area projection (whole Earth). The Arctic Ocean closed by restoring transform slip of Alaska-Chukotka (Patrick & McClelland 1995). Arrows schematically denote the motion of Cimmerian landmasses in transit across the Tethys gulf, originating by rifting off the margin of Gondwana, toward Mesozoic accretion along the southern flank of Eurasia by closure of Paleothys as Neotethys opened. AC, Alaska-Chukotka; Af, Africa; AM, Asia Minor; An, Antarctica; AO, Arctic Ocean (closed); Ar, Arabia; Au, Australia; EA, Eurasia; G, Greenland; GI, Greater India; I, India; J; Japan; M, Madagascar; NA, North America; NC, New Caledonia; NG, New Guinea; NZ, New Zealand; Ph-In, Philippine-Indonesian archipelago; SA, South America.

supercontinent. Continental blocks suggested as conjugate to the Cordilleran rifted margin of Laurentia include Siberia (Sears & Price 2000), Antarctica-Australia (Dalziell 1992), Australia together with an unknown block farther north (Karlstrom et al. 1999), and China (Li et al. 2002). Of the various options, Siberia currently seems the most viable (Sears & Price 2003).

Annu. Rev. Earth Planet. Sci. 2004.32:13-45. Downloaded from arjournals.annualreviews.org
by Montana State University - Bozeman on 03/20/07. For personal use only.

PRECAMBRIAN–PALEOZOIC MIOGEOCLINE

Along the Cordilleran margin of Laurentia, an elongate belt of thick sediment was deposited in Neoproterozoic and lower Paleozoic time as a miogeoclinal prism draped over a passive continental margin formed by rifting during the breakup of Rodinia (Figure 1). The narrow miogeoclinal belt truncates disrupted older Precambrian age provinces of interior Laurentia (Figure 5). The miogeoclinal prism thickened westward from a zero edge along a hinge line at the edge of the Laurentian craton. Miogeoclinal sedimentation continued, unbroken by tectonic disruption, until Late Devonian time, but the timing of its inception was apparently diachronous.

Cordilleran Rifting

North of the trans-Idaho discontinuity (Yates 1968), where the elongate trend of the miogeocline is offset by >250 km (Figure 5), basaltic rocks associated with glaciomarine diamictite in basal horizons of the miogeoclinal succession have been dated isotopically at 770–735 Ma (Armstrong et al. 1982, Devlin et al. 1988, Rainbird et al. 1996, Colpron et al. 2002). This time frame provides an age bracket for rifting that initiated deposition of the Windermere Supergroup along a newly formed passive continental margin open to the west in Canada (Ross 1991, MacNaughton et al. 2000). South of the trans-Idaho discontinuity, coeval rifting apparently formed only intracontinental basins in which redbed units such as the Chuar Group (775–735 Ma) of the Grand Canyon were deposited (Timmons et al. 2001), with continental separation delayed in the Death Valley region to the west until after 600 Ma (Prave 1999).

The subparallelism of the trans-Idaho discontinuity and a paleotransform delimiting the southwest margin of Laurentia (Figure 5) suggests that both originated as transform offsets of the nascent Cordilleran margin. Miogeoclinal strata present locally along the trans-Idaho discontinuity form a narrow band exposed only within roof pendants of the Idaho batholith (Lund et al. 2003) and contain intercalated bimodal volcanic rocks (685 Ma), which perhaps reflect prolonged deformation along a marginal offset at the edge of the continental block during the evolution of the rifted Cordilleran margin.

Published subsidence analyses for the Cordilleran miogeocline in both Canada and the USA imply that postrift thermotectonic subsidence of the passive continental margin did not begin until 560–555 Ma in Early Cambrian time (Bond et al. 1983, Armin & Mayer 1983, Bond & Kominz 1984, Levy & Christie-Blick 1991). Replotting the subsidence curves for revised estimates of the beginning of Cambrian time (545 Ma versus 570 Ma) puts onset of thermotectonic subsidence at 525–515 Ma, still within Early Cambrian time on the revised timescale. Projecting subsidence curves backward in time to allow for 1.1–1.2 km of synrift tectonic subsidence (∼2 km of sediment accumulation) in the Great Basin area of the USA (Levy & Christie-Blick 1991) suggests that rifting that led directly to

Annu. Rev. Earth Planet. Sci. 2004.32:13-45. Downloaded from arjournals.annualreviews.org
by Montana State University - Bozeman on 03/20/07. For personal use only.

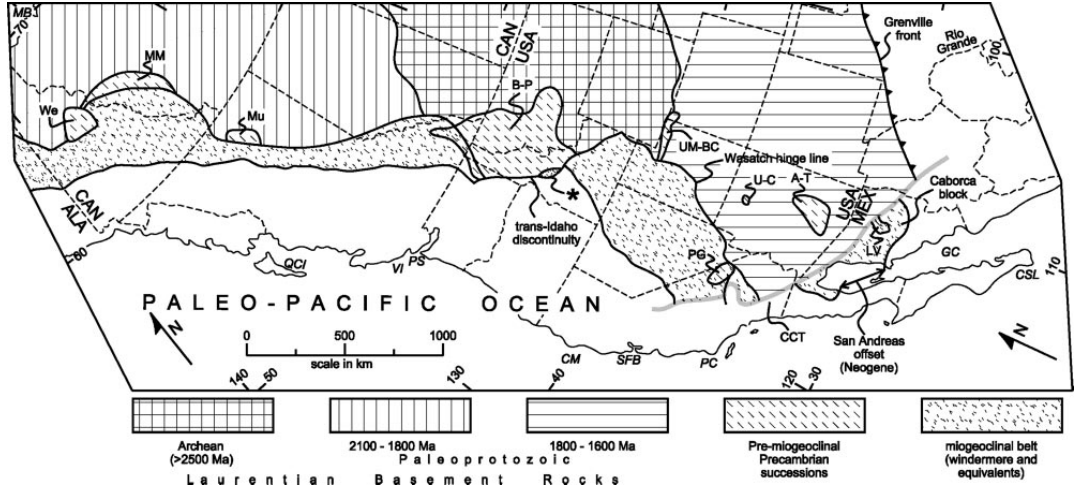


Figure 5 Neoproterozoic-Early Paleozoic Cordilleran miogeocline and premiogeoclinal sedimentary basins along the trend of the North American Cordillera (rock assemblages now present west of the miogeoclinal belt were added to the continental block after mid-Late Devonian time). Asterisk (*) denotes miogeoclinal strata along trans-Idaho discontinuity (Lund et al. 2003). Grenville front is margin of Mesoproterozoic Grenville orogen along which Rodinia was assembled. CCT is Permian-Triassic California-Coahuila transform (Dickinson 2000), which offset the Cordilleran miogeoclinal assemblage of the Caborca block by overprinting an older paleotransform system that delimited the early Paleozoic southwest margin of Laurentia (Dickinson & Lawton 2001a). See text for ages of premiogeoclinal successions. (A-T, Apache-Troy; B-P, Belt-Purcell; LV, Las Víboras; MM, Mackenzie Mountains; Mu, Muskwa; PG, Pahrump Group; U-C, Unkar-Chuar; UM-BC, Uinta Mountain—Big Cottonwood; We, Wernecke). Coastal locales (*italics*): CM, Cape Mendocino; CSL, Cabo San Lucas; GC, Gulf of California; MB, Mackenzie Bay of Arctic Ocean; PC, Point Conception; PS, Puget Sound; QCI, Queen Charlotte Islands; SFB, San Francisco Bay; VI, Vancouver Island.

Annu. Rev. Earth Planet. Sci. 2004.32:13-45. Downloaded from arjournals.annualreviews.org
by Montana State University - Bozeman on 03/20/07. For personal use only.

continental separation south of the trans-Idaho discontinuity occurred during the interval 600–575 Ma (Armin & Mayer 1983). Isotopic dating of synrift volcanic rocks in southern British Columbia at 570 ± 5 Ma (Colpron et al. 2002) documents that active rifting persisted into latest Neoproterozoic time, north as well as south of the trans-Idaho discontinuity.

The indicated time span of 45–65 million years between initial rifting and onset of passive thermotectonic subsidence is comparable to the time span of 55 million years between initial development of Triassic rift basins and the first emplacement of Jurassic oceanic crust along the modern Atlantic continental margin (Manspeizer & Cousminer 1988). Cordilleran unconformities near the Precambrian-Cambrian time boundary (Devlin & Bond 1988, Lickorish & Simony 1995) may stem from reactivation of rift faults or from the influence of eustasy on a rift hinge undergoing flexure from sediment loading of oceanic crust offshore (Fedo & Cooper 2001).

The evidence for two rift events (Colpron et al. 2002), spaced 160–170 million years apart in pre-Windermere and latest Neoproterozoic time, suggests the possibility that two different continental blocks, one west of Canada and one west of USA-Mexico, were once conjugate with Laurentia, but no current Rodinian models are readily compatible with that interpretation. In any case, the onset of thermotectonic subsidence at the same time in both Canada and southward implies that the Windermere passive margin was reactivated at the time of the second rifting event, as suggested by stratal relationships near the USA-Canada border (Devlin 1989).

Precursor Rifts

A number of premiogeoclinal Precambrian sedimentary successions occur along the trend of the Cordillera but lack the longitudinal continuity of the overlying miogeocline (Figure 5). Each was deposited within an intracratonic basin formed by incipient rift extension within Rodinia or before its assembly (Figure 1). From the trans-Idaho discontinuity northward, isotopic dating of basin substratum, intercalated volcanics, and local intrusions establishes age brackets as follows for deep local rift troughs: Wernecke Supergroup, 1820–1710 Ma (Ross et al. 2001); Muskwa Assemblage, 1760–1660 Ma (Ross et al. 2001); Belt-Purcell Supergroup, 1470–1370 Ma (Evans et al. 2000, Luepke & Lyons 2001); Mackenzie Mountains Supergroup, 975–775 Ma (Rainbird et al. 1996); Uinta Mountain Group (and Big Cottonwood Formation), 975?–725? Ma. Farther south, thinner premiogeoclinal successions, deposited either in rift basins or on the craton, include the following: Unkar Group, Apache Group (including Troy Quartzite), and lower Pahrump Group, 1220–1070 Ma (Timmons et al. 2001), with the lowermost Apache Group as old as 1335 Ma (Stewart et al. 2001); Las Víboras Group, 1050?–850? Ma (Stewart et al. 2002); and the Chuar Group, 775–735 Ma (Timmons et al. 2001).

The precursor rift troughs may have acted as subregional guides helping to control the trend of eventual continental separation that initiated miogeoclinal

Annu. Rev. Earth Planet. Sci. 2004.32:13-45. Downloaded from arjournals.annualreviews.org
by Montana State University - Bozeman on 03/20/07. For personal use only.

sedimentation. In the Death Valley region, for example, diamictites of the Kingston Peak Formation in the upper Pahrump Group probably include correlatives of both syn-Windermere (~750 Ma) rift fill and younger (~600 Ma) synrift deposits at the base of the miogeoclinal succession (Prave 1999). Recent interpretations from deep seismic reflection profiles propose that pre-Windermere Canadian assemblages (Wernecke, Muskwa, Mackenzie Mountains) in the region north of the Belt-Purcell basin are all parts of a composite sediment prism built westward along an evolving passive continental margin that flanked the youngest basement components of the Laurentian craton and persisted over a time span that exceeded a billion years (Snyder et al. 2002). If so, no continental separation by Neoproterozoic rifting was required to form the Windermere continental margin, but the disparate age ranges and outcrop discontinuity of the pre-Windermere successions are difficult to reconcile with the postulate of a pre-Windermere passive continental margin continuous for the length of the Canadian Cordillera.

LATE PALEOZOIC–EARLY TRIASSIC ACCRETION

Between Late Devonian and Early Triassic time, internally deformed allochthons (Figure 6) of oceanic strata were thrust eastward as accretionary prisms across the seaward flank of the miogeoclinal belt when the margin of the Laurentian continental block was drawn into the subduction zones of intraoceanic island arcs that faced the Cordilleran margin and subducted offshore oceanic crust of marginal seas downward to the west (Dickinson 2000). Lithic constituents of the allochthons include pillow basalts, peridotite, and serpentinite of oceanic crust and subjacent mantle, as well as more voluminous argillite, ribbon chert, and turbidites of overlying seafloor sediment profiles. The turbidites of the allochthons include continental slope and rise deposits originally transported off the Laurentian margin and then thrust back toward the craton over the miogeoclinal shelf edge. Exposures where later tectonism and erosion has exhumed the thrust contact show that the allochthons traveled 100+ km across the structurally underlying miogeoclinal assemblage.

Antler-Sonoma Allochthons

Stratigraphic and structural analysis of the overthrust allochthons has documented their emplacement during two discrete episodes of incipient continental subduction termed the Antler and Sonoma orogenies in the USA. The two events were spaced ~110 million years apart during comparatively brief intervals of time (~25 million years each) spanning the Devonian-Mississippian and Permian-Triassic time boundaries (Figure 1). The two separate allochthons have been delineated with greatest confidence in the Great Basin of Nevada (USA), where allochthonous but unmetamorphosed oceanic facies of multiple Paleozoic horizons were thrust over autochthonous miogeoclinal facies of the same ages along the Roberts Mountains

Annu. Rev. Earth Planet. Sci. 2004.32:13-45. Downloaded from arjournals.annualreviews.org
by Montana State University - Bozeman on 03/20/07. For personal use only.

(Antler) and Golconda (Sonoma) thrusts (Figure 6). Farther north, the lack of clearcut evidence for the presence of either allochthon along the trend of the trans-Idaho discontinuity (Figures 5 and 6) may stem from engulfment by batholiths, widespread erosion, and burial beneath volcanic cover, but may also reflect anomalous tectonic behavior along that atypical segment of the Cordilleran margin.

Within Canada, post-Triassic internal deformation and tectonic transport of Paleozoic Antler-Sonoma allochthons during Mesozoic arc-continent collision and subsequent retroarc thrusting complicate interpretations of their original character and positions (Hansen 1990, Ghosh 1995). Allochthons of both Antler (Smith & Gehrels 1991; 1992a,b) and Sonoma (Roback et al. 1994, Roback & Walker 1995) age have been identified in the Kootenay structural arc (Figure 6) spanning the USA-Canada border. Farther north, the Sylvester allochthon emplaced above the Cassiar platform (Figure 6) is composed exclusively of post-Devonian rocks (Nelson 1993) and apparently represents only the younger allochthon of Sonoma age. Nearby, however, the widespread and internally complex Yukon-Tanana terrane (Hansen 1988) probably includes both allochthons as well as underthrust miogeoclinal facies (Hansen & Dusel-Bacon 1998). Blueschists of both Devonian (∼345 Ma) and Permian (270–260 Ma) ages are present in allochthonous Yukon-Tanana assemblages lying structurally above miogeoclinal strata along the west flank of the Cassiar platform and in the isolated Anvil allochthon (Figure 6) to the east (Erdmer et al. 1998). Juxtaposition of the Anvil allochthon against the Cassiar platform implies ∼485 km of post-thrust dextral displacement along the Tintina fault (Figure 6).

Antler-Sonoma Foreland

Tectonic loads of the overthrust Antler-Sonoma allochthons downflexed the Laurentian margin to form an elongate system of markedly asymmetric proforeland sedimentary basins extending across the miogeoclinal belt into the fringe of the interior craton (Lawton 1994, Savoy & Mountjoy 1995). The extent of the Antler foreland basin is defined by an apron of clastic sediment shed toward carbonate platforms of the interior craton, but the Sonoma foreland basin is defined only by the limit of Triassic marine strata (Figure 6). Widespread syndepositional normal faulting of Antler age along the foreland belt in Canada (Gordey et al. 1987) can be interpreted as a response to local extension induced by flexure of the foreland basin floor (Smith et al. 1993).

Proximal sandstone petrofacies along the western fringe of the Antler foreland belt are dominantly quartzolithic, a composition reflective of sediment recycling from the uplifted accretionary prisms of allochthons exposed farther west as sediment sources (Smith et al. 1993). Near the Canada-Alaska border, the ages of detrital zircons in Cambrian and Devonian sandstones suggest derivation of foreland sediment near the northern end of the Cordilleran orogen (Figure 6) from the Paleozoic Innuitian-Ellesmerian orogen of the Canadian Arctic to the northeast (Gehrels et al. 1999).

During the time interval between Antler and Sonoma thrusting along the Cordilleran margin, part of the continental block extending as far west as the Antler foreland basin and thrust front in the USA was disrupted by intracontinental reverse faulting to form yoked basins and uplifts of the Ancestral Rocky Mountains province (Figure 6). The intracontinental deformation, centered on Pennsylvanian time (Figure 1), was related to sequential intercontinental suturing along the Ouachita orogenic belt (Figure 6), where the southern flank of the Laurentian craton was drawn progressively, from east to west, into a subduction zone along the leading edge of Gondwana during the assembly of Pangea (Dickinson & Lawton 2003).

Annu. Rev. Earth Planet. Sci. 2004.32:13-45. Downloaded from arjournals.annualreviews.org
by Montana State University - Bozeman on 03/20/07. For personal use only.

Accreted Island Arcs

Segments of accreted Devonian and Permian island arcs, composed of volcanic and volcaniclastic strata and paired geotectonically with Antler and Sonoma accretionary prisms to the east, are present in the Klamath-Sierran region (Figure 6) of the Cordilleran orogen to the south of volcanic cover in the Pacific Northwest (USA). The Paleozoic Klamath-Sierran arc system evolved as a system of frontal arcs and remnant arcs during slab rollback related to closure of marginal seas between the offshore arc complex and the Cordilleran continental margin (Dickinson 2000).

Farther north in Canada, remnants of comparable Devonian to Permian arc assemblages (Rubin et al. 1990, Brown et al. 1991), underlying the Mesozoic arc assemblages of Quesnellia and Stikinia (Figure 6), are interpreted here as northern analogues of the accreted Klamath-Sierran island arcs. Both east and west of the Cassiar platform (Figure 6), overthrust allochthonous assemblages include both Devonian (365–340 Ma) and Permian (~260 Ma) granitic plutons of arc affinity (Mortensen 1992). Permian island-arc volcanics are closely associated with deformed seafloor volcanics within the internally complex Sylvester allochthon emplaced structurally above the Cassiar platform (Nelson 1993) and in correlative assemblages farther south (Ferri 1997). These occurrences of island-arc remnants within allochthonous Paleozoic assemblages suggest that severe structural telescoping in Canada during superposed mid-Mesozoic arc-continent suturing and later Mesozoic-Cenozoic retroarc thrusting closely juxtaposed island-arc and subduction-zone tectonic elements of Antler-Sonoma age that remain largely separate farther south.

MESOZOIC-CENOZOIC ARC-TRENCH SYSTEM

A Permian-Triassic (284–232 Ma) magmatic arc, built along the edge of Gondwanan crust in eastern Mexico (Dickinson & Lawton 2001a), was sustained by subduction of oceanic crust beneath present-day central Mexico (Figure 6). The northern margin of the subducting Mezcalera plate along the southwestern edge of

Annu. Rev. Earth Planet. Sci. 2004.32:13-45. Downloaded from arjournals.annualreviews.org
by Montana State University - Bozeman on 03/20/07. For personal use only.

Laurentia was defined by the sinistral California-Coahuila transform, which offset the Caborca block of miogeoclinal strata, together with underlying basement and a structurally superposed allochthon of overthrust Paleozoic strata (Figure 6), from southern California into northwestern Mexico (Dickinson 2000, Dickinson & Lawton 2001a). Farther northwest, the transform fault obliquely truncated, along a northwest-southeast trend, island-arc complexes trending northeast-southwest that were accreted to the continental block in the Klamath-Sierran region by Antler-Sonoma orogenesis. Initiation of subduction beneath the truncated continental margin in mid-Early Triassic time (Dickinson 2000) closely preceded the breakup of Pangea, and was the earliest record of Cordilleran orogenesis as an integral facet of the circum-Pacific orogenic belt.

Subsequent evolution of the active Cordilleran continental margin was marked by incremental accretion of subduction complexes at a trench along the continental slope, and by arc magmatism involving both plutonism and volcanism along the edge of the continental block. Multiple imbricate thrust panels of accretionary mélange belts incorporate disrupted stratal successions of seafloor turbidites, argillite, and chert, together with pillow lavas of underlying oceanic crust and structural slices of peridotite and serpentinite derived from oceanic mantle, and with limestone enclaves representing carbonate platforms built on oceanic seamounts. Combined plutonic and volcanic contributions to arc magmatism were emplaced into and erupted through the composite Cordilleran crustal profile along a shifting belt of igneous activity that lay 100–250 km inland from the evolving subduction zone along the continental margin (Armstrong 1988, Armstrong & Ward 1991). The principal record of arc magmatism is a discontinuous alignment of deeply eroded Cretaceous granitic batholiths extending the full length of the Cordilleran orogen. Isotopic studies indicate that the granitic magmas were composed in part of juvenile mantle components and in part of recycled crustal materials (DePaolo 1981, Samson et al. 1991).

Mid-Triassic to Mid-Jurassic Cordilleran Arc

Volcanic assemblages and associated plutons of Upper Triassic to Middle Jurassic age developed within a continuous magmatic arc established along the margin of North America as modified by Antler-Sonoma tectonism. The central segment of the Triassic-Jurassic arc transected miogeoclinal and Laurentian cratonic crust along the truncated continental margin of the southwest USA (Busby-Spera 1988, Schweickert & Lahren 1993), but the arc trend extended southward across the Ouachita suture into Gondwanan crust of eastern Mexico (Dickinson & Lawton 2001a) and northward along the continental margin, as expanded by tectonic accretion, to merge with the Quesnellia or Nicola arc (Mortimer 1987) of the Canadian Cordillera (Figure 7).

The local preservation of forearc basins along the western flank of the nascent Cordilleran arc in both the Canadian Cordillera (Travers 1978) and the USA Pacific Northwest (Dickinson 1979) show that the arc-trench system faced west,

Annu. Rev. Earth Planet. Sci. 2004.32:13-45. Downloaded from arjournals.annualreviews.org
by Montana State University - Bozeman on 03/20/07. For personal use only.

subducting seafloor downward beneath North America, even where relations of the arc assemblage to Laurentian basement or miogeoclinal strata are unexposed. Past speculation that the Quesnellia arc was a freestanding intraoceanic structure only accreted to North America by later collapse of an intervening marginal sea or open ocean has been discounted by recent isotopic studies (Unterschutz et al. 2002, Erdmer et al. 2002). The backarc region was flooded in Canada by marine waters, but was occupied in the USA by desert ergs (Figure 7), with the accommodation space for both sedimentary assemblages probably provided by subsidence of the flank of the continental block under the geodynamic influence of a subducted slab in the mantle beneath (Lawton 1994).

West of the Triassic-Jurassic Cordilleran arc assemblage lies a paired subduction complex of mélange and variably deformed thrust panels of oceanic strata forming the Cache Creek terrane and its correlatives in the Canadian Cordillera, the central mélange belt (Baker terrane) of the Pacific Northwest, coeval assemblages in the central Klamath Mountains and the Sierra Nevada foothills of California, and remnants of the Arperos oceanic realm formed on the Mezcalera plate in central Mexico. This nearly continuous alignment of disrupted oceanic materials, conveniently termed the Cache Creek belt (Mortimer 1986), forms a suture zone trapped between the Triassic-Jurassic continental margin and various accreted arc assemblages lying farther west (Figure 7).

The suture belt is probably a compound subduction complex formed of combined tectonic elements added to the flank of North America at a trench lying just offshore from the Triassic-Jurassic Cordilleran arc but also accreted to the flank of intraoceanic arc structures as they approached the Cordilleran margin, with both components representing offscrapings from intervening paleo-Pacific seafloor. Cache Creek blueschists formed by subduction-zone metamorphism have yielded isotopic ages of 230–210 Ma (Late Triassic) in both Canada and the USA (Erdmer et al. 1998), where stratal components of the suture belt range in age from Carboniferous (locally Devonian) to Early or Middle Jurassic (Cordey et al. 1987, Blome and Nestell 1991, Cordey & Schiarizza 1993, Dickinson 2000, Struik et al. 2001, Orchard et al. 2001). In Mexico, where accretion of an intraoceanic arc to the continental margin occurred much later than farther north, only Permian to Early Cretaceous rocks are present within the suture belt of central Mexico (Dickinson & Lawton 2001a).

Mid-Jurassic to Mid-Cretaceous Arc Accretion

In Jurassic-Cretaceous time, tectonic accretion at the Cordilleran subduction zone was punctuated by the arrival of intraoceanic island arcs subducting seafloor downward to the west, rather than to the east, to produce arc-continent collisions (Godfrey & Dilek 2000, Ingersoll 2000, Dickinson 2001). For evaluating accretionary tectonism, a distinction must be drawn (Wright 1982) between incremental accretion within evolving subduction complexes (so-called disrupted terranes), even where far-traveled oceanic components are incorporated, and bulk accretion

Annu. Rev. Earth Planet. Sci. 2004.32:13-45. Downloaded from arjournals.annualreviews.org
by Montana State University - Bozeman on 03/20/07. For personal use only.

of tectonic elements transported intact, as integral exotic terranes, to the continental margin. Arc accretion expanded the continental edge by closing the Cache Creek suture and induced the subduction zone and the magmatic arc along the Cordilleran margin to step outward away from the continental interior. Subsequent Cordilleran arc magmatism was widely superimposed on the accreted arc and mélange terranes (van der Heyden 1992, Friedman & Armstrong 1995). The ages of the oldest superimposed plutons of the Cordilleran magmatic arc reflect north-south diachroneity of arc accretion from Middle Jurassic (~170 Ma) as far south as central California (Schweickert et al. 1999) to Early Cretaceous (~120 Ma) in Mexico (Dickinson & Lawton 2001a).

CANADIAN TECTONIC ELEMENTS In Canada, two principal accreted tectonic elements, the Stikinia arc and the Insular superterrane, lie west of the Cache Creek suture belt (Figure 7). The Insular superterrane along the present continental fringe includes the Alexander terrane, a Paleozoic arc assemblage of largely pre-Devonian rocks overlain by less deformed Devonian to Permian strata including abundant limestone (Butler et al. 1997), and the Wrangellia terrane, a largely post-Carboniferous succession of Permian arc volcanics and overlying Triassic basalt capped by Upper Triassic limestone (Jones et al. 1977). The two components of the Insular superterrane were amalgamated by Carboniferous time, long before their joint incorporation into the Cordilleran continental margin, for they were both locally intruded by the same pluton (Gardner et al. 1988).

The Stikinia arc farther east is composed dominantly of Upper Triassic to Middle Jurassic volcanic and volcaniclastic rocks, intruded by cogenetic plutons (Marsden & Thorkelson 1992, Mihalynuk et al. 1994, Anderson 1993, Currie & Parrish 1997, MacIntyre et al. 2001). The arc assemblage is flanked on the northeast by a forearc basin (Dickie & Hein 1995, Johannson et al. 1997), lying adjacent to the Cache Creek suture in a position showing that the Stikinia arc faced the Cordilleran margin and subducted seafloor downward to the west. The ages of the youngest arc-forearc strata and the oldest strata in the postaccretion Jurassic-Cretaceous Bowser basin (MacLeod & Hills 1990), resting unconformably on Stikinia (Figure 7), indicate accretion of the northern part of Stikinia by early Middle Jurassic closure of the Cache Creek suture in either Aalenian (Ricketts et al. 1992) or early Bajocian (Thomson et al. 1986, Anderson 1993) time. The youngest strata known from the adjacent segment of the Cache Creek suture belt are Early Jurassic in age (Struik et al. 2001), but farther south in Canada deformed strata of the Cache Creek belt include strata as young as late Middle Jurassic (Callovian) in the Bridge River terrane (Cordey & Schiarizza 1993). The difference in stratal ages along tectonic strike suggest progressive southward closure of the Cache Creek suture from a tectonic hinge point on the north.

STIKINIA-QUESNELLIA OROCLINE Along tectonic strike to the north, the Stikinia arc merges, around the northern limit of the Cache Creek belt, with the northern end of the petrologically and lithologically similar Quesnellia arc along the edge

Annu. Rev. Earth Planet. Sci. 2004.32:13-45. Downloaded from arjournals.annualreviews.org
by Montana State University - Bozeman on 03/20/07. For personal use only.

of Triassic-Jurassic North America (Figure 7). This spatial relationship suggests that the Stikinia arc formed originally as a northern extension of the Quesnellia arc, but that oroclinal bending of the Quesnellia-Stikinia arc trend during continued subduction backfolded Stikinia against the Cordilleran margin to juxtapose Stikinia against Quesnellia across the Cache Creek suture, which was thereby enclosed within the tectonic orocline (Nelson & Mihalynuk 1993, Mihalynuk et al. 1994). Paleomagnetic data (May & Butler 1986, Vandall & Palmer 1990) showing no detectable latitudinal movement of Stikinia with respect to North America are compatible with the enclosure interpretation, and isotopic data indicating juvenile crustal origins are similar for Stikinia and Quesnellia arc assemblages (Samson et al. 1989, Smith et al. 1995). Pre-Mesozoic underpinnings of both Stikinia and Quesnellia include Devonian to Permian arc assemblages (Brown et al. 1991, Currie & Parrish 1997), inferred here to have been accreted to Laurentia during Antler-Sonoma events (Figure 6). Both Mesozoic arc assemblages also overlap depositionally upon deformed Paleozoic assemblages (Mortensen 1992, Roback & Walker 1995, Dostal et al. 2001, Acton et al. 2002), interpreted here as overthrust Antler-Sonoma allochthons.

Most of the contact zone between the Stikinia arc and the Insular superterrane is occupied by a sliver of strongly deformed pre-Mesozoic strata, forming a western arm of the Yukon-Tanana terrane (Gehrels et al. 1991, 1992) including the Taku terrane (Gehrels 2002), which underlie the Mesozoic arc assemblage of Stikinia and are regarded here as a product of Antler-Sonoma orogenesis oroclinally deformed along with Stikinia (Figures 6 and 7). The contact zone was overlapped by thick Upper Jurassic (Oxfordian) to Lower Cretaceous (Albian) strata of the intraarc Gravina basin (McClelland et al. 1992), but underlying metavolcanic rocks that also overlap the contact zone document initial accretion of the Insular superterrane to the western flank of Stikinia by Middle Jurassic (~175 Ma) time (Gehrels 2001). Mid-Cretaceous thrusting later carried rocks east of the contact zone over the Gravina basin and the Insular superterrane (Gehrels et al. 1990, Rubin & Saleeby 1992).

INSULAR ARC ACCRETION As the Stikinia arc demonstrably faced east, subduction along its western flank could not have drawn the Insular superterrane toward the continental margin. Accordingly, Early to Middle Jurassic arc magmatism (190–165 Ma) within the Insular superterrane, as displayed in the Queen Charlotte Islands (Lewis et al. 1991) and on Vancouver Island (DeBari et al. 1999), is viewed here as evidence for activation of subduction along the eastern flank of the Insular superterrane, to draw the Insular superterrane closer to the back side of the Stikinia arc by subducting intervening seafloor downward to the west. The polarity of the Jurassic arc along the Insular superterrane is seemingly confirmed along tectonic strike to the northwest, beyond the head of the Gulf of Alaska, where Lower to Middle Jurassic plutons intruding the Wrangellia component of the Insular superterrane on the Alaska Peninsula display transverse compositional gradients indicative of a magmatic arc facing the continent (Reed et al. 1983).

Annu. Rev. Earth Planet. Sci. 2004.32:13-45. Downloaded from arjournals.annualreviews.org
by Montana State University - Bozeman on 03/20/07. For personal use only.

Paleomagnetic data suggest that the Alexander terrane lay in the Arctic region near Baltica in mid-Paleozoic time, but that the associated Wrangellia terrane lay near the paleolatitude of the Pacific Northwest by Late Triassic time (Butler et al. 1997). Apparently, the Insular superterrane drifted as an intraoceanic arc structure within the paleo-Pacific Ocean, along paths that cannot be specified with present information, through late Paleozoic and early Mesozoic time before its accretion to the Cordilleran margin along the back side of Stikinia. If the sliver of the Yukon-Tanana terrane along the west flank of Stikinia includes miogeoclinal facies, as seems likely (Gehrels 2000), the oroclinal rotation of Stikinia was apparently initiated by calving of Stikinia off the edge of the Laurentian margin during backarc rifting. The complex plate motions required to achieve accretion of both the Stikinia arc and the Insular superterrane to the Cordilleran margin in the same general time frame (intra-Jurassic) are indeterminate with present information.

PACIFIC NORTHWEST RECONSTRUCTION The longitudinal correlation of premid-Cretaceous tectonic elements southward across the Pacific Northwest from Canada into the USA has long been a challenge (Monger et al. 1982) because of widespread Neogene volcanic cover (Figure 8*A*), the complex kinematics of an intersecting knot of strike-slip faults of latest Cretaceous to Eocene age spanning the USA-Canada border (Figures 7, 9), and structural complexity within the metamorphic cores of mountain ranges near the USA-Canada border where Cretaceous structural telescoping obscured earlier tectonic relationships between older rock masses.

An apparently satisfactory tectonic reconstruction is achieved here (Figure 8*B*) by reversing 105–110 km of Eocene (44–34 Ma) dextral slip on the Fraser River–Straight Creek fault zone and 110–115 km of previous dextral slip on the offset Yalakom–Ross Lake fault system of latest Cretaceous (<75 Ma) to Eocene age (Kleinspehn 1985, Umhoefer & Kleinspehn 1995, Umhoefer & Miller 1996, Umhoefer & Schiarizza 1996) and by backrotating the Oregon-Washington Coast Range and the Blue Mountains by 50° each (Figure 8) to recover clockwise tectonic rotations imposed during Eocene time (Heller et al. 1987, Dickinson 2002).

In Figure 8, the southern extension of the Stikinia arc assemblage includes the Cadwallader terrane of southern British Columbia (Rusmore 1987, Rusmore et al. 1988, Umhoefer 1990, Rusmore & Woodsworth 1991) and the Triassic-Jurassic Cascade River–Holden belt (Hopson & Mattinson 1994) in the Cascade Mountains east of the Straight Creek fault. Inland extensions of the Insular superterrane include the Chilliwack, Bowen Lake, and Harrison Lake terranes of southern British Columbia (Friedman et al. 1990, Mahoney et al. 1995), the Swakane Gneiss (Nason terrane) east of the Straight Creek fault in the Cascade Mountains (Mattinson 1972), and the Wallowa–Seven Devils segment of Wrangellia in the Blue Mountains. The Cache Creek suture belt flanking the Triassic-Jurassic continental margin is reconstructed as an alignment of similar lithologic units, including the Cache Creek and Bridge River terranes of southern British Columbia, the Hozameen terrane spanning the USA-Canada border, the Baker terrane of the Blue Mountains, and

Annu. Rev. Earth Planet. Sci. 2004.32:13-45. Downloaded from arjournals.annualreviews.org
by Montana State University - Bozeman on 03/20/07. For personal use only.

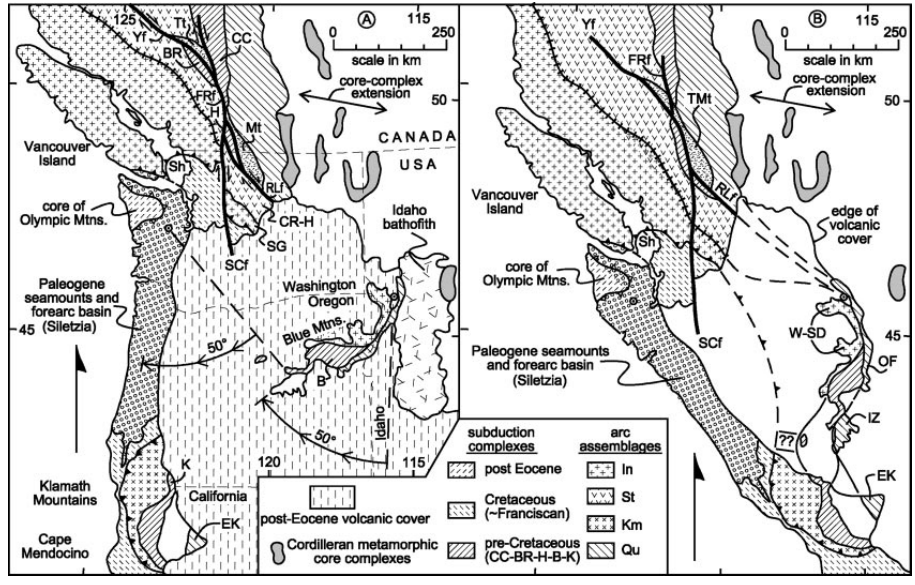


Figure 8 Pre-Oligocene geotectonic features in the Pacific Northwest (USA) and adjacent Canada at present (*A*) and as reconstructed (*B*) before clockwise rotations of the Oregon-Washington Coast Range and Blue Mountains provinces, and before dextral slip on branching faults near the USA-Canada border. Arc assemblages: In, Insular (SG, Swakane Gneiss; W-SD, Wallowa–Seven Devils); Km, accreted western Klamath Mountains arcs; Qu, Quesnellia and related terranes (IZ, Izee forearc basin; EK, eastern Klamath Mountains Mesozoic arc, OF, Olds Ferry terrane or Huntington arc); St, Stikinia (CR-H, Cascade River–Holden belt). Pre-Late Jurassic subduction-complex terranes: B, Baker; BR, Bridge River; CC, Cache Creek; H, Hozameen, K, central Klamath Mountains mélange belt. Other geologic features: Sh, Shuksan thrust system (schematic); TMt, Tyaughton–Methow trough (offset segments: Mt, Methow trough; Tt, Tyaughton trough).

Annu. Rev. Earth Planet. Sci. 2004.32:13-45. Downloaded from arjournals.annualreviews.org
by Montana State University - Bozeman on 03/20/07. For personal use only.

the central mélange belt of the Klamath Mountains (Figure 8*B*). Closer proximity of restored tectonic elements near the USA-Canada border to counterparts in the Blue Mountains could be achieved by additional recovery of the significant Eocene intracontinental extension recorded by Cordilleran core complexes (Figure 8) in southeastern British Columbia (Dickinson 2002).

The Tyaughton-Methow trough (Figure 8) was initiated in Early Jurassic time as a forearc basin flanking the Quesnellia arc (Anderson 1976), but evolved during Late Jurassic and Early Cretaceous time to overlap the accreted Stikinia arc (Garver 1992, Umhoefer et al. 2002). West and south of the Shuksan thrust system (Figure 8), an internally deformed underthrust assemblage, including Upper Jurassic to Lower Cretaceous blueschists and clastic strata (Brown 1987, Brandon et al. 1988, Monger 1991), is presumed to be a northern counterpart of the late Mesozoic Franciscan subduction complex and associated forearc basins of coastal California to the south (Brown & Blake 1987).

USA-MEXICO ARC ACCRETION The Insular superterrane extends as far south as the Blue Mountains (Figure 8) of the Pacific Northwest, where intense mid-Cretaceous crustal telescoping near the Snake River has thrust strata of Wrangellia beneath the Mesozoic continental margin (Lund & Snee 1988). Stratigraphic analysis of Blue Mountains terranes indicates, however, that initial accretion of the Wrangellia component of the Insular superterrane was completed in Middle Jurassic (Bajocian) time (Follo 1992, White et al. 1992, Avé Lallemant 1995), coordinate with accretion farther north in Canada. The oroclinally deformed Stikinia arc apparently does not extend farther south than the Cascades Mountains along the USA-Canada border (Figure 8), and there is no indication that active magmatism was still underway at the southern end of the Insular superterrane when the Wallowa–Seven Devils segment (Figure 8) of Wrangellia was drawn passively into a subduction zone along the continental margin (Dickinson 1979).

Accreted intraoceanic arc assemblages of Jurassic age in the Klamath Mountains and Sierra Nevada foothills of California rest on ophiolitic basement formed near the Triassic-Jurassic time boundary (Dilek 1989, Edelman 1990, Hacker & Ernst 1993, Wright & Wyld 1994, Hacker et al. 1995), as does the Guerrero superterrane (Figure 7) of western Mexico (Dickinson & Lawton 2001a). The accreted Mesozoic arc complexes in the USA and Mexico can perhaps be regarded as southern extensions and descendants of the Jurassic arc along the Insular superterrane where subduction continued southward across paleo-Pacific oceanic crust lying beyond the southern limits of the older Alexander and Wrangellia terranes. In California, severely deformed mélange belts separate accreted arc assemblages on the west from the pre-Jurassic continental margin (Wright 1982, Edelman & Sharp 1989, Edelman et al. 1989b, Dilek et al. 1990, Hacker et al. 1993), but a superimposed magmatic arc built along the Cordilleran continental margin across the accreted tectonic elements by late Middle Jurassic (Callovian) time (Wright & Fahan 1988, Edelman 1990, Edelman et al. 1989a, Harper et al. 1994, Girty et al. 1995) implies arc accretion during early Middle Jurassic (Bajocian) time (170–165 Ma).

Annu. Rev. Earth Planet. Sci. 2004.32:13-45. Downloaded from arjournals.annualreviews.org
by Montana State University - Bozeman on 03/20/07. For personal use only.

In the southwestern USA and Mexico, final closure of the oceanic realm between accreted Mesozoic arcs and the Cordilleran continental margin in Early Cretaceous time promoted slab rollback of the Mezcalera plate to induce crustal extension within the overriding continental block (Dickinson & Lawton 2001a). The resulting border rift belt, including the Bisbee basin and Chihuahua trough, supplanted arc magmatism along the USA-Mexico border region (Figure 7), with Late Jurassic rifting accompanied by bimodal magmatism and followed by Early Cretaceous thermotectonic subsidence (Dickinson & Lawton 2001b). Farther north, the extensional Utah-Idaho trough (Figure 7) of Middle to Late Jurassic age and development of a wide zone of Late Jurassic to Early Cretaceous backarc magmatism (Figure 7) closely followed arc accretion along the California continental margin to the west (Dickinson 2001). Earlier Middle Jurassic thrusting along the Luning-Fencemaker thrust (Wyld 2002), which carried the fill of the Auld Lang Syne backarc basin eastward (Figure 7), coincided closely in timing with arc accretion farther west.

Mid-Cretaceous to Mid-Tertiary Cordilleran Arc

Following Jurassic-Cretaceous arc accretion at the evolving subduction zone along the continental margin, the Cordilleran magmatic arc stepped oceanward to a trend that was largely superimposed upon accreted terranes (Figure 9). Massive Late Cretaceous plutonism, continuing until mid-Eocene time in Canada, formed the major Cordilleran batholith belt along the arc axis. To the west, a parallel belt of Jurassic-Cretaceous forearc basins is prominent along the coastal fringes of the USA and Mexico, and lies immediately inland from exposures of the Jurassic-Cretaceous subduction complex forming the Franciscan superterrane (Figure 9). Farther north in Canada, however, Cenozoic modification of the continental margin by strike slip along the Cenozoic Queen Charlotte transform and its splays has largely disrupted or submerged tectonic elements of the late Mesozoic forearc region.

Past speculation (Cowan et al. 1997), based on paleomagnetic data, that the western part of the Canadian Cordillera, including a large segment of the Cretaceous batholith belt, was transported northward in Cretaceous-Paleocene time from an origin along the continental margin of California or Mexico encounters the insuperable difficulty that no segment of the Cretaceous arc-trench system is missing from California or Mexico (Figure 9). The anomalously shallow paleomagnetic vectors that gave rise to the hypothesis of large lateral displacements can be interpreted instead as the result of widespread pluton tilt coupled with compaction in sedimentary strata (Butler et al. 2001).

Crustal shortening across the Cordilleran orogen gave rise by Late Jurassic time in Canada (Cant & Stockmal 1989) and mid-Early Cretaceous time in the USA (Dickinson 2001) to initiation of a backarc thrust belt that was continuous from the interior flank of the Canadian Cordillera into the Sevier thrust belt (Figure 9). The tectonic load of the thrust sheets downflexed an extensive retroforeland basin with a

Annu. Rev. Earth Planet. Sci. 2004.32:13-45. Downloaded from arjournals.annualreviews.org
by Montana State University - Bozeman on 03/20/07. For personal use only.

distal fringe that extended well into the continental interior. Deformation within the Canadian Cordillera produced intraorogen thrusting associated with development of the Skeena foldbelt (Evenchick 1991) accompanied by downflexure of the Sustut basin, and analogous intraorogen deformation formed the Eureka thrust belt in the USA (Figure 9).

Scattered plutons of Late Cretaceous age present in the interior hinterland of the backarc thrust belt, but most prominent in the Omineca region of the Canadian Cordillera (Figure 9), were not an integral facet of the arc magmatism active farther west, but instead were derived largely from sources within underthrust continental crust. Backarc thrusting and the associated retroforeland basin did not extend as far south as the region occupied until mid-Cretaceous time by the Bisbee basin and related rift troughs along the USA-Mexico border. Although somewhat diachronous in timing, backarc rifting (Figure 7) and backarc thrusting (Figure 9) occupied different realms marked by distinct contrasts in geodynamics along the Cordilleran orogen.

In Canada, arc magmatism along the eastern flank of the Coast batholith continued until mid-Eocene time (~45 Ma), as did deformation along the backarc thrust belt. Farther south, however, in both the USA and Mexico, subhorizontal subduction of the Farallon plate during latest Cretaceous through Eocene time altered the progress of both magmatism and tectonism (Dickinson & Snyder 1978). Inland migration and diminution of igneous activity led to a magmatic null through much of the USA Cordillera (Figure 1), and basement-involved crustal shortening produced yoked uplifts and basins of the Laramide Rocky Mountains well inland from the continental margin (Figure 9).

Deformation began ~70 Ma throughout the Laramide Rocky Mountains while thrusting was still underway along the Sevier thrust belt to the west, but its termination was diachronous (Dickinson et al. 1988). The development of Laramide basins and uplifts was complete in the northern part of the Laramide province by mid-Eocene time (~50 Ma), coincident with the terminal phase of deformation along the Sevier thrust belt to the west (DeCelles 1994). Farther south, however, Laramide deformation continued until the end of Eocene time. In Mexico, south of the magmatic null, Laramide basin evolution (Figure 9) during Late Cretaceous and Paleocene time (Dickinson & Lawton 2001b) was accompanied by arc magmatism that migrated inland from the Cretaceous batholith belt near the coast. The time-space pattern of Laramide magmatism and deformation suggests that the shallow angle of plate descent that gave rise to both resulted from subduction of a buoyant oceanic plateau beneath the continental margin (Dickinson et al. 1988).

In the Pacific Northwest, the elongate oceanic seamount chain of Siletzia (Figure 9), which formed during Paleocene-Eocene time (Figure 1) at some unknown distance offshore, was accreted in bulk to the Cordilleran margin early in Eocene time, and was subsequently buried beneath the Eocene forearc basin (Figure 8) of the Oregon-Washington Coast Range (Heller et al. 1987). A subduction complex (Brandon & Vance 1992), composed of premid-Miocene Cenozoic

strata underthrust beneath the accreted mass of Siletzia, forms the core of the Olympic Mountains near the USA-Canada border (Figure 9). Incrementally accreted Paleocene-Eocene components of the Franciscan subduction complex are exposed along the coastal fringe of California farther south, but elsewhere most Cenozoic subduction along the Cordilleran margin occurred along an offshore zone still unexposed underwater.

CENOZOIC TAPHROGENY

Annu. Rev. Earth Planet. Sci. 2004.32:13-45. Downloaded from arjournals.annualreviews.org
by Montana State University - Bozeman on 03/20/07. For personal use only.

The Cordilleran arc orogen as a typical segment of the Circum-Pacific orogenic belt reached peak development in Late Cretaceous time. During Tertiary time, arrival at the Cordilleran margin of successive segments of spreading systems bounding the Pacific plate progressively converted segments of the continental margin into transform fault systems along the Pacific plate boundary. As the transform continental margin evolved, subsidiary strike slip and associated crustal extension disrupted the adjacent continental block and gave rise to the rift trough of the Gulf of California, an incipient ocean basin that is expanding obliquely within the transform regime (Figure 10).

North of the Tofino triple junction (Figure 10), subduction associated with waning phases of batholith generation along the coastal fringe of the Canadian Cordillera was supplanted in mid-Eocene time (Hyndman & Hamilton 1993) by dextral slip along the Queen Charlotte transform fault. The change in coastal geodynamics, from convergence to strike slip, was triggered by amalgamation of the offshore Kula and Pacific plates at ~42.5 Ma (Lonsdale 1988). Subsequent Oligocene-Miocene magmatism within the Queen Charlotte Islands was associated with evolution of a slab window (Hamilton & Dostal 2001), and the Neogene Queen Charlotte basin farther east (Figure 10) developed as a pull-apart basin within the transform system (Lewis et al. 1991). The Chatham Strait–Denali fault system, initiated in mid-Eocene time as a branch of the Queen Charlotte transform (Cole et al. 1999), has displaced segments of the Insular superterrane laterally along the continental margin (Figure 10). A discrepancy between 370 km of slip along the Denali fault and 150 km of slip along the linked Chatham Strait fault suggests that 220 km of slip parallel to the continental margin, southward from the elbow where those two fault segments meet, was accommodated by the Coast shear zone along the eastern flank of the Insular superterrane (Gehrels 2000).

Farther south, subduction along the Cordilleran margin continues at the foot of the continental slope along an offshore trend parallel to and coextensive with the active Cascades volcanic arc of the Pacific Northwest (Figure 10). Arc volcanism, which extended southward through the USA in Miocene time (Figure 10), was progressively extinguished south of the Cascades arc by evolution of the San Andreas transform system along the continental margin as the Mendocino triple junction (Figure 10) migrated northward to shorten the Cascades subduction zone. Beginning near the Oligocene-Miocene time boundary, slab-window volcanism evolved in coastal California along a belt parallel to the evolving San Andreas

Annu. Rev. Earth Planet. Sci. 2004.32:13-45. Downloaded from arjournals.annualreviews.org
by Montana State University - Bozeman on 03/20/07. For personal use only.

transform (Dickinson 1997). Neogene arc volcanism was extinguished in similar fashion within Baja California when the Rivera triple junction (Figure 10) migrated southward in mid-Miocene time to a position near the mouth of the modern Gulf of California.

Following Laramide events, establishment of mid-Cenozoic arc magmatism along a trend near the USA-Mexico continental margin had been accomplished by the migration of successive volcanic fronts toward the coast (Figure 10) as the slab of oceanic lithosphere subducting beneath the Cordilleran orogen steepened or foundered (Dickinson 2002). Subsequent initiation of the San Andreas transform along the continental margin in Early Miocene time triggered crustal extension within the Basin and Range taphrogen (Figure 10), where multiple fault blocks distended the Cordilleran orogen once the continental block was partly coupled to the Pacific plate. A largely intact remnant of the mid-Cenozoic arc assemblage lies along the Sierra Madre Occidental (Figure 10), where flat-lying volcanic strata form an enclave of largely undistended crust enclosed within the Basin and Range taphrogen. Baja California was calved from mainland Mexico when the San Andreas transform plate boundary south of the USA jumped inland in Late Miocene time to open the Gulf of California by oblique extension.

In the Pacific Northwest (USA), extensive volcanic fields of flood basalt that have erupted behind the Cascades volcanic arc since Early Miocene time mask older rock assemblages over wide areas (Figure 10). The volcanism may have been related to mantle advection induced by deformation of the continental lithosphere after shear was imposed on the continental block by interaction of the Pacific and American plates along the San Andreas transform system at the continental margin (Dickinson 1997). Less voluminous but comparably extensive Middle Miocene and younger volcanic fields of basaltic character in the Canadian Cordillera (Edwards & Russell 2000) may reflect analogous shear coupling of the Pacific and American plates along the nearby Queen Charlotte transform.

SUMMARY PERSPECTIVES

The questions posed in the introduction can be answered as follows:

1. The Cordilleran system, as an integral segment of the circum-Pacific orogenic belt, was established when subduction was initiated between Early and Late Triassic time along a continental margin that had been delineated by Neoproterozoic rifting during the breakup of Rodinia, and later modified in late Paleozoic and earliest Mesozoic time by the emplacement of oceanic allochthons upon the edge of the continental block during the final assembly of Pangea.
2. Rock masses native to the Cordilleran margin include the miogeoclinal prism deposited between Neoproterozoic and Late Devonian time along a passive continental margin, volcanic and plutonic rocks of the Cordilleran magmatic

arc built along an active continental margin from mid-Triassic time to the present, and the sedimentary and volcanic assemblages of basins and lava fields superimposed upon the miogeoclinal succession and the arc assemblage.

3. Accreted tectonic elements include subduction complexes thrust bodily over the miogeoclinal prism in Devonian-Mississsippian and Permian-Triassic time; intraoceanic island arcs sutured to the continental block at those times and also later, between Middle Jurassic and Early Cretaceous time; and subduction complexes accreted incrementally to the continental block at the Cordilleran subduction zone between Late Triassic and mid-Cenozoic time.
4. Postmid-Cenozoic internal distension and incipient dislocation of Cordilleran crust has occurred in response to transform tectonism imposed on the continental margin when intra-Pacific seafloor spreading systems impinged on the Cordilleran trench.

The *Annual Review of Earth and Planetary Science* is online at http://earth.annualreviews.org

Annu. Rev. Earth Planet. Sci. 2004.32:13-45. Downloaded from arjournals.annualreviews.org by Montana State University - Bozeman on 03/20/07. For personal use only.

LITERATURE CITED

Acton SL, Simony PS, Heaman LM. 2002. Nature of the basement to Quesnel terrane near Christina Lake, southeastern British Columbia. *Can. J. Earth Sci.* 39:65–78

Anderson P. 1976. Oceanic crust and arc-trench gap tectonics in southwestern British Columbia. *Geology* 4:443–46

Anderson RG. 1993. A Mesozoic stratigraphic and plutonic framework for northwestern Stikinia (Iskut River area), northwestern British Columbia, Canada. In *Mesozoic Paleogeography of the Western United States—II*, ed. GC Dunne, KA McDougall, Book 74, pp. 477–94. Los Angeles: Pacif. Sect. SEPM (Soc. Sediment. Geol.)

Armin RA, Mayer L. 1983. Subsidence analysis of the Cordilleran miogeocline: implications for timing of late Proterozoic rifting and amount of extension. *Geology* 11:702–5

Armstrong RL. 1988. Mesozoic and early Cenozoic magmatic evolution of the Canadian Cordillera. In *Processes in Continental Lithospheric Deformation*, ed. SP Clark Jr, BC Burchfiel, J Suppe, Spec. Pap. 218, pp. 55– 91. Boulder, CO: Geol. Soc. Am.

Armstrong RL, Ward PL. 1991. Late Triassic to earliest Eocene magmatism in the North America Cordillera: implications for the Western Interior Basin. In *The Evolution of the Western Interior Basin*, ed. WGE Caldwell, EG Kauffman, Spec. Pap. 39, pp. 49–72. Ottawa, Can: Geol. Assoc. Can.

Armstrong RL, Eisbacher GH, Evans PD. 1982. Age and stratigraphic-tectonic significance of Proterozoic diabase sheets, Mackenzie Mountains, northwestern Canada. *Can. J. Earth Sci.* 19:316–23

Avé Lallemant HG. 1995. Pre-Cretaceous tectonic evolution of the Blue Mountains province, northeastern Oregon. *U.S. Geol. Surv. Prof. Pap.* 1438:271–304

Blome CD, Nestell MK. 1991. Evolution of a Permo-Triassic sedimentary mélange, Grindstone terrane, east-central Oregon. *Geol. Soc. Am. Bull.* 103:1280–96

Bond GC, Kominz M. 1984. Construction of tectonic subsidence curves for the early Paleozoic miogeocline, southern Canadian Rocky Mountains: implications for subsidence mechanisms, age of breakup, and crustal thinning. *Geol. Soc. Am. Bull.* 95: 155–73

Annu. Rev. Earth Planet. Sci. 2004.32:13-45. Downloaded from arjournals.annualreviews.org
by Montana State University - Bozeman on 03/20/07. For personal use only.

Bond GC, Kominz MA, Devlin WR. 1983. Thermal subsidence and eustasy in the lower Palaeozoic miogeocline of western North America. *Nature* 306:775–79

Brandon MT, Vance JA. 1992. Tectonic evolution of the Cenozoic Olympic subduction complex, Washington state, as deduced from fission track ages for detrital zircons. *Am. J. Sci.* 292:565–636

Brandon MT, Cowan DS, Vance JA. 1988. *The Late Cretaceous San Juan Thrust System, San Juan Islands, Washington*, Spec. Pap. 221. Boulder, CO: Geol. Soc. Am. 81 pp.

Brown EH. 1987. Structural geology and accretionary history of the northwest Cascades system, Washington and British Columbia. *Geol. Soc. Am. Bull.* 99:201–14

Brown EH, Blake MC, Jr. 1987. Correlation of Early Cretaceous blueschists in Washington, Oregon, and northern California. *Tectonics* 6:795–806

Brown DA, Logan JM, Gunning MH, Orchard MJ, Bamber WE. 1991. Stratigraphic evolution of the Paleozoic Stikine assemblage in the Stikine and Iskut River area, northwestern British Columbia. *Can. J. Earth Sci.* 28:958–72

Busby-Spera CJ. 1988. Speculative tectonic model for the early Mesozoic arc of the southwest Cordilleran United States. *Geology* 16:1121–25

Butler RF, Gehrels GE, Bazard DR. 1997. Paleomagnetism of Paleozoic strata of the Alexander terrane, southeastern Alaska. *Geol. Soc. Am. Bull.* 109:1372–88

Butler RF, Gehrels GE, Kodama KP. 2001. A moderate translation alternative to the Baja British Columbia hypothesis. *GSA Today* 11(6):4–10

Cant DE, Stockmal GS. 1989. The Alberta foreland basin: relationship between stratigraphy and Cordilleran terrane-accretion events. *Can. J. Earth Sci.* 26:1964–75

Challand G, Rageau J-P. 1985. *A Strategic Atlas.* New York: Harper & Row. 224 pp.

Cole RB, Ridgway KD, Layer PW, Drake J. 1999. Kinematics of basin development during the transition from terrane accretion to strike-slip tectonics, Late Cretaceous–early Tertiary Cantwell Formation, south central Alaska. *Tectonics* 18:1224–44

Colpron M, Logan JM, Mortensen JK. 2002. U-Pb zircon age constraint for late Neoproterozoic rifting and initiation of the lower Paleozoic passive margin of western Laurentia. *Can. J. Earth Sci.* 39:133–43

Coney PJ, Jones DL, Monger JWH. 1980. Cordilleran suspect terranes. *Nature* 288: 329–33

Cordey F, Schiarizza P. 1993. Long-lived Panthalassic remnant: the Bridge River accretionary complex, Canadian Cordillera. *Geology* 21:263–66

Cordey F, Mortimer N, DeWever P, Monger JWH. 1987. Significance of Jurassic radiolarians from the Cache Creek terrane, British Columbia. *Geology* 15:1151–54

Cowan DS, Brandon MT, Garver JI. 1997. Geologic tests of hypotheses for large coastwise displacements—a critique illustrated by the Baja British Columbia controversy. *Am. J. Sci.* 297:117–73

Currie LD, Parrish RK. 1997. Paleozoic and Mesozoic rocks of Stikinia exposed in northwestern British Columbia: implications for correlations in the northern Cordillera. *Geol. Soc. Am. Bull.* 109:1402–20

Dalziell IWD. 1992. Antarctica: a tale of two supercontinents? *Annu. Rev. Earth Planet. Sci.* 20:501–26

DeBari SM, Anderson RG, Mortensen JK. 1999. Correlation among lower to upper crustal components in an island arc, Vancouver Island, Canada. *Can. J. Earth Sci.* 36:1371–413

DeCelles PG. 1994. Late Cretaceous-Paleocene synorogenic sedimentation and kinematic history of the Sevier thrust belt, northeast Utah and southwest Wyoming. *Geol. Soc. Am. Bull.* 106:32–56

DePaolo DJ. 1981. A neodymium and strontium isotopic study of the Mesozoic calc-alkaline granitic batholiths of the Sierra Nevada and Peninsular Ranges, California. *J. Geophys. Res.* 86:10470–88

Annu. Rev. Earth Planet. Sci. 2004.32:13-45. Downloaded from arjournals.annualreviews.org
by Montana State University - Bozeman on 03/20/07. For personal use only.

Devlin WJ. 1989. Stratigraphy and sedimentology of the Hamill Group in the northern Selkirk Mountains, British Columbia: evidence for latest Proterozoic–Early Cambrian extensional tectonism. *Can. J. Earth Sci.* 26:515–33

Devlin WJ, Bond GC 1988. The initiation of the early Proterozoic Cordilleran miogeocline: evidence from the uppermost Proterozoic–Lower Cambrain Hamill Group of southeastern British Columbia. *Can. J. Earth Sci.* 25:1–19

Devlin WJ, Brueckner HK, Bond GC. 1988. New isotopic data and a preliminary age for volcanics near the base of the Windermere Supergroup, northeastern Washington, U.S.A. *Can. J. Earth Sci.* 25:1906–11

Dickie JR, Hein FJ. 1995. Conglomeratic fan deltas and submarine fans of the Jurassic Laberge Group, Whitehorse trough, Yukon Territory, Canada: fore-arc sedimentation and unroofing of a volcanic island arc complex. *Sediment. Geol.* 98:263–92

Dickinson WR. 1977. Subduction tectonics in Japan. *Am. Geophys. Union Trans.* 58:948–52

Dickinson WR. 1979. Mesozoic forearc basin in central Oregon. *Geology* 7:166–70

Dickinson WR. 1997. Tectonic implications of Cenozoic volcanism in coastal California. *Geol. Soc. Am. Bull.* 109:936–54

Dickinson WR. 2000. Geodynamic interpretation of Paleozoic tectonic trends oriented oblique to the Mesozoic Klamath-Sierran continental margin in California. In *Paleozoic and Triassic Paleogeography and Tectonics of Western Nevada and Northern California*, ed. MJ Soreghan, GE Gehrels, Spec. Pap. 347, pp. 209–45. Boulder, CO: Geol. Soc. Am.

Dickinson WR. 2001. Tectonic setting of the Great Basin through geologic time: implications for metallogeny. In *Regional Tectonics and Structural Control of Ore: The Major Gold Trends of Northern Nevada*, ed. DR Shaddrick, E Zbinden, DC Mathewson, C Prenn, Spec. Publ. 33, pp. 27–53. Reno, NV: Geol. Soc. Nev.

Dickinson WR. 2002. The Basin and Range province as a composite extensional domain. *Int. Geol. Rev.* 44:1–38

Dickinson WR, Lawton TF. 2001a. Carboniferous to Cretaceous assembly and fragmentation of Mexico. *Geol. Soc. Am. Bull.* 113:1142–60

Dickinson WR, Lawton TF. 2001b. Tectonic setting and sandstone petrofacies of the Bisbee basin (USA-Mexico). *J. S. Am. Earth Sci.* 14:475–501

Dickinson WR, Lawton TF. 2003. Sequential intercontinental suturing as the ultimate control for Pennsylvanian Ancestral Rocky Mountains deformation. *Geology* 31:609–12

Dickinson WR, Snyder WS. 1978. Plate tectonics of the Laramide orogeny. In *Laramide Folding Associated With Basement Block Faulting in the Western United States*, ed. V Mathews III, Mem. 151, pp. 355–66. Boulder: Geol. Soc. Am.

Dickinson WR, Swift PN, Coney PJ. 1986. Tectonic strip maps of Alpine-Himalayan and Circum-Pacific orogenic belts (great circle projections). *Geol. Soc. Am. Map Chart Ser.* MC-58

Dickinson WR, Klute MA, Hayes MJ, Janecke SU, Lundin ER, et al. 1988. Paleogeographic and paleotectonic setting of Laramide sedimentary basins in the central Rocky Mountain region. *Geol. Soc. Am. Bull.* 100:1023–39

Dilek Y. 1989. Tectonic significance of post-accretion rifting of an early Mesozoic oceanic basement in the northern Sierra Nevada metamorphic belt, California. *J. Geol.* 97:503–18

Dilek Y, Thy P, Moores EM, Grundvig S. 1990. Late Paleozoic–early Mesozoic oceanic basement of a Jurassic arc terrane in the northwestern Sierra Nevada, California. See Harwood & Miller 1990, pp. 351–69

Dilek Y, Moores EM, Elthon D, Nicolas A, eds. 2000. *Ophiolites and Oceanic Crust: New Insights from Field Studies and the Ocean Drilling Program*, Spec. Pap. 349. Boulder, CO: Geol. Soc. Am.

Annu. Rev. Earth Planet. Sci. 2004.32:13-45. Downloaded from arjournals.annualreviews.org
by Montana State University - Bozeman on 03/20/07. For personal use only.

Dostal J, Church BN, Hoy T. 2001. Geological and geochemical evidence for variable magmatism and tectonics in the southern Canadian Cordillera: Paleozoic to Jurassic suites, Greenwood, southern British Columbia. *Can. J. Earth Sci.* 38:75–90

Dunne GC, McDougall KA, eds. 1993. *Mesozoic Paleogeography of the Western United States—II*. Los Angeles: Pacif. Sect., SEPM (Soc. Sediment. Geol.). Book 71

Edelman SH. 1990. *Paleozoic and Early Mesozoic Paleogeographic Relations; Sierra Nevada, Klamath Mountains, and Related Terranes*, See Harwood & Miller 1990, pp. 371–78

Edelman SH, Sharp WD. 1989. Terranes, early faults, and pre-Late Jurassic amalgamation of the western Sierra Nevada metamorphic belt, California. *Geol. Soc. Am. Bull.* 101:1420–33

Edelman SH, Day HW, Bickford ME. 1989a. Implications of U-Pb ages for the tectonic settings of the Smartville and Slate Creek complexes, northern Sierra Nevada, California. *Geology* 17:1032–35

Edelman SH, Day HW, Moores EM, Zigan SM, Murphy TP, Hacker BR. 1989b. *Structure Across a Mesozoic Ocean-Continent Suture Zone in the Northern Sierra Nevada, California*, Spec. Pap. 224. Boulder, CO: Geol. Soc. Am. 56 pp.

Edwards BR, Russell JK. 2000. Distribution, nature, and origin of Neogene-Quaternary magmatism in the northern Cordilleran volcanic province, Canada. *Geol. Soc. Am. Bull.* 112:1280–95

Erdmer P, Ghent ED, Archibald DA, Stout MZ. 1998. Paleozoic and Mesozoic high-pressure metamorphism at the margin of ancestral North America in central Yukon. *Geol. Soc. Am. Bull.* 110:615–29

Erdmer P, Moore JM, Heaman L, Thompson RI, Daughtry KL, Creaser RA. 2002. Extending the ancient margin outboard in the Canadian Cordillera: record of Proterozoic crust and Paleocene regional metamorphism in the Nicola horst, southern British Columbia. *Can. J. Earth Sci.* 39:1605–23

Evans KV, Aleinikoff JN, Obradovich JD, Fanning JM. 2000. SHRIMP U-Pb geochronology of volcanic rocks, Belt Supergroup, western Montana: evidence for rapid deposition of sedimentary strata. *Can. J. Earth Sci.* 37:1287–300

Evenchick CA. 1991. Geometry, evolution, and tectonic framework of the Skeena fold belt, north central British Columbia. *Tectonics* 10:527–46

Fedo CM, Cooper JD. 2001. Sedimentology and sequence stratigraphy of Neoproterozoic and Cambrian units across the craton-margin hinge zone, southeastern California, and implications for the early evolution of the Cordilleran margin. *Sediment. Geol.* 141-142:501–22

Ferri F. 1997. Nina Creek Group and Lay Range assemblage, north-central British Columbia: remnants of late Paleozoic oceanic and arc terranes. *Can. J. Earth Sci.* 34:854–74

Follo MF. 1992. Conglomerates as clues to the sedimentary and tectonic evolution of a suspect terrane: Wallowa Mountains, Oregon. *Geol. Soc. Am. Bull.* 104:1561–76

Foster DA, Gray DR. 2000. Evolution and structure of the Lachlan fold belt (orogen) of eastern Australia. *Annu. Rev. Earth Planet. Sci.* 28:47–80

Friedman RM, Armstrong RL. 1995. Jurassic and Cretaceous geochronology of the southern Coast Belt, British Columbia, 49° to 51° N. See Miller & Busby 1995, pp. 95–139

Friedman RM, Monger JWH, Tipper HW. 1990. Age of the Bowen Island Group, southwestern Coast Mountains, British Columbia. *Can. J. Earth Sci.* 27:1456–61

Gardner MC, Bergman SC, Cushing GW, MacKevett EM Jr, Plafker G, et al. 1988. Pennsylvanian stitching of Wrangellia and the Alexander terrane, Wrangell Mountains, Alaska. *Geology* 16:967–71

Garver JI. 1992. Provenance of Albian-Cenomanian rocks of the Methow and Tyaughton basins, southern British Columbia: a mid-Cretaceous link between North America and the Insular terrane. *Can. J. Earth Sci.* 29:1274–95

Annu. Rev. Earth Planet. Sci. 2004.32:13-45. Downloaded from arjournals.annualreviews.org
by Montana State University - Bozeman on 03/20/07. For personal use only.

Gehrels GE. 2000. Reconnaissance geology and U-Pb geochronology of the western flank of the Coast Mountains between Juneau and Skagway, southeastern Alaska. In *Tectonics of the Coast Mountains, Southeastern Alaska and British Columbia*, ed. HH Stowell, WC McClelland, Spec. Pap. 343, pp. 213–33. Boulder, CO: Geol. Soc. Am.

Gehrels GE. 2001. Geology of the Chatham Sound region, southeast Alaska and coastal British Columbia. *Can. J. Earth Sci.* 38: 1579–99

Gehrels GE. 2002. Detrital zircon geochronology of the Taku terrane, southeast Alaska. *Can. J. Earth Sci.* 39:921–31

Gehrels GE, McClelland WC, Samson SD, Patchett PJ, Jackson JL. 1990. Ancient continental margin assemblage in the northern Coast Mountains, southeast Alaska and northwest Canada. *Geology* 18:208–11

Gehrels GE, McClelland WC, Samson SD, Patchett PJ. 1991. U-Pb geochronology of detrital zircons from a continental margin assemblage in the northern Coast Mountains, southeastern Alaska. *Can. J. Earth Sci.* 28:1285–300

Gehrels GE, McClelland WC, Samson SD, Patchett PJ. 1992. Geology of the western flank of the Coast Mountains between Cape Fanshaw and Taku Inlet, southeastern Alaska. *Tectonics* 11:567–85

Gehrels GE, Johnsson MJ, Howell DG. 1999. Detrital zircon geochronology of the Adams Argillite and Nation River Formation, east-central Alaska, U.S.A. *J. Sediment. Res.* 69:135–44

Girty GH, Hanson RE, Girty MS, Schweickert RA, Harwood DS, et al. 1995. Timing of emplacement of the Haypress Creek and Emigrant Gap plutons: implications for the timing and controls of Jurassic orogenesis, northern Sierra Nevada, California. See Miller & Busby 1995, pp. 191–201

Ghosh DK. 1995. Nd-Sr isotopic constraints on the interactions of the Intermontane Superterrane with the western edge of North America in the southern Canadian Cordillera. *Can. J. Earth Sci.* 32:1740–58

Godfrey NJ, Dilek Y. 2000. Mesozoic assimilation of oceanic crust and island arc into the North American continental margin in California and Nevada: insights from geophysical data. See Dilek et al. 2000, pp. 365–82

Gordey SP, Abbott JG, Tempelman-Kluit DJ, Gabrielse H. 1987. "Antler" clastics in the Canadian Cordillera. *Geology* 15:103–7

Hacker BR, Ernst WG. 1993. Jurassic orogeny in the Klamath Mountains: a geochronological analysis. See Dunne & McDougall 1993, pp. 37–59

Hacker BR, Ernst WG, McWilliams MO. 1993. Genesis and evolution of a Permian-Jurassic magmatic arc/accretionary wedge, and reevaluation of terranes in the central Klamath Mountains. *Tectonics* 12:387–409

Hacker BR, Donato MM, Barnes CG, McWilliams MO, Ernst WG. 1995. Timescales of orogeny: Jurassic construction of the Klamath Mountains. *Tectonics* 14:677–703

Hamilton TS, Dostal J. 2001. Melting of heterogeneous mantle in a slab window environment: examples from the middle Tertiary Masset basalts, Queen Charlotte Islands, British Columbia. *Can. J. Earth Sci.* 38:825–38

Hansen VL. 1988. A model for terrane accretion, Yukon-Tanana and Slide Mountain terranes, northwest North America. *Tectonics* 6:1167–77

Hansen VL. 1990. Yukon-Tanana terrane: a partial acquittal. *Geology* 18:365–69

Hansen VL, Dusel-Bacon C. 1998. Structural and kinematic evolution of the Yukon-Tanana upland tectonites, east-central Alaska: a record of late Paleozoic to Mesozoic crustal assembly. *Geol. Soc. Am. Bull.* 110:211–30

Harper GD, Saleeby JB, Heizler M. 1994. Formation and emplacement of the Josephine ophiolite and the Nevadan orogeny in the Klamath Mountains, California-Oregon: U/Pb sircon and $^{40}Ar/^{39}Ar$ geochronology. *J. Geophys. Res.* 99:4293–321

Harwood DS, Miller MM, eds. 1990. *Paleozoic and Early Mesozoic Paleogeographic*

Annu. Rev. Earth Planet. Sci. 2004.32:13-45. Downloaded from arjournals.annualreviews.org
by Montana State University - Bozeman on 03/20/07. For personal use only.

Relations; Sierra Nevada, Klamath Mountains, and Related Terranes, Spec. Pap. 225. Boulder, CO: Geol. Soc. Am.

Heller PL, Tabor RW, Suczek CA. 1987. Paleogeographic evolution of the United States Pacific Northwest during Paleogene time. *Can. J. Earth Sci.* 24:1652–67

Hopson CA, Mattinson JM. 1994. Chelan migmatite complex, Washington: field evidence for mafic magmatism, crustal anatexis, mixing, and protodiapiric emplacement. In *Guides to Field Trips, 1994 Geological Society of America Annual Meeting, Seattle, Washington*, ed. DA Swanson, RA Haugerud, pp. 22–23. Seattle: Univ. Wash.

Hyndman RD, Hamilton TS. 1993. Queen Charlotte area Cenozoic tectonics and volcanism and their association with relative plate motions along the northeastern Pacific margin. *J. Geophys. Res.* 98:14257–77

Ingersoll RV. 2000. Models for emplacement of Jurassic ophiolites of northern California. See Dilek et al. 2000, pp. 395–402

Johannson GG, Smith PL, Gordey SP. 1997. Early Jurassic evolution of the northern Stikinian arc: evidence from the Laberge Group, northwestern British Columbia. *Can. J. Earth Sci.* 34:1030–57

Jones DJ, Silberling NJ, Hillhouse J. 1977. Wrangellia—a displaced terrane in northwestern North America. *Can. J. Earth Sci.* 14:2565–77

Karlstrom KE, Harlan SS, Williams HL, McClelland J, Geissman JW, Ahäll KI. 1999. Refining Rodinia: geologic evidence for the Australia–western U.S. connection in the Proterozoic. *GSA Today* 9(10):1–7

Kleinspehn KL 1985. Cretaceous sedimentation and tectonics, Tyaughton–Methow basin, southwestern British Columbia. *Can. J. Earth Sci.* 22:154–74

Lawton TF. 1994. Tectonic setting of Mesozoic sedimentary basins, Rocky Mountain region, United States. In *Mesozoic Systems of the Rocky Mountain Region, USA*, ed. MV Caputo, JA Peterson, KJ Franczyk, pp. 1–25. Denver, CO: Rocky Mountain Sec., SEPM (Soc. Sediment. Geol.).

Lawver LA, Scotese CR. 1987. A revised reconstruction of Gondwanaland. In *Gondwanaland Six: Structure, Tectonics, and Geophysics*, Monogr. 40, pp. 17–23. Washington, DC: Am. Geophys. Union Geophys.

Le Pichon X. 1983. Pangée, géoïde et convection. *C.R. Acad. Sci. Paris (Ser. II).* 296:1313–20

Le Pichon X, Huchon P, Barrier, E. 1985. Pangea, the geoid and the evolution of the western margin of the Pacific Ocean. In *Formation of Active Ocean Margins*, ed. N Nasu, K Kobayashi, S Uyeda, I Kushiro, H Kagami, pp. 3–42. Tokyo: Terra Sci.

Levy M, Christie-Blick N. 1991. Tectonic subsidence of the early Paleozoic passive continental margin in eastern California and southern Nevada. *Geol. Soc. Am. Bull.* 103:1590–606

Lewis PD, Haggart JW, Anderson RG, Hickson CJ, Thompson RI, et al. 1991. Triassic to Neogene geologic evolution of the Queen Charlotte region. *Can. J. Earth Sci.* 28:854–69

Li Z-X, Li X-H, Zhou H, Kinny PD. 2002. Grenvillian continental collision in south China: new SHRIMP U-Pb zircon results and implications for the configuration of Rodinia. *Geology* 30:163–66

Lickorish HW, Simony PS. 1995. Evidence for late rifting of the Cordilleran margin outlined by stratigraphic division of the Lower Cambrian Gog Group, Rocky Mountain main ranges, British Columbia and Alberta. *Can. J. Earth Sci.* 32:860–74

Lonsdale P. 1988. Paleogene history of the Kula plate: offshore evidence and onshore implications. *Geol. Soc. Am. Bull.* 100:733–54

Luepke JJ, Lyons TW. 2001. Pre-Rodinian (Mesoproterozoic) supercontinental rifting along the western margin of Laurentia: geochemical evidence from the Belt-Purcell Supergroup. *Precambrian Res.* 111:79–90

Lund K, Snee LW. 1988. Metamorphism, structural development, and age of the continent–island arc juncture in west-central Idaho. In *Metamorphism and Crustal Evolution of the Western United States*, ed. WG Ernst,

Annu. Rev. Earth Planet. Sci. 2004.32:13-45. Downloaded from arjournals.annualreviews.org
by Montana State University - Bozeman on 03/20/07. For personal use only.

pp. 296–331. Englewood Cliffs, NJ: Prentice Hall

Lund K, Aleinikoff JN, Evans KV, Fanning CM. 2003. SHRIMP U-Pb geochronology of the Neoproterozoic Windermere Supergroup, central Idaho: implications for rifting of western Laurentia and synchroneity of Sturtian glacial deposits. *Geol. Soc. Am. Bull.* 113:349–72

MacIntyre DG, Villeneuve ME, Schiarizza P. 2001. Timing and tectonic setting of Stikine terrane magmatism, Babine–Takla Lakes area, central British Columbia. *Can. J. Earth Sci.* 38:579–601

MacLeod SE, Hills LV. 1990. Conformable Late Jurassic–Early Cretaceous strata, northern Bowser basin, British Columbia: a sedimentological and paleontological model. *Can. J. Earth Sci.* 27:988–98

MacNaughton RB, Narbonne GM, Dalrymple RW. 2000. Neoproterozoic slope deposits, Mackenzie Mountains, northwestern Canada: implications for passive-margin development and Ediacaran faunal ecology. *Can. J. Earth Sci.* 37:997–1020

Mahoney JB, Friedman RM, McKinley SD. 1995. Evolution of a Middle Jurassic volcanic arc: stratigraphic, isotopic, and geochemical characteristics of the Harrison Lake Formation, southwestern British Columbia. *Can. J. Earth Sci.* 32:1759–76

Manspeizer W, Cousminer HL. 1988. Late Triassic–Early Jurassic synrift basins of the U.S. Atlantic margin. In *The Atlantic Continental Margin*, ed. RE Sheridan, JA Grow, Vol. I-2, pp. 197–216. Boulder, CO: Geol. Soc. Am. Geol. N. Am.

Marsden H, Thorkelson DJ. 1992. Geology of the Hazelton volcanic belt in British Columbia: implications for the Early to Middle Jurassic evolution of Stikinia. *Tectonics* 11:1266–87

Mattinson JM. 1972. Ages of zircons from the northern Cascade Mountains, Washington. *Geol. Soc. Am. Bull.* 83:3769–84

May SR, Butler RF. 1986. North American Jurassic apparent polar wander: implications for plate motion, paleogeography, and Cordilleran tectonics. *J. Geophys. Res.* 91:11519–44

McClelland WC, Gehrels GE, Saleeby JB. 1992. Upper Jurassic–Lower Cretaceous basinal strata along the Cordilleran margin: implications for the accretionary history of the Alexander-Wrangellia-Peninsular terrane. *Tectonics* 11:823–35

Meert JG, Van der Voo R. 1997. The assembly of Gondwana 800–550 Ma. *J. Geodyn.* 23:223–35

Mihalynuk MG, Nelson JL, Diakow LJ. 1994. Cache Creek terrane entrapment: oroclinal paradox within the Canadian Cordillera. *Tectonics* 13:575–95

Miller DM, Busby C, eds. 1995. *Jurassic Magmatism and Tectonics of the North American Cordillera*, Spec. Pap. 299. Boulder, CO: Geol. Soc. Am.

Monger JWH. 1991. Correlation of the Settler Schist with the Darrington Phyllite and Shuksan Greenschist and its tectonic implications, Coast and Cascade Mountains, British Columbia and Washington. *Can. J. Earth Sci.* 28:447–58

Monger JWH, Price RA, Tempelman-Kluit DJ. 1982. Tectonic accretion and the origin of the two major metamorphic and plutonic welts in the Canadian Cordillera. *Geology* 10:70–75

Mortensen JK. 1992. Pre-mid-Mesozoic tectonic evolution of the Yukon-Tanana terrane, Yukon and Alaska. *Tectonics* 11:836–53

Mortimer N. 1986. Late Triassic, arc-related, potassic igneous rocks in the North American Cordillera. *Geology* 14:1035–38

Mortimer N. 1987. The Nicola Group: Late Triassic and Early Jurassic subduction-related volcanism in British Columbia. *Can. J. Earth Sci.* 24:2521–36

Nelson JL. 1993. The Sylvester allochthon: upper Paleozoic marginal-basin and island-arc terranes in northern British Columbia. *Can. J. Earth Sci.* 30:631–43

Nelson JA, Mihalynuk M. 1993. Cache Creek ocean: closure or enclosure? *Geology* 21:173–76

Orchard MJ, Cordey F, Rui L, Bamber EW, Mamet B, et al. 2001. Biostratigraphic and

Annu. Rev. Earth Planet. Sci. 2004.32:13-45. Downloaded from arjournals.annualreviews.org
by Montana State University - Bozeman on 03/20/07. For personal use only.

biogeographic constraints on the Carboniferous to Jurassic Cache Creek terrane in central British Columbia. *Can. J. Earth Sci.* 38:551–78

Patrick BE, McClelland WC. 1995. Late Proterozoic granitic magmatism on Seward Peninsula and a Barentian origin for Alaska-Chukotka. *Geology* 23:81–84

Prave AR. 1999. Two diamictites, two cap carbonates, two δ^{13} excursions, two rifts. *Geology* 27:339–42

Rainbird RH, Jefferson CW, Young GM. 1996. The early Neoproterozoic sedimentary succession B of northwestern Laurentia: correlations and paleogeographic significance. *Geol. Soc. Am. Bull.* 108:454–70

Ramos VA, Aleman A. 2000. Tectonic evolution of the Andes. In *Tectonic Evolution of South America*, ed. UG Cordani, EJ Milani, AT Filho, DA Campos, pp. 635–85. Rio de Janeiro: Int. Geol. Congr. (31st)

Reed BL, Miesch AT, Lanphere MA. 1983. Plutonic rocks of Jurassic age in the Alaska-Aleutian Range batholith: chemical variations and polarity. *Geol. Soc. Am. Bull.* 94:1232–40

Ricketts BD, Evenchick CA, Anderson RG, Murphy DC. 1992. Bowser basin, northern British Columbia: constraints on the timing of initial subsidence and Stikinia–North America terrane interactions. *Geology* 20:1119–22

Roback JC, Walker NW. 1995. Provenance, detrital zircon U-Pb geochronometry, and tectonic significance of Permian to Lower Triassic sandstone in southeastern Quesnellia, British Columbia and Washington. *Geol. Soc. Am. Bull.* 107:665–75

Roback RC, Sevigny JH, Walker NW. 1994. Tectonic setting of the Slide Mountain terrane, southern British Columbia. *Tectonics* 13:1242–58

Ross GM. 1991. Tectonic setting of the Windermere Supergroup revisited. *Geology* 19:1125–28

Ross GM, Parrish RR, Winston W. 1992. Provenance and U-Pb geochronology of the Mesoproterozoic Belt Supergroup (northwestern United States): implications for age of deposition and pre-Panthalassa reconstructions. *Earth Planet. Sci. Lett.* 113:57–76

Ross GM, Villenueve ME, Theriault RJ. 2001. Isotopic provenance of the lower Muskwa assemblage (Mesoproterozoic, Rocky Mountains, British Columbia): new clues to correlation and source areas. *Precambrian Res.* 111:57–77

Rubin CM, Saleeby JB. 1992. Tectonic history of the eastern edge of the Alexander terrane, southeast Alaska. *Tectonics* 11:586–602

Rubin CM, Miller MM, Smith GM. 1990. Tectonic development of Cordilleran mid-Paleozoic volcano-plutonic complexes: evidence for convergent-margin tectonism. See Harwood & Miller 1990, pp. 1–16

Rusmore ME. 1987. Geology of the Cadwallader Group and the Intermontane–Insular superterrane boundary, southwestern British Columbia. *Can. J. Earth Sci.* 24:2279–91

Rusmore ME, Woodsworth GJ. 1991. Distribution and tectonic significance of Upper Triassic terranes in the eastern Coast Mountains and adjacent Intermontane Belt, British Columbia. *Can. J. Eath Sci.* 28:532–41

Rusmore ME, Potter CJ, Umhoefer PJ. 1988. Middle Jurassic terrane accretion along the western edge of the Intermontane Superterrane, southwestern British Columbia. *Geology* 16:891–94

Samson SD, McClelland WC, Patchett PJ, Gehrels GE, Anderson RG. 1989. Evidence from neodymium isotopes for mantle contributions to Phanerozoic crustal genesis in the Canadian Cordillera. *Nature* 337:705–9

Samson SD, Patchett PJ, McClelland WC, Gehrels GE. 1991. Nd and Sr isotopic constraints on the petrogenesis of the west side of the northern Coast Mountains batholith, Alaskan and Canadian Cordillera. *Can. J. Earth Sci.* 28:939–46

Savoy LE, Mountjoy EW. 1995. Cratonic-margin and Antler-age foreland basin strata (Middle Devonian to Lower Carboniferous) of the southern Canadian Rocky Mountains and adjacent plains. In *Stratigraphic Evolution of Foreland Basins*, ed. DL Dorobek,

Annu. Rev. Earth Planet. Sci. 2004.32:13-45. Downloaded from arjournals.annualreviews.org
by Montana State University - Bozeman on 03/20/07. For personal use only.

GM Ross, Spec. Publ. 52, pp. 213–31. Tulsa, OK: SEPM (Soc. Sediment. Geol.)

Schweickert RA, Hanson RE, Girty GH. 1999. Accretionary tectonics of the western Sierra Nevada metamorphic belt. In *Geologic Field Trips in Northern California*, ed. DL Wagner, SA Graham, Spec. Publ. 119, pp. 33–79. Sacramento: Calif. Div. Mines Geol.

Schweickert RA, Lahren MM. 1993. Triassic-Jurassic magmatic arc in eastern California and western Nevada: arc evolution, cryptic tectonic breaks, and significance of the Mojave–Snow Lake fault. See Dunne & McDougall 1993, pp. 227–46

Sears JW, Price RA. 2000. New look at the Siberian connection: no SWEAT. *Geology* 28:423–26

Sears JW, Price RA. 2003. Tightening the Siberian connection to western Laurentia. *Geol. Soc. Am. Bull.* 115:943–53

Silberling NJ, Jones DL, Monger JW, Coney PJ. 1992. Lithotectonic terrane map of the North American Cordillera. *U.S. Geol. Surv. Misc. Inv. Ser. Map* I-2176

Smith AD, Brandon AD, Lambert RStJ . 1995. Nd–Sr systematics of Nicola Group volcanic rocks, Quesnel terrane. *Can. J. Earth Sci.* 32:437–46

Smith MT, Gehrels GE. 1991. Detrital zircon geochronology of upper Proterozoic to lower Paleozoic continental margin strata of the Kootenay arc: implications for the early Paleozoic tectonic development of the eastern Canadian Cordillera. *Can. J. Earth Sci.* 28:1271–84

Smith MT, Gehrels GE. 1992a. Structural geology of the Lardeau Group near Trout Lake, British Columbia: implications for the structural evolution of the Kootenay arc. *Can. J. Earth Sci.* 29:1305–19

Smith MT, Gehrels GE. 1992b. Stratigraphic comparison of the Lardeau and Covada Groups: implications for revision of stratigraphic relations in the Kootenay arc. *Can. J. Earth Sci.* 29:1320–29

Smith MT, Dickinson WR, Gehrels GE. 1993. Contractional nature of Devonian-Mississippian Antler tectonism along the North American continental margin. *Geology* 21:21–24

Snyder DB, Clowes RM, Cook FA, Erdmer P, Evenchick CA, et al. 2002. Proterozoic prism arrests suspect terranes: insights into the ancient Cordilleran margin from seismic reflection data. *GSA Today* 12 (10):4–10

Stewart JH, Amaya-Martínez R, Palmer AR. 2002. Neoproterozoic and Cambrian strata of Sonora, Mexico: Rodinian supercontinent to Laurentian continental margin. In *Contributions to Crustal Evolution of the Southwestern United States*, ed. A Barth, Spec. Pap. 365, pp. 5–48. Boulder, CO: Geol. Soc. Am.

Stewart JH, Gehrels GE, Barth AP, Link PK, Christie-Blick N, Wrucke CT. 2001. Detrital zircon provenance of Mesoproterozoic to Cambrian arenites in the western United States and northwestern Mexico. *Geol. Soc. Am. Bull.* 113:1343–56

Struik LC, Schiarizza P, Orchard MJ, Cordey E, Sano H, et al. 2001. Imbricate architecture of the upper Paleozoic to Jurassic oceanic Cache Creek terrane, central British Columbia. *Can. J. Earth Sci.* 38:496–514

Thomson RC, Smith PL, Tipper HW. 1986. Lower to Middle Jurassic (Pliensbachian to Bajocian) stratigraphy of the northern Spatsizi area, north-central British Columbia. *Can. J. Earth Sci.* 23:1965–73

Timmons JM, Karlstrom KE, Dehler CM, Geissman JW, Heizler MT. 2001. Proterozoic multistage (ca. 1.1 and 0.8 Ga) extension recorded in the Grand Canyon Supergroup and establishment of northwest- and north-trending tectonic grains in the southwestern United States. *Geol. Soc. Am. Bull.* 113:163–80

Travers WB. 1978. Overturned Nicola and Ashcroft strata and their relation to the Cache Creek Group, southwestern Intermontane Belt, British Columbia. *Can. J. Earth Sci.* 15:99–116

Umhoefer PJ. 1990. Stratigraphy and tectonic setting of the upper part of the Cadwallader terrane, southwestern British Columbia. *Can. J. Earth Sci.* 27:702–11

Umhoefer PJ, Kleinspehn KL. 1995. Mesoscale and regional kinematics of the northwestern Yalakom fault system: major Paleogene dextral faulting in British Columbia, Canada. *Tectonics* 14:78–94

Umhoefer PJ, Miller RB. 1996. Mid-Cretaceous thrusting in the southern Coast Belt, British Columbia, after strike-slip reconstruction. *Tectonics* 15:545–65

Umhoefer PJ, Schiarizza P. 1996. Latest Cretaceous to early Tertiary dextral strike-slip faulting on the southeastern Yalakom fault system, southeastern Coast Belt, British Columbia. *Geol. Soc. Am. Bull.* 108:768–85

Umhoefer PJ, Schiarizza P, Robinson M. 2002. Relay Montain Group, Tyaughton–Methow basin, southwest British Columbia: a major Middle Jurassic to Early Cretaceous terrane overlap assemblage. *Can. J. Earth Sci.* 39:1143–67

Unterschutz JLE, Creaser RA, Erdmer P, Thompson RI, Daughtry KL. 2002. North American origin of Quesnel terrane strata in the southern Canadian Cordillera: inferences from geochemical and Nd isotopic characteristics of Triassic metasedimentary rocks. *Geol. Soc. Am. Bull.* 114:462–75

Vandall TA, Palmer HC. 1990. Canadian Cordilleran displacement: paleomagnetic results from the Early Jurassic Hazelton Group, Terrane I, British Columbia, Canada. *Geophys. J. Int.* 103:609–19

Van der Heyden P. 1992. A Middle Jurassic to early Tertiary Andean-Sierran arc model for the Coast Belt of British Columbia. *Tectonics* 11:82–97

White JDL, White DL, Vallier TL, Stanley GD Jr, Ash SR. 1992. Middle Jurassic strata link Wallowa, Olds Ferry, and Izee terranes in the accreted Blue Mountains island arc, northeastern Oregon. *Geology* 20:729–32

Wright JE. 1982. Permo-Triassic accretionary subduction complex, southwestern Klamath Mountains, northern California. *J. Geophys. Res.* 87:3805–18

Wright JE, Fahan MR. 1988. An expanded view of Jurassic orogenesis in the western United States Cordillera: Middle Jurassic (pre-Nevadan) regional metamorphism and thrust faulting within an active arc environment, Klamath Mountains, California. *Geol. Soc. Am. Bull.* 100:859–76

Wright JE, Wyld SJ. 1994. The Rattlesnake Creek terrane, Klamath Mountains, California: an early Mesozoic volcanic arc and its basement of tectonically disrupted oceanic crust. *Geol. Soc. Am. Bull.* 106:1033–56

Wyld SJ. 2002. Structural evolution of a Mesozoic backarc fold-thrust belt in the U.S. Cordillera: new evidence from northern Nevada. *Geol. Soc. Am. Bull.* 114:1452–68

Yates RG. 1968. The trans-Idaho discontinuity. *23rd Int. Geol. Congr.* 1:117–23

Annu. Rev. Earth Planet. Sci. 2004.32:13-45. Downloaded from arjournals.annualreviews.org
by Montana State University - Bozeman on 03/20/07. For personal use only.

Annu. Rev. Earth Planet. Sci. 2004.32:13-45. Downloaded from arjournals.annualreviews.org
by Montana State University - Bozeman on 03/20/07. For personal use only.

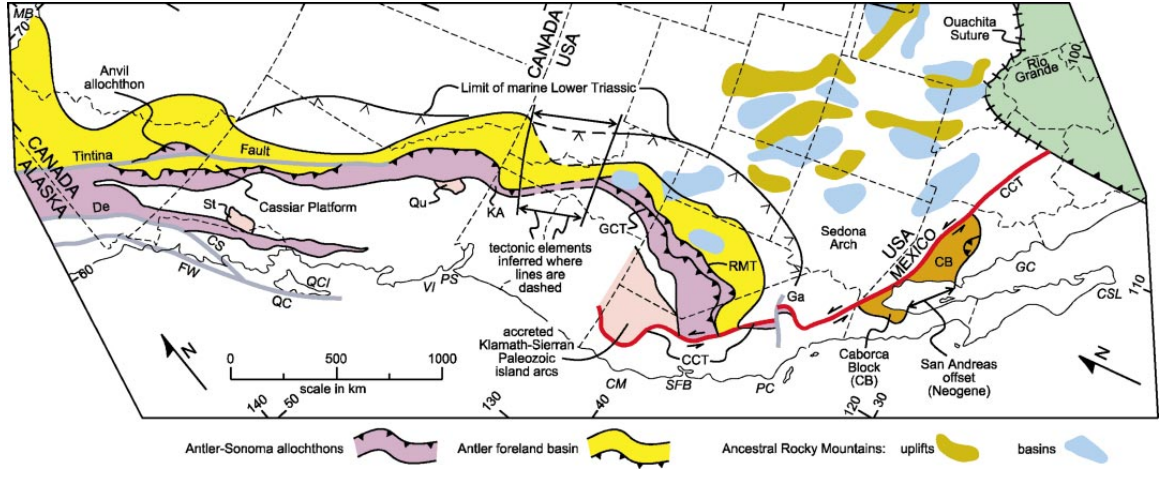


Figure 6 Geotectonic features of the Antler orogen (Late Devonian–Early Mississippian), the Ancestral Rocky Mountains province (Pennsylvanian–Early Permian), and the Sonoma orogen (Late Permian–Early Triassic) of the North American Cordillera (allochthons of Antler and Sonoma age are combined, but note the uncertain continuity of tectonic trends along the trans-Idaho discontinuity of Figure 5). See text for discussion of Kootenay structural arc (KA) and remnants of Paleozoic arc assemblages in Quesnellia (Qu) and Stikinia (St). Key active faults: RMT, Devonian-Mississippian Roberts Mountains thrust; GCT, Permian-Triassic Golconda thrust; CCT, Permian-Triassic California-Coahuila transform. Gondwanan Mexico restored (after Dickinson & Lawton 2001a) to position before mid-Mesozoic opening of the Gulf of Mexico. Tintina and De-CS-FW-QC fault systems are Cenozoic structures. See Figure 5 for geographic legend.

Annu. Rev. Earth Planet. Sci. 2004.32:13-45. Downloaded from arjournals.annualreviews.org
by Montana State University - Bozeman on 03/20/07. For personal use only.

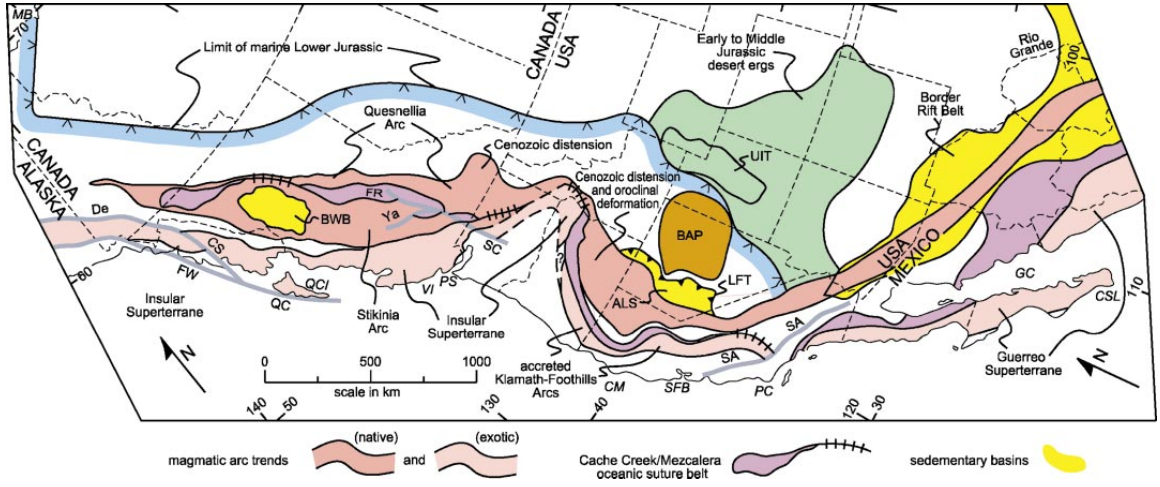


Figure 7 Mid-Early Triassic (~247.5 Ma) to mid-Early Cretaceous (~120 Ma) geotectonic features of the Cordilleran arc-trench system, including intraoceanic arc structures accreted to the Cordilleran continental margin between Middle Jurassic and Early Cretaceous time. Selected geologic features: ALS, Late Triassic to Early Jurassic Auld Lang Syne backarc basin; LFT, Middle Jurassic Luning-Fencemaker backarc thrust system; BAP, zone of diffuse Middle to Late Jurassic backarc plutonism (Nevada-Utah); UIT, Middle to Late Jurassic Utah-Idaho backarc trough; BWB, Late Jurassic to Early Cretaceous Bowser successor basin (superimposed on accreted Stikinia arc). Border rift belt (Late Jurassic to Early Cretaceous) includes Bisbee basin and Chihuahua trough. Cenozoic faults (*gray*): De-CS, Denali-Chatham Strait; FR, Fraser River; FW, Fairweather; QC, Queen Charlotte; RL, Ross Lake; SA, San Andreas; SC, Straight Creek; Ya, Yalakom. See Figure 5 for geographic legend.

Annu. Rev. Earth Planet. Sci. 2004.32:13-45. Downloaded from arjournals.annualreviews.org
by Montana State University - Bozeman on 03/20/07. For personal use only.

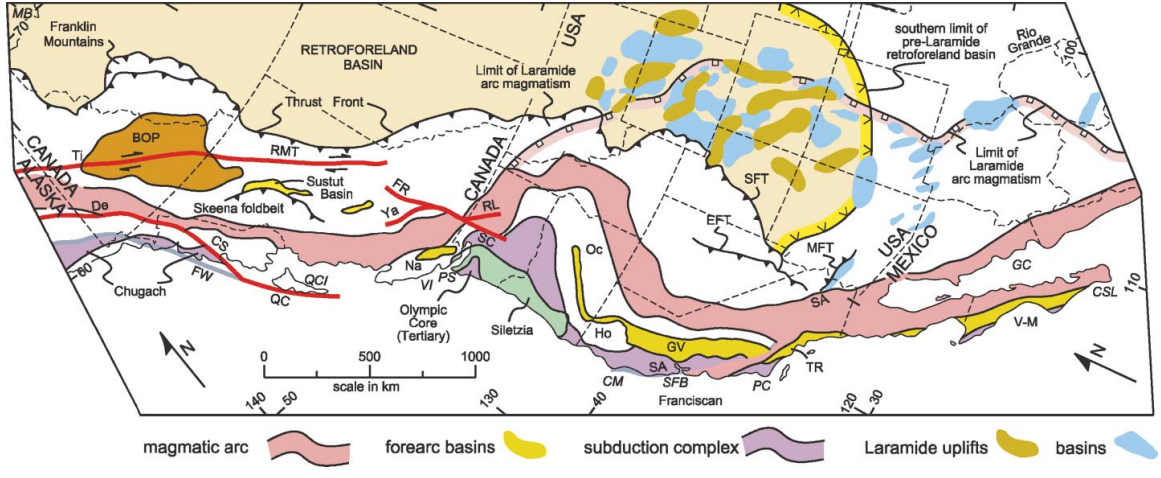


Figure 9 Mid-Early Cretaceous (~120 Ma) to mid-Cenozoic (Eocene/Oligocene boundary) geotectonic features of the Cordilleran arc-trench system, including the Laramide province of intracontinental deformation. The main batholith belt is delineated as the magmatic arc, but subsidiary arc magmatism spread inland for varying distances (BOP, Omineca zone of backarc mid-Cretaceous plutonism). Active Paleogene strike-slip faults (*red lines*): De-CS, Denali-Chatham Strait; FR, Fraser River; QC, Queen Charlotte; RL, Ross Lake; SC, Straight Creek; Ti-RMT, Tintina–Rocky Mountain Trench; Ya, Yalakom. Younger Neogene strike-slip faults (*gray lines*): FW, Fairweather; SA, San Andreas. Key active fold-thrust belts: EFT, Eureka; MFT, Maria; SFT, Sevier. Key forearc basin segments: GV, Great Valley (California); Ho, Hornbrook; Oc, Ochoco; Na, Nanaimo; TR, Transverse Ranges; V-M, Vizcaino-Magdalena. See Figure 5 for geographic legend.

Annu. Rev. Earth Planet. Sci. 2004.32:13-45. Downloaded from arjournals.annualreviews.org
by Montana State University - Bozeman on 03/20/07. For personal use only.

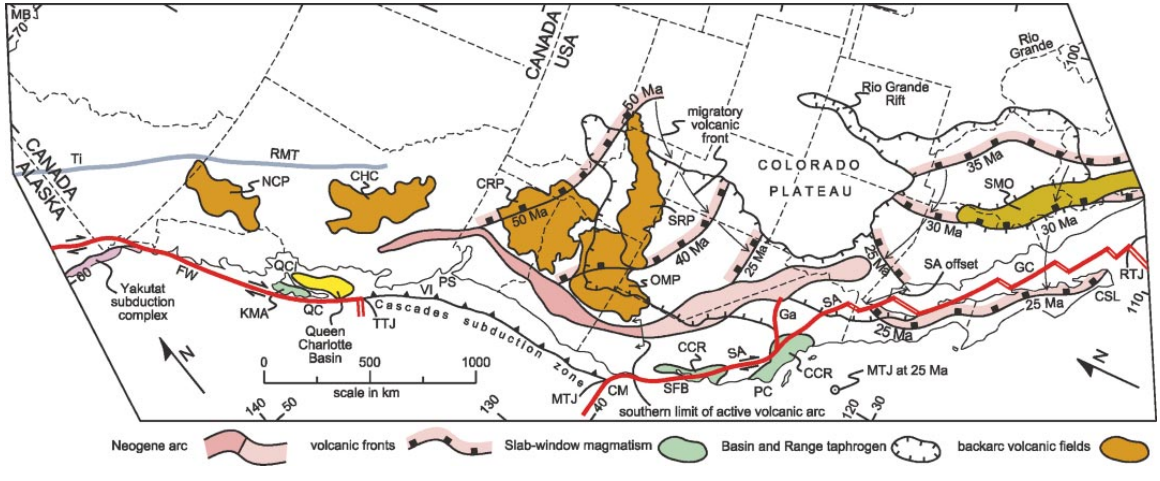


Figure 10 Post-Eocene geotectonic features of the North American Cordillera, including the Basin and Range taphrogen (SMO, Paleogene magmatic arc remnant in the Sierra Madre Occidental). Active Neogene strike-slip faults (*red lines*): FW, Fairweather; Ga, Garlock; QC, Queen Charlotte; SA, San Andreas. Offshore triple plate junctions: MTJ, Mendocino (FFT); RTJ, Rivera (RTF); TTJ, Tofino (RTF). Slab-window magmatism (near the coastal transform systems): CCR, California Coast Ranges (28–0 Ma); KMA, Queen Charlotte Islands (46–17 Ma). Backarc lava fields (erupted inland from main Cordilleran arc trend): CHC, Chilcotin (14–6 Ma); CRP, Columbia River Plateau (17–8 Ma); NCP, Northern Cordilleran Province (8–0 Ma); OMP, Oregon-Modoc Plateau (17–7 Ma); SRP, Snake River Plain (16–0 Ma). See Figure 5 for geographic legend.

Origin and Tectonic Implications of Across-Strike Geochemical Variations in the Eocene Absaroka Volcanic Province, United States

T. C. Feeley

Department of Earth Sciences, Montana State University, Bozeman, Montana 59717, U.S.A.
(e-mail: tfeeley@montana.edu)

ABSTRACT

In order better to understand the origin and significance of across-strike geochemical variations in the Eocene Absaroka volcanic province (AVP), this article compares compositional data for magmatic rocks from two eruptive centers that define type localities for major stratigraphic subdivisions of the Absaroka Volcanic Supergroup. Geochemical variations for evolved lavas indicate that the calc-alkaline differentiation trend at Washburn volcano results from mixing compositionally diverse mafic and silicic magmas, whereas the shoshonitic trend at the more easternly Sunlight volcano reflects assimilation-fractional crystallization. The mantle source for both volcanoes is, as shown by incompatible trace element contents and radiogenic isotopic ratios of mafic lavas, largely within ancient depleted lithospheric mantle later enriched by a metasomatic event characterized by low Sm/Nd and Rb/Sr ratios. The approximate timing of the enrichment event, as calculated from Nd isotopic data (2.2–2.0 Ga), is similar to estimates from other magmatic fields in the Wyoming Province. Large variations in trace element ratios of mafic lavas involving large ion lithophile elements (LILE) and light rare earth element that are not obviously reflected in isotopic ratios also indicate a recent (<100 Ma) metasomatic enrichment event. Superficially, the mantle source for Sunlight volcano appears to contain larger amounts of the young metasomatic component, as measured by high LILE/high field strength element (HFSE) ratios. Parental magmas at both volcanoes have similar HFSE contents and HFSE/heavy rare earth element ratios, however, suggesting comparable degrees of source region melting and metasomatism. Rather than variable degrees of metasomatism and partial melting, the geochemical differences between the mafic rocks are best explained by compositional heterogeneity in metasomatic fluids inherited from breakdown of different phases in hydrous peridotite. A consistent geodynamic model to account for generation of AVP magmas involves metasomatism of asthenosphere and subcontinental mantle lithosphere during shallow subduction of the Farallon plate during the Late Cretaceous through Paleocene, followed in the Eocene by foundering of the slab and primary basalt generation through major heating associated with upwelling and influx of hot asthenosphere.

Introduction

An intense episode of compositionally diverse magmatism affected large areas of the northwest United States and Canadian Cordilleras in the Eocene following Laramide crustal shortening (Armstrong 1978). One of the most voluminous magmatic fields associated with this event is the Absaroka volcanic province (AVP), which comprises ~30,000 km^3 of basaltic to rhyolitic magmatic rocks distributed over an area in excess of 23,000 km^2 in northwest Wyoming and southwest Montana (Sundell 1993; fig. 1). The traditional interpretation of the Absaroka magmatic event is that it represents a generation of mantle-derived mafic magmas and associated differentiates related to subduction of the Farallon plate beneath the northwest United States during the Eocene (Lipman et al. 1972; Armstrong 1978; Lipman 1980; Bird 1984). The principal evidence cited to support a subduction origin for the Absaroka magmas are the calc-alkaline, andesitic compositions of many of the rocks and eastward increasing K_2O contents (Chadwick 1970). The latter feature has been considered to reflect eastward increasing depths to an Eocene Benioff zone in a manner analogous to the "K-*h*" relationship of Dickinson and Hatherton (1967), which has been documented for numerous modern arcs (e.g.,

Manuscript received January 14, 2002; accepted September 30, 2002.

[The Journal of Geology, 2003, volume 111, p. 329–346] © 2003 by The University of Chicago. All rights reserved. 0022-1376/2003/11103-0006$15.00

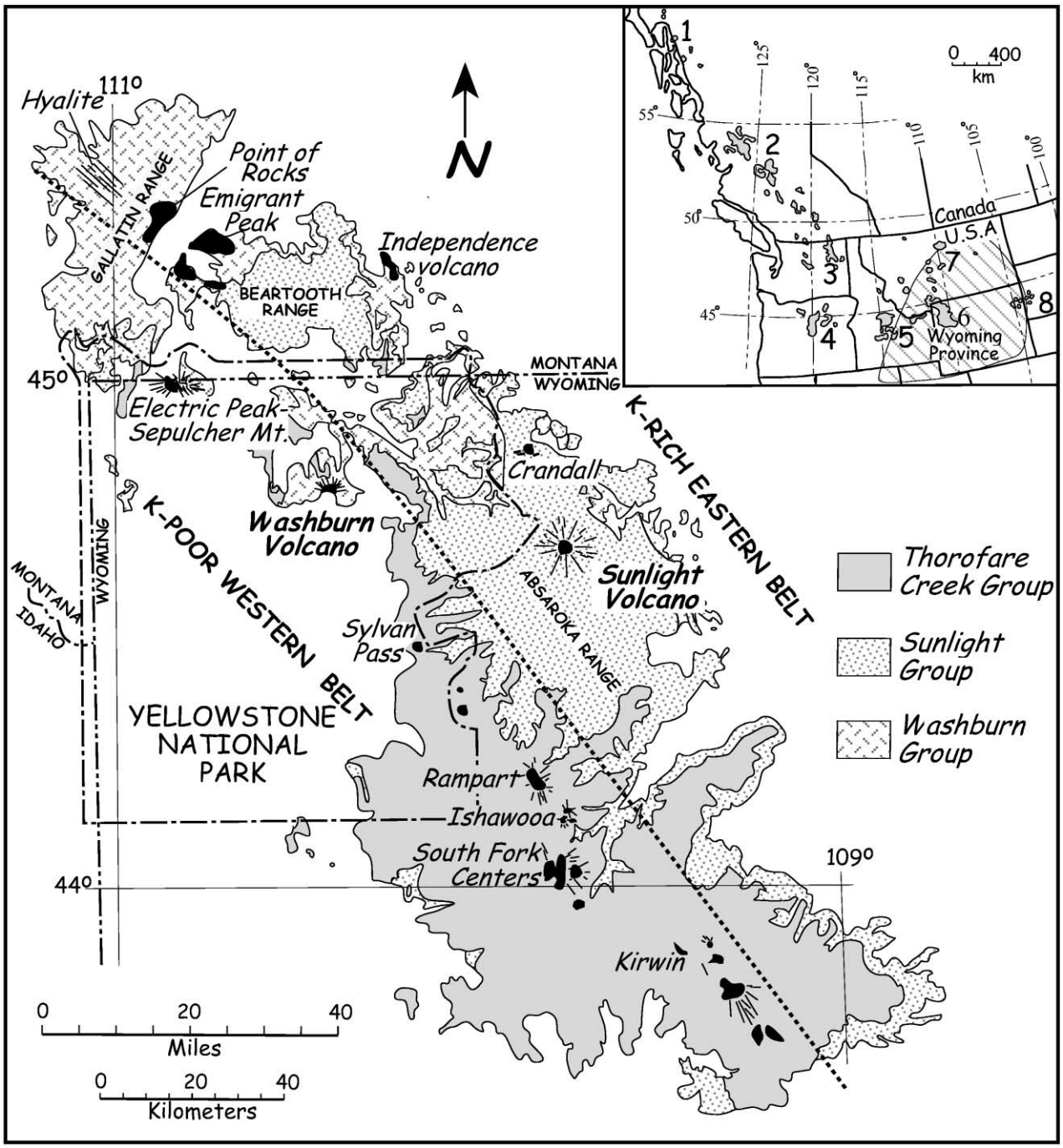


Figure 1. Map of the Absaroka volcanic province showing the stratigraphic units of the Absaroka Volcanic Supergroup of Smedes and Prostka (1972). Labeled black areas represent locations of principal vent complexes and intrusive centers discussed by Chadwick (1970). Thick dashed line shows the approximate division between western calc-alkaline and eastern shoshonitic belts (after Chadwick 1970). Single dot dashed line is the boundary of Yellowstone National Park. Inset shows the locations of early to middle Eocene magmatic fields (after Chadwick 1985; Holder and Holder 1988; Dudás 1991; Norman and Mertzman 1991; Wheeler et al. 1991; Luedke 1994). *1*, Sloko volcanic province; *2*, Francois Lake igneous complex; *3*, Colville igneous complex; *4*, Clarno volcanics; *5*, Challis volcanic province; *6*, Absaroka volcanic province; *7*, Montana alkalic province; *8*, Black Hills. Diagonally ruled field shows inferred extent of Archean cratonic Wyoming Province (Dutch and Nielsen 1990).

Gill 1981). However, a subduction origin for the Absaroka magmas has recently been indirectly challenged through work on other Eocene igneous complexes in the northwest United States and Canadian Cordilleras. These studies emphasize the contemporaneous nature of magmatism over a broad area with no linear continuity or obvious alignment of centers and the close temporal and, in some cases, spatial relationship between eruption of the Eocene magmas and crustal extension and formation of metamorphic core complexes (Wernicke et al. 1987; Dudás 1991; Hooper et al. 1995; Morris and Hooper 1997).

A proper understanding of the eastward increasing K_2O contents in the AVP has important bearings on models for the Eocene tectonic setting of the northwest United States. Previous investigations of the trend were experimental in nature and appealed to various crustal-level processes acting on uniform, subalkaline basaltic andesitic parental magmas (Meen 1987). These include variations in (1) pressures, (2) water contents, and (3) extents of fractional crystallization of parental magmas before crustal contamination. Discrimination between these options and testing whether mantle compositions and processes are also important has been hindered, however, by the lack of parallel, detailed geochemical studies on both calc-alkaline and shoshonitic eruptive centers.

In an attempt to more fully understand the origin of the across-strike K_2O trend, this article focuses on comparison of geochemical data for magmatic rocks in the central region of the AVP from two recently well-characterized Absaroka eruptive centers that define type localities for major stratigraphic subdivisions of the Absaroka Volcanic Supergroup. These are the calc-alkaline Washburn volcano and the shoshonitic Sunlight volcano (fig. 1; Feeley et al. 2002; Feeley and Cosca 2003). The objective of this article is to demonstrate that across-strike geochemical variations in the AVP, as exemplified by data from these centers, reflect a complex interplay between variable crustal differentiation processes and mantle sources. Shoshonitic series rocks at Sunlight volcano are generally more fractionated than Washburn volcano calc-alkaline rocks, whereas the latter have been modified to a larger extent by mixing with diverse composition silicic melts derived from the lower continental crust. Moreover, mafic rocks at Sunlight and Washburn volcanoes have compositional distinctions that provide unmistakable evidence for recent modification of mantle source regions by metasomatic slab-derived fluids, possibly added during an extended episode of shallow subduction of the Farallon plate during the early Tertiary.

Background: Tectonic and Geologic Setting

Regional Setting. The AVP is an important part of the widespread Eocene Challis-Kamloops volcanic belt that stretches from the northwestern United States into central British Columbia and continues to the central part of the Yukon (fig. 1). Although magmatism within the belt was initially associated with active subduction of the Farallon plate beneath North America (e.g., Lipman et al. 1972), the petrogenetic role of a subducted slab for the rocks is now controversial. For example, magmatic rocks in several volcanic fields are interpreted to contain a significant slab component, possibly added during an episode of relatively rapid, shallow angle subduction of the Farallon plate beneath the North American plate during the Cretaceous to Eocene (e.g., O'Brien et al. 1991; MacDonald et al. 1992; du Bray and Harlan 1996). In contrast, other fields show no direct evidence for subduction-related processes (Meen and Eggler 1987; Dudás 1991; Norman and Mertzman 1991; Morris and Hooper 1997). In these studies, the "arc-like" trace element signatures (e.g., high large ion lithophile element [LILE]/high field strength element [HFSE]) that characterize many of the mafic rocks are attributed to melting of ancient, metasomatically enriched lithospheric mantle by other heating or decompression mechanisms mainly associated with extensional tectonics. These models attempt to provide an explanation for the association of Eocene magmatic rocks in Idaho, northeastern Washington, and south-central British Columbia with extensional deformation and the contemporaneous nature of magmatism over a broad area with no linear continuity or obvious alignment of centers. As emphasized by Hooper et al. (1995), however, distinguishing between recent and ancient subduction-enrichment events can be difficult because both carry the same whole-rock chemical signature. In this case, the only obvious difference would be time-related changes in isotopic ratios resulting from the geochemical changes.

The bulk of the AVP magmas erupted between 55 and 45 Ma from 13 major volcanic centers situated along two subparallel northwest-trending belts: a western low-K (calc-alkaline) belt and an eastern high-K (shoshonitic) belt (fig. 1; Chadwick 1970; Harlan et al. 1996; Hiza 1999; Feeley et al. 2002; Feeley and Cosca 2003). The Absaroka volcanic rocks are traditionally divided into three groups that collectively form the Absaroka Vol-

canic Supergroup (Smedes and Prostka 1972). In ascending stratigraphic order, these are (1) the Washburn Group, (2) the Sunlight Group, and (3) the Thorofare Creek Group. The AVP magmas erupted through Archean crystalline rocks of the Wyoming Province, which are mainly granitoid gneisses that intruded high-grade metasedimentary and metavolcanic rocks ~2.8 b.yr. ago, and shallow marine carbonate and clastic sedimentary rocks ranging in age from Cambrian to Cretaceous (Ruppel 1972; Wooden and Mueller 1988). Seismic refraction studies indicate that the crust beneath the AVP is presently 45–50 km thick (Prodehl and Lipman 1989). Petrologic studies of mantle-derived xenoliths in volcanic rocks erupted north of the AVP also indicate the existence of a thick (150–180 km), metasomatically enriched lithospheric mantle keel beneath the Wyoming Province during the Eocene. Isotopic model ages of Wyoming Province mafic magmatic rocks and mantle-derived xenoliths suggest that metasomatism of the lithosphere may have commenced in the Archean, continued into the Early Proterozoic, and peaked in the middle Proterozoic (Eggler et al. 1988).

Geology of Washburn and Sunlight Volcanoes. Washburn volcano (~55–52 Ma; Feeley et al. 2002) is the largest Eocene volcanic center exposed in Yellowstone National Park. Rocks associated with the edifice represent the type stratigraphic section for the Washburn Group, which is the least potassic of the three groups comprising the Absaroka Volcanic Supergroup (Chadwick 1970; Smedes and Prostka 1972). The preserved northern flank of Washburn volcano consists of ~1300 m of volcanic strata that includes lava flows, flow breccias, and debris flow deposits. The lava flows are largely calc-alkaline (sensu stricto) pyroxene and pyroxene-amphibole andesites, although minor basaltic andesitic and amphibole- and biotite-bearing dacitic lava flows are present near the base of the sequence. The southern flank of Washburn volcano is truncated by the northern fault scarp of the Yellowstone caldera, resulting in exposure of the edifice interior, where small plugs of medium-grained biotite diorite geochemically similar to the andesite lavas are present.

Sunlight volcano (49.6–48.1 Ma; Feeley and Cosca 2003) is the largest eruptive center in the AVP. Rocks associated with the volcano comprise the type stratigraphic section for the Sunlight Group, which is the most mafic and potassic of the three groups of the Absaroka Volcanic Supergroup. The volcanic center is comprised of numerous small stocks of medium- to coarse-grained syenite, monzonite, potassic gabbro, and diorite within the ancestral central vent region, hundreds of mafic to silicic dikes radially arranged around the vent region, and a thick sequence (up to 1800 m) of shoshonitic series lava flows and volcaniclastic rocks. All of the extrusive rocks belong to the Wapiti Formation and overlying Trout Peak Trachyandesite within the Sunlight Group (Nelson and Pierce 1968). The Wapiti Formation is a thick sequence of volcaniclastic rocks with smaller amounts of intercalated shoshonitic to latitic lava flows. The Trout Peak Trachyandesite is a massive sequence of shoshonitic to latitic lava flows overlain by potassic trachybasaltic lava flows and minor volcaniclastic rocks.

Results: Geochemical Comparison of the Eruptive Centers

Summary of Magma Differentiation Processes. Recent detailed studies of Washburn and Sunlight rocks focused on documenting crystallization histories, crustal differentiation processes, and sources for evolved magmas (Feeley et al. 2002; Feeley and Cosca 2003). The collective conclusion from these studies is that many of the geochemical differences between the calc-alkaline and shoshonitic magmas likely developed in crustal-level magma chambers (table 1). For example, major and trace element trends for Washburn volcano rocks on figure 2 are shallow and roughly linear, implying an important role for mixing between variably fractionated mantle-derived mafic magmas and heterogeneous silicic melts of Archean mid- to lower-crustal rocks (Feeley et al. 2002). In contrast, evolved Sunlight rocks have relatively low MgO and Cr (and Ni; not shown on fig. 2) contents and compositional trends showing pronounced inflections corresponding to changes in modal phenocryst assemblages. These features imply that fractional crystallization was the dominant differentiation process in the evolution of the rocks (Feeley and Cosca 2003). In detail, the major and trace element data for Sunlight rocks define multiple arrays on figure 2 that require diverse composition parental magmas, phenocryst fractionation and accumulation, and assimilation of crustal rocks in order to account for all of the geochemical features in the suite. These include multiple, subparallel arrays for some major and trace elements (e.g., K_2O, Rb, Ba), significantly elevated contents of Ni, Cr, and Sr (>2000 ppm) in some rocks, and correlations between isotopic ratios and indices of differentiation.

Variations of initial Sr and Nd isotopic ratios with silica contents define distinct arrays for the Washburn and Sunlight rocks, with both implicat-

Table 1. Major and Trace Element Compositions of Select Sunlight and Washburn Rocks

	Sunlight volcano							Washburn volcano						
	SV9804	SV9820	SV9807	SV9903	SV9909	SV9737	SV9916	MW9713[a]	MW9730[a]	MW9736	MW9733	MW9731[a]	MW9743[a]	MW9704[a]
Major elements (wt%):														
SiO_2	49.90	52.66	53.81	55.94	57.95	60.98	62.94	52.39	55.11	56.17	57.23	58.94	61.74	67.11
TiO_2	.69	.88	.96	.60	.48	.40	.26	.89	.84	.85	.77	.74	.54	.43
Al_2O_3	12.15	15.46	17.31	19.04	20.14	18.10	17.68	14.98	16.32	15.84	16.38	17.52	16.21	15.31
Fe_2O_3	8.31	8.37	8.69	5.65	4.65	4.42	3.42	9.98	7.78	7.69	7.31	6.97	5.05	3.48
MnO	.14	.12	.15	.14	.12	.09	.08	.16	.12	.13	.13	.09	.08	.05
MgO	13.57	4.58	3.92	2.80	1.74	2.08	.88	8.65	4.17	5.33	4.94	2.92	3.42	1.61
CaO	8.55	7.64	7.53	4.22	2.94	3.26	2.30	8.58	7.43	8.07	7.31	6.08	5.40	3.45
Na_2O	2.66	3.71	3.62	5.27	5.71	5.95	5.91	2.58	3.09	3.17	3.32	3.92	3.47	3.75
K_2O	2.32	4.69	3.12	4.62	4.83	4.47	5.63	1.25	1.96	2.16	1.87	2.11	2.63	2.61
P_2O_5	.51	.64	.60	.61	.44	.30	.15	.181	.273	.333	.211	.319	.232	.147
Total	98.28	98.11	99.11	98.28	98.55	99.75	99.10	99.65	97.09	99.74	99.47	99.60	98.77	97.94
Trace elements (ppm):														
Ni	390	67	28	13	5	22	10	134	16	41	26	3	41	25
Cr	846	164	86	27	8	49	21	415	54	133	83	7	99	42
Sc	26	21	22	7	9	8	4	26	19	23	21	14	13	8
Ba	2009	2737	2104	2627	2500	2515	2465	589	1268	1907	982	1453	1640	1445
Rb	98	151	69	135	126	125	123	22	33	30	35	38	46	81
Sr	997	1251	1299	2686	2816	1830	1507	463	841	1037	620	953	1025	510
Zr	120	160	148	196	206	237	353	104	137	168	123	158	160	180
Hf	2.5	3.0	…	…	…	…	…	2.4	3.2	…	…	3.7	2.6	3.7
Y	14	16	17	12	12	13	14	17	16	18	15	14	12	13
Nb	5.1	9.2	7.2	20.5	18.8	24.6	20.5	5.0	4.2	7.4	4.1	7.6	5.8	6.5
Ta	.32	.36	…	…	…	…	…	.25	.30	…	…		.33	.42
Pb	17	21	16	40	33	26	44	6	13	20	10	16	24	22
Th	5	8	7	16	17	18	23	6	6	5	6	5	5	5
La	31.4	35.5	…	…	…	…	…	15.7	34.6	…	…	47.5	40.1	37.5
Ce	56.7	62.7	…	…	…	…	…	31.0	67.4	…	…	90.8	67.2	61.4
Nd	25.9	27.6	…	…	…	…	…	14.6	28.3	…	…	30.9	27.7	25.7
Sm	5.11	5.54	…	…	…	…	…	3.20	4.87	…	…	5.49	3.92	3.58
Eu	1.54	1.65	…	…	…	…	…	1.19	1.56	…	…	1.64	1.27	1.1
Tb	.53	.59	…	…	…	…	…	.56	.63	…	…	.46	.37	.36
Yb	1.1	1.3	…	…	…	…	…	1.6	1.8	…	…	1.3	1.0	1.0
Lu	.18	.21	…	…	…	…	…	.22	.27	…	…	.14	.17	.15

Note. Analytical procedures and Sr and Nd isotopic compositions of Washburn and Sunlight rocks are reported in Feeley et al. (2002) and Feeley and Cosca (2003).
[a] Data from Feeley et al. (2002).

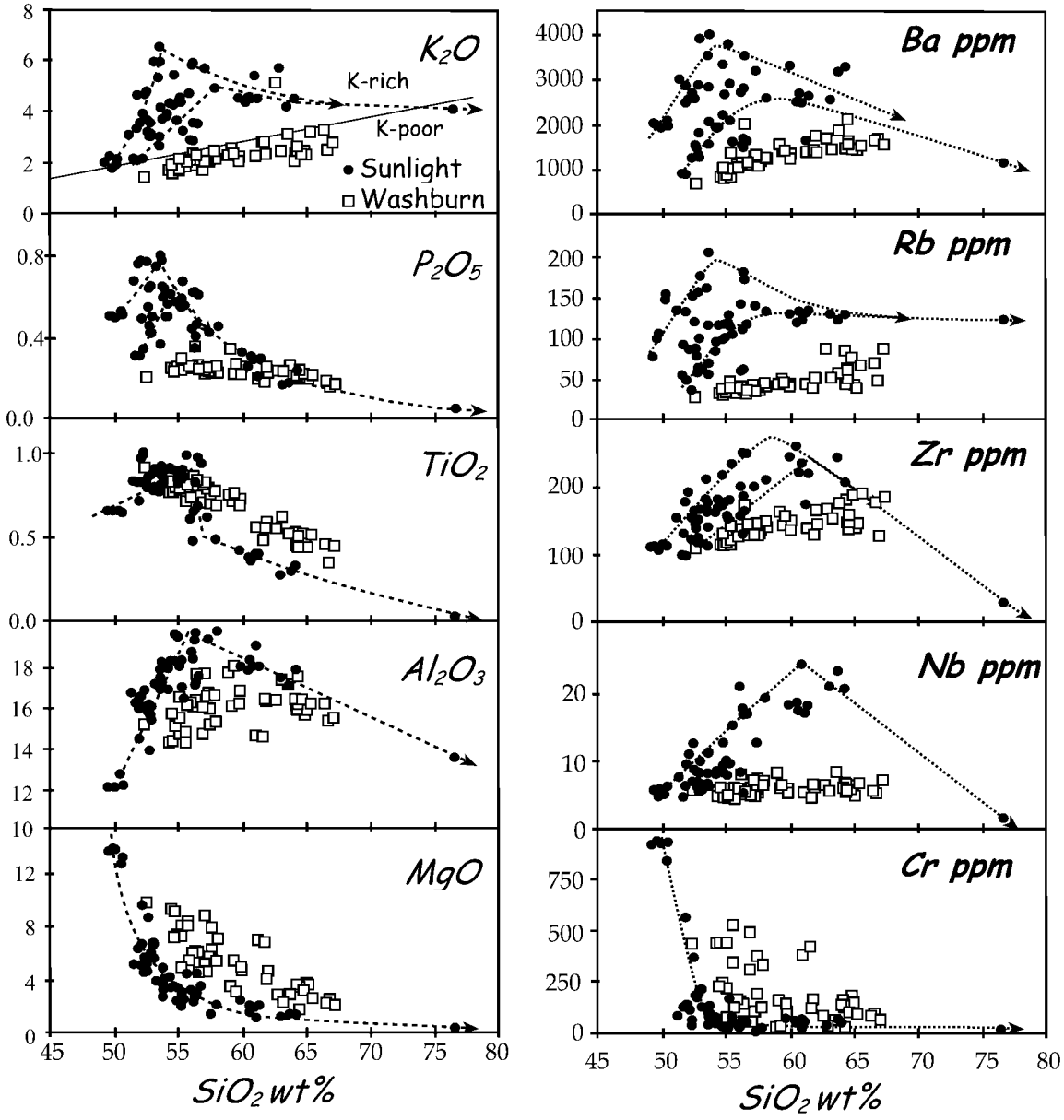


Figure 2. Plots of select major and trace element compositions of Washburn (*open squares*) and Sunlight (*filled circles*) igneous rocks versus SiO_2. Dashed curves show inferred differentiation trends for Sunlight magmas. Solid line on K_2O diagram separates K-rich fields from K-poor fields of Chadwick (1970).

ing involvement of magmas derived from the continental crust during differentiation (fig. 3). Notably, the Sunlight data define unusual negative and positive correlations versus silica contents for Sr and Nd isotopic ratios, respectively. Isotopic data for Washburn rocks define more common trends of increasing Sr and decreasing Nd isotopic ratios with increasing silica contents, although isotopic compositions of mafic rocks are similar to or project toward the compositions of mafic lavas from Sunlight volcano. Together, the trends indicate that whereas crustal sources for the two groups were distinct, parental magmas at Washburn and Sunlight volcanoes had similar Sr and Nd isotopic ratios in spite of significant differences in LILE and light rare earth element (LREE) contents.

Nature and Variability of Parental Melts. This section describes key compositional features of parental magmas at Washburn and Sunlight volcanoes. Discussion and interpretation of the tectonic sig-

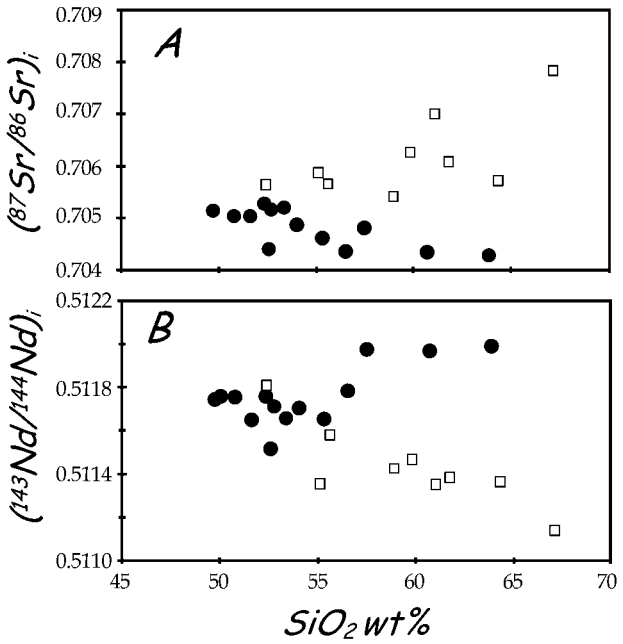


Figure 3. $(^{87}Sr/^{86}Sr)_i$ (*A*) and $(^{143}Nd/^{144}Nd)_i$ (*B*) versus SiO_2 for Washburn and Sunlight rocks. Symbols as in figure 2. Symbol size illustrates analytical uncertainty (2σ precision).

nificance of these features follow. Two aspects of the geochemistry of the parental magmas are addressed. The first is general comparison of the compositions with young basaltic magmas of known tectonic affinity. The second is more detailed analysis of chemical variations among mafic magmas erupted at Washburn and Sunlight volcanoes.

Figure 4 illustrates mid-ocean ridge basalt (MORB)–normalized incompatible element patterns for least-evolved lavas from Washburn and Sunlight volcanoes (table 1). The important features of the patterns with respect to the above issues are as follows. First, the Washburn and Sunlight patterns closely resemble in form the pattern for high-K, calc-alkaline arc basalt, except for significant enrichments in Ba and Th for both rocks and further enrichments in K, P, and LREE for the Sunlight basalt. Second, HFSE and heavy rare earth element (HREE) contents in both rocks are similar to or lower than contents in MORB and arc-basalt, and they are significantly lower than contents in ocean island basalt. Third, the Sunlight basalt has elevated abundances of K, P, LILE (especially Rb), and LREE (e.g., Ce) relative to the Washburn basalt. In contrast, HREE (e.g., Yb) and HFSE contents are nearly identical in both rocks.

The relatively low HFSE and HREE contents in mafic rocks from Washburn and Sunlight volcanoes are characteristics of primitive rocks from other Eocene magmatic fields in the Wyoming Province. These features are generally interpreted to indicate primary basalt generation from mantle source regions depleted by previous partial melting events (Eggler et al. 1988; Dudás 1991; O'Brien et al. 1991). By contrast, high LILE and LREE contents have also been noted from other centers and are interpreted to reflect enrichment processes that may or may not (e.g., Dudás et al. 1987) be related to dehydration of subducted oceanic lithosphere. The exact timing of the LILE and LREE enrichments is unclear, as is the number of enrichment events. Meen and Eggler (1987), Eggler et al. (1988), and Dudás (1991) note the differences in the trace element characteristics of the Eocene Wyoming Province magmas and arc basalts, particularly the extreme enrichments in Ba. On the basis of these distinctions and the unique Sr and Nd isotopic compositions of the rocks, these authors interpret the arc-like trace element patterns as indicators of source regions in subcontinental lithospheric mantle depleted in Archean times and subsequently enriched by a regional mid-Proterozoic (2.2–0.95 Ga; Dudás et al. 1987; O'Brien et al. 1991; MacDonald et al. 1992) and possibly older (3.8 Ga; Meen and Eggler 1987) metasomatic event.

To some extent, the high LILE and LREE contents of Washburn and Sunlight mafic rocks also reflect

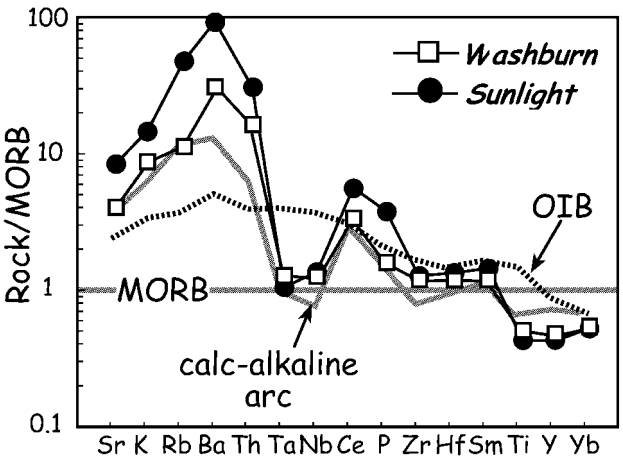


Figure 4. Mid-ocean ridge basalt (*MORB*)–normalized trace element diagrams for least-evolved basaltic rocks from Washburn and Sunlight volcanoes. Symbols as in figure 2. Normalizing values and element order after Pearce (1982). Also shown for reference are typical patterns for tholeiitic ocean island basalt (*OIB*) and calc-alkaline volcanic arc basalt (Pearce 1982).

an ancient enrichment event. Radiogenic isotopic compositions of mafic Sunlight and Washburn volcano magmas are characterized by relatively low $(^{87}Sr/^{86}Sr)_i$ and $(^{143}Nd/^{144}Nd)_i$ ratios, such that they plot well below the field defined by modern subduction-related basalts and the "mantle array" defined by asthenospheric melts in Sr-Nd isotopic space (fig. 5). These features are similar to other Wyoming Province magmas, and they indicate primary magma source regions predominately within ancient Sr (+Ba)-LREE-enriched (but HREE-HFSE-depleted) subcontinental lithospheric mantle. The precise timing of the ancient enrichment event is difficult to calculate, although it may be estimated from Nd isotopic data. Depleted mantle Nd model ages for least-evolved basaltic lavas from Sunlight and Washburn volcanoes are between 2.2 and 2.0 Ga. This range is within the range of computed Nd model ages (2.3–1.4 Ga; Eggler et al. 1988) for mafic rocks from Independence volcano, AVP, and elsewhere in the Wyoming Province (2.2–0.95 Ga; Dudás et al. 1987), indicating that enrichment of subcontinental lithospheric mantle beneath Washburn and Sunlight volcanoes was probably associated with the regional mid-Proterozoic event identified by other authors.

In addition to an ancient enrichment event, first-order compositional distinctions also exist among Washburn and Sunlight mafic magmas (i.e., Mg # = 100 $Mg/(Mg + Fe^{2+}) > 60$ and $SiO_2 < 56$ wt%) that indicate intrinsic variability in primary melts associated with a recent mantle enrichment event. The principal evidence for this younger event is similar values of $(^{87}Sr/^{86}Sr)_i$ and $(^{143}Nd/^{144}Nd)_i$ ratios for the mafic magmas, but wide ranges in K_2O, P_2O_5, LILE, and LREE contents, and LILE/HFSE and Rb/Sr abundance ratios (fig. 6). The order of elemental enrichment, based on comparison of Sun-

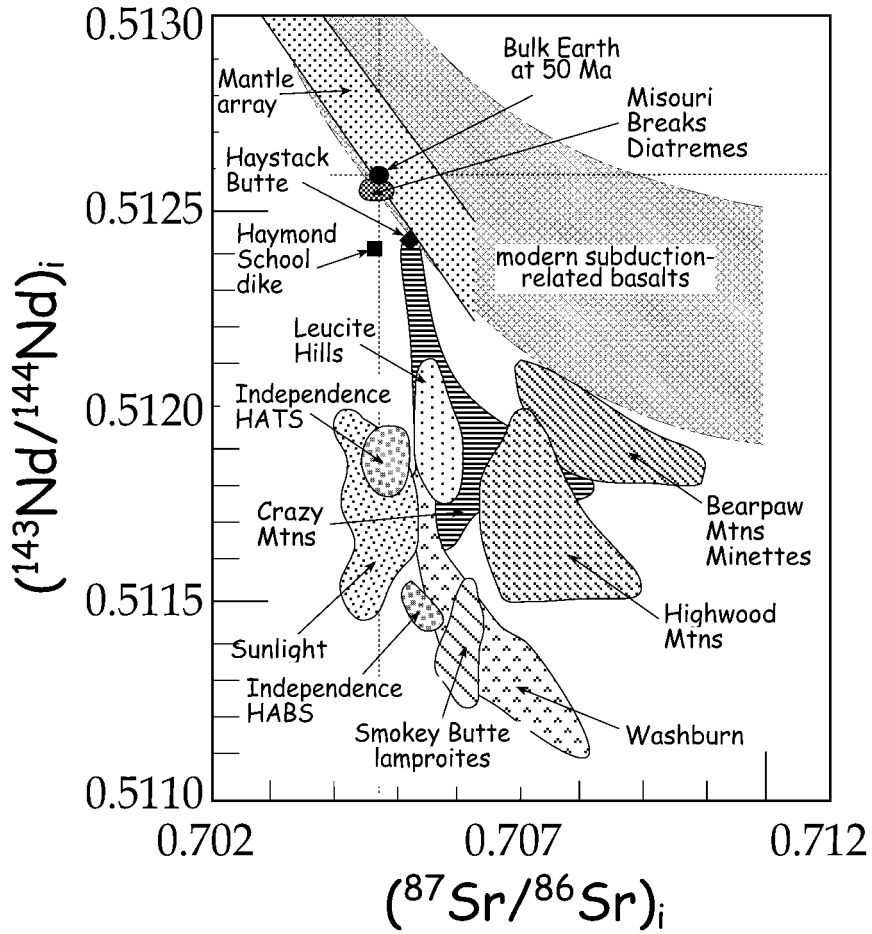


Figure 5. Comparison of initial Sr and Nd isotopic compositions of Washburn (at 53 Ma) and Sunlight (at 48.75 Ma) igneous rocks with other Eocene and alkalic rocks from the Wyoming Province. Data from Carlson and Irving (1994), O'Brien et al. (1995), Dudás and Harlan (1999), and references therein.

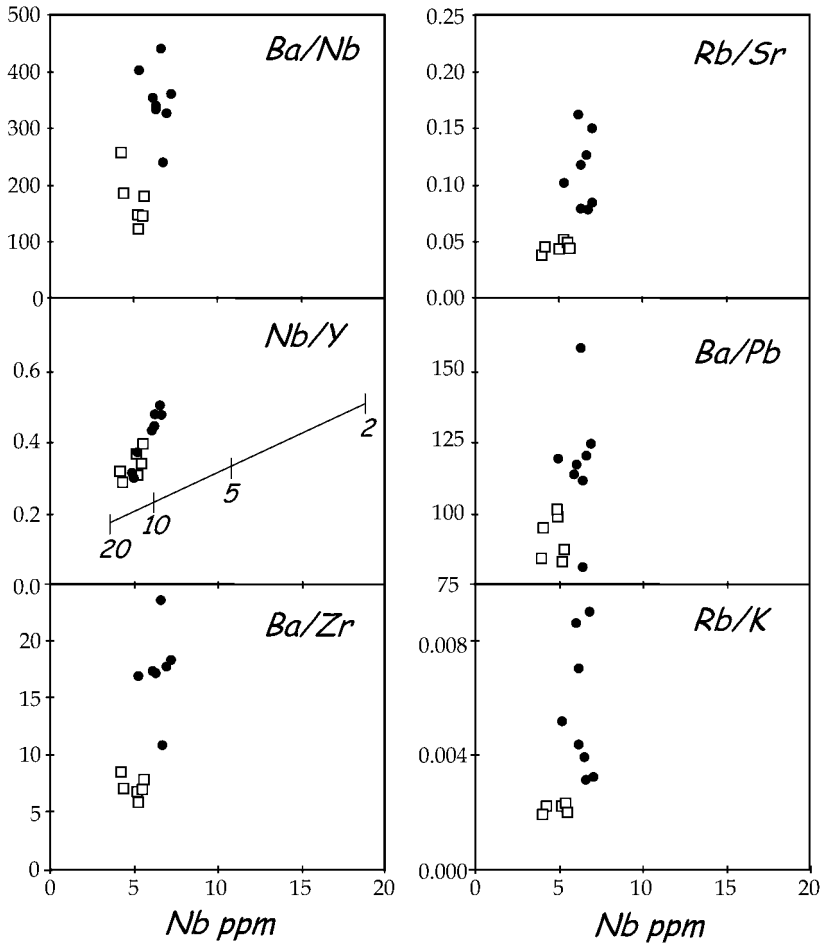


Figure 6. Select trace element abundance ratios for mafic (e.g., Mg # = 100 Mg/(Mg + Fe^{2+}) > 60 and SiO_2 < 56 wt%) rocks from Washburn and Sunlight volcanoes versus Nb contents. Symbols as in figure 2. Nb/Y versus Nb diagram illustrates partial melting model for garnet peridotite from Gill (1987). Initial source concentrations are 0.66 ppm and 6 ppm for Nb and Y, respectively. Tick marks give degree of melting (after Walker et al. 1995).

light mafic rocks with the highest LILE contents and Washburn mafic rocks with the lowest LILE contents, is Rb > Ba > K > Sr > La > Ce. This order is nearly identical to the order of enrichments inferred for volcanic rocks in arcs of the western Pacific relative to MORB (Pearce and Peate 1995).

The wide ranges in LILE and LREE contents of Sunlight and Washburn mafic rocks are consistent with recent mantle metasomatism by slab-derived, LILE-rich hydrous fluids (Tatsumi et al. 1986; Hawkesworth et al. 1993). Because LILE are mobile in hydrous fluids, especially relative to HFSE (Tatsumi et al. 1986; Brenan and Watson 1991), particularly strong evidence for recent mantle metasomatism is found in plots of Nb versus Ba/Nb and Ba/Zr for mafic Sunlight and Washburn magmas (fig. 6). In the absence of a fluid component or hydrous potassic phase such as phlogopite, the large variations in Ba/Nb (120–435) and Ba/Zr (six to 24) ratios at similar Nb contents of the mafic rocks cannot be generated by variable degrees of uniform source rock partial melting. The degrees of incompatibility for Ba, Nb, and Zr are Ba > Nb > Zr, although the differences are very small (D_{Ba}, D_{Nb}, and D_{Zr} are estimated to be 0.01, 0.04, and 0.08, respectively [Hofmann 1988]). It is therefore impossible to produce the large variations in Ba/Nb and Ba/Zr ratios at roughly constant Nb contents by different degrees of mantle melting. In general, the elevated LILE/HFSE ratios of mafic Sunlight lavas are consistent with higher degrees of metasomatism for Sunlight primary magma source rocks. By contrast, there appears to be little difference in the degree of melting for Sunlight and Washburn parental magmas, because the most primitive rocks from both volcanoes have nearly identical Nb/Y

(~0.3; fig. 6) and Zr/Nb (~20; not shown), ratios that are strongly fractionated during partial melting of a garnet-bearing peridotite source.

Alternatively, large variations in LILE and LREE for mafic magmas within individual volcanic fields have been attributed to numerous other processes. The most frequently cited of these includes contamination of asthenospheric melts with geochemically and isotopically extreme melts derived from the subcontinental lithospheric mantle (O'Brien et al. 1991), partial fusion of mantle peridotite with a variable contribution of metasomatic phlogopite in veins (Carmichael et al. 1996; Feldstein and Lange 1999), and crustal contamination (Feeley 1993). As discussed below, none of these processes adequately explains the geochemical differences between Washburn and Sunlight mafic magmas.

First, there are no positive correlations between K_2O, P_2O_5, and LILE with TiO_2 (fig. 7), as expected for a series of magmas related by a common liquid line of descent involving variable contributions of partially melted phlogopite in which these elements are all compatible (Esperança and Holloway 1987; Righter and Carmichael 1992; Carmichael et al. 1996; Feldstein and Lange 1999). Second, the similarity in initial Sr and Nd isotopic ratios of the most mafic Washburn and Sunlight rocks precludes variations in the degree of crustal contamination or compositions of assimilated crustal rocks as controlling the LILE variations. Indeed, trends in initial Sr and Nd isotopic compositions of evolved rocks in figure 3 indicate incorporation of isotopically disparate crustal melts during differentiation of the two suites. Isotopic compositions of mafic rocks, however, indicate derivation of primary magmas from mantle source regions with similar long-term LILE and LREE characteristics. Likewise, comparable Sr and Nd isotopic ratios of mafic rocks in the two suites also appear to preclude more complex models involving variable degrees of mixing between melts of asthenosphere and ancient enriched lithosphere with contrasting isotopic characteristics (e.g., O'Brien et al. 1991). Small differences in isotopic compositions of Washburn and Sunlight mafic rocks more likely reflect contrasting differentiation processes and extents of evolution

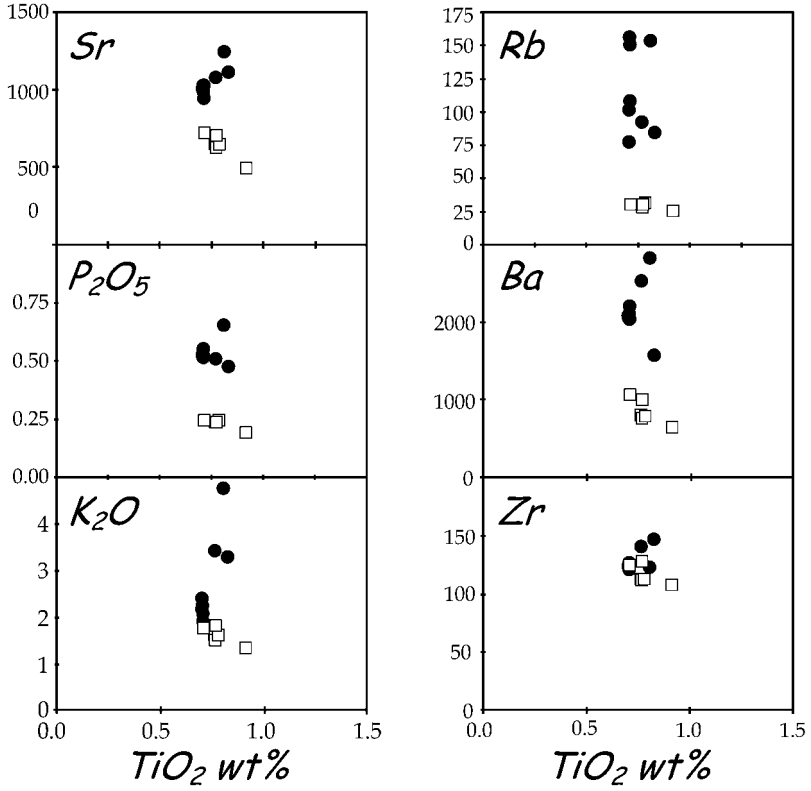


Figure 7. Plots of K_2O, P_2O_5, Sr, Zr, Ba, and Rb versus TiO_2 for mafic rocks from Washburn and Sunlight volcanoes. Symbols as in figure 2.

(e.g., as measured by MgO contents) than variable mixing of melts derived from distinct mantle source regions.

Discussion

Interpretation: Petrologic Role of Subducted Material in Magmagenesis. Comparison of geochemical data for mafic rocks from Sunlight and Washburn volcanoes provides unmistakable evidence for recent modification of mantle source regions by metasomatic, LILE-rich fluids. Similar to nearly all studied Eocene magmatic rocks in the Wyoming Province, Sunlight and Washburn mafic rocks have distinctive radiogenic isotopic compositions and trace element contents that indicate source regions largely within ancient depleted lithospheric mantle later enriched by a Proterozoic metasomatic event characterized by low Sm/Nd and Rb/Sr ratios. At the same time, the mafic rocks also show large variations in ratios involving LILE and LREE that are not obviously reflected in their initial Sr and Nd isotopic compositions. This suggests a recent (<100 Ma) metasomatic event, possibly associated with subduction of the Farallon plate.

In terms of the latter process, a paradox exists if the LILE variations among the Washburn and Sunlight mafic magmas are considered analogous to those in a conventional subduction model wherein east-directed subduction of the Farallon plate beneath the North American plate is associated with continuous dehydration of the slab and mantle partial melting. In this case, one might expect negative correlations between the extent of source region modification (as measured by LILE/HFSE ratios) and depth to the slab (e.g., Hickey-Vargas et al. 1989; Ryan et al. 1995; Tatsumi and Eggins 1995; Walker et al. 1995; Patino et al. 1997). If this were the case, Sunlight mafic magmas should show compositional evidence for weaker source region metasomatism (e.g., lower LILE/HFSE ratios) and correlated lower degrees of partial melting (e.g., higher LILE and HFSE). An opposite but related problem is that, given the apparently larger extents of metasomatism by LILE-rich fluids inferred for Sunlight parental magma sources, one might also expect correspondingly higher degrees of partial melting because of correlated lowering of the solidus of mantle peridotite (e.g., Stolper and Newman 1994). The degrees of melting by which Sunlight and Washburn parental magmas were generated appear to be very similar for both suites, however, implying comparable proportions of hydrous fluids added to their source regions (fig. 7).

The similar HFSE contents but variable LILE contents of Washburn and Sunlight mafic magmas could, alternatively, reflect first-order variations in the compositions of metasomatic fluids, with higher LILE/HFSE abundance ratios for fluids infiltrating source regions of Sunlight primary magmas. This explanation is plausible because relatively high Rb/K and Ba/Pb ratios in Sunlight mafic rocks compared with Washburn mafic rocks (fig. 6) are identical to variations described by Jakes and White (1972) and Tatsumi and Eggins (1995), who observed that these ratios are commonly elevated in primary magma sources for back-arc volcanoes of modern arcs. Tatsumi and Eggins (1995) attributed these characteristics to fluid equilibration with residual phlogopite formed from decomposition of pargasitic amphibole beneath volcanic front volcanoes and equilibration with residual K-rich amphibole formed from breakdown of phlogopite beneath back-arc volcanoes. This explanation differs from those that emphasize partial fusion of mantle peridotite with a variable contribution of melted phlogopite in that fluid elemental compositions and abundance ratios reflect equilibration with the residual phases formed by dehydration reactions. Thus, there is no expectation of positive correlations between LILE and TiO_2 (cf. fig. 7), as observed for magma series related by a common liquid line of descent involving variable contributions of partially melted phologopite (e.g., Carmichael et al. 1996; Feldstein and Lange 1999).

Regional Implications: A Possible Model for the Tectonic Setting of AVP Magmas. A consistent geodynamic model to explain the origin of the AVP magmas that attempts to take into account all of the tectonic and geochemical complexities of Washburn and Sunlight volcanoes is illustrated in figure 8. In the model, which is similar in many respects to that proposed by O'Brien et al. (1991; see their fig. 12) for Eocene magmatic rocks in the Highwood Mountains, Montana, LILE-rich, HFSE-poor hydrous fluids are initially released at low pressures from the shallow subducted Farallon plate because of decomposition of hydrous phases within the slab. These buoyant fluids migrate upward into a narrow asthenospheric wedge, where they react with peridotite and recrystallize hydrous minerals. The resultant hydrated peridotite carapace is then dragged laterally along the top of the subducted plate because of viscous coupling between the rigid oceanic lithosphere and the mantle wedge (e.g., McKenzie 1969; Andrews and Sleep 1974). As the carapace is transported to greater depths and consequent higher pressures and temperatures, hydrous minerals undergo dehydration initially involving breakdown of pargasitic amphibole (~3.5

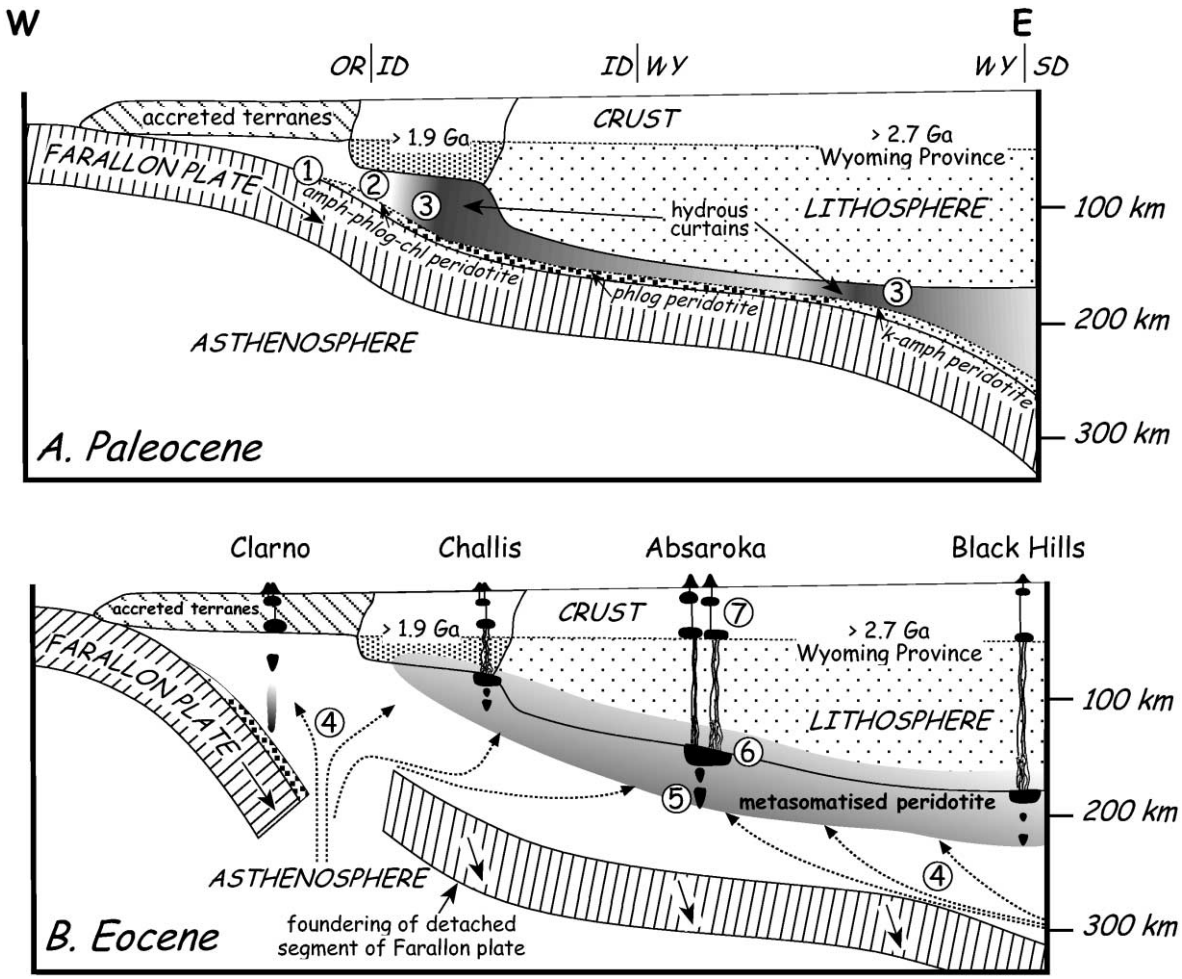


Figure 8. Schematic summary (highly simplified) of tectonomagmatic processes involved in the generation and evolution of Washburn and Sunlight volcano magmas. Cross section (1 : 2 scale) is near 45°S (see fig. 1 inset). *A*, Shallow subduction of the Farallon plate beneath the western margin of North America during the Paleocene. Stage *1*: initial loss of fluid from slab and creation of hydrous peridotite carapace. Stage *2*: downward transport of hydrous peridotite. Stage *3*: breakdown of pargasitic amphibole at ~3.5 GPa followed by phlogopite at ~6 GPa in carapace creates variable composition fluids that ascend as hydrous curtains into asthenosphere and base of lithosphere without partial melting. *B*, Foundering of the Farallon plate during the early Eocene, possibly by the mechanism described by Humphreys (1995). Stage *4*: upwelling and influx of hot asthenosphere into metasomatized zone of asthenosphere. Stage *5*: partial melting of metasomatized asthenosphere creates basaltic magmas that rise along and into base of the lithosphere. Stage *6*: melting within ancient depleted harzburgite and enclosed Ba-rich metasomes or homogeneous contamination of asthenospheric melts produced in stage *5* creates primary magmas for Washburn and Sunlight volcanoes. Primary magmas for both volcanoes are considered to result from similar degrees of melting of similar proportions of source materials. Compositional variability is suggested to reflect differences in fluid compositions inherited from breakdown of different phases in hydrous peridotite. Stage *7*: differentiation of parental magmas by magma mixing (calc-alkaline series) and assimilation-fractional crystallization (shoshonitic series).

GPa) followed by phlogopite at deeper levels (~6 GPa; Sudo and Tatsumi 1990). This two-step process creates variable composition fluids that ascend as hydrous curtains into asthenosphere and the base of overlying subcontinental lithospheric mantle, resulting in a relatively recent episode of metasomatism. I suggest that this metasomatic event does not immediately trigger melting and primary basalt generation, however, because of the cool thermal conditions prevalent in the narrow zone between the shallow subducted slab and lithosphere.

The exact timing of the young metasomatic event is difficult to determine. Although Sunlight mafic rocks have large relative enrichments in Rb/

Sr ratios that are not obviously reflected in their Sr isotopic compositions (fig. 6), a model wherein AVP magmas are produced as a consequence of contemporaneous, eastward shallow subduction of the Farallon plate is by no means proved and may, in fact, be untenable when all geologic and tectonic complexities of the region are considered (Dudás 1991). Alternatively, the Rb-Sr systematics are sufficiently uncertain such that the recent metasomatic event could have occurred during or following the first major episode of Phanerozoic magmatism in the region during the Late Cretaceous (Chadwick 1985). This explanation is plausible because, relative to an Eocene event, a metasomatic event at 85 Ma would result in indiscernible differences in $^{87}Sr/^{86}Sr$ compositions (~0.0002) of parental magmas at Sunlight and Washburn volcanoes, assuming that differences in Rb/Sr ratios between these rocks solely reflect differences in the compositions of the metasomatic fluids (i.e., they are not produced by variable degrees of melting). This ambiguity in isotopic systematics has been noted by other authors (e.g., Eggler et al. 1988; Hooper et al. 1995), who attribute the Eocene magmatic event in the northwest United States to alternative tectonic models, most notably lithospheric thinning and extension associated with asthenospheric upwelling in the back-arc region of a more traditional, steeply dipping subduction zone. Note that the variation in Rb/Sr ratios of the mafic rocks cannot reflect the often cited mid-Proterozoic enrichment event beneath the Wyoming Province, however, because this would lead to clear differences (~0.23) in $^{87}Sr/^{86}Sr$ compositions.

On the basis of the geochemical data presented here, I cannot differentiate between an Eocene or Late Cretaceous enrichment event. However, a young slab-derived component has been detected in several other Eocene magmatic fields in the Wyoming Province, most of which occur well to the east of the main locus of late Cretaceous subduction-related Laramide magmatism in the Idaho and Boulder batholiths (Lipman 1980; O'Brien et al. 1991; MacDonald et al. 1992; du Bray and Harlan 1996). This indicates significant eastward transfer of metasomatically enriched asthenosphere during the Paleocene, a period of relative magmatic quiescence in the northern Rocky Mountains and Great Plains. On the basis of these considerations and following the suggestions of numerous authors (e.g., Bird 1984; Dudás 1991; Baker 1992; Humphreys 1995; O'Brien et al. 1995; du Bray and Harlan 1996), I propose that, following a period of accelerated, relatively amagmatic convergence between the North American and Farallon plates in the Paleocene, large-scale magmatism in the AVP and elsewhere in the Wyoming Province recommenced in the Eocene in response to breakup and foundering of the subhorizontally subducting oceanic slab (Gurnis and Hager 1988). This interpretation is consistent with abundant evidence for dramatic changes in the overall tectonic configuration of the northwestern United States after about 58 Ma. The evidence includes a decrease in the convergence rate between the Farallon and North American plates, an increase in slab dip, and a change in crustal deformation style from compressional to extensional (e.g., Christiansen and Lipman 1972; Engebretson et al. 1985; Wernicke et al. 1987; Severinghaus and Atwater 1990).

The precise manner in which the slab was removed from beneath the region is speculative, and many ideas have already been proposed. The conceptually simplest models are those in which the slab rolled back toward the west to a steep angle. These models, however, are difficult to reconcile with the apparently contemporaneous nature of magmatism over a broad east-west trending area of the Northern Cordillera and low calculated velocities for slab rollback (Kincaid and Olsen 1987). A more difficult model to exclude involves tearing and downward buckling of the slab along an approximately east-northeast-trending axis (Humphreys 1995). This model is intriguing because, in many ways, it accounts for the space-time evolution of post-Laramide, Tertiary magmatism in the western United States. Whatever the exact mechanism, however, it is likely that mantle partial melting and primary basalt generation were triggered across a large region through major heating associated with upwelling and influx of hot asthenosphere between the sinking slab and lithosphere, particularly if it was associated with crustal uplift and extension (Harry and Leeman 1995; Hooper et al. 1995).

At this stage, the details of the petrogenetic model proposed here differ slightly from those in the model of O'Brien et al. (1991). In that model, dehydration of residual phlogopite in metasomatized peridotite produces a hydrous curtain that triggers melting as it ascends into hotter regions of the asthenospheric wedge (Tatsumi et al. 1986; Tatsumi 1989). Relatively homogeneous basaltic magmas produced by this process are thought to migrate into overlying mantle lithosphere through preexisting pathways, assimilating to variable degrees Ba-LREE-phlogopite-rich metasomes and surrounding depleted harzburgite. Chemical variability among parental magmas in the Highwood Mountains is thus a function of the degree of meta-

some assimilation, which O'Brien et al. (1991) interpret to reflect the residence time of individual batches of basaltic magma within the lithosphere.

In contrast to the model of O'Brien et al. (1991), I interpret the data presented here to indicate that primary magmas for both Sunlight and Washburn volcanoes were derived from similar combinations of source materials and degrees of melting. Compositional variability among parental magmas is thus interpreted to mainly reflect heterogeneity in fluid compositions inherited from breakdown of different phases in hydrous peridotite. Consideration of the long duration of shallow subduction of the Farallon plate in the Late Cretaceous through Eocene suggests these relationships may have resulted from periodic fluctuations in the angle of subduction (and hence depth of the slab) and variations in slab topography, laterally shifting positions of the hydrous curtains illustrated in figure 8*A* and balancing the extent of metasomatism in the region beneath the AVP. Combined with any convective mixing that may have occurred, the integrated effect is that the Eocene mantle beneath the AVP may have been uniformly "wet" but compositionally heterogeneous as a result of fluxing by volumetrically similar proportions of fluids derived from dehydration of amphibole and phlogopite. A fundamental implication of this interpretation is that the locations of the western and eastern AVP belts do not directly reflect the positions of amphibole and phlogopite breakdown in downdragged hydrous peridotite, as is commonly inferred from the dual nature of volcanic chains (e.g., arc front and back arc) in modern subduction settings (Tatsumi and Eggins 1995). More likely, the positions of the belts were controlled by preexisting pathways for magma ascent because of the presence of Precambrian zones of crustal weakness reactivated during the mid-Mesozoic to early Tertiary Laramide Orogeny (Chadwick 1970).

Although primary magmas for both volcanoes appear to be derived from melting approximately the same composition source rocks, the relative proportions of asthenospheric and lithospheric components in these melts is unclear. On the one hand, basaltic magmas produced by melting of hydrated asthenosphere may have accumulated at the base of the lithosphere, releasing heat and volatiles and triggering melting entirely within ancient depleted harzburgite and Ba-rich metasomes. On the other hand, the lithospheric mantle may have served as a source of homogeneous mantle contamination for ascending asthenospheric melts (e.g., Menzies et al. 1987). This interpretation is preferable because it allows variable degrees of mixing between asthenospheric and lithospheric melts for other Eocene magmatic centers, thereby reconciling the slight differences between the model proposed here and the model of O'Brien et al. (1991). Furthermore, the Nd-Sr data arrays for Wyoming Province mafic rocks in figure 5 were interpreted by O'Brien et al. (1991) as mixing lines between heterogeneous lithospheric mantle melts and a relatively undepleted asthenospheric component similar to the monticellite peridotite from Haystack Butte, which plots near bulk earth.

Broad Implications. Deciphering the origins of across-strike K_2O and other geochemical variations in magmatic fields, particularly those related to contemporaneous subduction, has been a major objective for geochemists as a result of the broader implications for regional tectonic complexities and primary melt generation processes in addition to better understanding of arc magmatism in general (Gill 1981; Tatsumi and Eggins 1995). The conclusions of this study contribute to these endeavors because the AVP is the global type locality for shoshonitic series igneous rocks (Iddings 1895), and the magmas apparently erupted in an atypical tectonic setting not frequently investigated.

The recent literature includes numerous articles focused on interpreting across-arc variations in modern steeply dipping subduction zones as functions of the degree of mantle partial melting and variations in the composition and mass of slab-derived fluids (or melts). Although numerous alternative models exist, many authors credit the occurrence of K_2O-rich magmas with high incompatible element contents in back-arc regions to decreasing additions of slab-derived, LILE-enriched hydrous fluids to mantle source regions with concomitant decreases in the degree of partial melting (Hickey et al. 1989; Stolper and Newman 1994; Tatsumi and Eggins 1995). The across-strike geochemical patterns that characterize AVP mafic magmas, as documented at Sunlight and Washburn volcanoes, resemble in part the spatial geochemical variations at these localities. As described above, however, the patterns in detail are not consistent with decreasing slab contributions or degrees of mantle partial with distance from the trench presumably because of the preceding protracted episode of shallow subduction of the Farallon Plate beneath North America. The variations instead appear to correspond only to spatial heterogeneity in the composition of slab-derived fluids. It thus appears that one of the principal effects of prolonged subduction zone enrichment is to balance degrees of mantle metasomatism, at least over spatial scales comparable to the width of the AVP. Furthermore, if my con-

clusion that the AVP rocks contain a young slab-derived component is correct, this is additionally significant because it implies (1) that subducting oceanic crust can carry fluids and supply a slab-derived component to the mantle wedge to distances greater than 750 km from the trench and to depths exceeding 150 km and (2) that in areas characterized by extended periods of shallow subduction and reduced magmatism, there may be a time lag of perhaps several million years between fluid enrichment of the mantle and the onset of melt formation. Although the latter conclusion is not well constrained, it is in striking contrast to the results of U-series disequilibria studies of modern arc magmatism, where the elapsed time is inferred to be at most a few hundred thousand years (Sigmarsson et al. 1990; Gill et al. 1993; Clark et al. 1998).

The data described in this study also reinforce the notion that evolved shoshonitic rocks in the AVP are generally more fractionated than evolved calc-alkaline rocks, whereas the latter have been modified to a larger extent by mixing with silicic melts derived from the mid- to lower-continental crust. Thus, the occurrence of shoshonitic and calc-alkaline magmatic trends in individual volcanic fields may typically be a function of crustal-level differentiation processes and, as such, imply little about the role of subducted material in magmagenesis (Meen 1987; Feeley and Cosca 2003).

Conclusions

The AVP is one of the most voluminous magmatic fields associated with an intense episode of magmatism that affected large areas of the northwest United States during the Eocene. A proper understanding of across-strike geochemical variations in the AVP therefore has important bearings on models for the Eocene tectonic setting of this region. Insight into the origin of the trends is provided by the results of this study, which compares compositional data for two recently well-characterized Absaroka eruptive centers that define type localities for major stratigraphic subdivisions of the Absaroka Volcanic Supergroup. With respect to questions discussed in earlier sections of this article, the most important conclusions of this study are as follows.

1. Volcanic rocks erupted at Washburn volcano in the western AVP belt and Sunlight volcano in the eastern belt belong to high-K calc-alkaline and shoshonitic differentiation series, respectively. The mantle source for both magma series is, as shown by trace element contents and Sr and Nd isotopic ratios for the most mafic rocks, largely within ancient depleted lithospheric mantle later enriched by a metasomatic event characterized by low Sm/Nd and Rb/Sr ratios. The approximate timing of the ancient enrichment event, as calculated by Nd depleted mantle model ages (2.0–2.2 Ga), is similar to estimates from other magmatic fields in the Wyoming Province (0.95–2.2 Ga; Dudás 1991).

2. In addition to a mid-Proterozoic enrichment event, the most mafic rocks in each suite also show large variations in trace element abundance ratios involving LILE and LREE. Because these variations are not reflected in isotopic ratios, they indicate a recent (<100 Ma) metasomatic event by LILE- and LREE-rich hydrous fluids possibly derived from the shallow subducted Farallon plate. Superficially, magma sources for Sunlight volcano appear to contain larger amounts of the metasomatic component, as measured by relatively high LILE/HFSE ratios. However, parental magmas at both volcanoes have similar HFSE contents and HFSE/HREE ratios, suggesting similar degrees of source region melting and therefore similar extents of source region metasomatism. Rather than variable degrees of metasomatism and partial melting, the geochemical differences between Washburn and Sunlight volcanoes are best explained by compositional heterogeneity in the metasomatic fluids inherited from breakdown of different phases in hydrous peridotite.

3. A consistent geodynamic model to account for the generation of AVP magmas involves metasomatic alteration of asthenosphere and ancient subcontinental lithospheric mantle during an episode of relatively amagmatic, shallow subduction of the Farallon plate beneath the North American plate during the Paleocene. This was followed in the early Eocene by foundering and removal of the subhorizontally subducted plate. On removal of the slab from beneath the AVP, partial melting and primary basalt formation were triggered in the asthenosphere and lower lithosphere through major heating associated with upwelling and influx of hot asthenosphere. It is also possible that AVP primary magmas were derived solely from the subcontinental mantle lithosphere. In either case, however, the extents of mantle melting and relative proportions of lithologies melted were similar for both Sunlight and Washburn volcanoes so that compositional variability among parental magmas chiefly reflects differences in fluid compositions inherited from breakdown of different phases in hydrous peridotite.

ACKNOWLEDGMENTS

This work was supported by National Science Foundation grant EAR-9725287. I thank C. Lindsay, J. Hamblock, and M. O'Conner for field assistance and C. Lindsay, L. Lennon, and M. Hiza for helpful discussions that led to some ideas presented in this article. Constructive comments by S. Harlan, P. Hooper, and an anonymous reviewer and editorial comments by A. Anderson helped to improve the clarity and expand the scope of the manuscript.

REFERENCES CITED

Andrews, D. J., and Sleep, N. H. 1974. Numerical modeling of tectonic flow behind island arcs. Geophys. J. Astron. Soc. 38:237–251.

Armstrong, R. L. 1978. Cenozoic igneous history of the U.S. Cordillera from lat 42° to 49°N. Geol. Soc. Am. Mem. 42:265–282.

Baker, D. W. 1992. Central Montana alkalic province: critical review of Laramide plate tectonic models that extract alkalic magmas from abnormally thick Precambrian lithospheric mantle. Northwest Geol. 20/21:71–95.

Bird, P. 1984. Laramide crustal thickening event in the Rocky Mountain foreland and Great Plains. Tectonics 3:741–758.

Brenan, J. M., and Watson, E. B. 1991. Partitioning of trace elements between olivine and aqueous fluids at high P-T conditions: implications for the effect of fluid composition on trace-element transport. Earth Planet. Sci. Lett. 107:672–688.

Carlson, R. W., and Irving, A. J. 1994. Depletion and enrichment history of subcontinental lithospherice mantle: an Os, Sr, Nd and Pb isotopic study of ultramafic xenoliths from the northwestern Wyoming Craton. Earth Planet. Sci. Lett. 126:457–472.

Carmichael, I. S. E.; Lange, R. A.; and Luhr, J. F. 1996. Quaternary minettes and associated volcanic rocks of Mascota, western Mexico: a consequence of plate extension above a subduction modified mantle wedge. Contrib. Mineral. Petrol. 124:302–333.

Chadwick, R. A. 1970. Belts of eruptive centers in the Absaroka-Gallatin volcanic province, Wyoming-Montana. Geol. Soc. Am. Bull. 81:267–274.

———. 1985. Overview of Cenozoic volcanism in the west-central United States. *In* Flores, R. M., and Kaplan, S. S., eds. Cenozoic paleogeography of the west-central United States. SEPM Rocky Mt. Sec. Spec. Pub., p. 359–381.

Christiansen, R. L., and Lipman, P. W. 1972. Cenozoic volcanism and plate tectonic evolution of the western United States. II. Late Cenozoic. Proc. R. Soc. Lond. 271:249–284.

Clark, S. K.; Reagan, M. K.; and Plank, T. 1998. Trace element and U-series systematics for 1963–1965 tephras from Irazú Volcano, Costa Rica: implications for magma generation processes and transit times. Geochim. Cosmochim. Acta 62:2689–2699.

Dickinson, W. R., and Hatherton, T. 1967. Andesitic volcanism and seismicity around the Pacific. Science 157:801–803.

du Bray, E. A., and Harlan, S. S. 1996. The Eocene Big Timber stock, south-central Montana: development of extensive compositional variation in an arc-related intrusion by side-wall crystallization and cumulate glomerocryst remixing. Geol. Soc. Am. Bull. 108:1404–1424.

Dudás, F. Ö. 1991. Geochemistry of igneous rocks from the Crazy Mountains, Montana, and tectonic models for the Montana alkalic province. J. Geophys. Res. 96:13,261–13,277.

Dudás, F. Ö.; Carlson, R. W.; and Eggler, D. H. 1987. Regional Middle Proterozoic enrichment of the subcontinental mantle source of igneous rocks from central Montana. Geology 15:22–25.

Dudás, F. Ö., and Harlan, S. S. 1999. An ancient depleted mantle sample from a 42-Ma dike in Montana: constraints on persistence of the lithosphere during Eocene magmatism. J. Geol. 107:287–299.

Dutch, S. I., and Nielsen, P. A. 1990. The Archean Wyoming Province and its relations with adjacent Proterozoic provinces. *In* Lewry, J. F., and Stauffer, M. R., eds. The Early Proterozoic Trans-Hudson Orogen of North America. Geol. Assoc. Can. Spec. Pap. 37:287–300.

Eggler, D. H.; Meen, J. K.; Welt, F.; Dudás, F. Ö.; Furlong, K. P.; McCallum, M. E.; and Carlson, R. W. 1988. Tectonomagmatism of the Wyoming Province. *In* Drexler, J., and Larson, E. E., eds. Colorado volcanism. Colo. Sch. Mines Q. 33:25–40.

Engebretson, D. C.; Cox, A.; and Gordon, R. G. 1985. Relative motions between oceanic and continental plates in the Pacific Basin. Geol. Soc. Am. Spec. Pap. 206:34–42.

Esperança, S., and Holloway, J. R. 1987. On the origin of some mica-lamprophyres: experimental evidence from a mafic minette. Contrib. Mineral. Petrol. 95:207–216.

Feeley, T. C. 1993. Crustal modification during subduction zone magmatism: evidence from the southern Salar de Uyuni region (20°–22° S), central Andes. Geology 21:1019–1022.

Feeley, T. C., and Cosca, M. A. 2003. Time-composition v. composition trends of magmatism at Sunlight volcano, Absaroka volcanic province, Wyoming. Geol. Soc. Am. Bull. 115.

Feeley, T. C.; Cosca, M. A.; and Lindsay, C. R. 2002. Petrogenesis and implications of cryptic hybrid magmas from Washburn volcano, Absaroka volcanic province, USA. J. Petrol. 43:663–703.

Feldstein, S. N., and Lange, R. A. 1999. Pliocene potassic magmas from the Kings River region, Sierra Nevada,

California: evidence for melting of a subduction modified mantle. J. Petrol. 40:1301–1320.

Gill, J. 1981. Orogenic andesites and plate tectonics. Berlin, Springer, 390 p.

Gill, J. B. 1987. Early geochemical evolution of an ocean island arc and backarc: Fiji and the South Fiji Basin. J. Geol. 95:589–615.

Gill, J. B.; Morris, J. D.; and Johnson, R. W. 1993. Timescale for producing the geochemical signature of island arc magmas: U-Th-Po and Be-B systematics in recent Papua New Guinea lavas. Geochim. Cosmochim. Acta 57:4269–4283.

Gurnis, M., and Hager, B. H. 1988. Controls on the structure of subducted slabs. Nature 335:317–321.

Harlan, S. S.; Snee, L. W.; and Geissman, J. W. 1996. $^{40}Ar/^{39}Ar$ geochronology and paleomagnetism of Independence volcano, Absaroka Volcanic Supergroup, Beartooth Mountains, Montana. Can. J. Earth Sci. 33: 1648–1654.

Harry, D. L., and Leeman, W. P. 1995. Partial melting of melt metasomatized subcontinental mantle and the magma source potential of the lower lithosphere. J. Geophys. Res. 100:10,255–10,269.

Hawkesworth, C. J.; Gallagher, K.; Hergt, J. M.; and McDermott, F. 1993. Mantle and slab contributions in arc magmas. Annu. Rev. Earth Planet. Sci. 21: 175–204.

Hickey-Vargas, R.; Moreno Roa, H.; Lopez Escobar, L.; and Frey, F. A. 1989. Geochemical variations in Andean basaltic and silicic lavas from the Villarrica-Lanin volcanic chain (39.5° S): an evaluation of source heterogenity, fractional crystallization and crustal assimilation. Contrib. Mineral. Petrol. 103:361–386.

Hiza, M. M. 1999. The geochemistry and geochronology of the Eocene Absaroka volcanic province, northern Wyoming and southwest Montana, USA. Ph.D. dissertation, Oregon State University, Corvallis.

Hofmann, A. W. 1988. Chemical differentiation of the earth: the relationship between mantle, continental crust, and oceanic crust. Earth Planet. Sci. Lett. 90: 297–314.

Holder, R. W., and Holder, G. A. M. 1988. The Colville Batholith: Tertiary plutonism in northeast Washington associated with graben and core-complex (gneiss dome) formation. Geol. Soc. Am. Bull. 100:1971–1980.

Hooper, P. R.; Bailey, D. G.; and McCarley Holder, G. A. 1995. Tertiary calc-alkaline magmatism associated with lithospheric extension in the Pacific Northwest. J. Geophys. Res. 100:10,303–10,319.

Humphreys, E. D. 1995. Post-Laramide removal of the Farallon slab, western United States. Geology 23: 987–990.

Iddings, J. P. 1895. Absarokite-shoshonite-banakite series. J. Geol. 3:935–959.

Jakes, P., and White, A. J. R. 1972. Major and trace element abundances in volcanic rocks of orogenic areas. Geol. Soc. Am. Bull. 83:29–40.

Kincaid, C., and Olsen, P. 1987. An experimental study of subduction and slab migration. J. Geophys. Res. 92: 13,832–13,840.

Lipman, P. W. 1980. Cenozoic volcanism in the western United States: implications for continental tectonics. *In* Burchfield, J. C.; Oliver, J. E.; and Silver, L. T., eds. Studies in geophysics, continental tectonics. Washington, D.C., Natl. Acad. Sci., p. 161–174.

Lipman, P. W.; Prostka, H. J.; and Christiansen, R. L. 1972. Cenozoic volcanism and plate-tectonic evolution of the western United States. Philos. Trans. R. Soc. Lond. A Math. Phys. Sci. 271:271–248.

Luedke, R. G. 1994. Map showing the distribution, composition, and age of early and middle Cenozoic volcanic centers in Idaho, Montana, west-central South Dakota, and Wyoming. U.S. Geol. Surv. Map I-2291-C.

MacDonald, R.; Upton, B. G. J.; Collerson, K. D.; Hearn, B. C., Jr.; and James, D. 1992. Potassic mafic lavas of the Bearpaw Mountains, Montana: mineralogy, chemistry, and origin. J. Petrol. 33:305–346.

McKenzie, D. P. 1969. Speculations on the consequences and causes of plate motions. Geophys. J. Astron. Soc. 18:1–32.

Meen, J. K. 1987. Formation of shoshonites from calcalkaline basalt magmas: geochemical and experimental constraints from the type locality. Contrib. Mineral. Petrol. 104:309–331.

Meen, J. K., and Eggler, D. H. 1987. Petrology and geochemistry of the Cretaceous Independence volcanic suite, Absaroka Mountains: clues to the composition of the Archean sub-Montanan mantle. Geol. Soc. Am. Bull. 98:238–247.

Menzies, M. A.; Rogers, N.; Tindle, A.; and Hawkesworth, C. J. 1987. Metasomatic and enrichment processes in lithospheric peridiotites, an effect of asthenosphere-lithosphere interaction. *In* Menzies, M. A., and Hawkesworth, C. J., eds. Mantle metasomatism. London, Academic Press, p. 313–361.

Morris, G. A., and Hooper, P. R. 1997. Petrogenesis of the Colville igneous complex, northeast Washington: implications for Eocene tectonics in the northern U.S. Cordillera. Geology 25:831–834.

Nelson, W. H., and Pierce, W. G. 1968. Wapiti Formation and Trout Peak Trachyandesite, northwestern Wyoming. U.S. Geol. Surv. Bull. 1254-H, 11 p.

Norman, M. C., and Mertzman, S. A. 1991. Petrogenesis of Challis volcanics from central and southwestern Idaho: trace element and Pb isotopic evidence. J. Geophys. Res. 96:13,279–13,293.

O'Brien, H. E.; Irving, A. J.; and McCallum, I. S. 1991. Eocene potassic magmatism in the Highwood Mountains, Montana: petrology, geochemistry, and tectonic implications. J. Geophys. Res. 96B:13,237–13,260.

O'Brien, H. E.; Irving, A. J.; McCallum, I. S.; and Thirlwall, M. F. 1995. Strontium, neodymium and lead isotopic evidence for the interaction of post-subduction asthenospheric potassic magmas of the Highwood Mountains, Montana, U.S.A., with ancient Wyoming Cration lithospheric mantle. Geochim. Cosmochim. Acta 59:4539–4556.

Patino, L. C.; Carr, M. J.; and Feigenson, M. D. 1997. Cross-arc geochemical variations in volcanic fields in

Honduras, CA: progressive changes in source with distance from the volcanic front. Contrib. Mineral. Petrol. 129:341–351.

Pearce, J. A. 1982. Trace element characteristics of lavas from destructive plate boundaries. *In* Thorpe, R. S., ed. Andesites. New York, Wiley, p. 525–548.

Pearce, J. A., and Peate, D. W. 1995. Tectonic implications of the composition of volcanic arc magmas. Annu. Rev. Earth Planet. Sci. 23:251–285.

Prodehl, C., and Lipman, P. W. 1989. Crustal structure of the Rocky Mountain region. Geol. Soc. Am. Mem. 172:249–284.

Righter, K., and Carmichael, I. S. E. 1992. Hawaiites and related lavas in the Atenguillo graben, western Mexican Volcanic Belt. Geol. Soc. Am. Bull. 104:612–626.

Ruppel, E. T. 1972. Geology of pre-Tertiary rocks in the northern part of Yellowstone National Park, Wyoming. U.S. Geol. Surv. Prof. Pap. 729-A, 66 p.

Ryan, J. G.; Morris, J. D.; Tera, F.; Leeman, W. P.; and Tsvetkov, A. 1995. Cross-arc geochemical variations in the Kurile arc as a function of slab depth. Science 270:625–627.

Severinghaus, J., and Atwater, T. 1990. Cenozoic geometry and thermal state of the subducted slabs beneath western North America. *In* Wernicke, B. P., ed. Basin and range extension tectonics near the latitude of Las Vegas, Nevada. Geol. Soc. Am. Mem. 176:1–22.

Sigmarsson, O.; Condomines, M.; and Morris, J. D. 1990. Uranium and ^{10}Be enrichments by fluids in Andean arc magmas. Nature 346:163–165.

Smedes, H. W., and Prostka, H. J. 1972. Stratigraphic framework of the Absaroka Volcanic Supergroup in the Yellowstone National Park Region. U.S. Geol. Surv. Prof. Pap. 729-C, 33 p.

Stolper, E., and Newman, S. 1994. The role of water in the petrogenesis of Mariana trough magmas. Earth Planet. Sci. Lett. 121:293–325.

Sudo, A., and Tatsumi, Y. 1990. Phlogopite and K-amphibole in the upper mantle: implication for magma genesis in subduction zones. Geophys. Res. Lett. 17:29–32.

Sundell, K. A. 1993. A geologic overview of the Absaroka volcanic province. *In* Snoke, A. W.; Steidtmann, J. R.; and Roberts, S. M., eds. Geology of Wyoming. Geol. Surv. Wyo. Mem. 5:480–506.

Tatsumi, Y. 1989. Migration of fluid phases and genesis of basaltic magmas in subduction zones. J. Geophys. Res. 94:4697–4707.

Tatsumi, Y., and Eggins, S. 1995. Subduction zone magmatism. Cambridge, Blackwell, 211 p.

Tatsumi, Y.; Hamilton, D. L.; and Nesbitt, R. W. 1986. Chemical characteristics of fluid phase released from a subducted lithosphere and the origin of arc magmas: evidence from high-pressure experiments and natural rocks. J. Volcanol. Geotherm. Res. 29:293–309.

Walker, J. A.; Carr, M. J.; Patino, L. C.; Johnson, C. M.; Feigenson, M. D.; and Ward, R. L. 1995. Abrupt change in magma generation processes across the Central American arc in southeastern Guatemala: flux-dominated melting near the base of the wedge to decompression melting near the top of the wedge. Contrib. Mineral. Petrol. 120:378–390.

Wernicke, B. P.; Christiansen, R. L.; England, P. C.; and Sonder, L. J. 1987. Tectonomagmatic evolution of Cenozoic extension in the North American Cordillera. *In* Coward, M. P.; Dewey, J. F.; and Hancock, P. L., eds. Continental extensional tectonics. Geol. Soc. Lond. Spec. Publ. 28:203–221.

Wheeler, J. O.; Brookfield, A. J.; Gabrielse, H.; Monger, J. W.; Tipper, H. W.; and Woodsworth, G. J. 1991. Terrane map of the Canadian Cordillera. Geol. Surv. Can. Map 1713A.

Wooden, J. L., and Mueller, P. A. 1988. Pb, Sr, and Nd isotopic compositions of a suite of Late Archean, igneous rocks, eastern Beartooth Mountains: implications for crust-mantle evolution. Earth Planet. Sci. Lett. 87:59–72.

YELLOWSTONE NATIONAL PARK, ISLAND PARK, AND VICINITY FIELD TRIP GRIDE



Simultaneous eruptions of Castle and Beehive geysers, Upper Geyser Basin, Yellowstone National Park (July, 2004)

GEO 429R – Field Geology

Montana State University
Department of Earth Sciences

July 2-4, 2014

Introduction

This guide is complied with liberal use of previously published road logs by Smith and Downs (1989; AGU Field Trip Guidebook T305) and Smith and Siegel (2000; Windows into the Earth; Oxford University Press), Montagne and Chadwick (1976), Parsons (1978), and Fritz (1995). The guide provides an overview of Quaternary and Pliocene volcanic activity in and around Yellowstone National Park and Island Park, Idaho, focusing on the modern Yellowstone caldera and associated volcanic rocks. Additional optional stops focus on aspects of the Yellowstone geothermal system and regional geology of Gallatin Canyon and the Paradise Valley. The guide does not stress glacial or other aspects of the complex geologic history of the region in detail, which are depicted on the geologic maps in Christiansen (2001).

The field trip begins in Bozeman, Montana and is designed to be completed in three days (Figure 1). The formal stops are in Yellowstone National Park and Island Park with the aim of examining manifestations of volcanism to the north of and within the modern Yellowstone caldera and a "dead" caldera in Island Park. Collectively, the field trip will traverse a large part of the region known to geologists throughout the world as the Pliocene to Quaternary Yellowstone Plateau volcanic field.

Note to Field Trip Participants: Because of National Park regulations, no rock collection is allowed in the park at any time or any place. Bear in mind that geologic rock picks can be a quite disturbing sight for some guests. Therefore, it is best to leave your rock hammer in the vehicles while we are within the park boundaries. While none of the stops are physically demanding, because of the altitude, mid-summer heat or cold, and effects of geothermal fumes, participants should consider their physical condition. At the very least, bring water, snacks, sun screen, sunglasses, bug spray, a hat, a rain jacket, and a fleece jacket. Also consider that even though it is mid-summer, it is possible that days and nights in the northern Rocky Mountains can get quite cold, warm, rainy or even snowy. Special caution should also be exercised when visiting the thermal areas. These areas are both delicate and dangerous. Everyone should use designated walkways and follow posted Park regulations. **FINALLY, WHEN CAMPING WE MUST MAINTAIN A CLEAN CAMPSITE. BECAUSE OF WILDLIFE NOTHING CAN BE LEFT OUT AT NIGHT. ALSO, PLEASE STRICTLY ADHERE TO CAMPGROUND QUIET HOURS.**

Bring a notebook, which you will turn in at the end of the trip. Your notes should consist of a road log of the stops we make, official or unofficial. The notes should include a description of the location of each stop (including the date and time) and arranged in the order of the stops (for example: Stop 5: Grand Canyon of the Yellowstone River). The notes should describe any geological landmarks, volcanic features, tectonic features, etc. that are discussed at each stop. You should also try to incorporate your own observations and questions to the greatest extent possible. The purpose of the notebook is to provide you with a set of additional, personal notes from which you can retrace our steps and lead a similar field trip if required or asked to do so by friends, family, or in a professional situation. The notes should be legible (to the extent possible in a field situation) and supplemented by illustrations where feasible. Do not forget to put your name, date, name of field trip, etc. in the front of the notes.

Volcanic and Tectonic Setting of the Yellowstone Plateau Volcanic Field

By any number of measures, the Yellowstone Plateau volcanic field is one of the most spectacular areas of active volcanism on Earth. Nearly every geologist is familiar with Yellowstone National Park, as the area hosts what is perhaps the largest active rhyolitic caldera system in the world. During the past 2.5 million years, the volcanic field has erupted over 6,500 km^3 of lava and ash (actually, quenched magma) - nearly enough to fill the Grand Canyon of the Colorado River. Most of this material erupted catastrophically during three explosive “super-eruptions” larger and more powerful than any in the world's recorded history. These eruptions, which respectively were 2,500, 280, and 1,000 times larger than the 1980 eruption of Mount St. Helens in Washington State, formed three giant calderas, or volcanic depressions, and

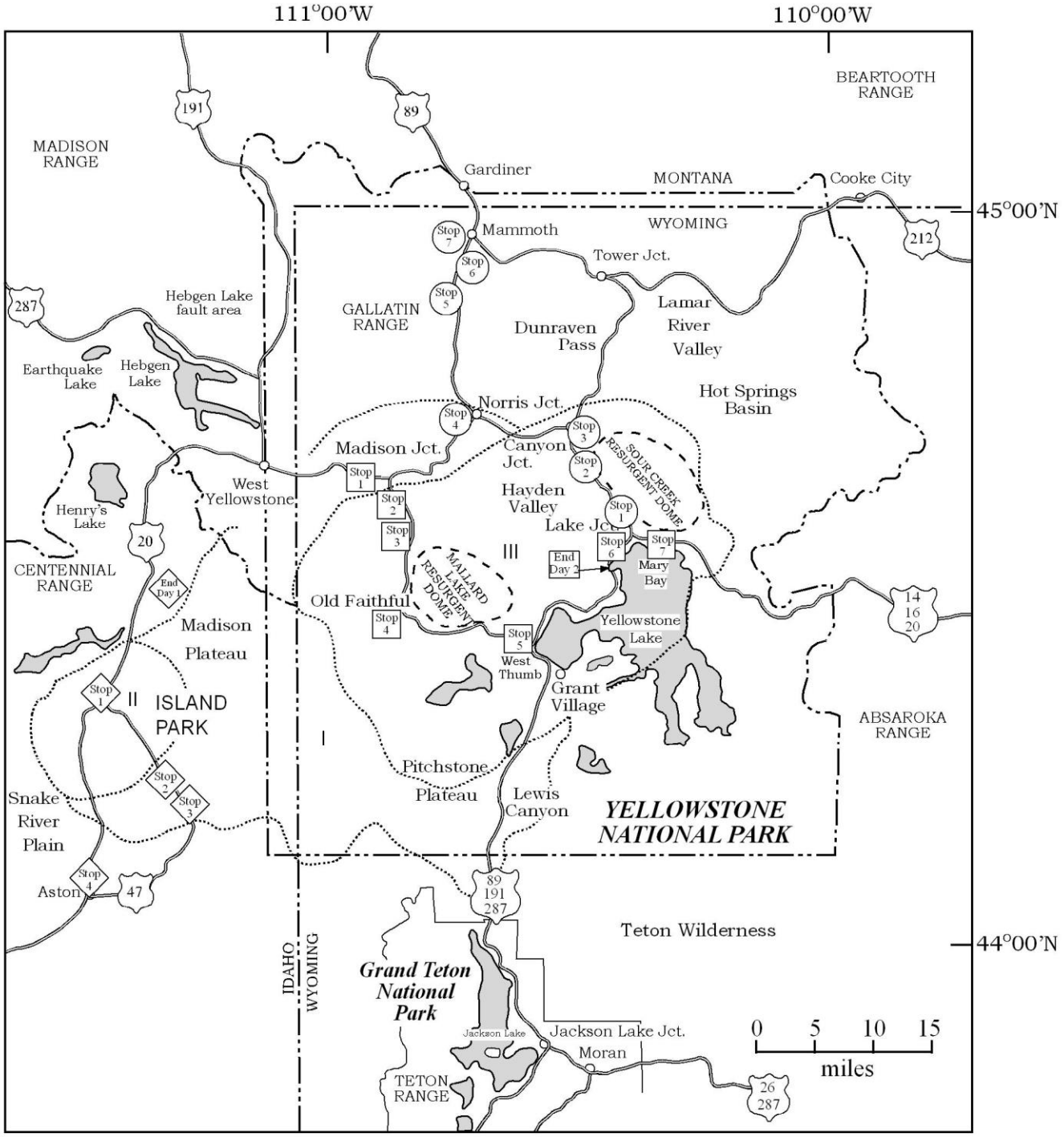


Figure 1. Index map with numbers for each "official" stop related to the Yellowstone Plateau Volcanic Field. Stops for Day 1 are in diamonds, stops for Day 2 are in squares, and stops for Day 3 are in squares. Dotted lines show outlines of ancient eruption calderas.

covered much of the United States with a thin layer of ash (Figure 2).The most recent of these, the 640 thousand year old Yellowstone caldera, measures 30 by 45 miles and covers much of central Yellowstone National Park. The heat emitted through the caldera floor is thirty to forty times greater than the average heat flow for North America. This high heat flow is interpreted to reflect crystallization of a midcrustal magma (magma and lava are nearly synonymous terms: when underground, molten rock is referred to as magma; when it erupts, it is referred to as lava) body beneath the caldera (Figure 3). Regionally, the collective magnitude of the three eruptions have been so great that the rugged topography characteristic of the northern Rocky Mountains that existed prior to the volcanism has to large extent been reduced to a relatively flat, forested plateau, much of which is above 7,700 feet. This landscape is the legacy of supervolcanism, in which mountains were blown away or swallowed up as caldera floors sank and topographic depressions became infilled with ash and lava.

Volcanism of the Yellowstone Plateau volcanic field is actually the most recent episode of caldera-related volcanism in the northwest United States that dates back to at least 16.5 million years ago. At this time, rhyolitic calderas began forming 500 miles to the southwest in the McDermitt region along the boarder of southeast Oregon and north-central Nevada. Since then, huge volumes of rhyolitic magma have erupted at least 100 times from giant calderas in at least seven and possibly as many as thirteen volcanic centers similar to the Yellowstone Plateau volcanic field. These older fields are now mostly hidden beneath younger basaltic lava flows of the Snake River Plain, but unambiguous evidence for their existence exists in the mountains that boarder the plain, in places where the Snake River has cut deep enough to create canyons exposing the rocks, and in deep drill cores. A distinctive feature of these rhyolitic volcanic fields, or "old Yellowstones" is that they become progressively younger to the northeast, culminating with the modern Yellowstone caldera (Figure 4).

The most popular interpretation for the origin of the Yellowstone Plateau volcanic field and the northeast age progression along the chain of calderas is that the North American plate of the Earth's crust is migrating at 1-2 centimeters per year in a southwest direction over a fixed and continuous plume of molten basaltic rock. Previously it was assumed that this plume, or "hotspot", rises from deep within the interior of the Earth, possibly originating near the boundary between the Earth's core and mantle 1000 miles beneath the surface. As the North American plate passes over the hotspot, heat from the basaltic magma melts rocks of the continental crust to create silica-rich magmas that collect in sponge-like chambers of partially molten rhyolite (Figure 5).

The theory of fixed hotspots creating chains of volcanoes with uniform age progressions is not new and is, in fact, very well documented at many places on Earth. For example, the Hawaiian hotspot has erupted through the Pacific plate for the past 80 million years creating the 3,600 mile long northwest trending chain of atolls, undersea volcanoes, and volcanic islands known as the Emperor-Hawaiian seamount chain. The Hawaiian hotspot is currently situated below the Island of Hawaii, the youngest island at the southeast end of the Hawaiian Islands, where the famed active shield volcanoes Kilauea, Mauna Loa, and Mauna Kea regularly erupt basaltic lava flows. In total, there are roughly 30 active hotspots on Earth, although almost all but the Yellowstone hotspot are located beneath oceans or near coastlines or other boundaries between the Earth's plates (Figure 6).

Although the theory of fixed deep hotspots is well established, recent research suggests that the ideas developed from areas like Hawaii may not be perfectly applicable to the Yellowstone-Snake River Plain system. Indeed, evidence suggests that the partly molten plume of the Yellowstone hotspot originates in the upper part of the Earth's mantle, only about 300 miles beneath

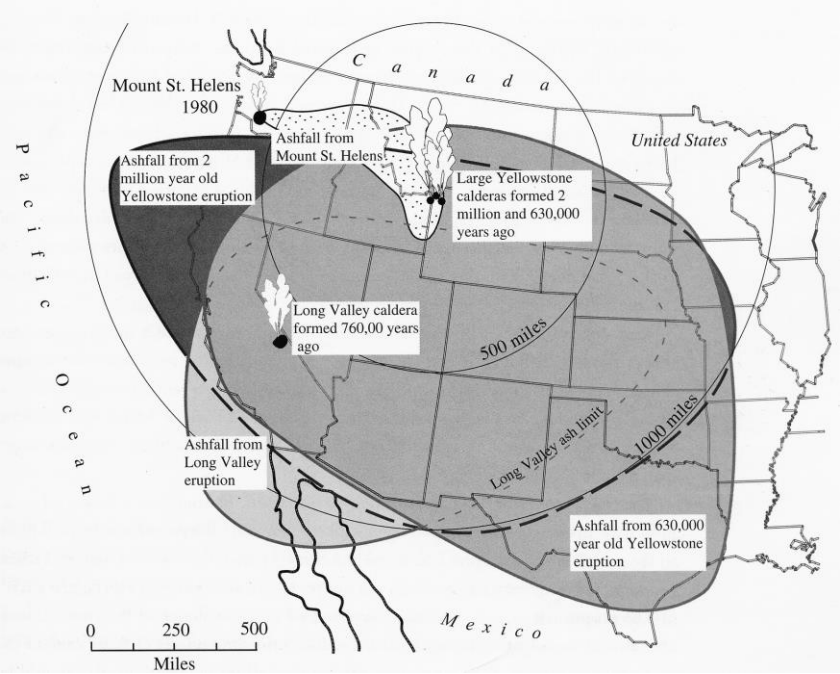


Figure 2. Areas of the United States once covered by ash from cycles 1 (~2.1 million years ago) and 3 (~640 thousand years ago) of the Yellowstone Plateau volcanic field along with the 760 thousand year old eruption of Long Valley caldera in California and the 1980 eruption of Mount St. Helens, Washington (from Smith and Siegel, 2000).

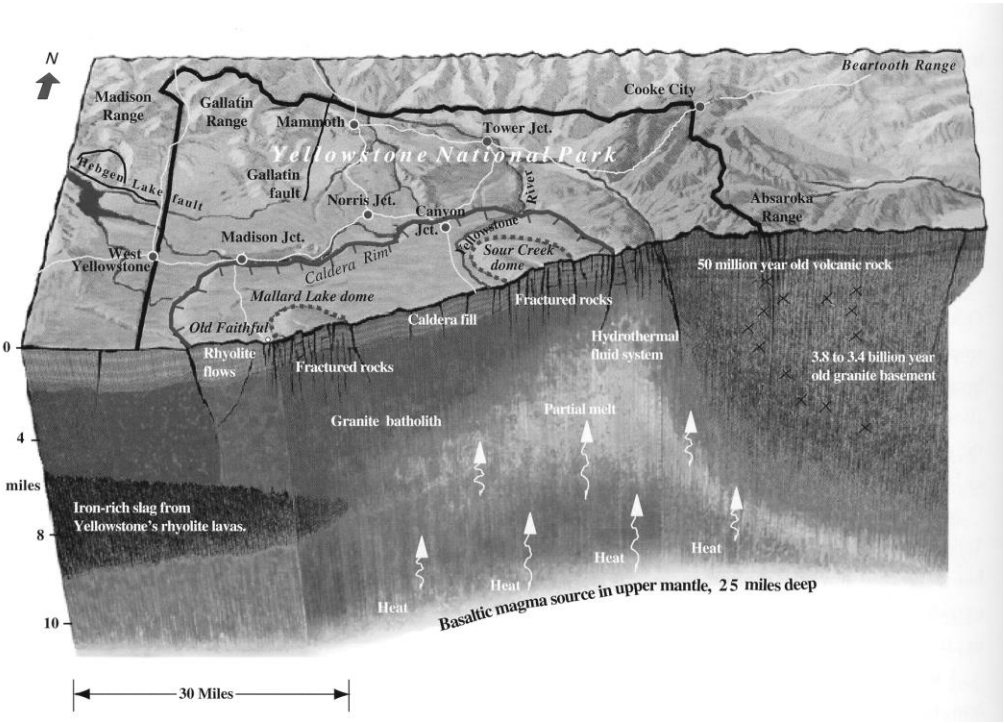


Figure 3. West to east cross section of Yellowstone National Park illustrates molten magma under the caldera at depths of about 3 to 8 miles (from Smith and Siegel, 2000).

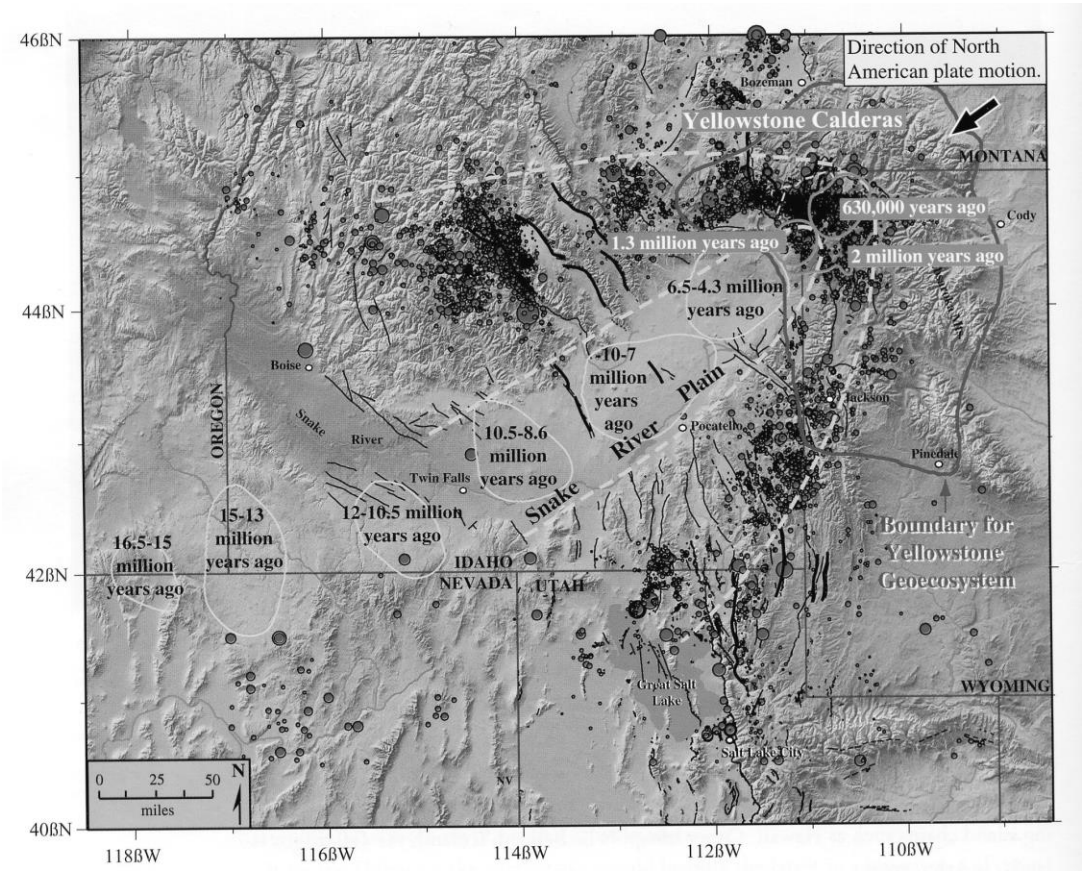


Figure 4. Path of the Yellowstone hotspot showing locations (yellow circles) where the hotspot produced one or more caldera eruptions in the time periods indicated. Also shown is parabola-shaped zone (brown and tan zone) of mountains and earthquakes (red dots) surrounding regions of low elevations (green zone; from Smith and Seigel, 2000).

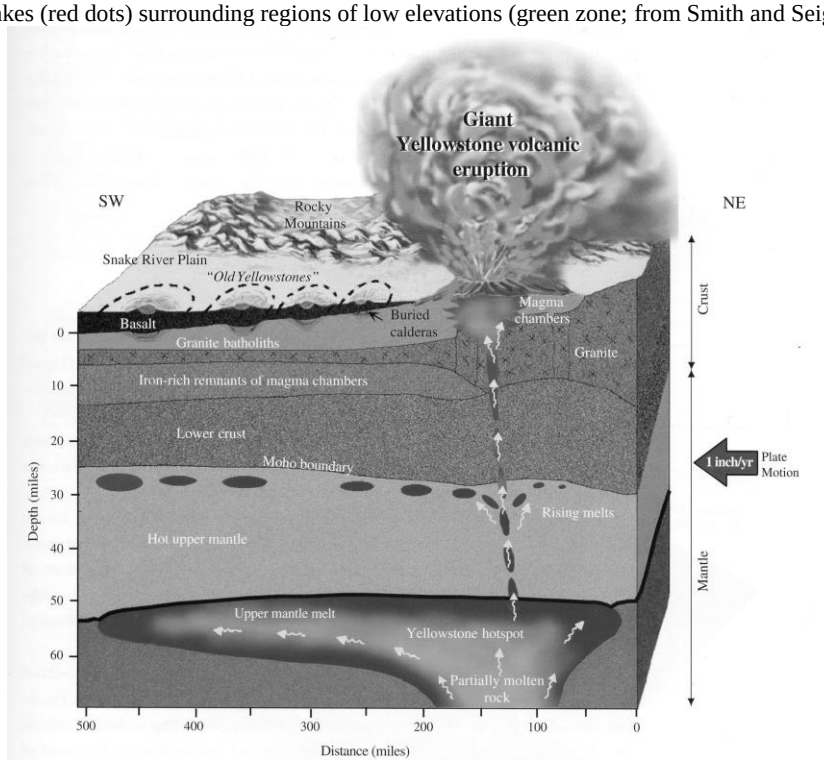


Figure 5. Cross section showing relationship of Yellowstone Plateau volcanic field and Snake River Plain to Yellowstone hotspot. Most magma rises directly from the hotspot to produce caldera forming eruptions by melting of granitic rocks in the continental crust. From Smith and Seigel (2000).

the surface (Figure 6). Moreover, although rhyolitic caldera related volcanism along the Yellowstone hotspot track shows a regular age-progression of younging to the northeast, basaltic volcanism has remained active along the entire length of the eastern Snake River Plain, even many hundreds of thousands to millions of years after the hotspot passed beneath any given area. For example, basaltic lava flows erupted as recently as 2,000 years ago in the Craters of the Moon volcanic field (and National Monument) near Arco, Idaho. For comparison, the youngest rhyolite lava flow erupted from the Yellowstone Plateau volcanic field is about 70,000 years old. Thus, when viewed on a regional scale, the Yellowstone-Snake River Plain system does not appear to fit the simple model of a hotspot track where volcanism dies out after the migrating plate has passed over the stationary plume.

In addition to the active volcanism, the Yellowstone Plateau is situated in a region of ongoing tectonic stretching, or extension. Young north to northwest trending extensional faults pass through the eastern margin of the plateau and extend southward paralleling the eastern margin of basin-range faulting in southeastern Idaho and western Wyoming (Figure 7). The most famous of these faults is the Teton fault, which trends in a north-south direction and has uplifted the Teton Range over the past 13 million years. To the west of the Teton Range and south of the Snake River Plain extensional faults are abundant and form a broad region of stretched crust known to geologists as the Basin and Range Province, which encompasses southern Idaho, southeastern California, parts of Arizona, and the entire state of Nevada (Figure 4). North of the Yellowstone Plateau-Snake River Plain the number of extensional faults and magnitude and area of crustal stretching are not nearly as extensive as they are south of the plain. This observation has led some geologists to suggest that the Yellowstone Plateau volcanic field is not a result of a fixed mantle plume at all, but instead marks the position of a "melting anomaly" associated with the northeastern propagating tip of an accommodation zone between regions of high and low crustal extension south and north of the Snake River Plain, respectively.

Regardless of its ultimate origin, volcanism of the Yellowstone Plateau and earlier volcanic fields strongly influence the pattern of earthquake activity and topography of the surrounding region. Just as when a boat moves through water it creates an arc- or parabola-shaped bow wave, the Yellowstone hotspot (or melting anomaly!) has left in its wake an arc-shaped belt of earthquake epicenters and high topography bordering both sides of the Snake River Plain and wrapping around the volcanic plateau (Figure 4). It is important to note that the hotspot did not create the mountains of the topographic swell or the earthquake faults. These were present prior to the arrival of the hotspot and have continued to develop following its passage. The hotspot did, however, uplift the volcanic plateau and mountains flanking the Snake River Plain to higher elevations, depress the Snake River Plain and destroy mountains that once crossed it, and provide a source of energy to trigger a larger number of earthquakes.

The area forming the band of earthquakes is known as the Intermountain Seismic Belt, the heart of which is centered on the Yellowstone area. In fact, although the Yellowstone Plateau represents only about 1 percent of the total area of the Intermountain Seismic Belt, it generates up to 20 percent of its earthquake energy (Figure 8). The two largest historic earthquakes in the belt, the magnitude 7.5 Hebgen Lake quake in 1959 and magnitude 7.3 Borah Peak quake in 1983 are both manifestations of this activity. Only faults in California produce more earthquakes today in the conterminous United States than the broad area encompassing Yellowstone National Park.

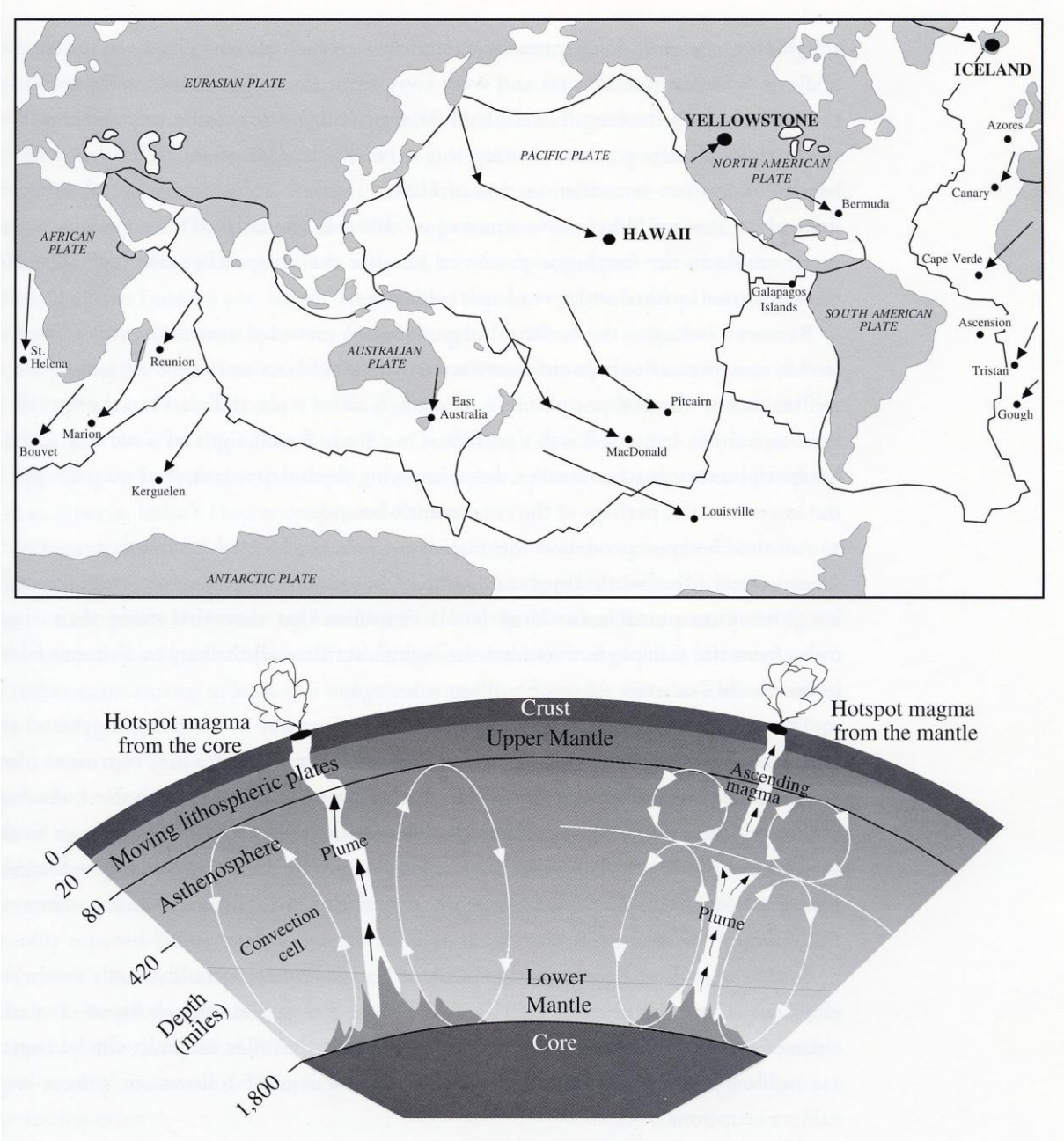


Figure 6. Upper figure shows locations of known hotspots (dots) on Earth. Arrows show apparent motion of hotspots as lithospheric plates of the Earth drift over them Lower figure shows cross section of Earth with traditional view of hotspots rising from the Earth's core on left and newer theory on right that Yellowstone hotspot originates at a much shallower depth. From Smith and Seigel (2000).

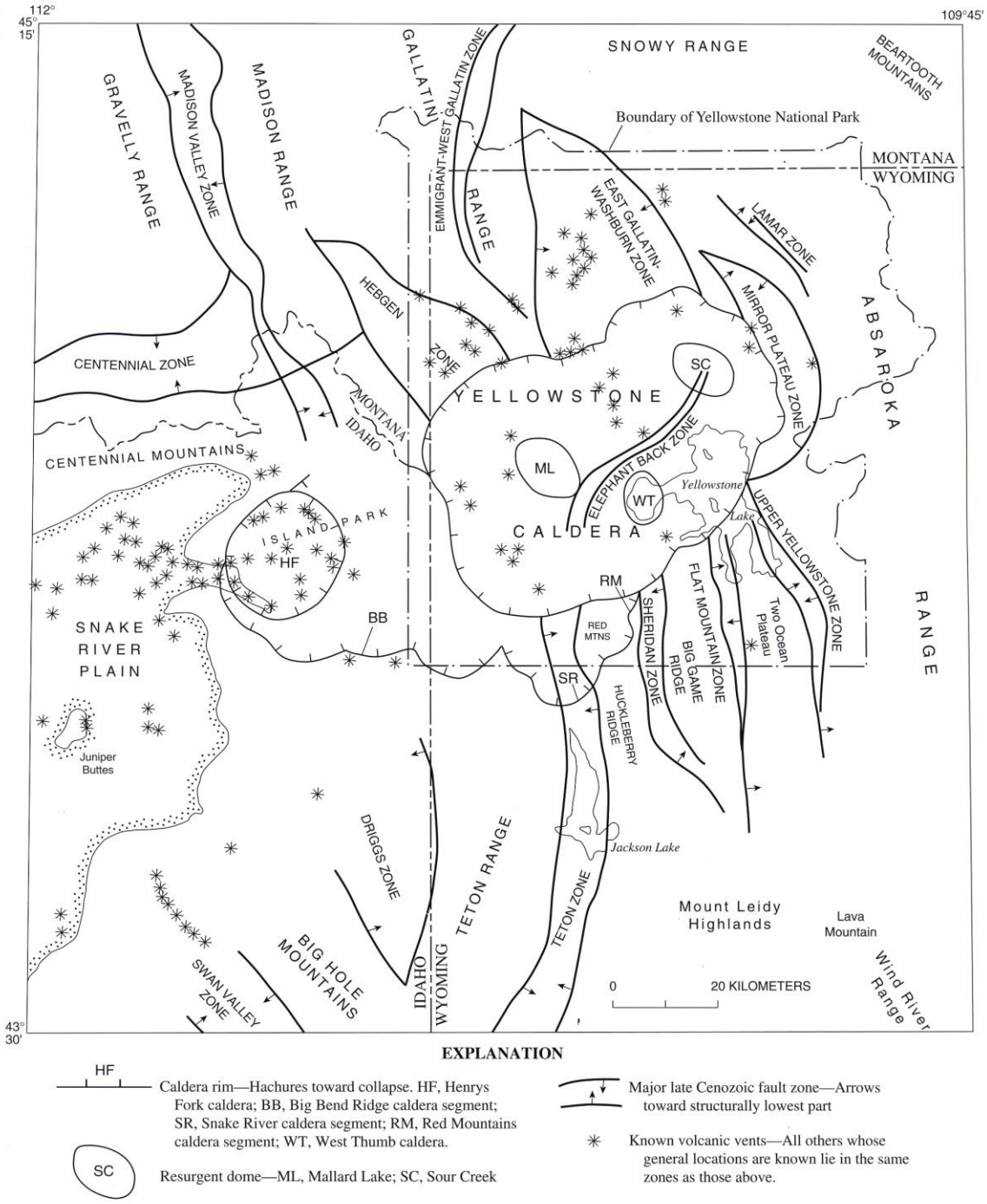


Figure 7. Map showing late Cenozoic volcanic and tectonic features of the Yellowstone Plateau volcanic field. From Christiansen (2001).

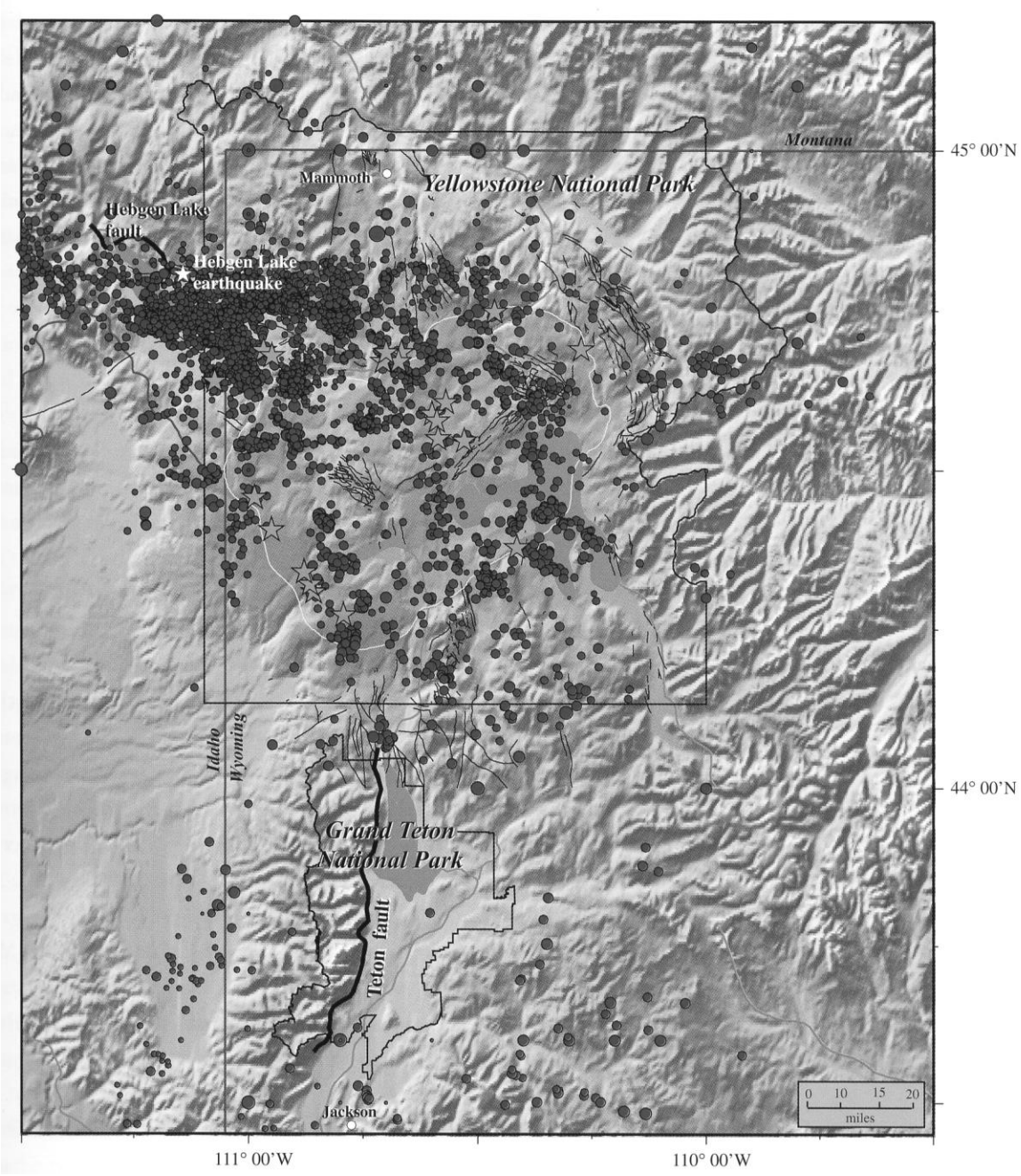


Figure 8. Map showing earthquake epicenters in the Yellowstone region from 1973 to 1996 (red dots). Most of the quakes were under magnitude 5. Active faults are shown are black lines and post-caldera volcanic vents are shown are orange stars (from Smith and Siegel, 2000)

Eruptive Styles and Resurgent Caldera Cycles

The Yellowstone Plateau volcanic field is a tectonically and erosionally dissected plateau that is the product of three main cycles of volcanism. These cycles all appear to have followed similar evolutionary patterns, each climaxing with the eruption of a large volume rhyolitic ash-flow tuff (a synonymous term for ash-flow tuff is "ignimbrite") from a huge caldera. An ash-flow tuff is a rock type consisting of a poorly sorted mixture of ash, pumice, and crystals deposited from a pyroclastic flow. Pyroclastic flows are hot (~800 ºC) and fast moving (up to 200 km/hr) avalanches of fragmented magma produced during highly explosive volcanic eruptions (Figure 9). The

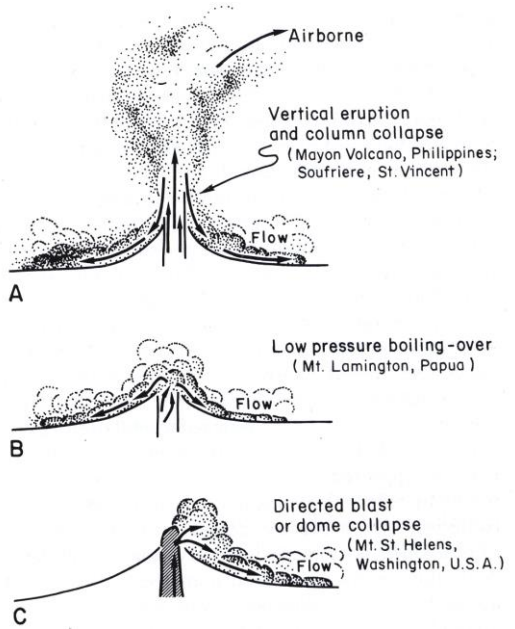


Figure 9. Mechanisms for producing pyroclastic flows (from Fisher and Schmincke, 1984).

three cycles of caldera and ash flow tuff formation recorded in the Yellowstone Plateau volcanic field are (figure 10):

- **The first cycle: various caldera segments and Huckleberry Ridge Tuff**, which erupted approximately 2.1 million years ago.
- **The second cycle: the Henrys Fork caldera and Mesa Falls Tuff** at approximately 1.3 million years ago.

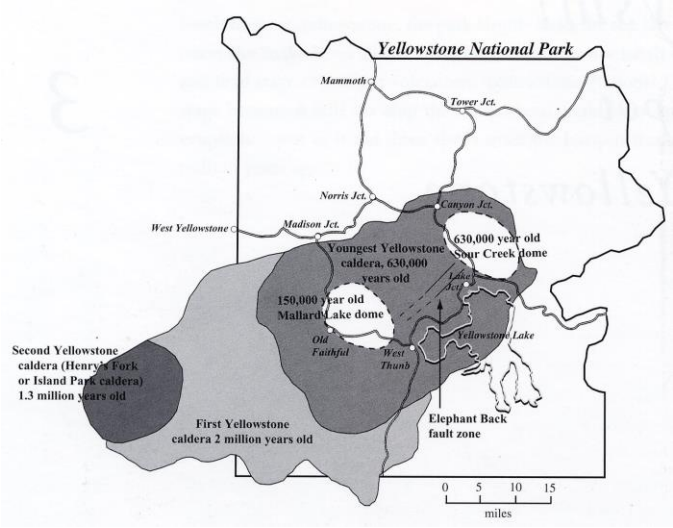


Figure 10. Locations of Yellowstone's three main calderas and resurgent domes of the modern caldera (from Smith and Siegel, 2000).

- **The third cycle: the Yellowstone caldera and Lava Creek Tuff** at approximately 640 thousand years ago.

In addition to the rhyolitic ash flow tuffs, significant volumes of magma also erupted as rhyolitic and basaltic lava flows.

Volcanic rocks erupted in the Yellowstone Plateau are almost exclusively basaltic (~ 50% SiO_2) or rhyolitic (~75% SiO_2) in composition. Compositionally, this style of volcanism is referred to by geologists as "bimodal" because there are virtually no volcanic rocks with silica concentrations intermediate between these two extremes. By contrast, stratovolcanoes such as Mount St. Helens in Washington State erupt vast amounts of andesite, intermediate composition magmas (~60% SiO_2).

When erupted as lava flows, the distributions of the rhyolitic and basaltic composition volcanic rocks are not random. For example, during the period when the volcanic system is active, rhyolitic lava flows are mainly confined to within the boundaries of the caldera, whereas basaltic lavas **only** erupt outside around the periphery. Basaltic lavas may, however, erupt within the boundaries of the caldera once rhyolitic volcanism has ceased or become extinct. The temporal distribution

of different rock types is also not random. For example, while the caldera is active, rhyolite magma erupts quietly as lava flows principally before and after caldera formation, whereas it erupts explosively as pyroclastic flows during caldera formation. In contrast, basaltic magma erupts exclusively as lava flows continuously throughout the eruptive cycles.

In detail, the evolutionary pattern of volcanism associated with each of the three caldera cycles is best understood in the context of the modern Yellowstone caldera, as tectonism, erosion, and burial have partially obscured the geologic record of the two older cycles. Geologists studying the Yellowstone Plateau volcanic field have identified three distinct stages in the evolutionary patterns of the caldera cycles. These are collectively called a "resurgent caldera cycle" and are characterized by the following processes (Figure 11).

- **Precaldera stage.** The volcanic cycle begins with eruptions of both basaltic and rhyolitic lava flows. In the case of the Yellowstone caldera, these eruptions preceded caldera formation by as much as 600 thousand years. Vents for the rhyolitic lava flows are inferred to have been mainly from developing ring-fracture or fault systems. The distribution of the early lava flows of the third volcanic cycle are shown in Figure 12. This activity reflects the growth of a shallow silicic magma chamber beneath the focus of volcanic activity, and climatic eruptions can be viewed as culminations of the growth of these chambers.

- **Caldera forming stage**. The climax of each cycle is marked by the rapid and explosive eruption of extremely large volumes of volcanic gas plus rhyolitic ash, pumice, and crystals. When mixed together, the ash, pumice, and crystals collectively have the identical composition as the rhyolitic lava flows of the preceding stage, they are just in a different physical state. Specifically, they are fragmented, or blown to bits, due to rapid expansion of volcanic gasses during the explosive eruption. The volume of the third cycle Lava Creek Tuff is approximately 1000 km^3; for comparison the 1980 eruption of Mount St. Helens produced about 1 km^3 of magma. The reconstructed distribution of the Lava Creek Tuff is illustrated in Figure 13.

The eruption of such large volumes of magma and gas during this phase of the eruption causes the roof of the magma chamber to lose structural integrity and collapse in a piston-like manner, forming a volcanic depression called a caldera (a similar, but not synonymous term is crater; a volcanic crater forms by lava reaming out a hole in the Earth). It is inferred that the formation of a caldera occurs when the ring fractures developing in the precaldera stage coalesce. The system of generally continuous and linked ring faults thus marks the semi-circular (sometimes elongate) outline of the roof of the magma chamber. For large calderas on Earth, several km's (~1.5-3.5) of subsidence are typical. Interestingly, although the Yellowstone caldera forms a single topographic basin, it actually comprises two distinct ring-fracture zones referred to as the **Mallard Lake** and **Sour Creek** caldera segments. These formed by subsidence of two separate segments of the roof over the highest parts of the very large Yellowstone magma chamber (Figure 13).

During the caldera forming eruption, about half of the volume of the pyroclastic flow escapes the caldera (**outflow facies**) to form widespread, but relatively thin sheets (10's of meters in thickness). About half of the volume of the pyroclastic material is deposited in the caldera (**intracaldera facies)** to form thick, syn-collapse accumulations reaching several km's in thickness. Often, and as in the case of the Yellowstone tuffs, the outflow facies forms a continuous deposit 360^o around the caldera if the volume of the eruption is sufficiently large. In smaller eruptions the ignimbrites are so modest in volume that they are confined to valleys around the calderas and do not form a continuous sheet. Frequently, the intracaldera pyroclastic flow contains within it large lenses of landslide

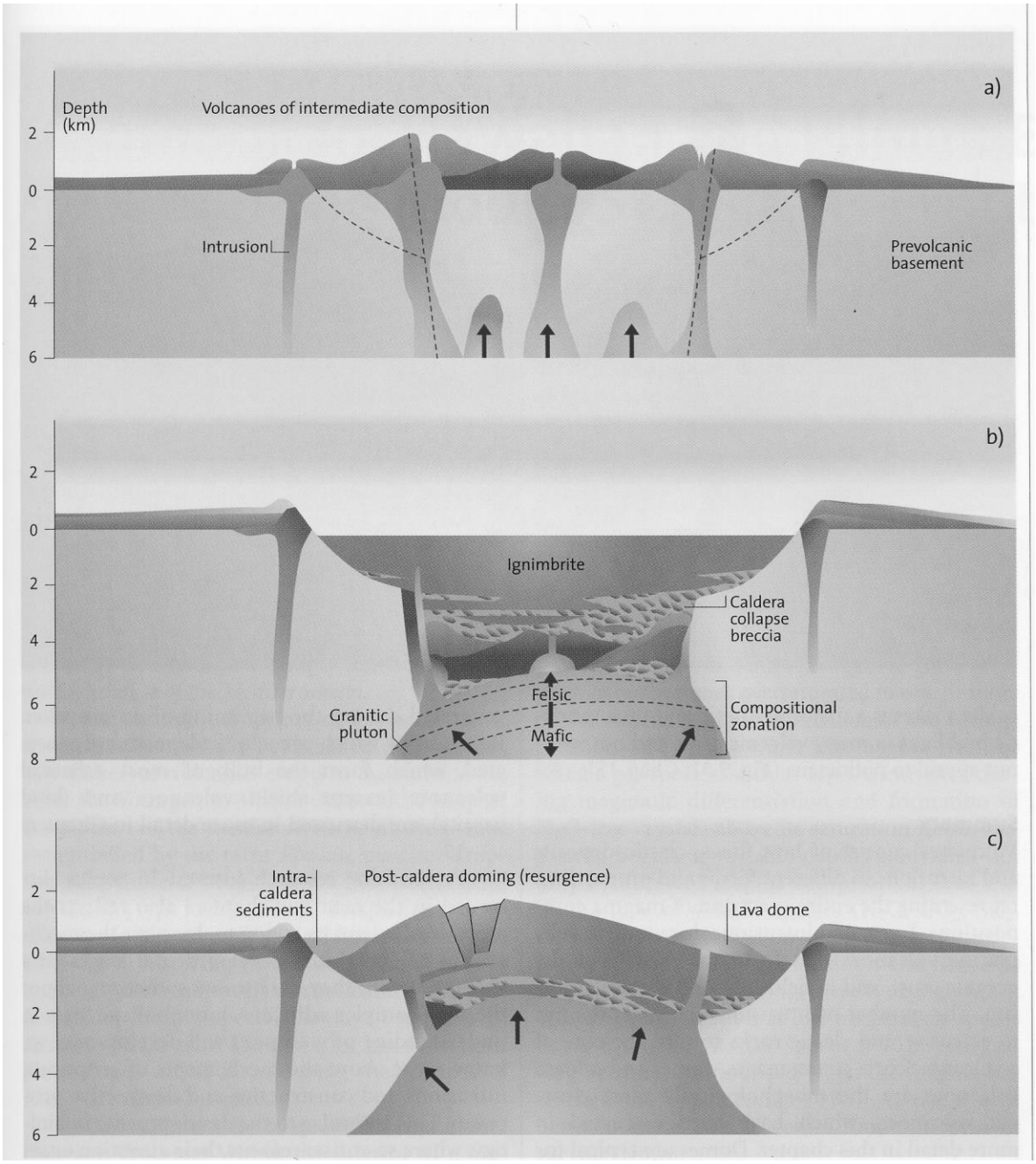


Figure 11. Stages in the evolution of a resurgent caldera system. Bright orange represents molten magma; dark orange and browns represent silicic volcanic rocks; gray represents basaltic lavas. Top figure shows early eruptions of precollapse lava flows and initial formation of ring fractures. Note that Yellowstone does not appear to erupt intermediate composition magmas during this stage; only rhyolite. Middle figure shows period after caldera collapse. Note thick intracaldera facies of ignimbrite, thin outflow facies, and enlargement of caldera walls by landslides. Bottom figure shows resurgent doming and post-collapse rhyolite lava domes within the caldera boundaries and basaltic volcanism outside boundaries. From Schmincke (2004).

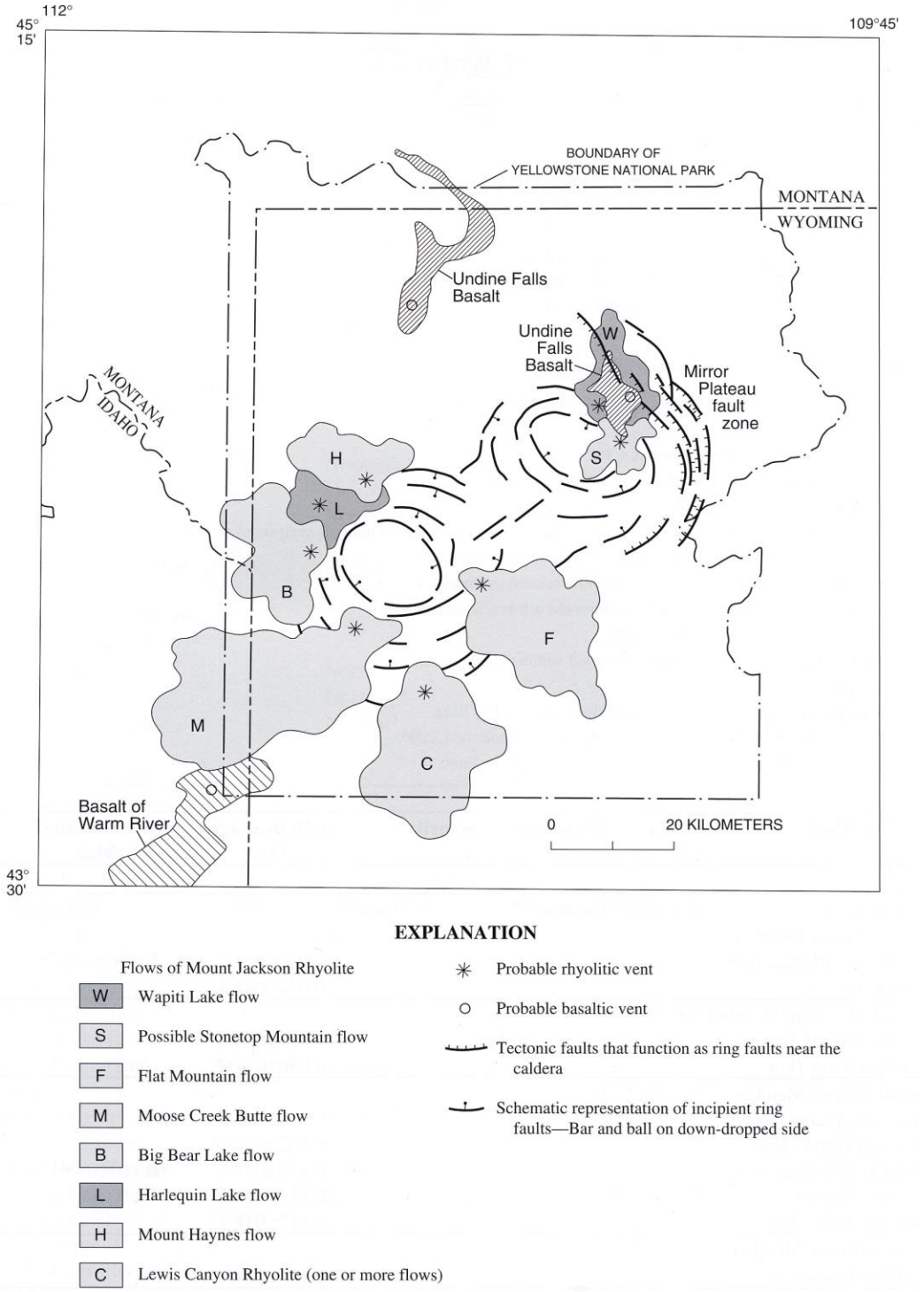


Figure 12. Distribution of early (precollapse) basaltic and rhyolitic lava flows of the third volcanic cycle. From Christiansen (2001).

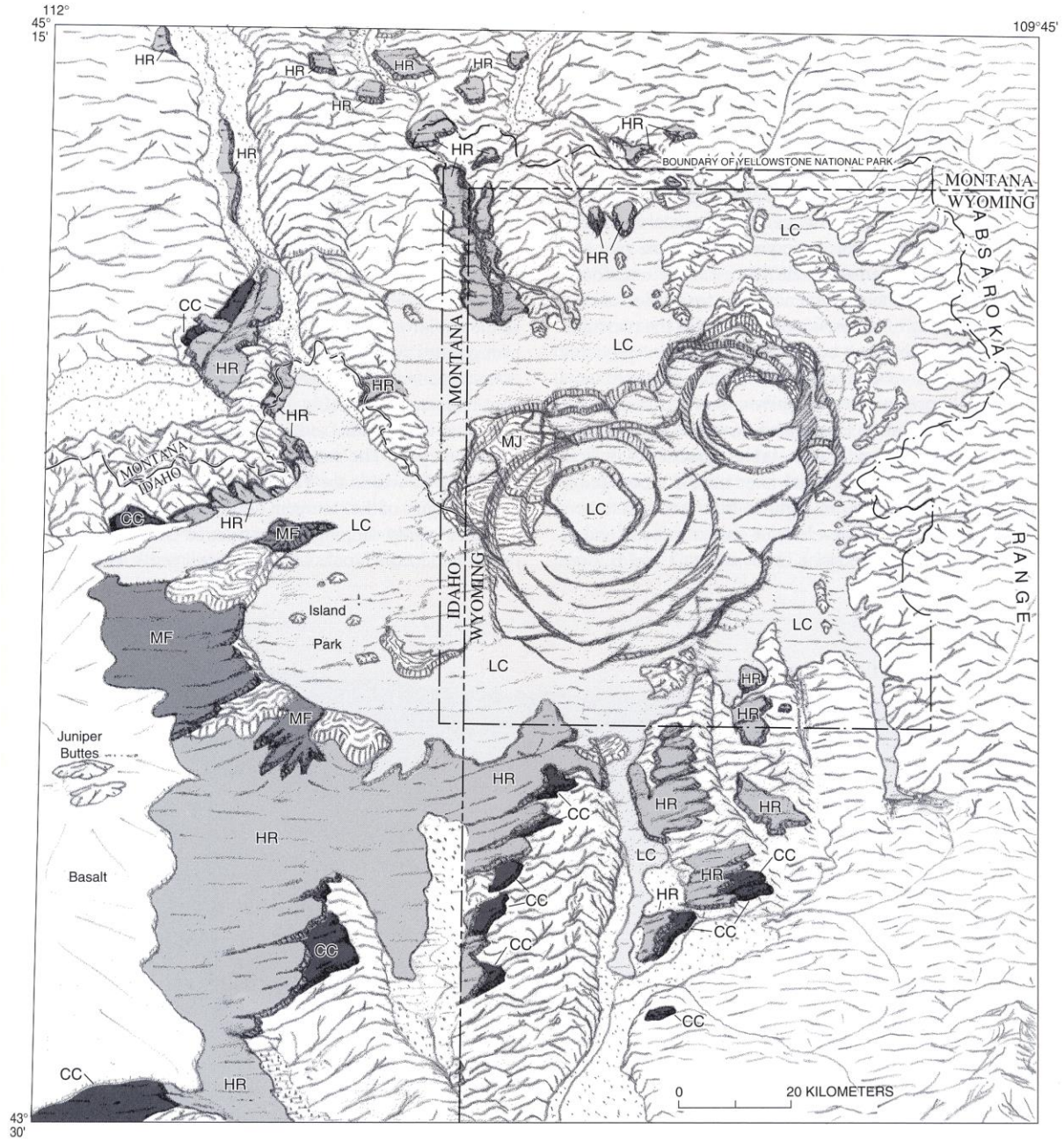


Figure 13. Reconstructed distribution of the Lava Creek Tuff (LC). Also shown are two caldera segments of the Yellowstone caldera. From Christiansen (2001).

breccia formed by slumping and shattering of unstable walls that have been oversteepened by structural collapse. These landslides enlarge the caldera beyond the dimensions defined by the ring faults, and they often create large irregularities (scallops) in the topographic caldera wall, leading to outlines far more complicated in detail than simple circular depressions (Figure 14).

- **Post-collapse volcanism and caldera resurgence stage.** After the caldera forming stage, a significant quantity of magma remains in the subcaldera magma chamber. As is common at other large calderas, at the Yellowstone caldera this magma rose and intruded the intracaldera tuff dooming up the roof of the caldera. This process is called **resurgence** and the associated dome is called a **resurgent dome**. Because the Yellowstone caldera consists of two independently subsided cauldron blocks, it should come as no surprise that it contains two resurgent domes: the Mallard Lake and Sour Creek resurgent domes (Figure 14).

The system of ring faults associated with caldera collapse provides pathways for magma to ascend to the surface. This results in eruption of post-collapse rhyolite lava flows and domes. The Yellowstone caldera has had a long, complex history of post-collapse rhyolitic volcanism. At least thirty lava flows erupted in the interval from about 640 thousand years ago to about 70 thousand years ago. These lava flows have erupted both within and outside the structural boundaries of the caldera. To large extent, these lava flows have obscured the actual location of the caldera boundaries (Figure 15). Eruptions of basaltic lava flows also continue outside the boundaries of the caldera during this period.

The system of ring faults also allows water to migrate down into hot intracaldera tuff, where it is heated and returns to the surface in the form of hydrothermal activity. The Yellowstone caldera system hosts the most diverse and intact collection of geysers, hot springs, mudpots, and fumaroles on Earth - more than 10,000 geothermal features in all. It contains more than 300 geysers that collectively make up two thirds of all those found on Earth. The distribution of the known present and past hydrothermal features associated with the modern Yellowstone caldera clearly shows the structural control (Figure 16). Most of the activity occurs within the ring fracture zones, but some is also associated with areas of resurgence and areas outside the caldera boundaries associated with zones of tectonic faulting.

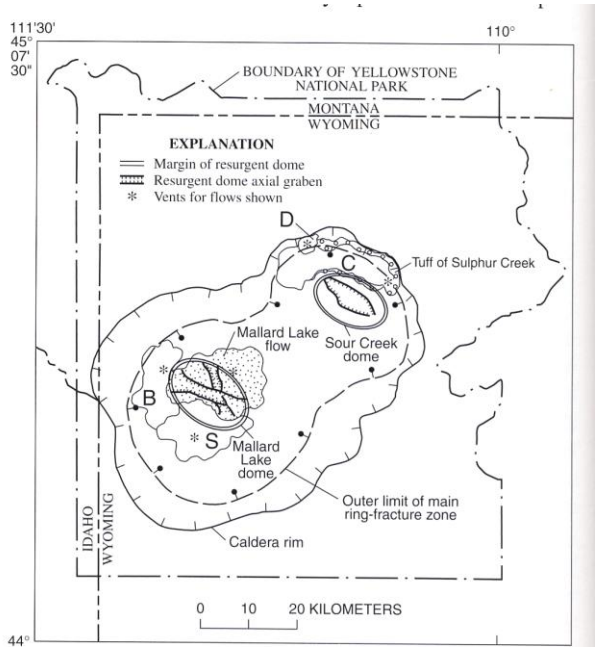


Figure 14. Distribution of early post-collapse rhyolite lava flows and inferred main ring fracture zone. Note widening of caldera by landsliding relative to main ring fracture zone. From Christiansen (2001).

The Yellowstone Magma Chamber

The Yellowstone caldera is an active volcano, although this generally was not recognized until the 1960's due to the relatively subdued Rocky Mountain topography and the widely forested volcanic structures of the Yellowstone Plateau. Convincing evidence for a relatively shallow magma body is the immense heat flow issuing from Yellowstone on a continual

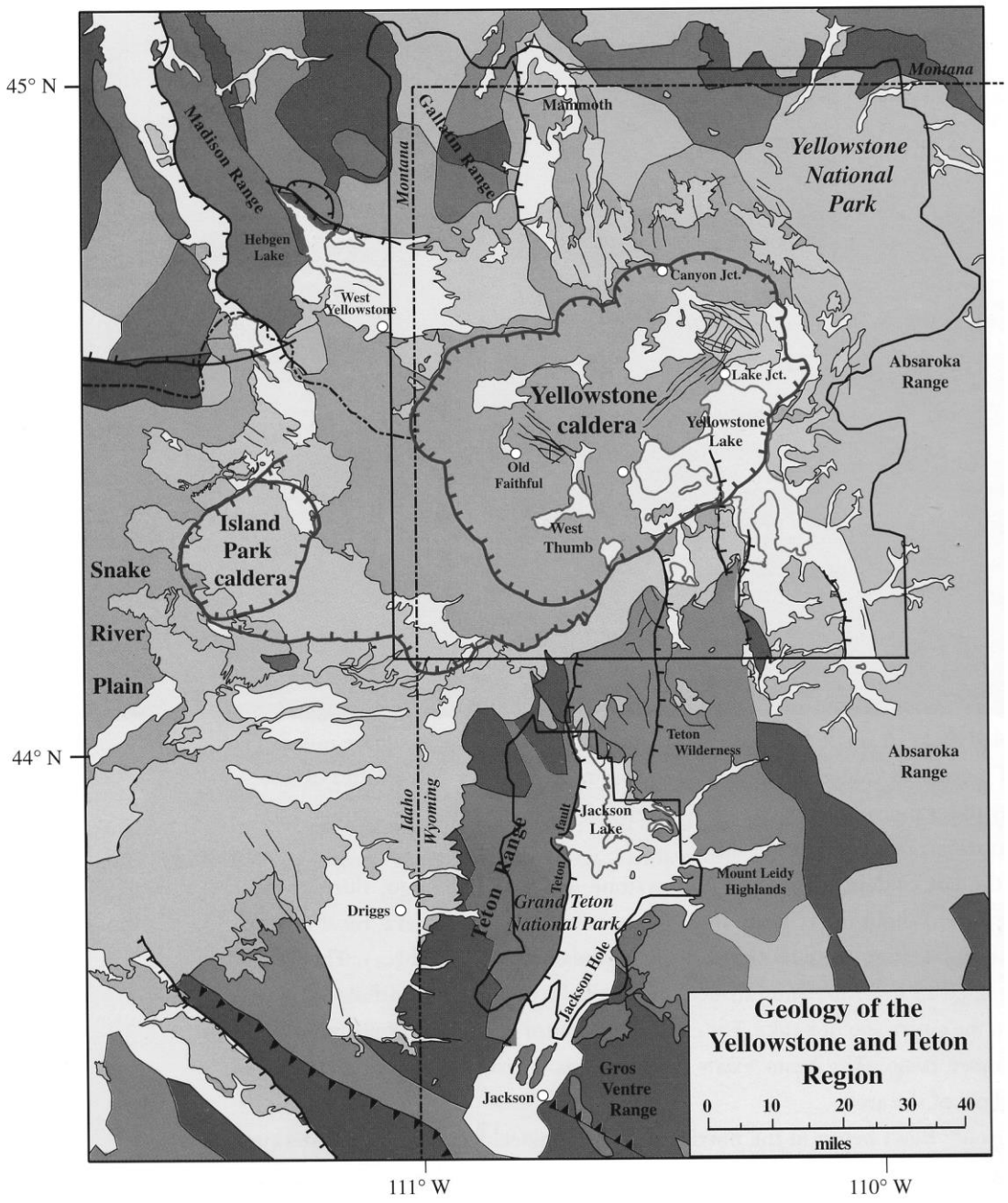


Figure 15. Generalized geologic map of the Yellowstone and Teton region. Note filling of Yellowstone caldera by post-collapse rhyolite lava flows (shown in intermediate grey). From Smith and Siegel (2000).

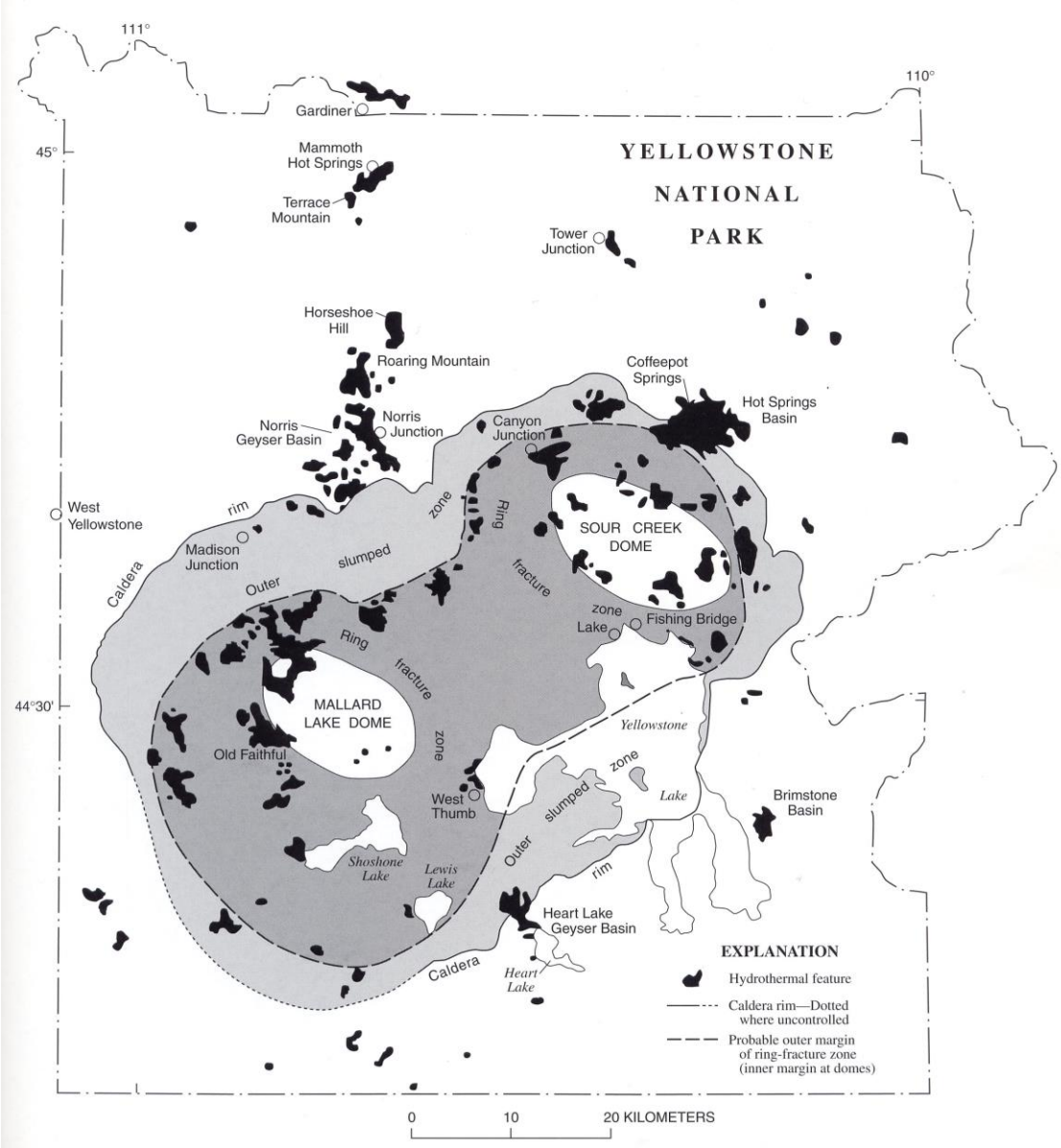


Figure 16. Map showing distribution of known hydrothermal features in Yellowstone Plateau region, both active and extinct. Note structural control of locations of hydrothermal features. Most are within the ring fracture zone of the Yellowstone caldera, although major extracaldera activity extends from Norris Geyser Basin to Mammoth Hot Springs. From Christiansen (2001).

basis. The estimated heat flow from Yellowstone is roughly 30 times greater that the average continental value. Estimates of gas flux also imply that Yellowstone is one of the Earth's most prolific sources of CO_2, releasing over 45,000 tons per day. Geophysical studies place constraints on the nature of the Yellowstone magma chamber. Seismic tomography based on local earthquakes indicates slowing of compressional (P) seismic waves starting at depths of ~5 miles. The seismic data can be interpreted as a partly molten zone with two ends located beneath the two resurgent domes (Figure 17). Strong slowing of shear (S) seismic waves at some seismic stations

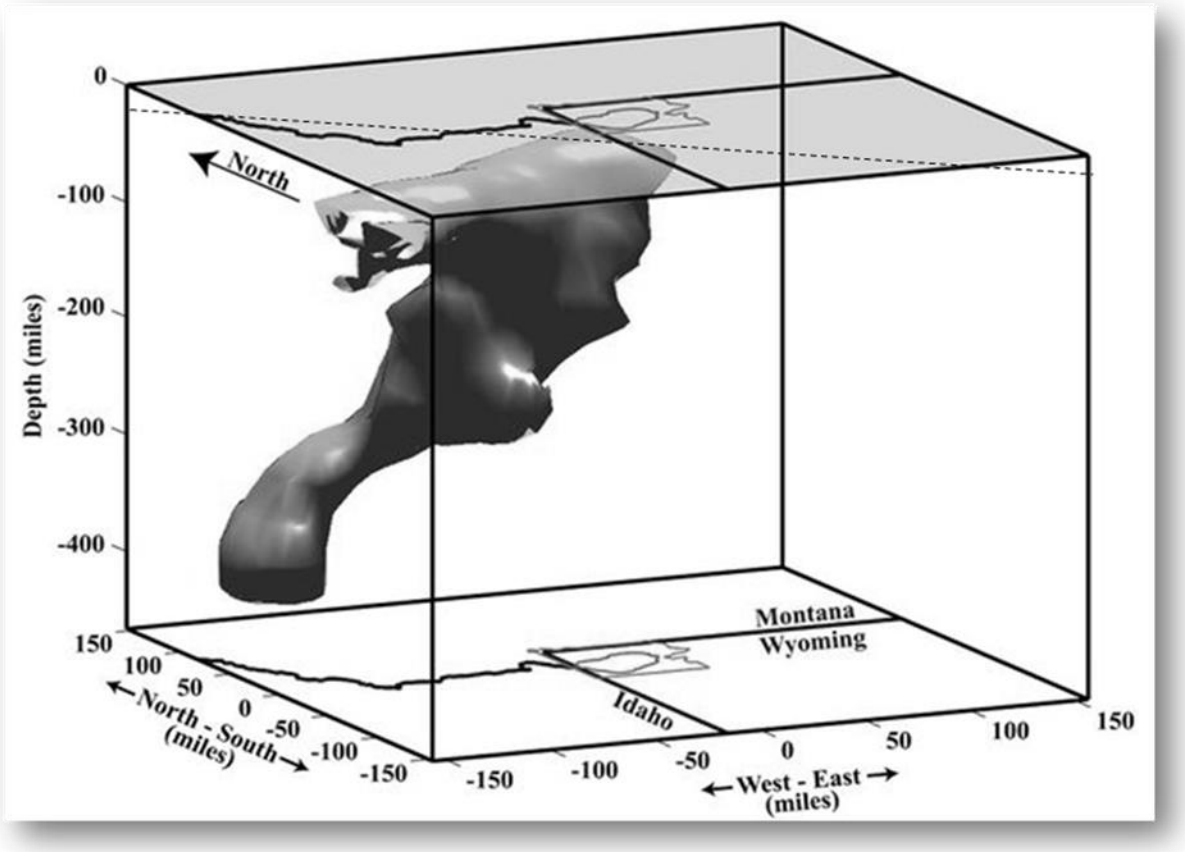


Figure 17. A new 3-D model shows the 45-mile-wide (72-kilometer-wide), 410-mile-deep (660-kilometer-deep) plume of hot, molten rock rising under Yellowstone's supervolcano.

is consistent with volumes of partly molten rock extending down to 12 miles or more. In addition, earthquake hypocenters only extend down to approximately 4 miles beneath the caldera, implying temperatures above 350 ºC at shallow depths. Outside the caldera, such temperatures are not achieved shallower than approximately 10 miles, suggesting much cooler rock.

Overall, the geophysical and geochemical evidence points strongly toward the presence of a large thermal anomaly (c.f., magma chamber?) in the shallow- to mid-crust. The big questions, however, are how much is eruptible magma and how much is hot rock or crystal mush? Given the size of the caldera and the depths discussed above, it is reasonable to infer that at least 25,000 km^3 of crystal-melt/mush are located beneath the Yellowstone caldera at depths from approximately 5 to 12 km. If melt fractions are 10 to 15%, then sufficient melt exists to form the mass for a super-eruption - if it can be extracted and accumulated into an eruptible volume. It is also plausible that volumes with high melt fractions (more than 60%) exist within pockets within the greater magma chamber and could erupt as moderate-volume (less than 100 km^3) lavas or pyroclastic flows. Current evidence suggests, however, that the seismic anomalies are not sufficiently large to allow for a larger, highly molten (and thereby eruptible) volume of magma beneath Yellowstone at this time.

ROAD LOG

The following road log gives cumulative and incremental mileage for each day of the field trip to designated stops and additional features we will pass by (see Figure 1). As odometer readings vary from vehicle to vehicle, the mileage readings were recorded with a GPS device. Note that due to road construction, the field trip may not follow the itinerary below exactly.

Geology from Bozeman to Island Park ID

The field trip begins at the parking lot on the northwest side of Brick Breeden Field House on the Montana State University campus, heads south on Huffine Lane to Four Corners. The main part of the route leads southward through Gallatin Canyon along Highway 191, bordering the west margin of the Gallatin Range and the east margin of the Madison Range (Figure 18). The Gallatin and Madison Ranges are geologically and topographically similar, an essential difference being a thick cap of Eocene lavas and volcaniclastic rocks (~ 50 Ma) that cover the high parts of the Gallatin Range. The road log starts at "Four Corners" (the intersection of Highways 84 [289] and 191, about 9 miles west of MSU and ends north of Ashton, Idaho.

To get to Four Corners, drive west for about 9 miles to Four Corners and turn left at the four-way traffic signal. Along the 9 mile stretch from MSU to Four Corners the road traverses the wide basin occupied by Bozeman, Belgrade, and other towns known as the Gallatin Valley. The valley is bordered to the south by the Gallatin Mountains, to the northeast by the Bridger Range, and to the west by the Tobacco Root Mountains. The Gallatin Valley is the northeastern most extensional basin of the Basin and Range. It is locally anomalous in that it is defined by two major faults: the NNW-trending Bridger Fault along the west side of the Bridger Range and the WSW-trending Gallatin Fault along the north flank of the Gallatin Range (most adjacent basin-bounding faults are dominantly NNE- to N-trending).

Cumulative mileage (increment mileage)

0.0 (0.0) Four Corners: junction of Highways 289 and 191. Southward from the junction the route is along the floodplain of the Gallatin River and proceeds directly toward the Gallatin Mountains range front.

5.3 (5.3) Gallatin Gateway Inn, a relic of the competition between the Milwaukee Railroad and other lines for the most popular approach to Yellowstone National Park. This was the change-over point from rail lines to the Gallatin Stage, which in its earlier period took two days to traverse Gallatin Canyon to the west entrance of the Park.

5.4 (0.1) Road right passes town of Gallatin Gateway, so named because of its position leading to Yellowstone National Park. Continue straight ahead on Highway 191. From here the road follows various terrace levels toward the mouth of Gallatin Canyon. To the west (right) across the Gallatin River can be seen several terrace and pediment systems, older than the Wisconsin age glaciers that discharged into the Gallatin River in the canyon ahead. Timbered hills to the southwest are Archean metamorphic rocks flanked by Cambrian strata on the north side and faulted against younger Paleozoic rocks on the south side.

6.5 (1.1) Road traverses poorly exposed Wisconsin-age outwash gravels discharged and spread by the Gallatin River.

10.5 (4.0) At 3 o'clock, across the river Archean metamorphic complex, Cambrian Flathead Quartzite, and Cambrian Meagher Limestone (Figure 19) ridges mark range-front flexure truncated to the north by a fault, which raised Archean up against the Paleozoic strata. The counterpart of this structure on the east (left) side of the canyon mouth can be seen in the prominent gray limestone dip-slab at 9 o'clock. A large normal fault marking the north front of the Gallatin Range has offset this limestone from its projection to the west side of the river here. Small saddle at 11 o'clock just east of Archean knob at the canyon mouth

contains in-faulted Eocene andesitic volcanic rocks, the northernmost exposure of this material in this area. The "V" shape of the Gallatin Canyon straight ahead, a result of the uplift of resistant Archean rocks along the Gallatin Range front, soon gives way to a broad valley in the next down-faulted alcove to the south.

11.2 (0.7) Cross Gallatin River and enter Gallatin Canyon.

12.9 (1.7) To right of road are excellent exposures of typical Wyoming Province Archean gneiss saturated by pegmatite veins and dikes. Zircon ages for the gneiss range from 3.4 to 3.5 Ga. The canyon here is cut roughly parallel to the strike of the gneiss, which dips steeply to the west.

13.4 (0.5) Spanish Creek, a strike-oriented stream discharging from the north slope of the Spanish Peaks uplift.

13.8 (0.4) Mississippian Lodgepole Limestone Formation in prominent cliffs ahead. Archean metamorphic rocks directly to left in timbered slopes with Laramide Squaw Creek reverse fault in between. Along strike to the southeast, throw on the fault progressively decreases. Rocks to the south of the fault dip moderately to the northeast into the fault. The Squaw Creek Fault extends at least as far west as the Madison River, where it is called the Cherry Creek Fault. To the southeast, the fault is in line with Eocene volcanic and intrusive centers of the Absaroka Volcanic Supergroup including upper Swan Creek, Point of Rocks, Emigrant Peak, Independence, and Cooke City. The fault may represent a zone of weakness along which magmas rose during the Eocene. Note how the valley widens upon crossing the Squaw Creek Fault due to more efficient erosion of less resistant sedimentary rocks.

14.5 (0.7) Road traverses Gallatin River terrace, which can be traced upstream to outwash from late Wisconsin valley glaciers that discharged onto the canyon floor.

14.8 (0.3) Rock Haven Chapel: Lodgepole Formation in prominent cliffs directly across river.

14.9 (0.1) Roadcut on right shows contact between brownish Devonian Jefferson Dolomite below and yellowish marlstone at the base of the Devonian Three Forks Formation.

15.3 (0.4) View ahead of Garnet Mountain and to the left at about 11 o'clock of Stormcastle Mountain. These prominences are built of Paleozoic rocks ranging in age from Cambrian through the Mississippian Madison Limestone 2,000 feet up and show the northeast dips of the downdropped block south of the Stormcastle Creek Fault.

15.8 (0.5) Exposures in canyon wall along east bank of river are of northeast dipping Paleozoic rocks. Nearing Stormcastle Mountain the downsection part of this exposure consists of Cambrian Meagher Limestone, a thin ledge of Cambrian Wolsey Shale, and the cliff-forming Cambrian Pilgram Dolomite. The Pilgram here is unconformably overlain by estuarian channel fills of the Lower Devonian Beartooth Butte Formation, which contains scattered and obscure armored plates of placoderms and ostracoderms, two of the earliest fish.

16.4 (0.6) Stormcastle Creek Ranger Station turnoff and bridge to left. Continue straight ahead.

17.1 (0.7) Moundy topography to right of road at 3 o'clock is Wisconsin-age terminal moraine of the Hell Roaring glacier, which descended the valley of Hell Roaring Creek from the Spanish Peaks. Various terrace levels extending downstream from the mouth of Hell Roaring Creek are essentially outwash plains progressively abandoned and dissected by the Gallatin River.

17.3 (0.1) Cross Hell Roaring Creek. Latest Wisconsin moraine clogs inner channel of creek.

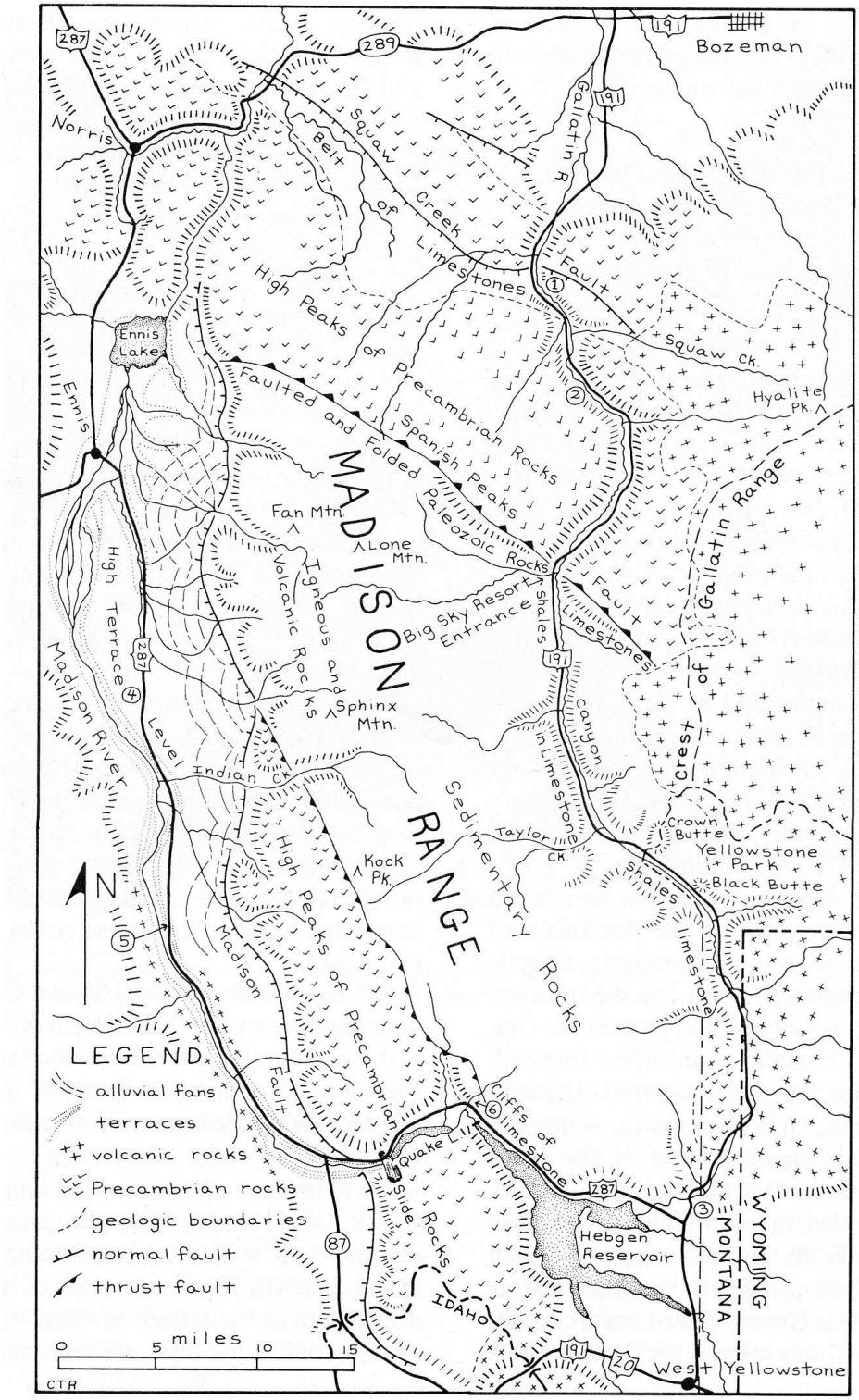


Figure 18. Map of area covered in road log from junction of Highways 289 and 191 to West Yellowstone (from Parsons, 1978).

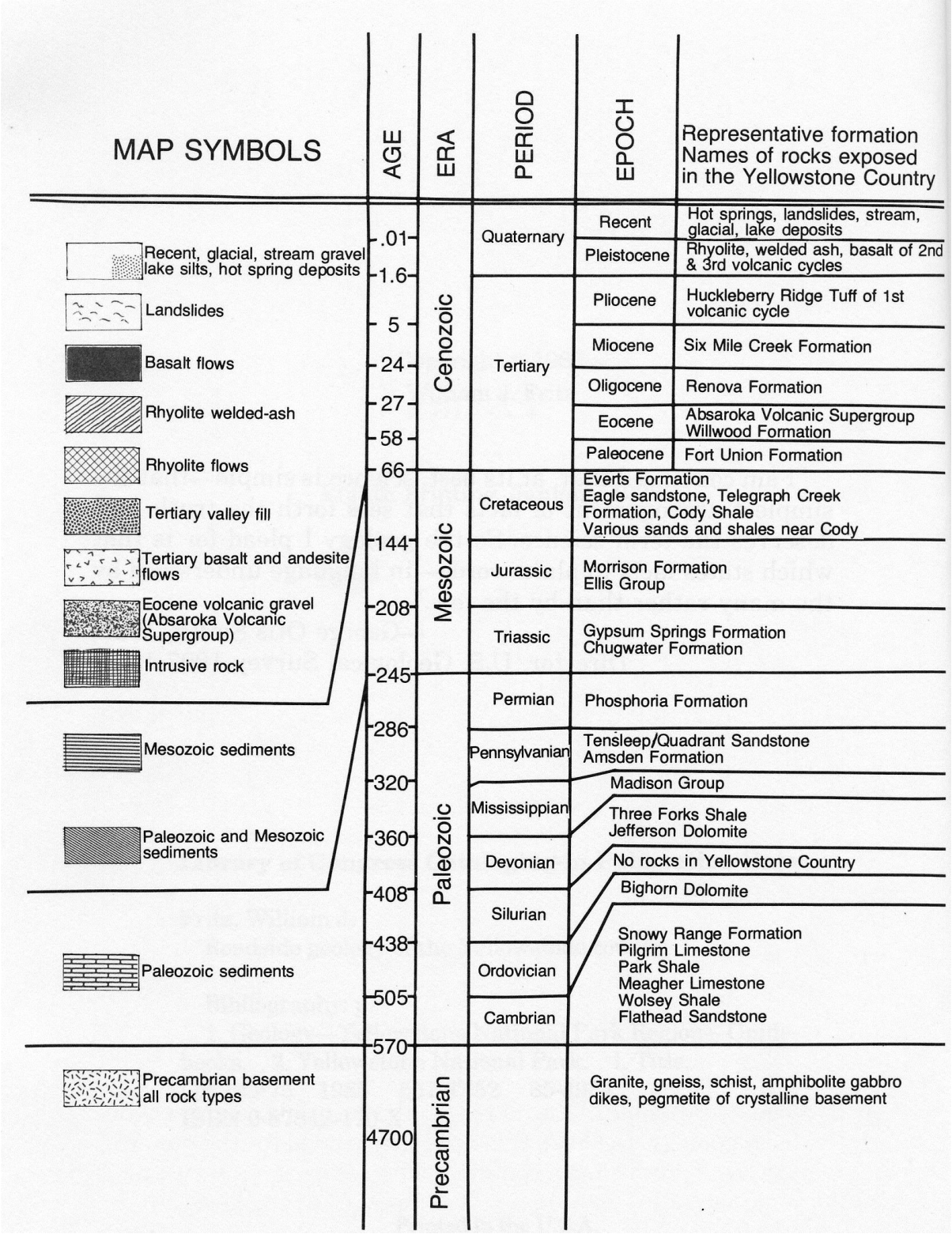


Figure 19. Stratigraphic nomenclature of rocks covered in road log (from Fritz, 1995)

17.5 (0.5) Stormcastle Meadows: one of several dark hornblende andesite porphyry sills may be seen in lower cliffs of Meagher Limestone at 9 o'clock (east). The large prominent sill has been dated at 80 Ma. This is the alleged collection site of Wards© Andesite Porphyry sample.

17.9 (0.1) Stormcastle Creek Canyon at 9 o'clock is cut in north dipping homocline developed in Paleozoic rocks along the downdropped block of the Stormcastle Fault. The fault and its related structural effects continue southeastward along the north side of Stormcastle Creek for several miles to a point where the entire assemblage becomes covered by Eocene volcanic rocks.

18.3 (0.4) Steeply dipping Paleozoic rocks here are underlain in the inner canyon by resistant Archean metamorphic rocks, thus accounting for the tendency of the canyon to narrow beyond this point.

18.8 (0.5) Exposures of Archean metamorphic rocks across river for next few miles display well developed foliation trends that define numerous folds, which strike perpendicular to the highway.

20.2 (1.4) "Circle Bridge" across Gallatin River. The river has been diverted by the Cascade Creek Glacier, the terminal moraine of which juts eastward into the path of the river just beyond the bridge to the right.

20.3 (0.1) Excellent exposures of Archean metamorphic complex in roadcut left of road.

22.0 (1.7) "Kitchen Rock" on left. This river-abraded gneissic exposure shows fine drag folds. This landmark was used as a camp kitchen by the Hayden Surveys in the late 19th century, hence the name.

22.5 (0.5) Glacial till on both sides of canyon. Here a large valley glacier extended from southwest to northeast across the canyon, blocking the river and forming a lake, which backed up as far as Portal Creek (ahead). The varved clay of the lake can be seen in several exposures on the southwest bank of the river for several miles upstream from here.

23.3 (0.8) Greek Creek Campground. Greek Creek, to the left, descends an extensive landslide.

23.6 (0.3) Curve in road follows course of Gallatin River, which again has been pushed northward by a valley glacier that descended Burnt Creek on the opposite side of the river.

24.2 (0.6) Poorly exposed outcrops on west side of river opposite Swan Creek show lacustrine beds capped by fluviatile gravel. Archean rocks surround the canyon, but the Gallatin Range to the left of road is capped here, as elsewhere, by Eocene volcanic rocks.

25.3 (0.9) Moose Creek Flat, the result of complex geomorphic events including deltaic deposition in the glacially dammed lake and heavily fuviatile discharge from Moose Creek. To the west of Mosse Creek Flat, across the river, is deposit of antohophyllitic asbestos mined sporadically through the years.

26.1 (0.8) Trailhead to asbestos mine.

32.0 (5.9) View south toward Madison Range to right. Prominent skyline peak is Sphinx Mountain. Limestone units descending from canyon walls are Cambrian beds on the footwall of the Spanish Peaks Fault.

32.5 (0.5) Mouth of Dudley Creek (west) and Levinski Creek (east across river). Levinski Ridge at 10 o'clock extends eastward on skyline along Laramide Spanish Peaks reverse Fault. Chalcopyrite in Archean complex of the ridge several miles east of here has yielded low-grade copper but was never commercially exploited. To the southeast, Spanish Peaks Fault is in line with Eocene eruptive centers at Porcupine Creek, Electric Peak, Mt. Washburn, and the Southern Absaroka Range.

33.1 (0.6) Cool-water springs along roadside and on both sides of river emanate from Cambrian limestone unites, a fracture

system, or both, along the Spanish Peaks Fault. The fault crosses the road beneath cover at about this point. The fault is a high angle reverse fault, with the north block up.

33.4 (0.3) Bridge across West Fork of the West Gallatin River. Entrance to Big Sky recreation area just beyond on right. Steeply dipping and descending strata both to the east and west have been flexed along the Spanish Peaks Fault. Softer Mesozoic units ahead, also involved in the flexure, have facilitated the widening of the main valley and yielded to a variety of pervasive mass movements.

Lone Mountain, a glacial horn, looms at the head of the West Fork Valley to the west. The mountain is the main center for ski runs of the Big Sky Resort. The mountain is one of several intrusive centers extending to the west along the general trend lines of the Spanish Peaks Fault zone, and is composed of hornfelsic Cretaceous shale intruded by hornblende andesite porphyry also of Cretaceous age. Mass wasting attacks the mountain of all sides and brings about several prominent rock glaciers at its base.

34.2 (0.8) Pleistocene outwash terraces of the Gallatin River glacial system to right. On hillslopes above the terraces Cretaceous rocks crop out in dark patches, and above these and other gravel deposits the wooded flat-topped hill consists of the 2.1 Ma Huckleberry Ridge Tuff. This is a remnant of the 2,000 km^3 ash-flow tuff erupted from the Yellowstone Caldera 50 miles farther south.

36.1 (1.9) Mouth of Porcupine Creek. Prominent pediment at mouth of creek is developed on Cretaceous strata. On the skyline far to the east, flat-lying Eocene volcanic deposits can be seen extending northward and obscuring the steeply-dipping Paleozoic limestone strata along the trend of the Spanish Peaks Fault. From this point, Cretaceous through Mississippian rock units lead downsection to the axis of the next cross-trending structure, the Buck Creek Anticline.

37.2 (1.1) Outcrops of Mississippian Madison Limestone along road. The Madison here tends to be stained red along its upper units by mud from the overlying Mississippian-Pennsylvanian Amsden Formation.

40.1 (2.9) Prominent cliffs in canyon across river developed in red-stained Madison Group.

41.7 (1.6) Prominent cliffs in canyon across river in Madison Group. Note gentle northerly dips.

43.9 (2.2) Sharp flexure in canyon wall across river to east is crest of the Buck Creek Anticline. Previous gentle northward dips farther downstream contrast to steep southerly dips, which rapidly bring Pennsylvanian and Permian strata to river level.

45.2 (1.3) Entrance to Three Twenty Ranch and Buffalohorn Creek. At 8 o'clock is Permian Shedhorn Sandstone overlain by Triassic Dinwoody and Chugwater Formations. The Dinwoody here is soft and obscure. Steeper southeast dips along the Buck Creek Anticline can be seen in the cliffs beyond at 7 o'clock; the Buck Creek Syncline is marked by dip reversal in the middleground.

45.7 (0.3) Cream-colored ledges on east canyon wall are Quadrant Sandstone units on the south flank of the Buck Creek Syncline. Stratigraphic section descends to the Madison Group. Overlying the Quadrant here is old river gravel, which in turn is overlain by Huckleberry Ridge Tuff.

47.7 (2.0) Prominent Madison Limestone outcrops show giant calcite veins along fractures in the limestone.

48.8 (1.1) Gentle north dips in the Madison Group give way to sharp over-turned dips along the Snowflake Springs fault zone to the left of the highway. The zone is marked on the west across the river by giant springs issuing from the Madison Group. To the east, several faults constitute the zone, the most obvious being indicated

by the relationship that places Quadrant upon Triassic redbeds, with the elimination of the Shedhorn and Dinwoody units. Overturned Jurassic through Cretaceous units can be seen toward the southeast along the downdropped block.

49.3 (0.5) "Soft" topography developed in Cretaceous shales south of Snowflake Springs Fault. Skyline is capped by Eocene Absaroka volcanic rocks, but Crown Butte, with flat top in middleground, is capped by Huckleberry Ridge Tuff. Lava Butte is a continuation of the Huckleberry Ridge Tuff to the south.

50.0 (0.7) Yellowstone National Park northwestern boundary. Crown Butte directly to east in middle ground.

50.8 (0.8) Skyline to east shows flat breccia and flows of the Eocene Absaroka volcanic rocks above Huckleberry Ridge Tuff on Lava Butte (middleground) at 11 o'clock. The Eocene volcanic rocks are co-extensive with Eocene Absaroka volcanic rocks southeast of Yellowstone Park.

53.0 (2.2) Flanks of Black Butte Stock at 9 o'clock, an intrusive igneous body associated with the Absaroka volcanic rocks.

55.5 (2.5) Specimen Creek Trailhead. The trail provides access to the Gallatin Petrified forest in Eocene volcanic rocks. The Eocene volcanic rocks in this vicinity lie on top of Madison Limestone, which are prominently exposed for a mile or so along the left side of the road.

59.1 (3.6) Fawn Pass Trailhead: On the far east skyline is Electric Peak, an Eocene intrusive body intruded into Cretaceous strata.

60.6 (1.5) Bighorn Trailhead: divide between Grayling Creek (ahead) and headwaters of the Gallatin River, which turns up into the mountains. View in far distance is of Southern Gallatin Range.

63.7 (3.1) Exposures on both sides of road for next several miles are predominately of Huckleberry Ridge Tuff (first caldera cycle Yellowstone tuff - 2.1 Ma) but also include Archean schists and Paleozoic and Mesozoic sedimentary rocks.

69.3 (5.6) Prominent exposures of Huckleberry Ridge Tuff to right of road.

69.8 (0.5) Yellowstone National Park northwestern boundry: exposures here and beyond are of Huckleberry Ridge Tuff.

71.8 (2.0) View of West Yellowstone Basin, which measures about 10 by 15 miles across. The basin was created by smoothing and flattening by a giant glacier flowing from the icecap that repeatedly covered the Yellowstone Plateau. Now the basin is filled with sand and gravel eroded from the lava flows in Yellowstone as they were scoured by the glacier. From 1 o'clock to 3 o'clock is the Madison Range, which gradually descends beneath the Madison Plateau. To the south (straight ahead) is the Madison Plateau, formed by post-collapse Plateau Rhyolite lava flows spilling over the west rim of the Yellowstone caldera. Gap at 10 o'clock in far distance is breach in Yellowstone caldera rim by Madison River. From 7 o'clock to 8 o'clock Southern Gallatin Range gradually descends beneath cover of outflow facies of Lava Creek Tuff, erupted 640 thousand years ago during formation of the modern Yellowstone caldera.

80.2 (8.4) Enter town of West Yellowstone.

80.6 (0.4) Turn right on Highway 191. The road leading west out of West Yellowstone crosses the West Yellowstone Basin, which measures about 10 by 15 miles across. The basin was created by smoothing and flattening by a giant glacier flowing from the icecap that repeatedly covered the Yellowstone Plateau. Now the basin is filled with sand and gravel eroded from the lava flows in Yellowstone as they were scoured by the glacier. Straight-ahead (west) and to the right (north) is the Madison Range. To the south is the Madison Plateau, formed by post-collapse Plateau Rhyolite lava flows spilling over the west rim of the Yellowstone caldera.

88.5 (7.9) Hills on south side of road are Lava Creek Tuff; view to northwest is "Lions Head" of Absaroka volcanic rocks.

89.4 (0.9) Outcrops on right (south) side are Huckleberry Ridge Tuff.

89.9 (0.5) Targhee Pass and continental divide: cross into Idaho at the southern extension of the Madison Range, exposing Paleozoic and Mesozoic sedimentary rocks capped by Eocene Absaroka volcanic rocks.

95.4 (5.5) View of Centennial Mountains at Pierre J. Desmet turnout. The Centennial Mountains are unusual in North American because they trend east-west, in contrast to most which trend generally north-south. The range is a south-tilted fault block (e.g., the fault uplifting the range is on the north side) exposing Precambrian metamorphic rocks at the base overlain by Paleozoic and Mesozoic sedimentary rocks, overlain by Eocene Absaroka volcanic rocks, as exposed on Sawtell Peak at the east end with the prominent aviation radar dome. The south slope of the range is onlapped by Huckleberry Ridge Tuff, the first and largest ash-flow tuff of the Yellowstone Plateau volcanic field. To the left (east) are distal ends of Madison Plateau rhyolite lava flows. Note how the Madison Range gradually dives beneath the plateau.

102.2 (6.8) Rise up onto a plateau of poorly exposed Lava Creek Tuff.

103.1 (0.9) Outcrops of Lava Creek Tuff.

104.3-105.9 Outcrops of Lava Creek Tuff on both sides of road

109.1 (3.2) Cross Buffalo River. We have now entered into both the first cycle caldera (Island Park caldera segment) and the second cycle caldera (Henry's Fork caldera) of the Yellowstone Plateau volcanic field. Roadcuts expose basalts that floor the Henrys Fork caldera.

113.2 (4.1) Exposures of Gerrit Basalt on right (south) side of road.

114.3-115.0 Exposures of Gerrit Basalt on both sides of road

116.5 (1.5) Turn left onto Mesa Falls Scenic Drive (Road 294) and park.

STOP 1: OVERVIEW OF HENRYS FORK AND ISLAND PARK CALDERAS: From this locality we are near the centers of the second cycle Henry's Fork caldera (1.3 million years old) and the southwestern segment of the Island Park Caldera (2.1 million years) old, sometimes referred to as the Big Bend Ridge segment. Unlike the modern Yellowstone caldera, with its numerous active geothermal fields, active uplift and deformation related to a large subsurface magma chamber, and abundant intercaldera rhyolite lava flows, these are "dead" calderas. The calderas are filled with the Gerrit Basalt; a third cycle basalt filling the second and first cycle calderas. This is possible because a large rhyolitic magma chamber no longer is present in the subsurface (although there is probably a granitic batholith). Thus, the rocks are cold, dense, and brittle, allowing basalt to leak to the surface and fill in the caldera.

To north is Thurmon Ridge, the shared north wall of the calderas. Thurmon Ridge is formed of Mesa Falls Tuff. In this vicinity the Mesa Falls Tuffs onlaps pre-Mesa Falls, post Huckleberry Ridge Tuff rhyolite present on Bishop Mountain. Moonshine Mountain in the foreground is a downdropped block of Bishop Mountain Rhyolite. To the east and south is Big Bend Ridge. The northern segment of Big Bend Ridge is the shared western walls of the calderas. The southern segment of Big Bend Ridge is the southern caldera wall of the Island Park caldera. The high points on the northern end of Big Bend Ridge are vents for younger basalts with affinities to those of the Snake River Plain. Thus, this the point where the Snake River Plain magmatic province begins and the Yellowstone Plateau volcanic field ends.

Drive south on Mesa Falls Scenic Drive.

The road crosses a flat, forested plain of Gerrit Basalt.

120.0 (3.5) Osborne Butte: The small hill to the left (east) is the top of Osborne Butte dome cropping out above surrounding Gerrit Basalt. This dome is one of a group of post-Mesa Falls Tuff rhyolitic domes that erupted following formation of the Henrys Fork caldera. The domes have a distinctive northwest trend, probably reflecting control of their locations by regional Basin and Range style faulting. The small hill to the right is a vent for the Garrit Basalt.

124.7 (4.7) Elk Butte: another post Mesa Falls Tuff rhyolite dome; forested and difficult to see.

125.0 (0.3) View on left side of road (east) of **Hatchery Butte**; a vent for Gerrit Basalt.

125.5 (0.5) Leave Henrys Fork caldera: the caldera boundary is buried by basalt lava flows. We have now entered a "moat" between the Henrys Fork caldera and the Island Park caldera.

129.4 (3.9) Turn right in to Upper Mesa Falls Drive.

129.6 (0.2) Platy Lava Creek Tuff on right side of road.

130.0 (0.4) Poorly exposed top of Mesa Falls Tuff on right side of road.

130.3 (0.3) Park in lot for Upper Mesa Falls.

STOP 2: UPPER MESA FALLS: Across the river, the cliff exposures are entirely the 1.3 million year old Mesa Falls Tuff. In the lower part of the cliff the tuff is "densely welded" and displays well developed columnar jointing. The upper parts of the cliff are more poorly welded and jointing is more crudely developed. The falls plunge over the top of the more resistant densely welded horizon.

Walk down the stairs and view basaltic lava flows on top of the densely welded Mesa Falls Tuff. Note that the more poorly welded section of tuff is missing. This is because an earlier period of river downcutting before eruption of the basalt stripped away the more easily erodable poorly welded section. The basaltic lava flow thus diverted the river to the west. Also, note the thickness of the Mesa Falls Tuff across the river. The tuff here is about 275 feet thick. This is somewhat remarkable because we are outside of the boundaries of the caldera and hence this is "outflow facies" of the Mesa Falls tuff. However, the tuff has ponded here in the "moat" between the Henrys Fork caldera and the Island Park caldera. Note, further downstream on southside of canyon "channel filling" basaltic lava flows.

Return to road.

131.2 (0.9) Turn right onto Mesa Falls Scenic Drive.

131.9 (0.7) Park in parking lot for overlook.

STOP 3: LOWER MESA FALLS: Again, the entire thickness of the opposite canyon wall is Mesa Falls Tuff ponded to over 300 feet in thickness. On this side of the river the terrace is composed of basalt lava flows, which also rims the canyon. Both the rim basalt and terrace basalt erupted from vents within the Henrys Fork caldera.

To the south-southwest is Snake River Butte - a pre Huckleberry Ridge Ruff rhyolitic lava flow truncated at the rim of the first cycle Island Park caldera.

Return to road and drive south toward Aston.

132.7 (0.8) Inferred first cycle caldera ring fault.

134.2 (1.5) Bear Gulch turnout. View of Snake River Butte and Big Bend Ridge caldera segment slump block.

135.4 (1.2) Small outcrop of Lava Creek Tuff on right side of road.

138.1 (2.7) At Warm River road curves to southwest around Snake River Butte to right. Outcrops are Huckleberry Ridge Tuff.

139.7 (1.6) View of Snake River Plain. Nice view of the west side of the Grand Tetons to the left (east) on a clear day.

142.4 (2.7) Ceder Buttes in distance. Ceder Buttes is thought to be the resurgent dome of the 4.3 Ma Heise caldera. At 11 o'clock is East Butte, a rhyolitic dome on the central axis of the Snake River Plain. The flat top is an uplifted section of basalt. At 9 o'clock are small basaltic shield volcanoes.

145.7 (3.3) Enter Ashton.

147.8 (2.1) Intersection with U.S. 20; turn right (north).

STOP 4: EXAMINE MESA FALLS TUFF: PARK ON RIGHT SIDE OF ROAD AND BE VERY CAREFUL CROSSING HIGHWAY AND CLIMBING SLOPE

148.9 (1.1) After crossing the Henrys Fork River. The road begins an incline exposing on both sides member B of the Huckleberry Ridge Tuff overlain by Mesa Falls Tuff. Note the thickness of the Mesa Falls Tuff through this stretch; it is much thinner than exposed at Upper and Lower Mesa Falls. This is because this is outflow facies of the tuff which has not ponded in a depression, and hence displays the typical thin nature of this facies. We will examine an outcrop of the Mesa Falls Tuff.

151.5 (2.5) Mesa Falls Tuff on both sides of road. On a sunny day look for glittering sanidine crystals.

153.8 (2.3) Cross back into Big Bend Ridge segment of the Island Park caldera (at Geology road-side exhibit!). Road for next mile or so traverses Snake River Plain basalt.

154.3 (0.5) Cross back into Henrys Fork Caldera. Again, caldera wall is not exposed because it is buried by basalt lava flows. Lookout Butte on right side of road; another post second cycle rhyolite lava flow.

156.5 (2.2) Exposures of Lava Creek Tuff.

158.9 (2.4) Exposures of Gerrit Basalt.

162.9 (4.0) Mesa Falls Scenic Drive. Drive to Big Springs campground. Let's go camping!

End of road log Day 1.

ROADLOG FROM WEST ENTERANCE TO YELLOWSTONE NATIONAL PARK TO BRIDGE BAY CAMPGROUND (DAY 2)

In the morning, we will drive from our campsite to the west entrance of Yellowstone National Park, which is about 55 miles.

0.0 (0.0) West Entrance Station.

2.5 (2.5) Madison River Basalt on hill on right (south). This unit is a post-collapse third cycle basalt .

5.4 (2.9) Madison River Basalt on hill on right (south).

6.6 (1.2) Terminal moraine of Pinedale glacier.

7.2 (0.6) "History Exhibit" turnout: contact between Mount Haynes flow and member A of Lava Creek Tuff on left. Distal flow lobe of Mount Haynes flow on right.

9.8 (2.6) "Mt. Haynes Overlook" turnoff on right (south) side of road.

STOP 1. VIEW OF BREACHED CALDERA WALL: This is one of the best places to see the ring fault zone that created the Yellowstone caldera. To the north of the road is a cliff exposing the pre-collapse Mount Haynes rhyolite lava flow overlain by member A of the Lava Creek Tuff. This south-facing cliff was created when the caldera collapsed about 640 thousand years ago during the last gigantic eruption. To the south is the West Yellowstone flow, banking against and, in places ahead, flowing over the caldera wall.

13.5 (3.7) Madison Junction. Turn right (south). Madison Junction is a geologic "triple point" because three geologic units are in contact here. To the south the Nez Perce Creek flow, a ~160 thousand year old post-collapse rhyolite lava flow, is present. To the west this flow is covered by the ~108 thousand year old West Yellowstone flow, which forms the prominent cliff of National Park Mountain. To the north is a thick

section of Lava Creek Tuff on the northwestern caldera wall. The contact between the West Yellowstone flow and the Nez Perce flow controls the stream path of the Firehole River. The contact between the northwestern caldera wall and the Nez Perce flow controls the drainage of the Gibbon River. These two rivers converge at Madison Junction to form the headwaters of the Madison River.

14.1 (0.6) Entrance to Firehole River one-way loop. Turn into one-way Firehole Canyon Drive. The road follows the Firehole River, which exploits the contact between the West Yellowstone lava flow and the Nez Perce Creek flow.

14.3 (0.2) Across the river is the steep (~700 feet high) eastern margin of the West Yellowstone lava flow. Note the complex internal jointing in the interior of the flow.

14.9 (0.6) Park in roadside turnout on left, just past large roadcut.

STOP 2: OUTCROP OF DISTAL FLOW BRECCIA OF NEZ PERCE CREEK FLOW: Watch out for oncoming traffic!! This is an excellent locality to view aspects of rhyolite lava flows. Much of the outcrop is broken-up rock, or breccia. This forms when the surface of a lava flow cools and becomes brittle against atmosphere (and in this case, perhaps, water), while the hot molten interior continues to flow, fragmenting the solidified surface. The breccia is thus termed an "auto-breccia" because brecciation of the lava flow occurs by flow of the lava itself. The breccia is laced with solid rhyolite, indicating places where the fluid, molten lava in the interior intruded the breccia; these could thus be term "auto-dikes" because they are dikes that cross-cut the same lava flow they are derived from.

15.3 (0.4) Parking area on left for Firehole Falls. The falls are supported by a ledge of vertically flow-layered Nez Perce Creek flow.

16.5 (1.2) Main Park road. Turn right toward Old Faithful. For the next four miles the road traverses over the western edge of the Nez Perce Creek flow. The road follows the Firehole River, which exploits the contact between the West Yellowstone lava flow (right) and the Nez Perce Creek flow (left).

20.7 (4.2) Porcupine Hills composed of hydrothermally cemented glacial kame deposits.

21.8 (1.1) Outcrop on left of ~153 thousand year old Elephant Back flow. Note complex flow banding.

22.6 (0.8) Turn right into parking lot for Fountain Paint Pots and Lower Geyser Basin.

STOP 3: LOWER GYSER BASIN: The Lower Geyser Basin is perhaps the most convenient place in Yellowstone Park where a short walk displays good examples of the four principal types of hydrothermal features: hot springs, geysers, fumaroles, and mud pots. The area also presents a small, but vivid demonstration of the effect of topographic control on water- and vapor-dominated hydrothermal systems. Note how at the base of the hill along the boardwalk hotsprings (Clestine Pool on left and Silex Spring on right) are present, representing the approximate level of the ground water table and where geothermal waters flow unrestricted to the surface. As you climb the boardwalk, you encounter Fountain Paint Pots, for which the Lower Geyser Basin is most noted. Analogous to the Mud Volcano area, the water present in Fountain Paint Pots is only from condensation of steam and from shallow groundwater from rain and snowmelt - that is we are now above the water table. The mud pots are muddy because hydrogen sulfide gas mixes with the water condensate to produce sulfuric acid, which breaks down the rocks. At the highest levels on the hill, fumaroles (steam vents), where only vapor finds access to the surface, are present because the surface rocks are mostly dry. Following the boardwalk down to the west side of the hill, a number of geysers are present. These are "wet" geothermal features, like hotsprings,

except that the plumbing systems cause local build up of pressure and eruption. The Lower Geyser Basin has formed in an area left uncovered by Plateau Rhyolite lava flows and where subsurface faults and fractures allow rain and snowmelt to percolate downward.

At the top of the hill, we will pause for a bit. From this vantage point, one has a spectacular view of the northwest part of the caldera. To the west on the skyline is the very large West Yellowstone rhyolite lava flow, an ~108 thousand year old flow that buries the western caldera margin. The valley in the foreground is Fountain Flats, formed from a recess in the West Yellowstone flow, which is also exposed to the south. The unusual form of the eastern margin of the West Yellowstone lava flow has been interpreted to reflect emplacement while a stagnating or retreating glacier remained in the area to the east (hence, the lack of a lava flow in Fountain Flats). In the foreground out on the flats are Twin Buttes, which are hydrothermally cemented sedimentary kame deposits formed during a subglacial explosion.. The view to the north in the foreground shows the West Yellowstone lava flow overlying the Nez Perce Creek lava flow; the Firehole River follows the contact between these two lava flows and forms Firehole Canyon. In the distance beyond is the northwest rim of the Yellowstone caldera and Mt. Holmes at the southern end of the Gallatin Range. To the northeast are the Porcupine Hills, which are similar, but smaller, examples of hydrothermally cemented deposits like Twin Buttes. To the east is the Elephant Back rhyolite lava flow. To the southeast is the gentle northwest flank of the Mallard Lake resurgent dome in the center of the western segment of the Yellowstone caldera, broken by normal faults that strike toward the geyser basin.

Return to main Park road and turn right toward Old Faithful. View of Great Fountain Geyser to left. This geyser is in the Firehole Lake Geyser Basin, which developed in a recess in the Elephant Back lava flow.

24.6 (2.0) Midway Geyser Basin. In the interest of time, we will skip this area. The basin features Grand Prismatic Pool, the largest hotspring in North America and deepest in Yellowstone Park at 111 feet. The basin also features Excelsior Geyser Crater, which discharges a large flow of hot water into the Firehole River. Excelsior Geyser crater was formed in the 1880's and 1890's by a series of powerful hydrothermal explosions.

In a similar way to the Lower and Upper Geyser Basins, Midway is located in a low created because plateau rhyolite lava flows left the area uncovered. Note also the faults on the Mallard Lake Dome, which trend directly toward Midway Geyser Basin. These faults probably extend northwest beneath Midway, allowing rain and snowmelt to percolate downward.

24.9 (0.3) Outcrop of ~516 thousand year old Biscuit Basin flow on left. This is the oldest third cycle post-collapse lava flow. Across the Firehole River to the west is the West Yellowstone flow. After this point the Firehole River flows around the western side of the Mallard Lake resurgent dome.

28.5 (3.6) Biscuit Basin: Another geyser basin; developed in the oldest post-collapse rhyolite lava flows: the ~516 thousand year old Biscuit Basin Flow. The small stream valley in the hills behind the basin is the contact between the West Yellowstone flow (north) and the ~112 thousand year old Summit Lake flow (south).

30.1 (1.6) Black Sand Basin: named for black sand formed from erosion of black volcanic glass, or obsidian.

30.3 (0.2) Exit park road toward Old Faithful.

31.0 (0.7) Turn left toward Old Faithful Inn.

31.4 (0.4) Park in Old Faithful Inn parking lot.

STOP 4: UPPER GEYSER BASIN: The Upper Geyser Basin is enclosed by large, young, post-collapse rhyolite lava flows (West Yellowstone, Summit Lake, and Scaup Lake) on the west, south, and southeast, and the Mallard Lake resurgent dome on the north. The large cliff face to the southwest from Old Faithful Lodge may resemble the margin of the caldera, but it is actually the steep front of the Summit Lake post-collapse rhyolitic lava flow (~112 thousand years old). The actual caldera margin has been difficult to locate directly and is inferred south and west of the Upper Geyser Basin, buried by lava flows of the Madison and Pitchstone Plateaus.

Uplift due to resurgence has exposed on the Mallard Lake dome the Mallard Lake rhyolitic lava flow. This lava flow is also post-collapse (e.g., younger than the Lava Creek Tuff and formation of the Yellowstone caldera) with an analytical age of ~160 thousand years old. This relatively "young" age for the Mallard Lake lava flow indicates that resurgence here occurred well after caldera formation, in contrast to resurgence of the Sour Creek dome. There is some evidence for resurgence contemporaneous with the Sour Creek dome near the Mallard Lake dome, but the relations exposed here indicate that resurgence can continue to occur well after caldera formation.

The Mallard Lake dome is an 11 by 19 km elliptical northwest trending uplifted feature. It has a complex northwest-trending fault pattern which, like the Sour Creek dome, shows its origin by domical uplift of the underlying block. From the open area near Old Faithful, one of the grabens that breaks across the Mallard Lake dome is visible on the skyline to the east.

The Upper Geyser Basin reportedly has the largest concentration of geysers on Earth; almost as many geysers occur here than are known altogether in the rest of the world. Many of geysers are large and periodic, such as Old Faithful, Castle, and Grand Geyser. These are typically isolated from other geysers and thus have individual plumbing systems that do not appear to be connected with the larger system. Others are smaller or more irregular eruption periodicity and these appear to have connected plumbing systems.

The location of the Upper Geyser Basin is due to three geologic features. First, post-caldera lava flows did not cover this area. Second, uplift on the Mallard Lake dome has fractured and broken the rocks not only on the dome, but also the rocks flanking the dome. Thus, water is able to percolate downward until it becomes superheated and eventually erupts through geysers or emerges as hotsprings. Third, the high standing Mallard Lake dome serves as an area of abundant recharge of water to the system.

We will spend approximately 90 minutes at this stop to ensure we see an eruption of Old Faithful and other features such as geothermal features on the boardwalk, the visitors center, and the historic Old Faithful Inn.

Leave Old Faithful Inn and head back toward main park road.

32.4 (1.0) Drive east toward West Thumb on main park road.

33.2 (0.8) Margin of the Scaup Lake flow.

34.7 (1.5) Lone Star geyser trailhead.

36.0 (1.3) Scaup Lake flow on left (north). Prominent flow to south over Scaup Lake flow is the Spring Creek rhyolite lava flow (post-collapse; age undetermined).

37.4 (1.4) Road traverses southern margin of Mallard Lake resurgent dome.

38.8 (1.4) Isa Lake and the Continental Divide. Isa Lake is believed to be the only lake in the world that drains to two different oceans *backwards*. The east side of the lake drains by way of the Lewis River to the Pacific Ocean and the west side of the lake drains by way of the Firehole River to the Atlantic Ocean via the Gulf of Mexico. This is the opposite of what one would expect because the Atlantic Ocean is east of the lake and the Pacific Ocean is west.

40.5 (1.7) View of the north shore of Shoshone Lake to the right (south). The area of flat topography beyond the lake is the Pitchstone Plateau formed by the ~71 thousand year old Pitchstone Plateau rhyolite lava flow – the youngest post-collapse magma eruption.

44.5 (4.0) Continental Divide again. How is this possible???

48.0 (3.5) Park in large turnout on left side of road (be careful crossing over!)

STOP 5: West Thumb Caldera: While most eruptions from the Yellowstone caldera following eruption of the Lava Creek Tuff and formation of the caldera have been effusive (i.e., lava producing), there have been a few explosive eruptions. The West Thumb lake basin is a deep, sub-circular extension of Yellowstone Lake and probably has its origin as a relatively small caldera within the larger Yellowstone caldera. The important word here is relative, however. The West Thumb caldera is comparable in size to the Crater Lake Caldera in the Oregon Cascades. The caldera formed during eruption of the 162 thousand year old Tuff of Bluff Point. The north, east, and south margins of the West Thumb caldera are largely buried by younger rhyolite lava flows, which are not exposed because of burial by younger sediments.

Directly in the foreground is the Duck Lake hydrothermal explosion crater. We will have the opportunity to see and discuss features such as this at a later stop.

To the south are the Red Mountains, which mark the southern caldera margin. Far to the east across Yellowstone Lake are the Absaroka Mountains and the eastern caldera margin. The Absaroka Mountains are the global type locality for high-K_2O shoshonitic series igneous rocks (see Figure 21). These volcanic and shallow intrusive rocks are completely unrelated to the Yellowstone Plateau volcanic field as they are much older (~50 Ma) and compositionally distinct (dominated by intermediate composition rocks). The volcanic event that produced them, however, was much larger than Yellowstone as they represent eruption of ~25,000 km^3 of magma, whereas Yellowstone has only erupted ~6,000 km^3.

48.2 (0.2) Turn north toward West Thumb.

48.4 (0.2) West Thumb Geyser Basin. We will skip this stop in the interest of time. West Thumb Geyser Basin geothermal features vary more than others in Yellowstone in terms of temperature and water discharge, perhaps due to periodic infiltration of water from the lake.

50.7 (2.3) Cross Little Thumb Creek. Along the lakeshore, good views to the southern margin of Yellowstone caldera are provided as the road winds around the northern margin of the West Thumb caldera.

51.9 (1.2) Exposure of Tuff of Bluff Point on left (west). Elephant Back Mountain in distance to north.

55.1 (3.2) Sandbar offshore forms a lagoon along the shore. The road beyond here traverses old lake terraces above the present lake level.

66.0 (10.9) View across northern half of Yellowstone Lake and Stevenson Island.

67.3 (1.3) Lake Junction.

68.2 (0.9) Park in large turnout on right side of road. Walk out on small footpath (this may not be possible depending on the time of year because of grizzly bear activity)

STOP 6: Raised Yellowstone Lake Shorelines: The view to the west from this point includes several old shoreline terraces of Yellowstone Lake (see Figure 21). The origin of these terraces is of interest to geologists because they indicate provide a record of movement of the Yellowstone caldera floor beyond historical records and thus the "heavy breathing" of the volcanic system. The basic idea is that subsidence of the caldera floor causes an increase in the

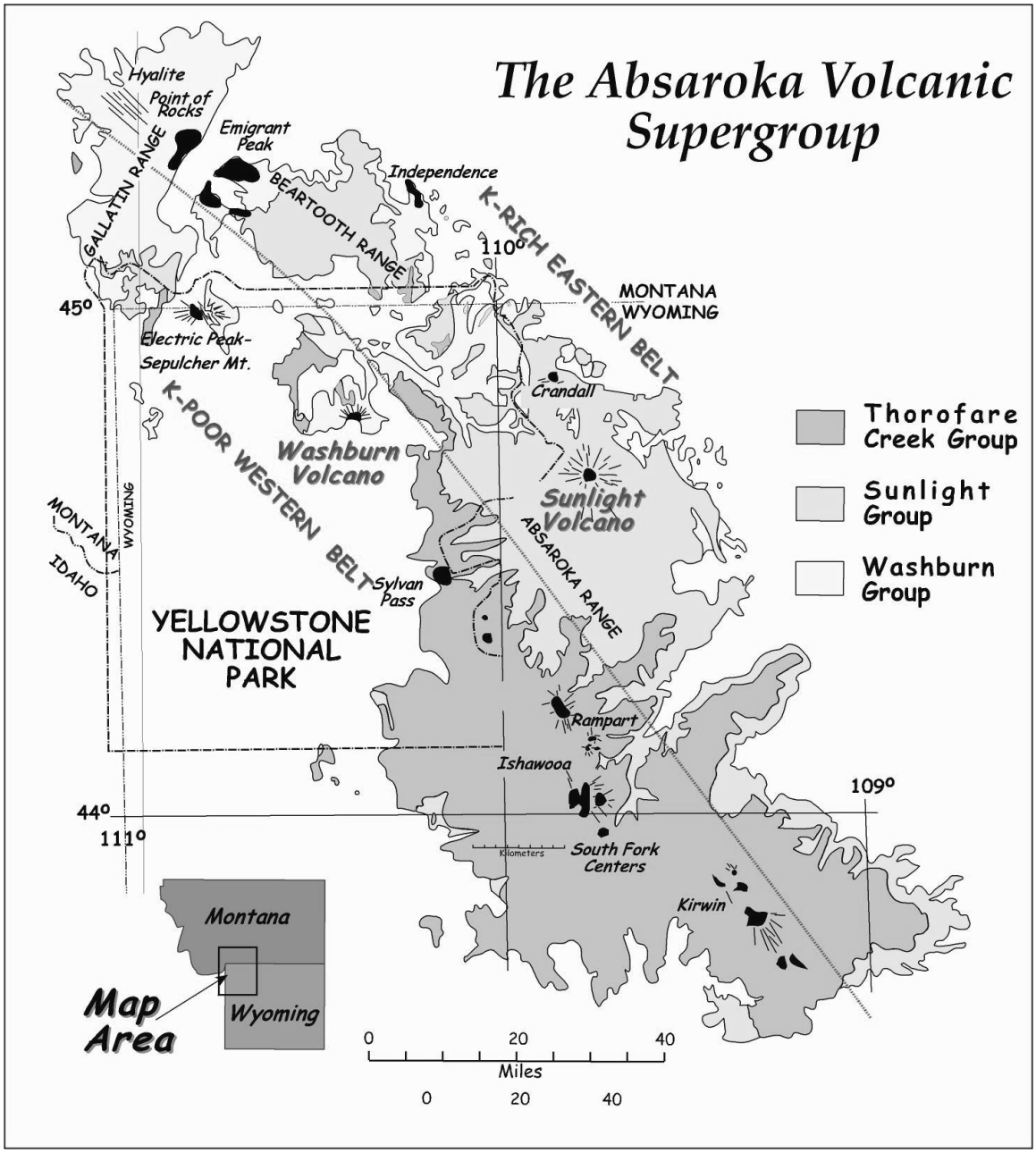


Figure 18. Simplified map of the Absaroka Volcanic Province.

gradient and discharge of the Yellowstone River and thus lowering of the Yellowstone Lake water level. Doming of the interior causes an opposite effect: a decrease in the Yellowstone River gradient and an increase in lake level. Associated with this increased lake level will be formation through erosion of a wave-cut platform and cliff, or terrace.

Based on detailed mapping of these shorelines around Yellowstone Lake, an overall oscillating lowering of lake level from ~14 thousand years to ~8 thousand years is suggested (Figure 22). This reflect erosion of the outlet accompanied by inflation-deflation cycles. From 8 thousand years to the present, the lake has been below or near its present level with general uplift since about 3-4 thousand years ago.

68.6 (0.4) Turn right toward Fishing Bridge.

70.6 (2.0) Pelican Creek.

72.2 (1.6) Indian Pond hydrothermal explosion crater. The crater formed by a shallow steam and hot-water eruption several thousand years ago.

73.3 (1.1) Mary Bay.

75.6 (2.3) Steamboat Point.

STOP 7: STEAMBOAT POINT: At this stop we look to the west over Mary Bay and the northern part of Yellowstone Lake. Mary Bay is another hydrothermal explosion crater formed about 13,800 years ago; it is the worlds largest type of these features. The bluff around the north shore of the bay is composed of deposits from this eruption (the ejecta ring). Studies of Mary Bay show a large hole at the bottom with water temperatures near boiling. The cliff behind us exposes breccias formed when Mary Bay exploded. On the east side of Steamboat Point is Sedge Bay, another hydrothermal explosion crater. Like Mary Bay, the lake floor water temperatures are very high.

Hydrothermal explosions occur due to a rapid reduction in pressure of superheated water (above the boiling point). As snowmelt and rainfall seep deep into the ground, they can absorb enough heat from the Yellowstone magma chamber to raise the temperature close to boiling. Because the boiling point of water increases with increasing pressure and pressure increases with depth, deep water can be hotter than boiling water near the surface (such water is referred to as being "superheated"). If the pressure that confines the water is reduced quickly, pockets of water may suddenly boil, causing an explosion as the water is converted to steam with a concomitant huge increase in volume. Triggers for these events might include earthquakes, increased gas emissions from below, or reduced hydrostatic pressure resulting from drought or deglaciation. Importantly, none of the hydrothermal events of the past 16,000 years has been followed by eruption of magma.

From this vantage point we can see all the important and potentially hazardous manifestations of volcanic activity at Yellowstone. These include (1) caldera-forming eruptions and production of large tuffs (super-eruptions); (2) lava flows; (3) strong earthquakes on fault lines; and (4) hydrothermal explosions. Figure 22 shows schematically the frequency of these events relative to their destructive power. The hydrothermal explosions are particularly important because although the effects are not particularly far-reaching, they occur relatively frequently. More than a dozen large hydrothermal-explosion craters formed between about 14,000 and 3,000 years ago (Figure 23).

From this site one also has a good view of Elephant Back Mountain. Elephant Back Mountain is important in understanding the caldera geology because across it runs the northeast trending Elephant Back fault zone. These faults are due to an area that is the axis of active uplift and subsidence within the caldera. The fault zone links but does not connect the two resurgent domes: the Sour Creek Dome in the northeast part of the caldera and the Mallard Lake Dome in the southwest. The fault zone accommodates upward bulging and downward sagging between the domes and strains that stretch the caldera from northwest to southeast.

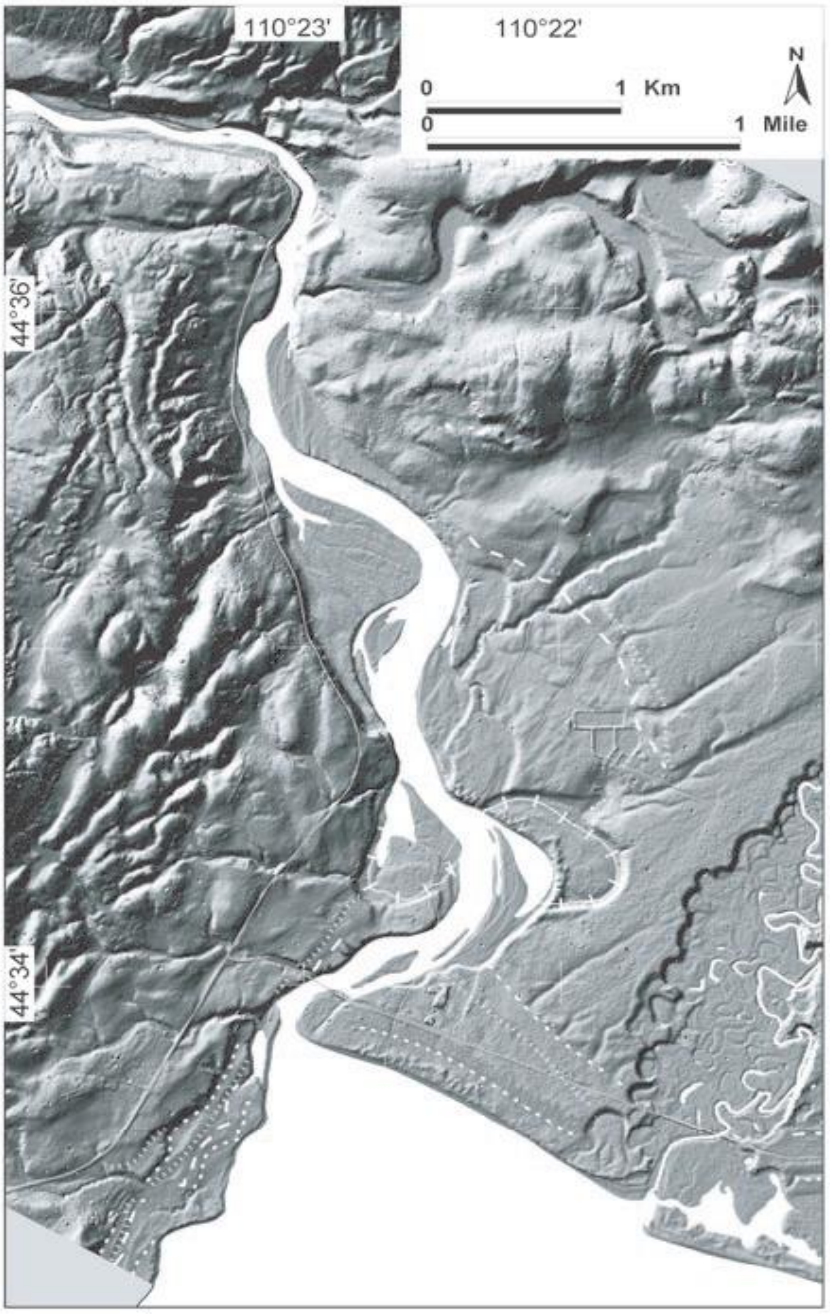


Figure 21. Image show post-glacial shorelines (dotted and dashed white lines) near outlet of Yellowstone Lake (from Pierce et al., 2002).

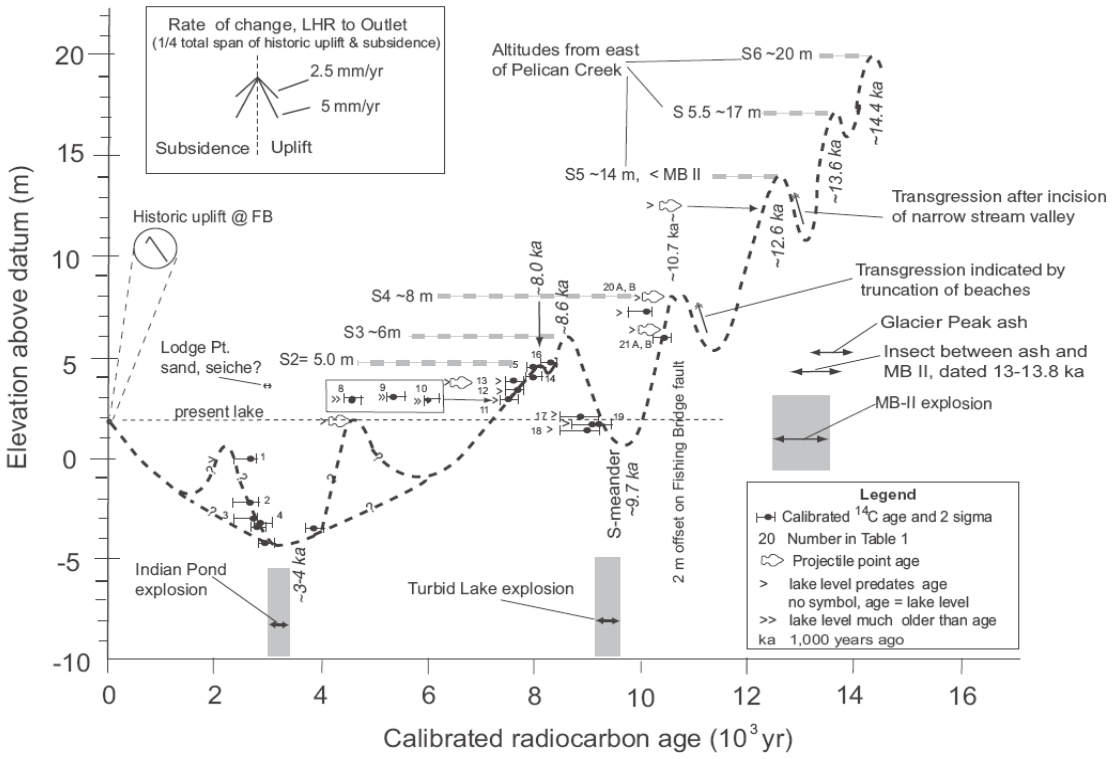


Figure 22. Reconstruction of changes in Yellowstone Lake level over the past 15 thousand years (from Pierce et al., 2002).

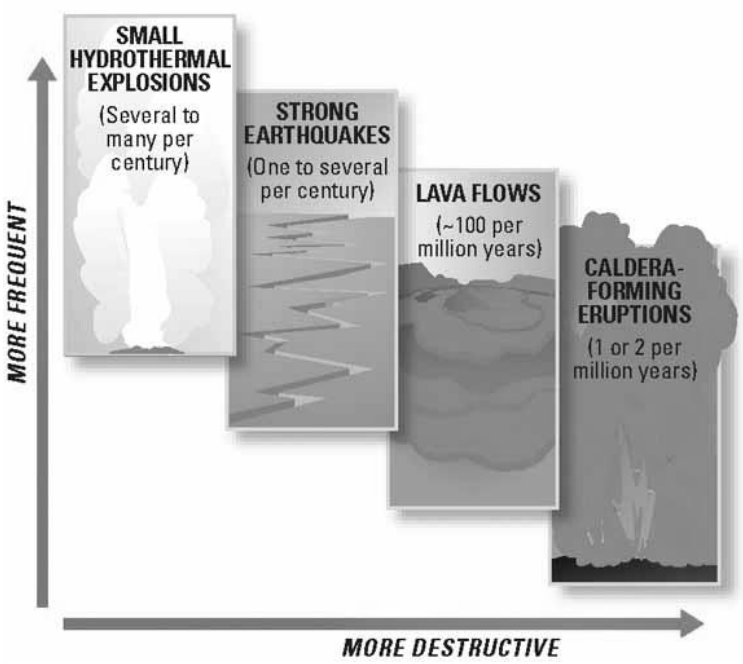


Figure 23. Scientists evaluate natural-hazard levels by combining their knowledge of the frequency and the severity of hazardous events. In the Yellowstone region, damaging hydrothermal explosions and earthquakes can occur several times a century. Lava flows and small volcanic eruptions occur only rarely—none in the past 70,000 years. Massive caldera-forming eruptions, though the most potentially devastating of Yellowstone's hazards, are extremely rare—only three have occurred in the past several million years. (Source: USGS).

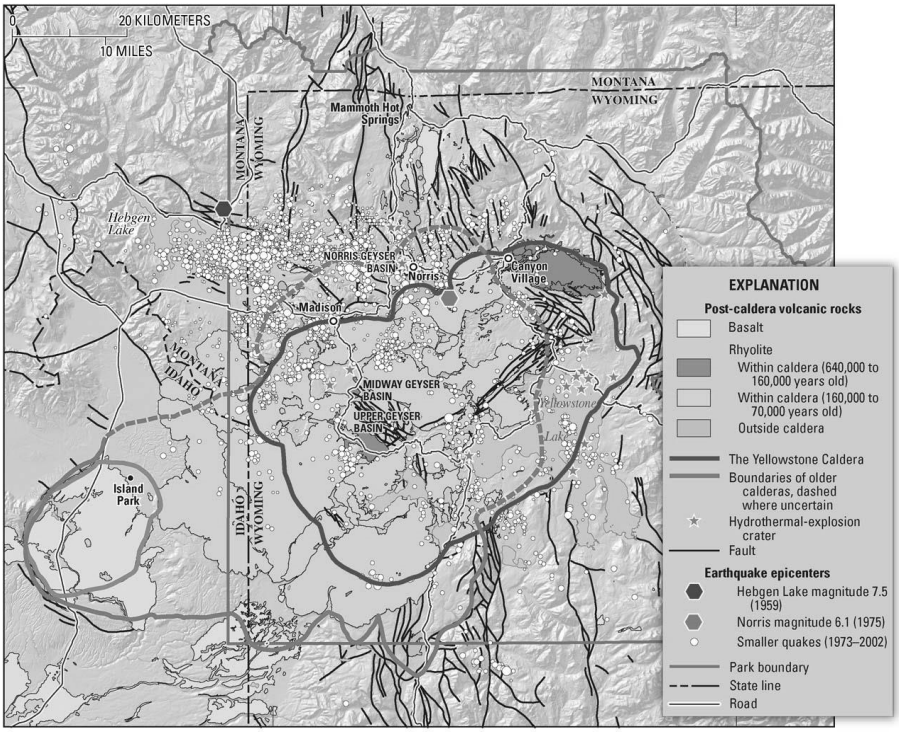


Figure 24. Map showing locations of volcanic and tectonic phenomena in and around the Yellowstone caldera (Source: USGS).

Side Trip (you can do this on your own some day with friends and family): Lake Butte (7.6 miles round trip)

1.0 miles. Sedge Bay, another hydrothermal explosion crater. Like Mary Bay, the lake floor water temperatures are very high.

1.9 miles. Outcrops of Eocene Absaroka volcanic rocks indicating we have crossed over the eastern margin of the Yellowstone caldera.

2.9 miles. Turn left to Lake Butte.

3.8 miles. Lake Butte.

STOP: LAKE BUTTE: the following is taken from Smith and Siegal (2000): *"If the weather is clear...(one has) a glorious view of Yellowstone Lake from this overlook, located on the eastern edge of the Yellowstone caldera.*

Lake Butte is volcanic rock crested by the eruptions that formed the Absaroka Range about 50 million years ago. It might have been a hill cut in two as the caldera floor dropped downward during the last major eruption 630,000 years ago. If such an eruption occurred now, anyone standing on Lake Butte would be incinerated instantly.

Also image what it would be like here during the Ice Age. The point where you are standing would be buried beneath an icecap some 3,500 feet thick. The ice helped carve out the basin for Yellowstone Lake – a job started by the last caldera explosion.

The view to the south encompasses the Southeast and South arms of the lake. The caldera boundary runs to Lake Butte from the northeast, then cuts roughly southwest across the lake. So most of the southeast portion of the lake is outside the giant crater. The basin occupied by that part of the lake was carved out by glaciers and also formed by faulting along the Southeast and South arms. The rest of the lake occupies only the eastern edge of the 45 by 30 mile caldera.

The deepest portion of Yellowstone Lake – about 300 feet deep – is located to the southwest roughly between where you are standing and Frank Island. Another underwater hot-water system is on the lake bottom just east of Stevenson Island, the island west of here.

To the southwest, the high mountain is 10,308-foot Mount Sheridan, located near the southern edge of the Yellowstone caldera. On a clear day, you may see the Teton Range farther southwest on the skyline and Yellowstone Lake's West Thumb to the west-southwest. As you take in the view from the southwest to the west, you can get a sense of the caldera's topography: A crater that was filled in with lava flows to form todays flattened Yellowstone Plateau surrounded by higher mountains.

To the northwest are Sedge and Mary bays, formed by steam eruption holes in the ground a mile or two wide."

Drive west back toward Fishing Bridge, turn left on Grand Loop Road and right into Bridge Bay campground (~ 1 mile beyond intersection).

End of road log Day 2.

ROADLOG FROM FISHING BRIDGE TO BOZEMAN VIA MAMMOTH HOT SPRINGS (DAY 3)

0.0 (0.0) The roadlog begins from intersection of Grand Loop Road and Fishing Bridge (~1.5 miles north of Bridge Bay campground).

1.3 (1.3) Outcrops on left (west) of Elephant Back lava flow.

2.9 (1.6) Park at turnout on east side of road for Le Hardy Rapids.

STOP 1: LE HARDY RAPIDS: The Yellowstone River here forms a series of rapids, which, while perhaps unimpressive, are important in understanding modern activity in the Yellowstone caldera and the water level in Yellowstone Lake. The rapids are present because the rocks over which the river flows (the Lava Creek Tuff) are uplifted by a series of active faults on the flank of the Sour Creek resurgent dome. The faults are associated with the northeast trending Elephant Back fault zone discussed

at the last stop yesterday. These faults are due to an area that is the axis of active uplift and subsidence within the caldera. For example, Figure 25 shows leveling data that demonstrate uplift of the caldera floor by as much as 2 centimeters per year here between 1923 and 1976 for a total of more than one meter vertically. From 1985 to the mid -1990's the caldera floor dropped downward by15 to 20 centimeters. Since then, the floor has been rising again. Studies of post-glacial Yellowstone Lake terraces discussed yesterday suggest that uplift/subsidence cycles of deformation at Yellowstone have taken place in the past 16 thousand years.

The uplift and down dropping of the caldera floor are creating the faults, which in turn create a stair step pattern in the rocks over which the rapids flow. The movement is related to the up-and-down breathing of the caldera, which in turn has been related by geologists to hydrothermal fluid sealing and inflation followed by cracking of the seal, pressure release, and deflation. Another possibility is magma injection. When new magma is injected, the ground rises. When the magma cools and degasses, the area subsides. Whatever the cause, the uplift has also helped to dam the Yellowstone River upstream creating Yellowstone Lake and controlling the lake level. The lake basin was largely created by collapse of the caldera floor 640 thousand years ago and more recently by scouring by glaciers. However, the uplift, faults, and rapids have raised the lake level to higher levels than it would be otherwise.

13.3 (10.4) Parking area for Mud Volcano Hydrothermal Area. We will skip this stop in the interest of time. Mud volcano hydrothermal area is the world's type locality for a vapor-dominated hydrothermal system. It is located here because the Elephant fault zone crosses the area, creating zones of weakness in the ground. Hot geothermal waters do not reach the surface here, only steam and other gases. The water present is thus only from condensation of steam and from shallow groundwater from rain and snowmelt. The Mud Volcano and other mud pots are muddy because hydrogen sulfide gas mixes with the water condensate to produce sulfuric acid, which breaks down the rocks. Because there is no flowing water to flush out the mud, it accumulates here. Nearly all of the rocks exposed here at glacial deposits.

13.6 (0.3) We are entering the Hayden Valley, in the heart of the northeast part of the Yellowstone caldera. The Hayden Valley is present because the post collapse lava flows that filled the Yellowstone caldera didn't quite reach this area, creating a natural basin. The Yellowstone icecap - a 3,500 foot thick layer of ice - sat atop this area during several glacial periods during the past 2 million years. The glacial ice along with a large lake - an ancestor to Yellowstone Lake - carved out the landscape and deposited thick sediments.

17.3 (3.7) Park at turnout on east side of road. Walk up small hill across road (watch out for traffic and animals!!).

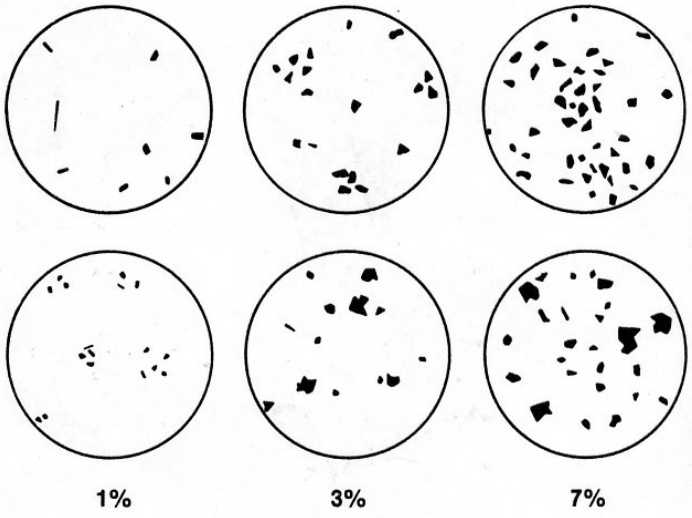
STOP 2: VIEW OF NORTHEAST PART OF YELLOWSTONE CALDERA: From this vantage point many features of the northeast part of the Yellowstone caldera are visible. To the north is the Washburn Range. The Washburn Range represents a Eocene (~55 million years old) stratovolcano that once was similar in size to volcanoes in the Cascades Mountains of the Pacific northwest. However, the southern half of the volcano is now missing, having sunk into the Yellowstone caldera and buried by various volcanic units of the Yellowstone Plateau volcanic field. In front of the Washburn Range are two early post collapse rhyolitic lava flows; the Canyon flow and the Dunraven Road flow. To the west is the Central Plateau, underlain by several large post-collapse rhyolite lava flows filling the heart of the caldera. To the east is the Sour Creek Resurgent dome. This structural dome has been uplifted, exposing mainly Lava Creek Tuff and minor areas of Huckleberry Ridge Tuff.

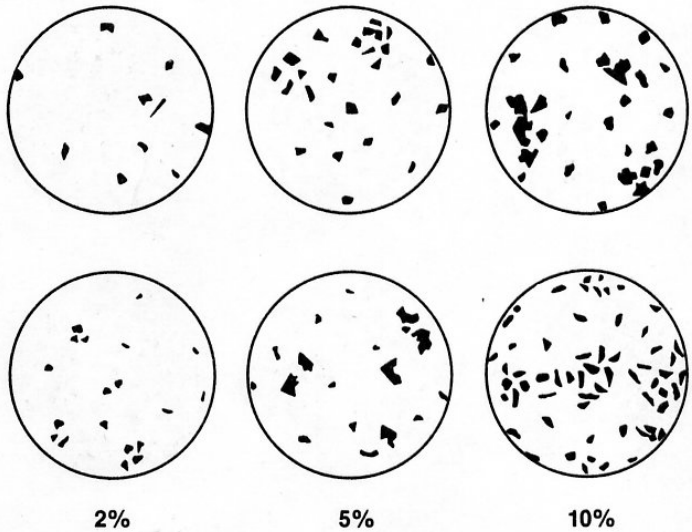
REFERENCE MATERIAL

AGI DATA SHEET 15.1

Comparison Chart for Estimating Percentage Composition

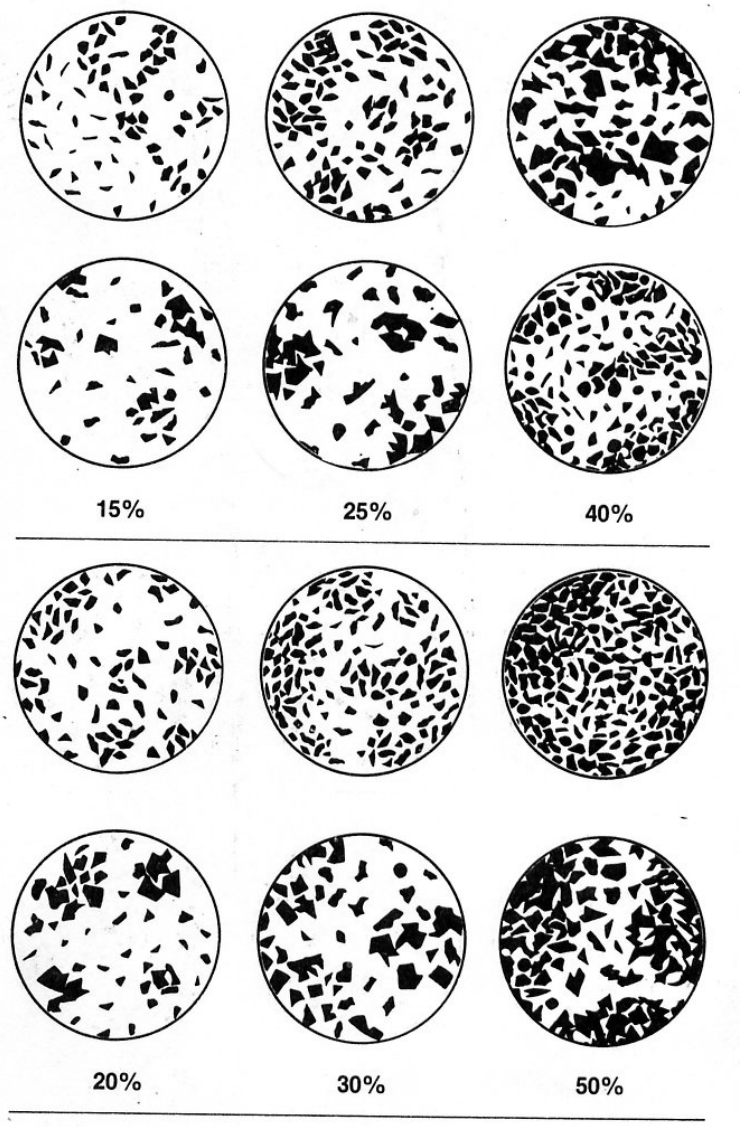
Prepared by Richard D. Terry and George V. Chilingar, Allen Hancock Foundation, Los Angeles. Reprinted from *Journal of Sedimentary Petrography*, v. 25, n. 3, p. 229–234, Sept. 1955.

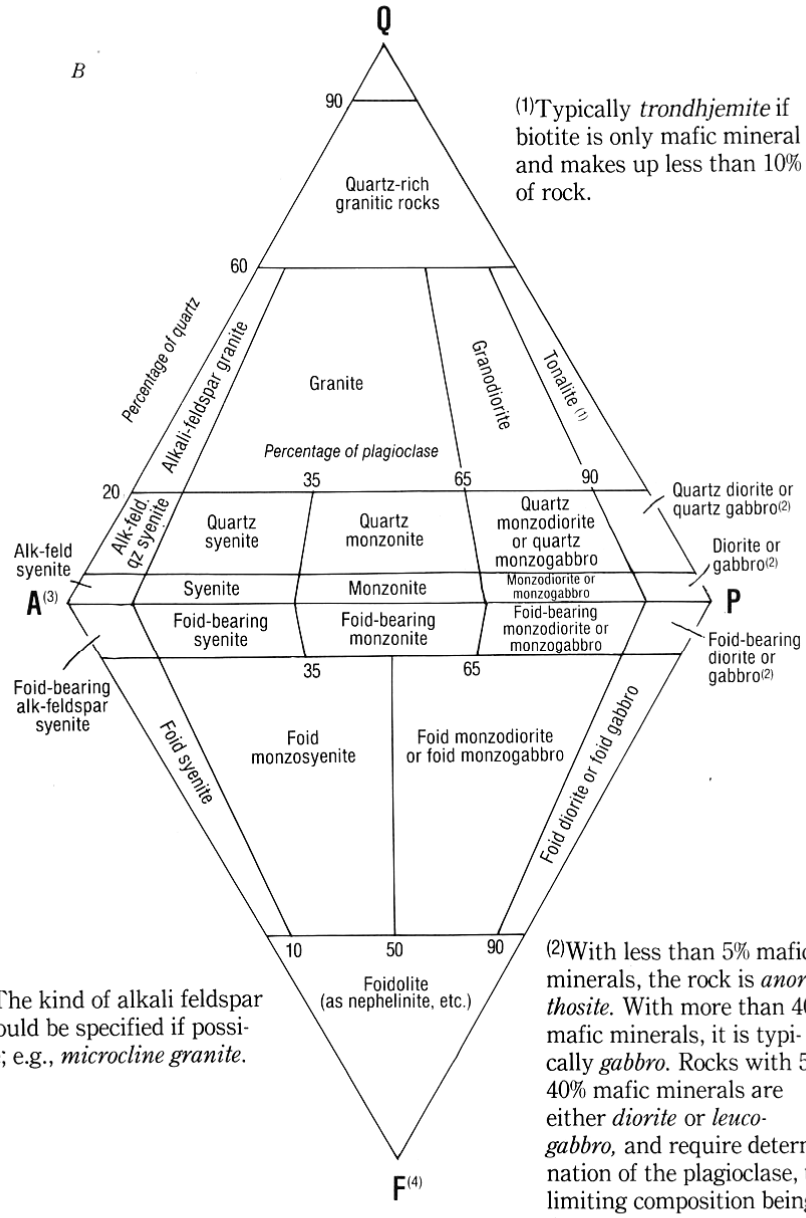




AGI-DS-65

AGI DATA SHEET 15.2





(1)Typically *trondhjemite* if biotite is only mafic mineral and makes up less than 10% of rock.

(2)With less than 5% mafic minerals, the rock is *anorthosite*. With more than 40% mafic minerals, it is typically *gabbro*. Rocks with 5-40% mafic minerals are either *diorite* or *leucogabbro,* and require determination of the plagioclase, the limiting composition being An_{50}.

(3)The kind of alkali feldspar should be specified if possible; e.g., *microcline granite*.

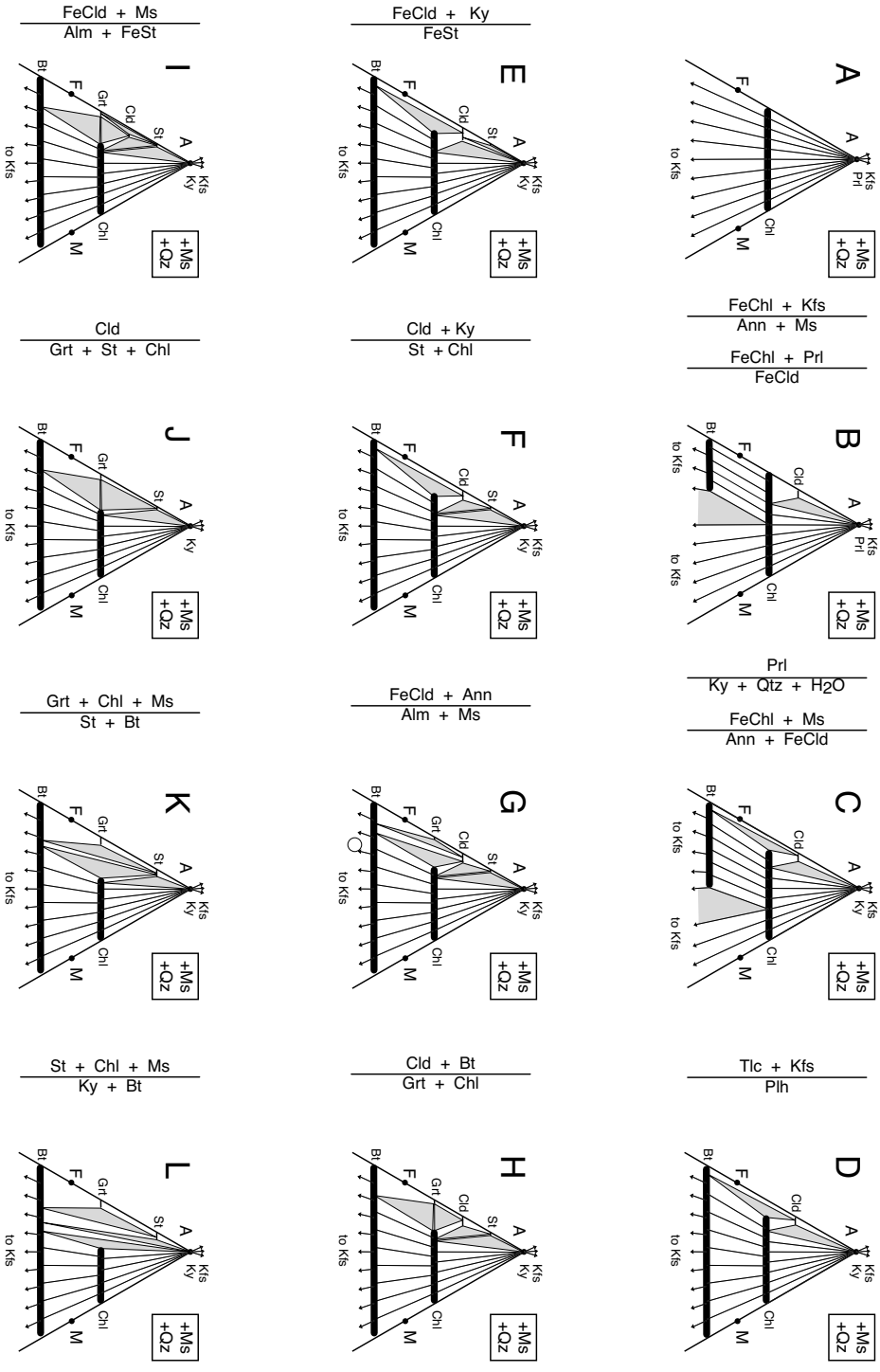
(4)The feldspathoid should be specified in each rock name; e.g., *nepheline syenite*.

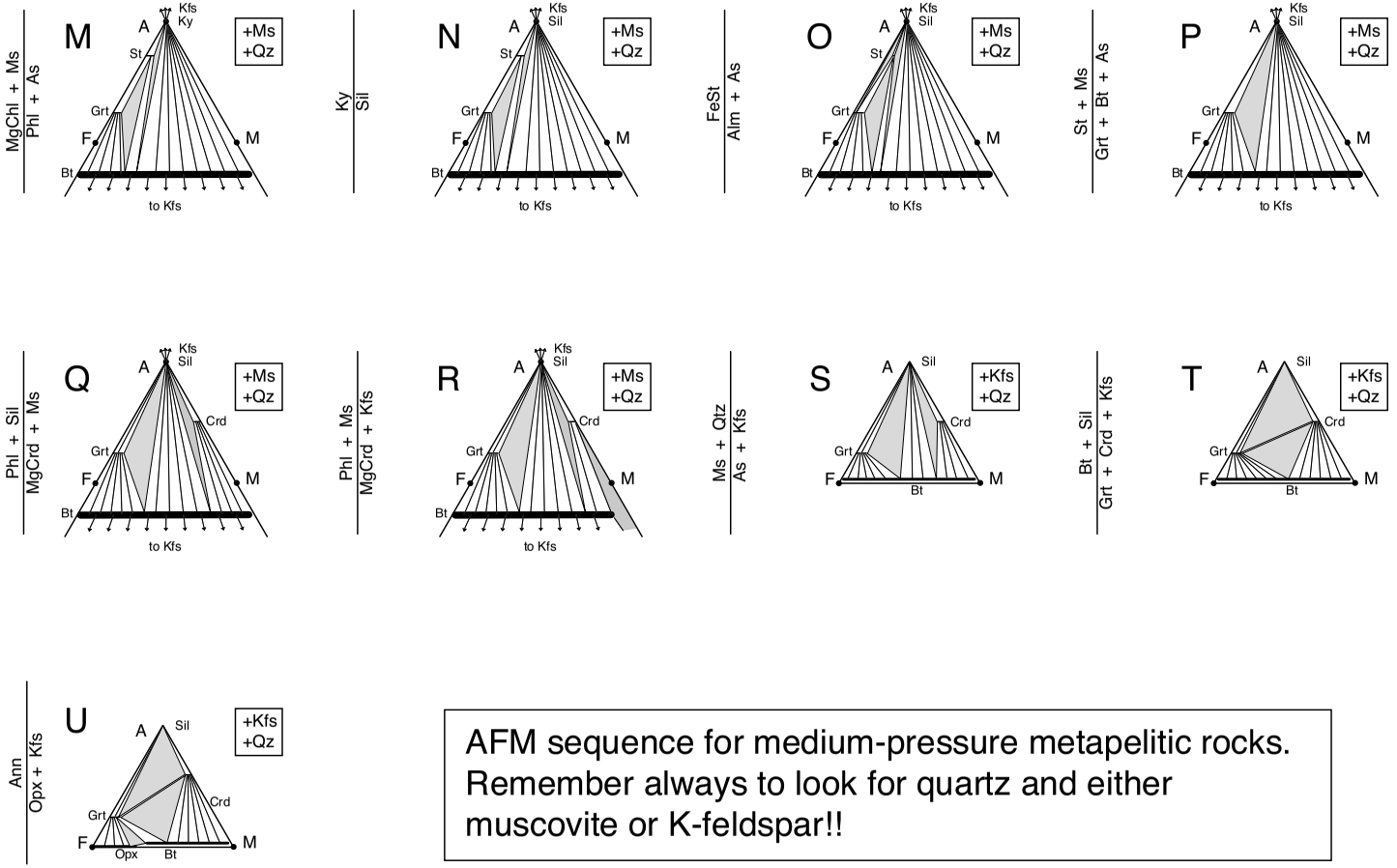
38

Table 4.6 Mineral properties in igneous rock hand specimens

Mineral	Typical chemical formula	Colour	Cleavage	Lustre	Habit	Hardness
Felsic minerals						
Quartz	SiO_2	Colourless to pale grey when surrounded by dark minerals; transparent	None; irregular, or curved fracture surfaces	Glassy, shiny	Rare trigonal pyramids but usually irregular, anhedral 	7
Alkali feldspar	$(K,Na)AlSi_3O_8$	White or pink, sometimes orange or yellow	2 sets at 90°, poorly visible	Usually dull, sometimes silky or vitreous	Tabular crystals; shiny cleavage surfaces may show simple twins. Elongate rectangular 'laths', lamellae, or irregular masses of plagioclase may be noted: perthite 	6
Plagioclase feldspar	$NaAlSi_3O_8$ to $CaAl_2Si_2O_8$	White or green, rarely pink or black	2 sets almost at 90°, poorly visible	Usually dull, sometimes silky or vitreous	Lath-shaped crystals; shiny cleavage surfaces may show multiple, parallel twins 	6–6.5
Nepheline	$NaAlSiO_4$	White to pale grey	2 poor cleavages, 1 occasionally distinct	Greasy, vitreous	Usually occurs in microcrystalline groundmass; occasional aggregates of crystals	5.5–6
Muscovite (mica)	$KAl_2(AlSi_3O_{10})(OH)_2$	Colourless to pale brown or green	1 excellent cleavage, cleaves into thin flexible sheets	Shiny, silver and pearly	Tabular crystals sometimes 6-sided, especially in pegmatites	2–2.5
Mafic minerals						
Olivine	$(Mg,Fe)_2SiO_4$	Olive green, yellow-green, sometimes brown	Very poor, usually fractures	Glassy when fresh, vitreous when altered	Usually rounded anhedral crystals, occasionally equidimensional tabular forms	6–7
Pyroxene	(i) $(Mg,Fe,Ca)_2Si_2O_6$ (augite, etc.) (ii) $NaFeSi_2O_6$ (aegirine)	Black to dark green or brown Yellowish-green	2 good sets meeting at nearly 90°	Vitreous when fresh, dull when altered	4- or 8-sided prismatic crystals occasionally showing cleavage  or  Aegirine more acicular	6
Amphibole	(i) $Ca_2(Mg,Fe)_5Si_8O_{22}(OH)_2$ (e.g. tremolite) (ii) $Na_2Fe_3^{2+}Fe_2^{3+}Si_8O_{22}(OH)_2$ (riebeckite)	Black to brownish black or dark green Dark blue	2 good sets meeting at 120°	Vitreous when fresh, dull when altered	Prismatic or lozenge-shaped crystals often showing cleavage or  Riebeckite more acicular	5–6
Biotite (mica)	$K(Mg,Fe)_3(AlSi_3O_{10})(OH)_2$	Black to dark brown or green	1 excellent cleavage; cleaves into thin flexible sheets	Very shiny	Thin tabular crystals, occasionally 6-sided, especially in ignimbrites and acid lavas	2.5–3
Tourmaline	$Na(Mg,Fe)_3Al_6B_3Si_6O_{22}(OH,F)_4$	Black, but varieties may be blue, red or green	Very poor	Vitreous shiny	Long thin prismatic needle-shaped crystals, sometimes longitudinally striated and often in clusters; occasionally striated curved surfaces 	7
Frequent accessory minerals						
Apatite	$Ca_5(PO_4)_3(OH)$	Pale green to yellow green	Very poor	Vitreous	Often euhedral, subhexagonal crystals; sometimes fibrous	5
Sphene	$CaTiSiO_4(OH)_2$	Colourless to yellow, green or brown	1 good cleavage	Vitreous	Characteristic  euhedral rhombic crystals	5

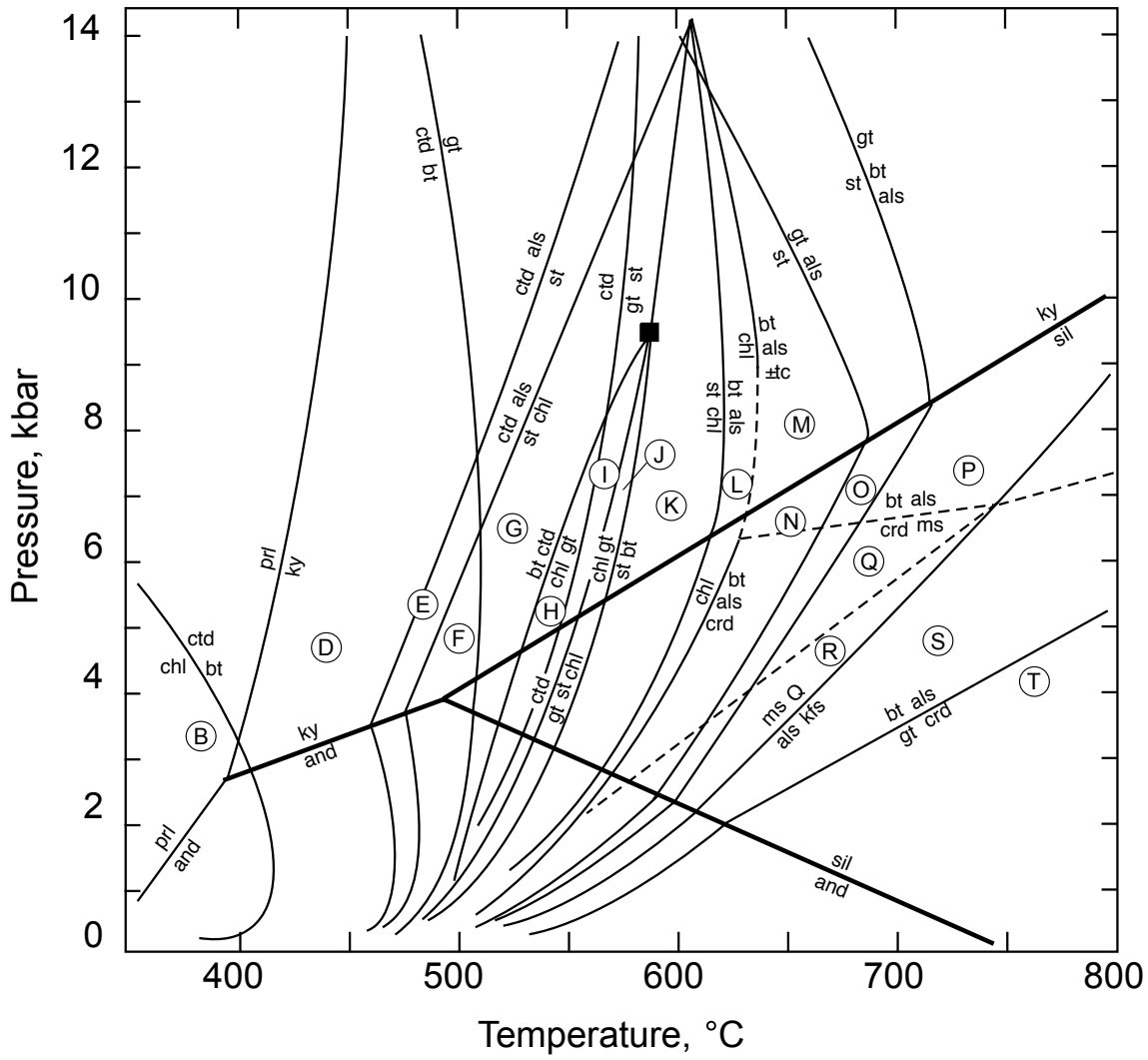
39


A
FeCld + Ms
Alm + FeSt
FeCld + Ky
FeSt
FeChl + Kfs
Ann + Ms
FeChl + Prl
FeCld
B
Cld
Grt + St + Chl
Cld + Ky
St + Chl
Prl
Ky + Qtz + H2O
FeChl + Ms
Ann + FeCld
C
Grt + Chl + Ms
St + Bt
FeCld + Ann
Alm + Ms
Tlc + Kfs
Plh
D
St + Chl + Ms
Ky + Bt
Cld + Bt
Grt + Chl
E
F
G
H
I
J
K
L
Bt
F
A
M
Cld
Grt
St
Chl
Kfs
Ky
Prl
to Kfs
+Ms
+Qz



AFM sequence for medium-pressure metapelitic rocks. Remember always to look for quartz and either muscovite or K-feldspar!!

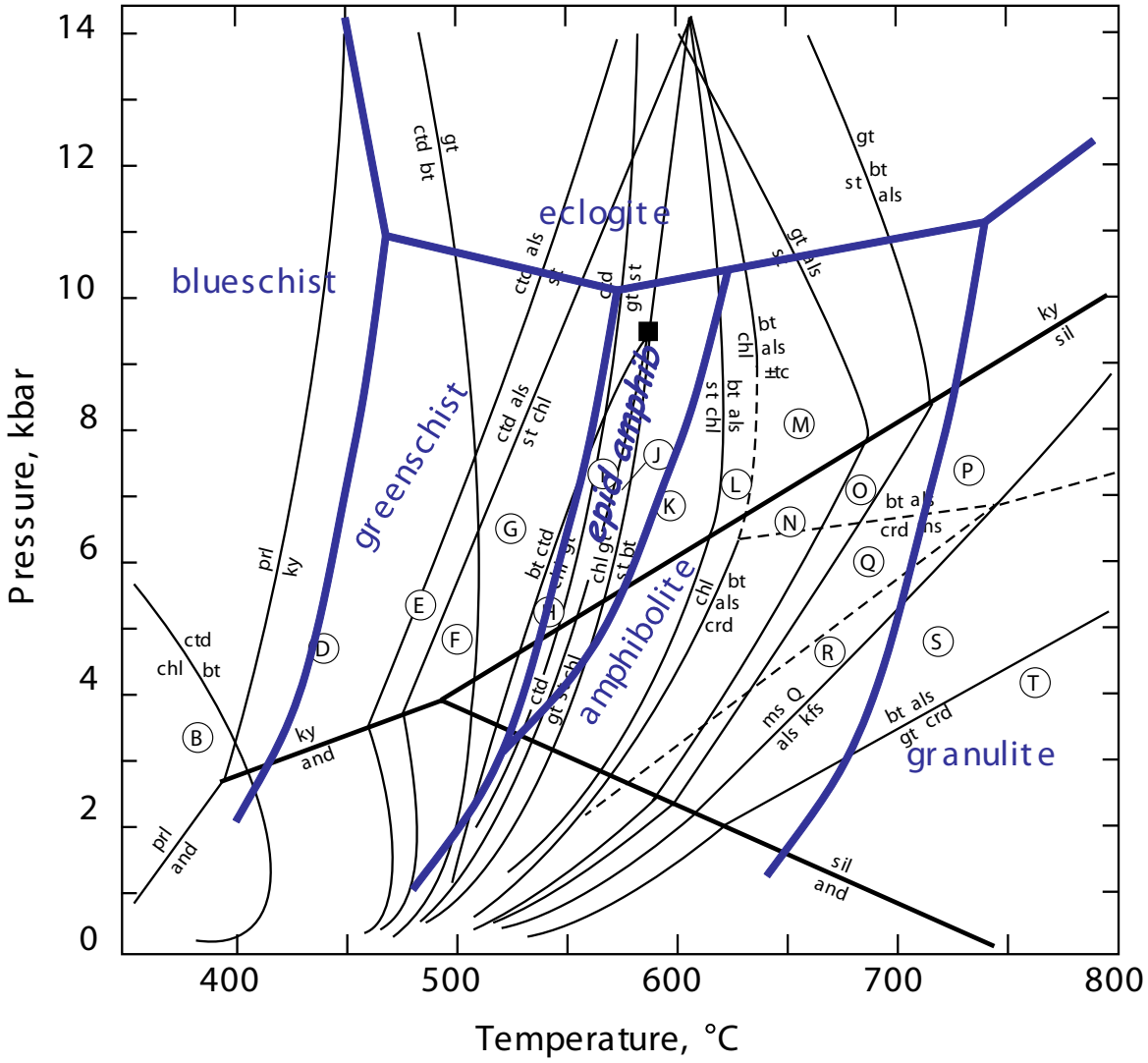
modified from Spear, 1993



Labeled fields represent divariant regions; the labels correspond to the specific AFM topologies shown on the attached page. Solid lines are for rocks that lie within the AFM diagram. Dashed lines are for Mg endmember system.

als = and, ky, or sil	ctd = chloritoid	prl = pyrophyllite
and = andalusite	gt = garnet	Q = quartz
bt = biotite	kfs = K-feldspar	sil = sillimanite
chl = chlorite	ky = kyanite	st = staurolite
crd = cordierite	ms = muscovite	tc = talc

Modified from Spear (1993)



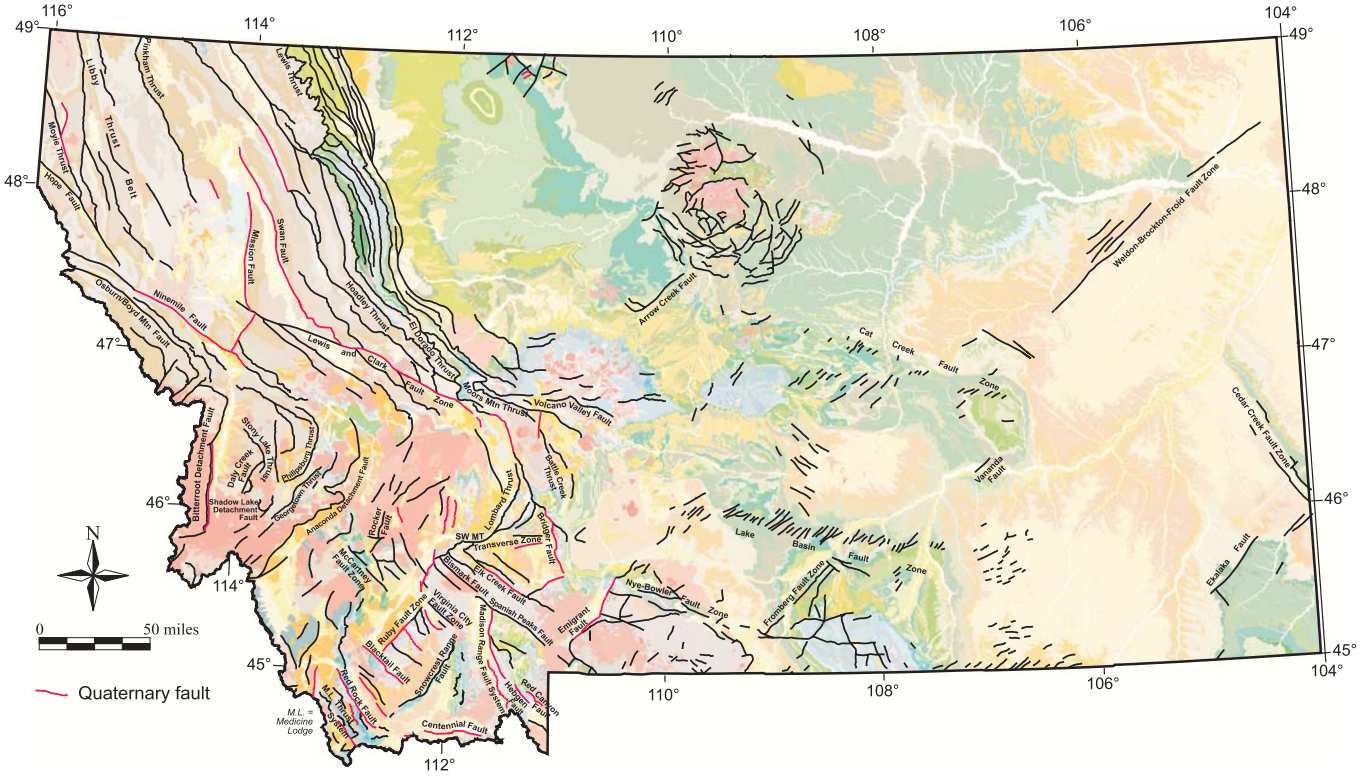
Labeled fields represent divariant regions; the labels correspond to the specific AFM topologies shown on the attached page. Solid lines are for rocks that lie within the AFM diagram. Dashed lines are for Mg endmember system.

als = and, ky, or sil	ctd = chloritoid	prl = pyrophyllite
and = andalusite	gt = garnet	Q = quartz
bt = biotite	kfs = K-feldspar	sil = sillimanite
chl = chlorite	ky = kyanite	st = staurolite
crd = cordierite	ms = muscovite	tc = talc

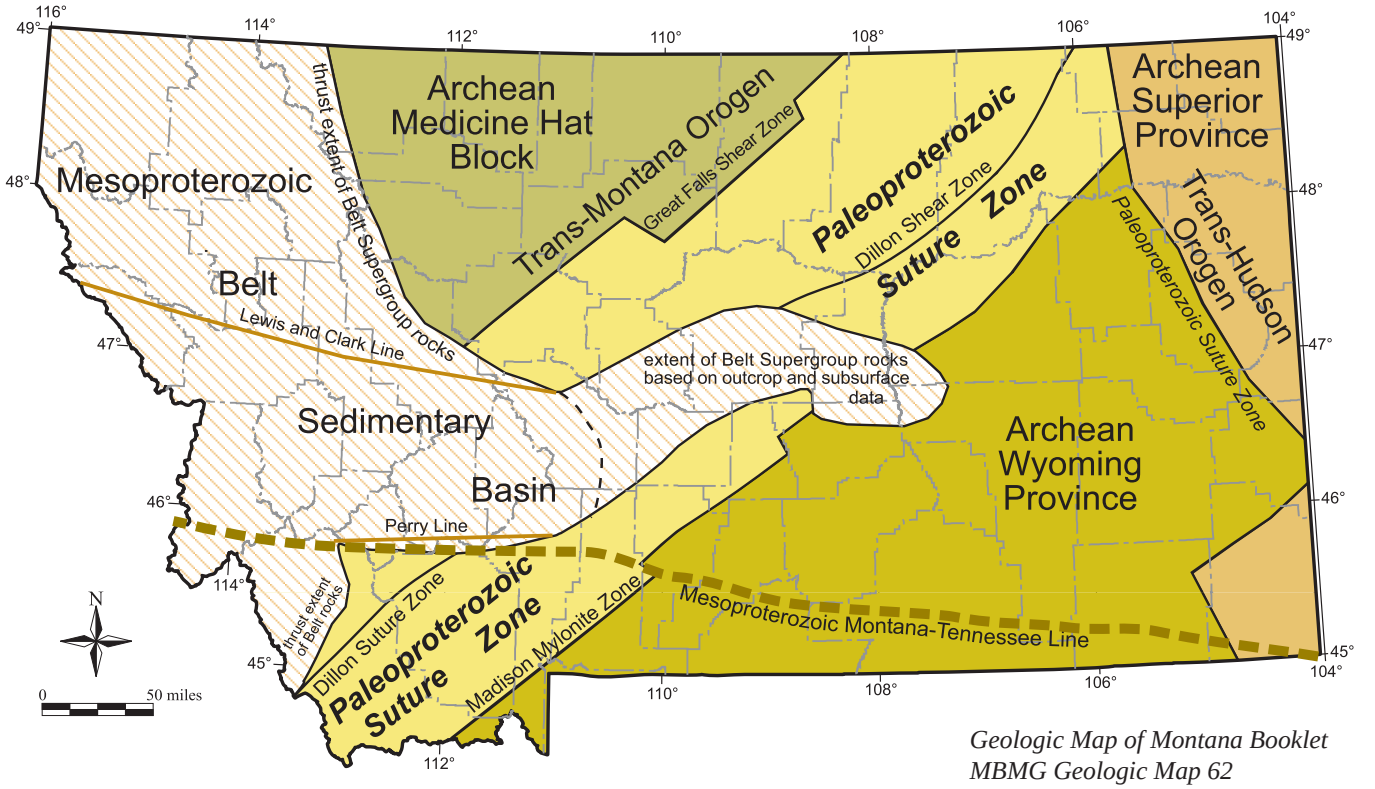
Modified from Spear (1993)

Structural Framework of Montana

Major faults. Base map from Geologic Map of Montana.
Quaternary faults from Stickney and others (2000).



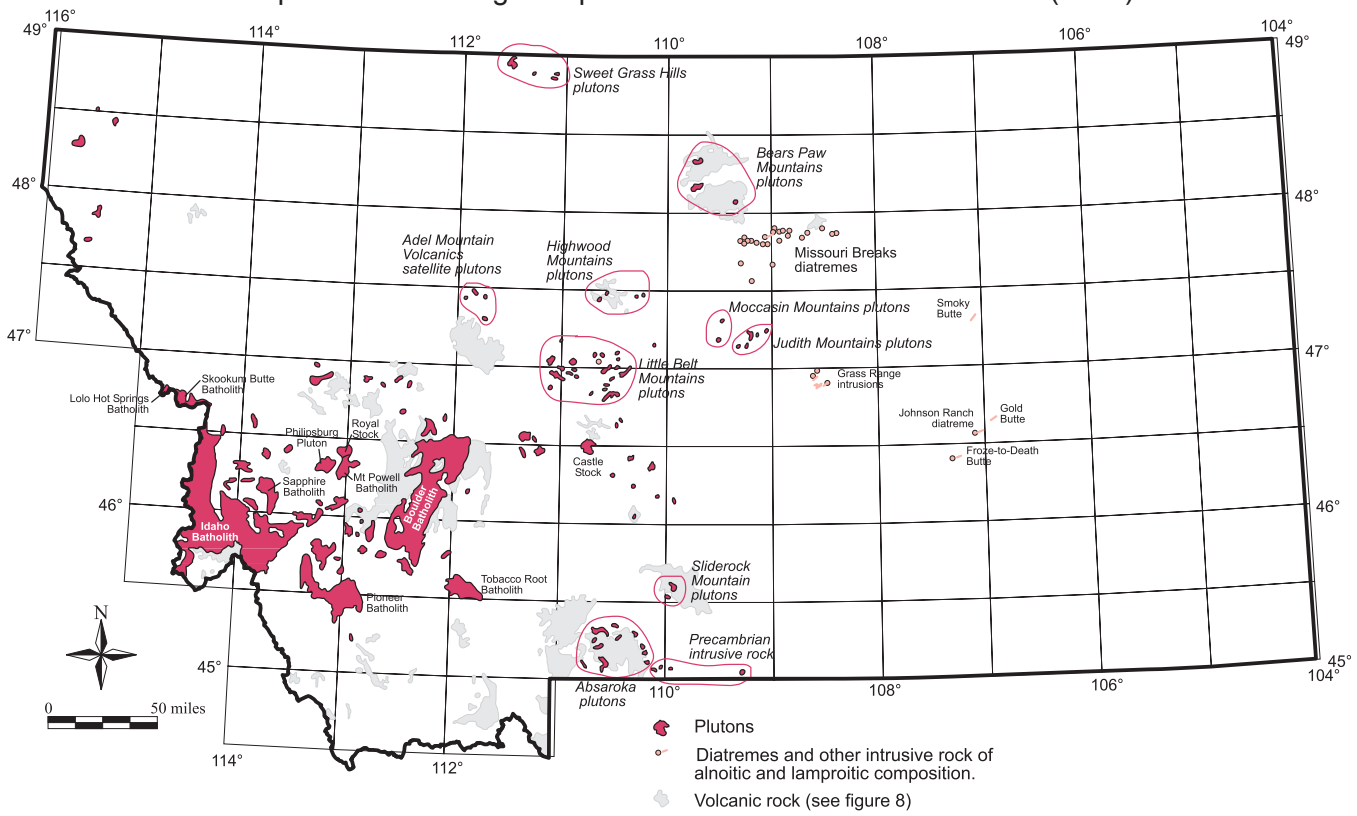
Precambrian Provinces. Modifed and compiled from Lisenbee and DeWitt (1993), Nelson (1993), Sears (2006), and Sims and others (2004).



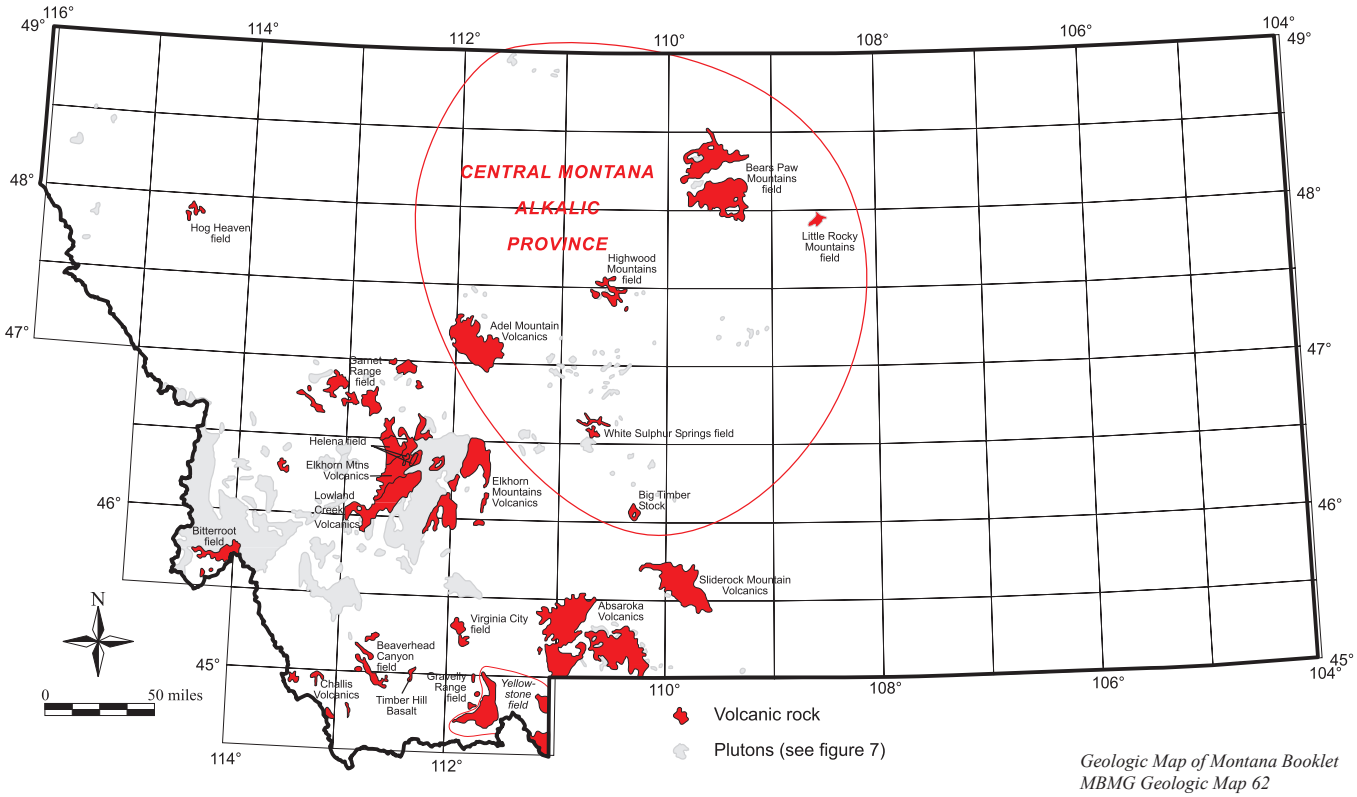
Geologic Map of Montana Booklet
MBMG Geologic Map 62

Igneous Rocks of Montana

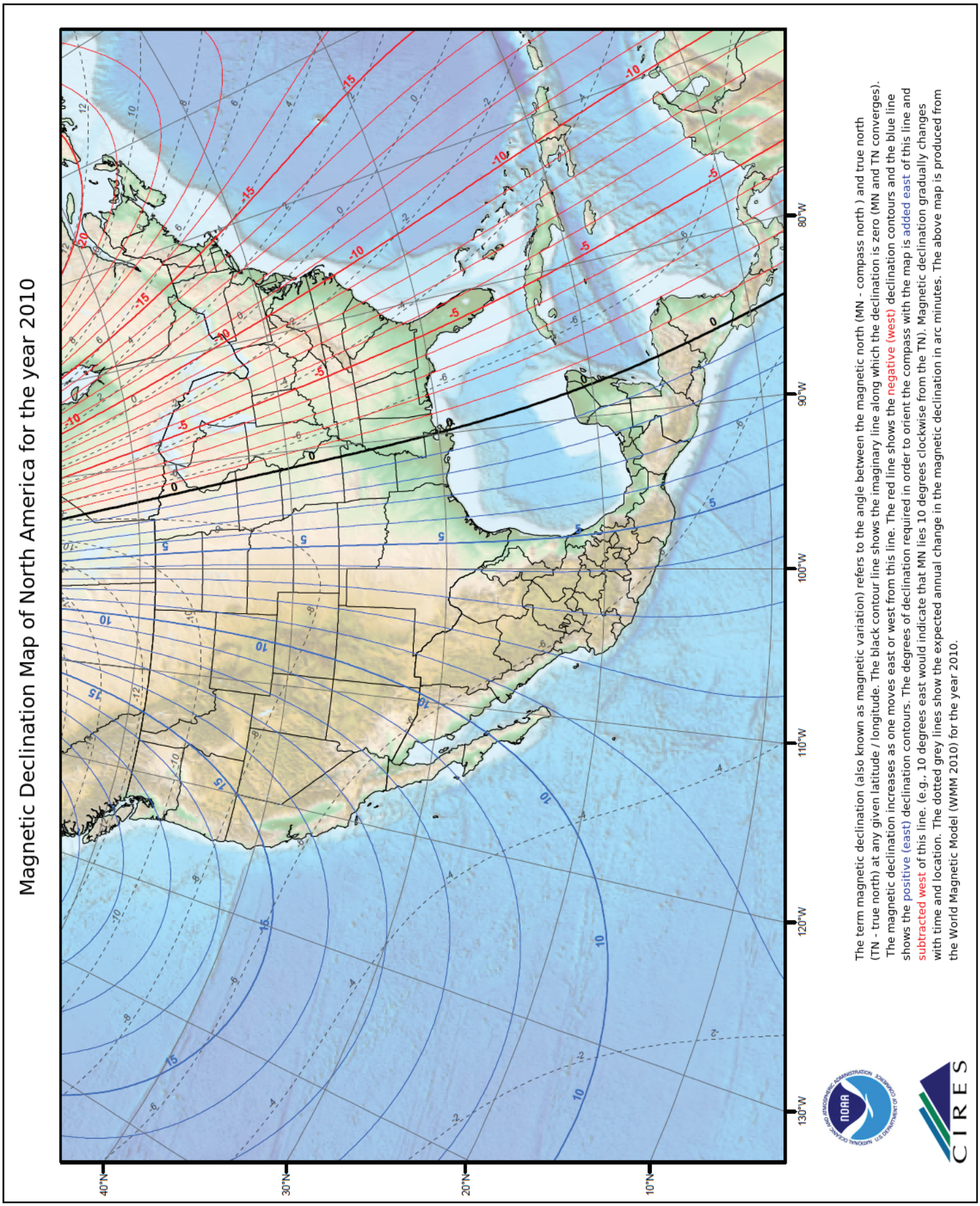
Plutons, diatremes, and other intrusive rock.
Compiled from Geologic Map of Montana and Hearn and others (1989).



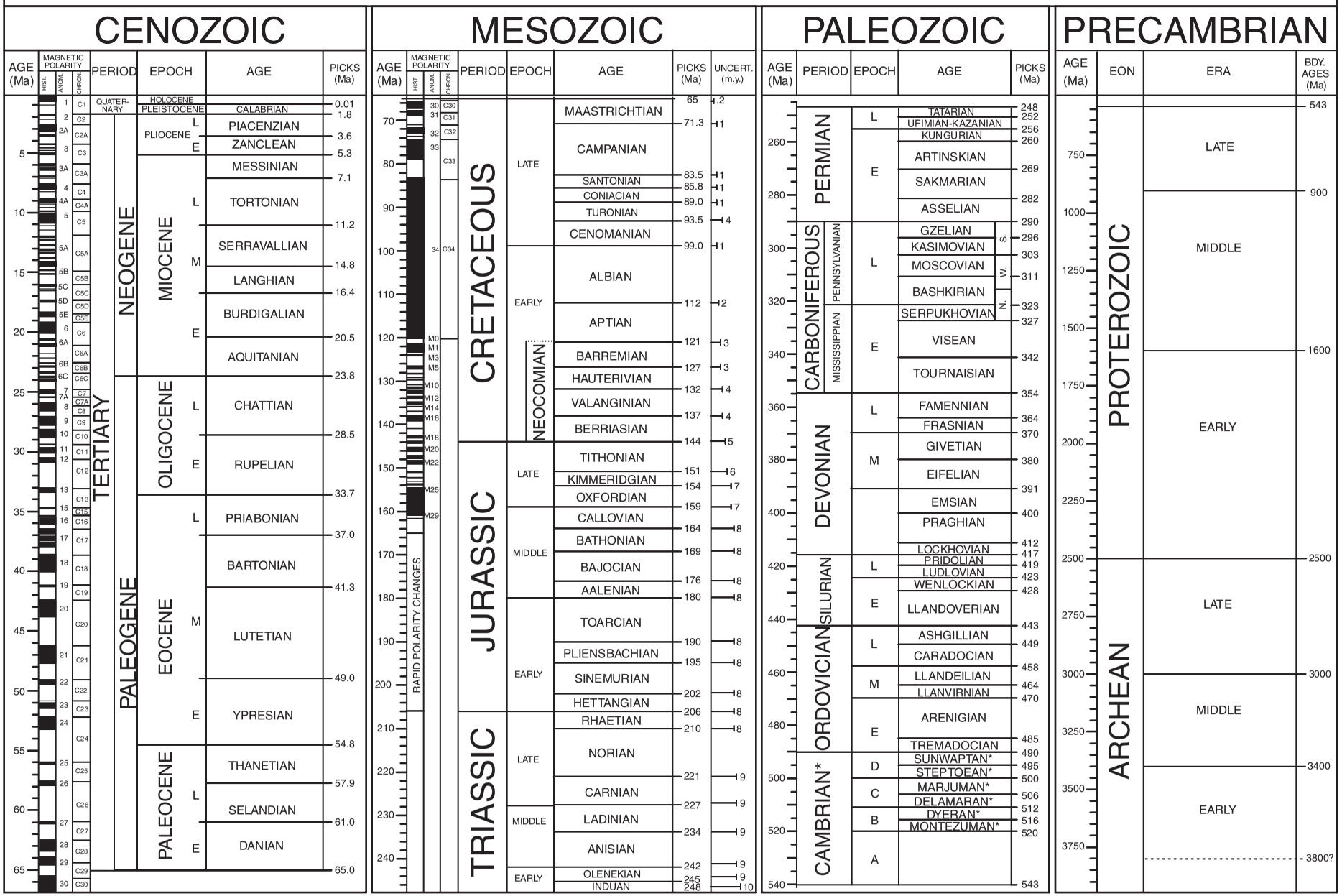
Volcanic rock. Compiled from Geologic map of Montana.



Geologic Map of Montana Booklet
MBMG Geologic Map 62


Magnetic Declination Map of North America for the year 2010
130°W
120°W
110°W
100°W
90°W
80°W
40°N
30°N
20°N
10°N
The term magnetic declination (also known as magnetic variation) refers to the angle between the magnetic north (MN - compass north) and true north (TN - true north) at any given latitude / longitude. The black contour line shows the imaginary line along which the declination is zero (MN and TN converges). The magnetic declination increases as one moves east or west from this line. The red line shows the negative (west) declination contours and the blue line shows the positive (east) declination contours. The degrees of declination required in order to orient the compass with the map is added east of this line and subtracted west of this line. (e.g., 10 degrees east would indicate that MN lies 10 degrees clockwise from the TN). Magnetic declination gradually changes with time and location. The dotted grey lines show the expected annual change in the magnetic declination in arc minutes. The above map is produced from the World Magnetic Model (WMM 2010) for the year 2010.
NOAA
CIRES

1999 GEOLOGIC TIME SCALE



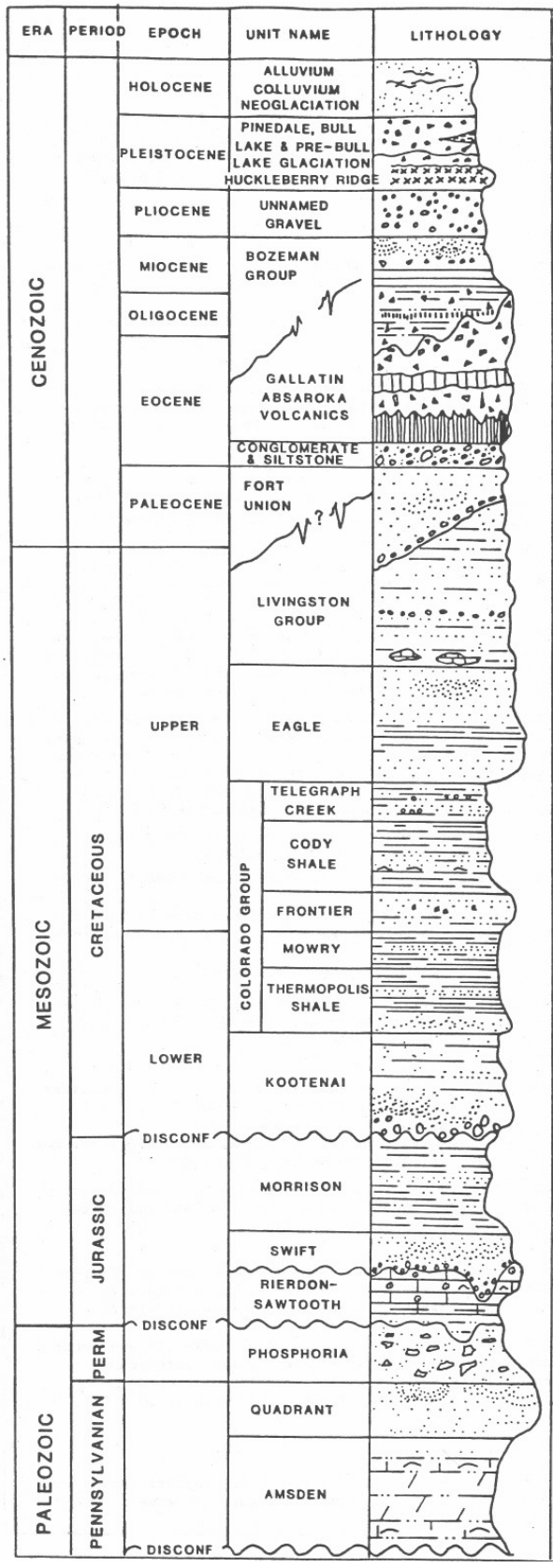
© 1999, The Geological Society of America. Product code CTS004. Compilers: A. R. Palmer, John Geissman

*International ages have not been established. These are regional (Laurentian) only. Boundary Picks were based on dating techniques and fossil records as of 1999. Paleomagnetic attributions have errors, Please ignore the paleomagnetic scale.

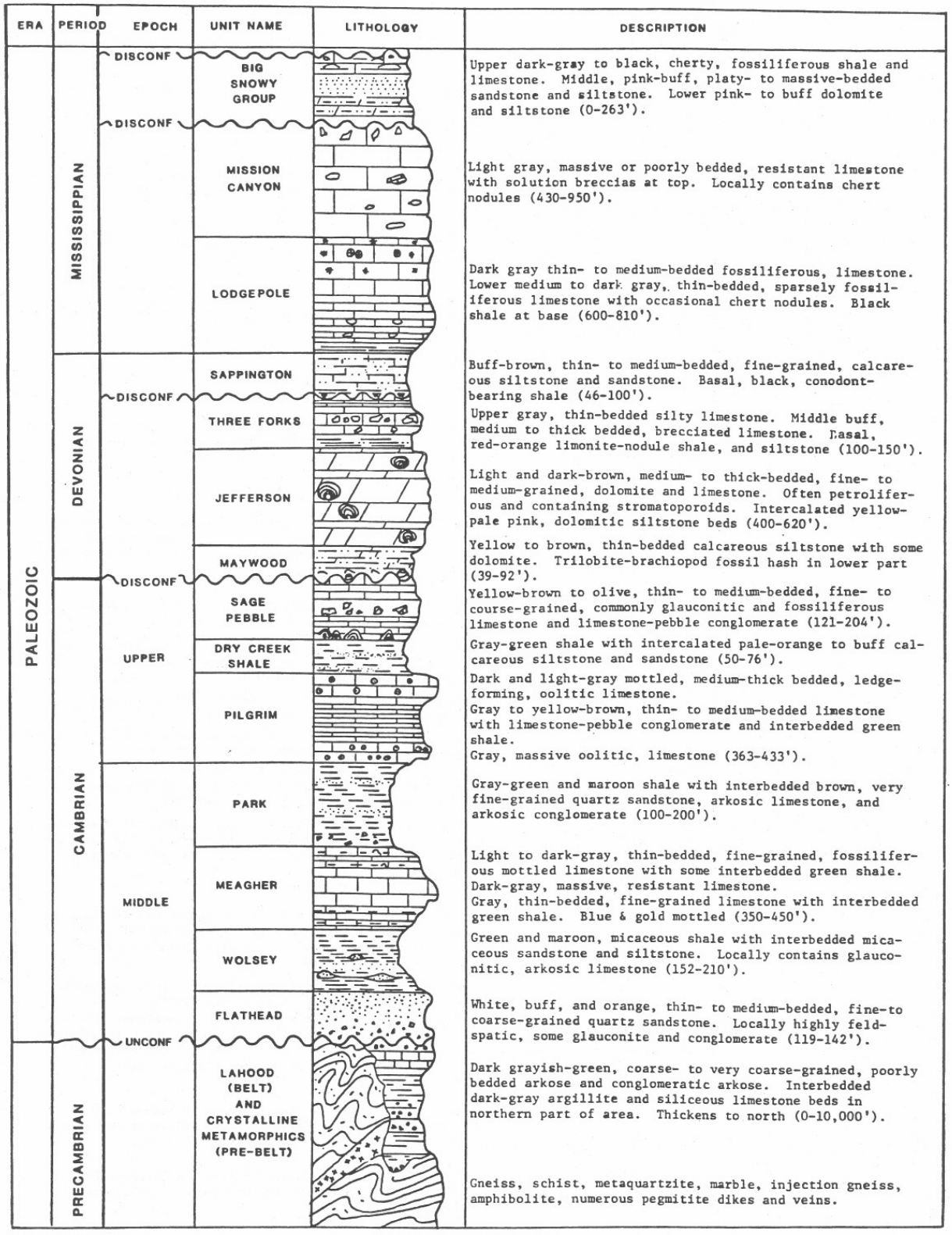
Sources for nomenclature and ages: Primarily from Gradstein, F., and Ogg, J., 1996, *Episodes*, v. 19, nos. 1 & 2; Gradstein, F., et al., 1995, SEPM Special Pub. 54, p. 95–128; Berggren, W. A., et al., 1995, SEPM Special Pub. 54, p. 129–212; Cambrian and basal Ordovician ages adapted from Landing, E., 1998, *Canadian Journal of Earth Sciences*, v. 35, p. 329–338; and Davidek, K., et al., 1998, *Geological Magazine*, v. 135, p. 305–309. Cambrian age names from Palmer, A. R., 1998, *Canadian Journal of Earth Sciences*, v. 35, p. 323–328.

GEOLOGICAL SOCIETY OF AMERICA

THREE FORKS BASIN STRATIGRAPHIC COLUMN



ERA	PERIOD	EPOCH	UNIT NAME	DESCRIPTION
CENOZOIC		HOLOCENE	ALLUVIUM COLLUVIUM NEOGLACIATION	Immature silt, sand and gravel; chaotic debris, till in cirques (0-100').
		PLEISTOCENE	PINEDALE, BULL LAKE & PRE-BULL LAKE GLACIATION	Lacustrine silt; fresh, weathered, and deeply weathered till (0-200').
			HUCKLEBERRY RIDGE	Welded phenocryst-rich rhyolitic ash-flow tuff (2 my B.P.) (0-200').
		PLIOCENE	UNNAMED GRAVEL	Unconsolidated stream gravel (0-100').
		MIOCENE	BOZEMAN GROUP	Light-colored alternating biosparite, tuffaceous biomicrite, tuffaceous silty shale, vitric ash, and conglomerate, with cross-bedded sandstone in upper part (0-5,000').
		OLIGOCENE		
		EOCENE	GALLATIN ABSAROKA VOLCANICS	Light to dark grayish-brown andesite and basalt flows, breccia, agglomerate, and tuff (0-6,000').
			CONGLOMERATE & SILTSTONE	Conglomerate consisting of Precambrian and later boulders and cobbles (0-50').
		PALEOCENE	FORT UNION	Light brown to dark gray sandstone and basal conglomerate (0-600').
MESOZOIC	CRETACEOUS	UPPER	LIVINGSTON GROUP	Light and dark grayish-green andesitic or tuffaceous siltstone, sandstone, and conglomerate with some fresh-water limestone lenses in the lower part (0-7,000').
			EAGLE	Light gray, thin- to thick-bedded, locally cross-bedded, fine to medium grained, salt and pepper sandstone with some intercalated carbonaceous shale and thin coal beds (0-600').
			COLORADO GROUP: TELEGRAPH CREEK	Medium gray, thin-bedded siltstone containing calcareous concretions and some resistant sandstone beds (0-250').
			COLORADO GROUP: CODY SHALE	Medium to dark gray and brown thin-bedded shale with some beds of siltstone and sandstone, especially in middle part. Locally fossiliferous (50-600').
			COLORADO GROUP: FRONTIER	Buff to medium gray thin- to medium-bedded, fine- to coarse-grained arkosic sandstone, locally silty (50-200').
			COLORADO GROUP: MOWRY	Grayish-brown and green shale and siltsone with some sandstone beds. Locally carbonaceous (25-400').
			COLORADO GROUP: THERMOPOLIS SHALE	Medium gray to black shale with numerous fine- to medium-grained gray sandstone beds. Locally arkosic, glauconitic, or carbonaceous. Lower resistant sandstone.
		LOWER	KOOTENAI	Buff to light gray, medium- to thick-bedded shale and sandstone with cross-bedded basal conglomerate. Locally contains fresh-water limestone nodules and beds near top (100-490').
		DISCONF		
	JURASSIC		MORRISON	Variegated red and green, thin- to medium-bedded shale and siltstone with intercalated yellowish-brown calcareous siltstone and sandstone. Upper part locally contains carbonaceous shale (110-444').
			SWIFT	Yellowish-brown, medium-bedded, fine-grained, calcareous sandstone. Basal chert conglomerate (100').
			RIERDON-SAWTOOTH	Upper massive gray, resistant oolitic limestone. Lower variegated and mostly dark gray limestone with interbedded siltstone and shale. Chert pebbles in lower part (200').
		DISCONF		
	PERM		PHOSPHORIA	Pale yellowish-brown, calcareous sandstone with chert nodules & breccias (0-26').
PALEOZOIC	PENNSYLVANIAN		QUADRANT	White to pinkish-gray, medium- to thick-bedded (locally cross-bedded), subrounded, fine- to medium-grained orthoquartzite; dolomitic in lower part (135-250').
			AMSDEN	Pale yellow to reddish-brown, medium- to thick-bedded siltstone with some dolomite and impure fossiliferous limestone beds (11-189').
		DISCONF		


ERA
PERIOD
EPOCH
UNIT NAME
LITHOLOGY
DESCRIPTION
PALEOZOIC
MISSISSIPPIAN
DEVONIAN
CAMBRIAN
PRECAMBRIAN
DISCONF
DISCONF
DISCONF
DISCONF
UNCONF
UPPER
MIDDLE
BIG SNOWY GROUP
MISSION CANYON
LODGEPOLE
SAPPINGTON
THREE FORKS
JEFFERSON
MAYWOOD
SAGE PEBBLE
DRY CREEK SHALE
PILGRIM
PARK
MEAGHER
WOLSEY
FLATHEAD
LAHOOD (BELT) AND CRYSTALLINE METAMORPHICS (PRE-BELT)
Upper dark-gray to black, cherty, fossiliferous shale and limestone. Middle, pink-buff, platy- to massive-bedded sandstone and siltstone. Lower pink- to buff dolomite and siltstone (0-263').
Light gray, massive or poorly bedded, resistant limestone with solution breccias at top. Locally contains chert nodules (430-950').
Dark gray thin- to medium-bedded fossiliferous, limestone. Lower medium to dark gray, thin-bedded, sparsely fossiliferous limestone with occasional chert nodules. Black shale at base (600-810').
Buff-brown, thin- to medium-bedded, fine-grained, calcareous siltstone and sandstone. Basal, black, conodont-bearing shale (46-100').
Upper gray, thin-bedded silty limestone. Middle buff, medium to thick bedded, brecciated limestone. Basal, red-orange limonite-nodule shale, and siltstone (100-150').
Light and dark-brown, medium- to thick-bedded, fine- to medium-grained, dolomite and limestone. Often petroliferous and containing stromatoporoids. Intercalated yellow-pale pink, dolomitic siltstone beds (400-620').
Yellow to brown, thin-bedded calcareous siltstone with some dolomite. Trilobite-brachiopod fossil hash in lower part (39-92').
Yellow-brown to olive, thin- to medium-bedded, fine- to course-grained, commonly glauconitic and fossiliferous limestone and limestone-pebble conglomerate (121-204').
Gray-green shale with intercalated pale-orange to buff calcareous siltstone and sandstone (50-76').
Dark and light-gray mottled, medium-thick bedded, ledge-forming, oolitic limestone.
Gray to yellow-brown, thin- to medium-bedded limestone with limestone-pebble conglomerate and interbedded green shale.
Gray, massive oolitic, limestone (363-433').
Gray-green and maroon shale with interbedded brown, very fine-grained quartz sandstone, arkosic limestone, and arkosic conglomerate (100-200').
Light to dark-gray, thin-bedded, fine-grained, fossiliferous mottled limestone with some interbedded green shale.
Dark-gray, massive, resistant limestone.
Gray, thin-bedded, fine-grained limestone with interbedded green shale. Blue & gold mottled (350-450').
Green and maroon, micaceous shale with interbedded micaceous sandstone and siltstone. Locally contains glauconitic, arkosic limestone (152-210').
White, buff, and orange, thin- to medium-bedded, fine-to coarse-grained quartz sandstone. Locally highly feldspatic, some glauconite and conglomerate (119-142').
Dark grayish-green, coarse- to very coarse-grained, poorly bedded arkose and conglomeratic arkose. Interbedded dark-gray argillite and siliceous limestone beds in northern part of area. Thickens to north (0-10,000').
Gneiss, schist, metaquartzite, marble, injection gneiss, amphibolite, numerous pegmitite dikes and veins.

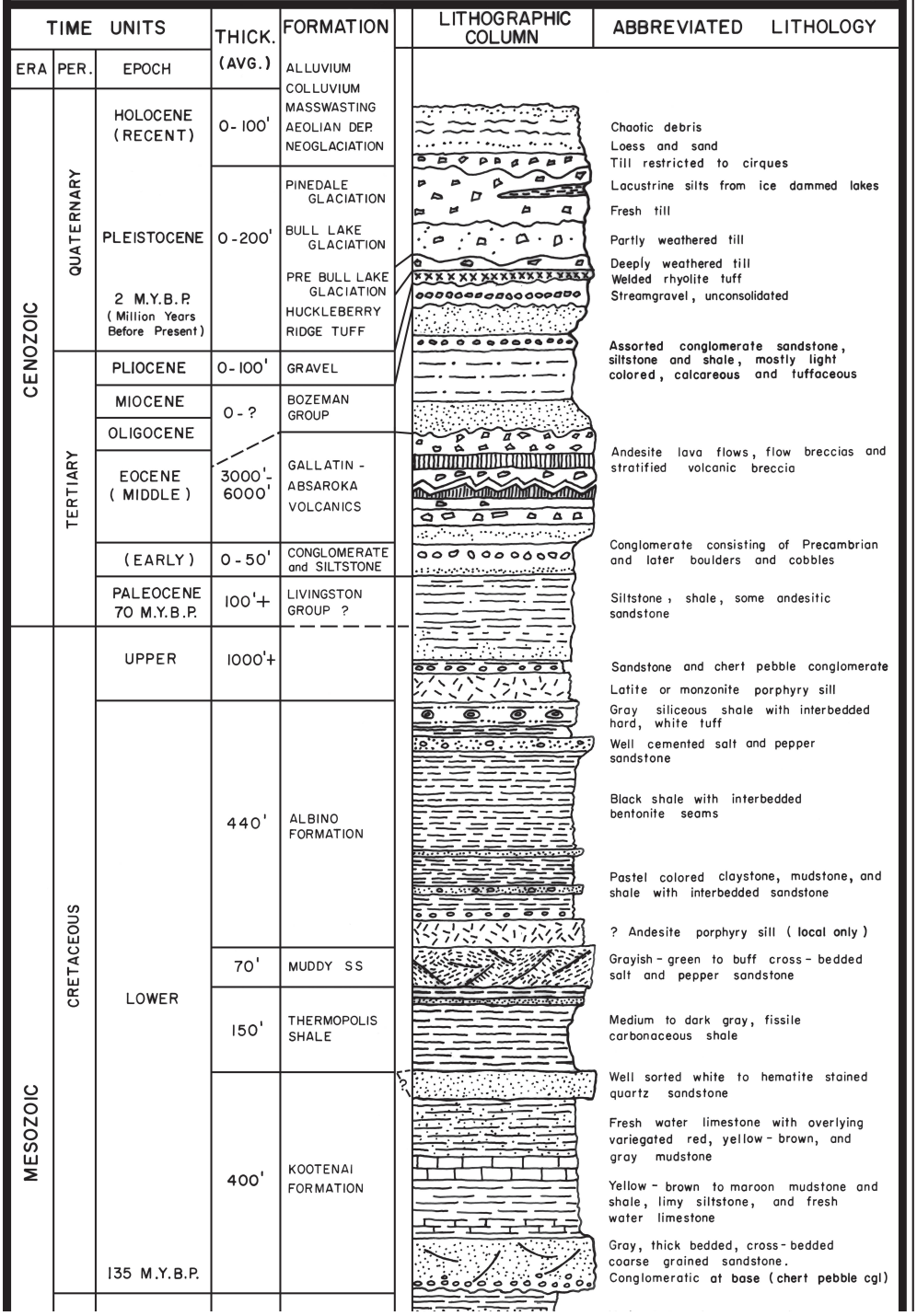
IDEALIZED STRATIGRAPHIC COLUMN
Northern Gallatin and Madison Ranges
Montana

Compiled by

John Montagne
Professor of Geology, Department of Earth Sciences
Montana State University

Assisted by John Goering
Drafting by Cecilia Vaniman

After: Hall, 1961; McMannis and Chadwick, 1964; Witkind, 1969; Kehew, 1971; Montagne, C., 1972; Montagne, J., 1975



*see next page for Jurassic & older rocks

*see previous page for Cretaceous & younger rocks

